PROTEOMIC PROFILING AND ROLE OF ACETYLCHOLINE BINDING PROTEIN IN AGED *LYMNAEA STAGNALIS*

Mohammed Aiyaz

27th January 2010

A thesis submitted in partial fulfilment of the requirements for the degree of

Doctor of Philosophy

University of Brighton

2010

Signature of candidate ……..

ABSTRACT

Age-related changes in the central nervous system (CNS) is a multi-factorial process involving subtle alterations to several subcellular systems, including a disturbance to cholinergic signalling that becomes a prominent feature in age-related neurodegenerative diseases (Giacobini, 1990). Previous work in the *L. stagnalis* nervous system highlighted synapse-specific alterations in subsets of neurons that are accompanied by a marked decline in feeding behaviour in chronologically aged animals (Arundell *et al.*, 2006; Yeoman *et al.*, 2008). To identify common elements that lead to a reduction in feeding behaviour, 2D Difference in-gel Electrophoresis (2D DIGE) analysis highlighted 49 proteins that were differentially expressed in the aged *L. stagnalis* CNS. Amongst them, three key protein groups involved in maintaining the cytoskeletal integrity, energy-dependent processes, and chaperones were significantly altered in the aged CBG. The expression level of cytoskeletal proteins such as tubulin and actin, putative chaperones such as 14-3-3, and kinases such as arginine kinase as well as mitochondrial proteins such as reductase were all significantly down-regulated in aged CNS ($p < 0.05$) and are well aligned with changes that are observed in normally aged higher vertebrates. This suggested that the alterations in functional neuronal circuits that accompany a reduction in feeding behaviour in *L. stagnalis* may encounter a similar set of biochemical challenges as those experienced in higher vertebrates.

The finding that acetylcholine binding protein (AChBP) that regulates cholinergic signalling through its release by *L. stagnalis* glial cells was significantly reduced by 1.70 fold ($p < 0.05$), suggested cholinergic signalling, in part through AChBP may also be impaired in aged animals. AChBP mRNA expression analysis revealed an 80% reduction ($p < 0.05$), that suggested AChBP levels were transcriptionally regulated in the aged animal. The participation of AChBP in the feeding network, examined using RNA interference (RNAi), suggested that knockdown of AChBP protein could occur in desheathed ganglia *in vitro* by 70% ($p < 0.05$), but not *in vivo* following Western blot analysis ($p > 0.05$). Therefore a conclusive role for AChBP could not be established in the feeding network. Together, this thesis highlights age-related changes in the molluscan nervous system using multiplex proteomics technology and illustrates how proteomics and reverse genetics could be used together to aid the understanding of gene function in an unsequenced organism.

TABLE OF CONTENTS

ABSTRACT 2

Chapter 1: GENERAL INTRODUCTION AND BACKGROUND 14

1.1 What is Ageing? 15
1.2 Why we age – postulated mechanisms 15
1.2.1 Free radical theory of ageing 16
1.2.2 Molecular inflammation theory of ageing 18
1.2.3 The Calcium Theory of ageing 19
1.2.4 Potential role of cellular senescence in brain ageing 21
1.2.5 Neurotrophic Theory 23
1.3.0 Age-related changes in invertebrate animal models 26
1.3.1 The L. stagnalis nervous system 27
1.3.2 The feeding behaviour is regulated by the cerebral and buccal ganglia in L.stagnalis 28
1.3.3 In vitro modelling of the feeding behaviour in Lymnaea stagnalis 30
1.3.4 Age-related changes to the feeding behaviour in L. stagnalis 31
1.3.5 Age-related electrophysiological changes in L. stagnalis 32
Summary of the thesis 35

Chapter 2: AGE-RELATED PROTEOMIC CHANGES IN THE CEREBRAL AND BUCCAL GANGLIA 36

***2.1. BACKGROUND:* 36**

2.1.1 Expression profiling in aged animals: 37
2.1.2 Protein separation technologies 39
2.1.3 Proteomic profiling using 2 dimensional electrophoresis 41

2.2 OBJECTIVE: 42

2.3 MATERIALS AND METHODS: 43

2.3.1 Animals 43
2.3.2 Chemicals and reagents 43
2.3.3 Instruments: 45
2.3.4 Behavioural analysis of feeding in L. stagnalis 45
2.3.5 Tissue dissection 46
2.3.6 Tissue Extraction in 2D Lysis buffer: 46
2.3.7 Acetone Precipitation 46
2.3.8 Determination of protein concentration: 47
2.3.9 2D PAGE/ 2D DIGE 47
2.3.9.1 Large format gel casting 47
2.3.9.2 First Dimension running conditions 48
2.3.9.3 Reduction and alkylation of IPG strips 48
2.3.9.4 Second Dimension gel running condition 48
2.3.9.5 2D DIGE experimental design 49
2.3.9.6 Digitisation and analysis of 2D DIGE image 50
2.3.9.7 Protein extraction from 2D PAGE gels 50
2.3.9.8 Trypsin Digestion 50
2.3.10 Mass Spectrometric Analysis Of Proteins 51
2.3.10.1 RP-LC fractionation of peptide digests 51
2.3.10.2 MS/MS spectral data acquisition from protein digest 51

2.3.11 De Novo Sequence Analysis of Protein Fragments 51
2.3.12 Western Blot analysis 52
2.3.12.1 Protein extraction and separation: 52
2.3.12.2 Gel transfer to PVDF membrane: 52
2.3.12.3 Antibody incubation 52
2.3.12.4 Chemiluminescent detection 52
2.3.12.5 Membrane stripping 53
2.3.13 Statistical analysis of data 53

2.4 RESULTS (1): DETERMINING PROTEOMIC CHANGES IN THE CEREBRAL AND BUCCAL GANGLIA OF L. STAGNALIS 54

2.4.1 Method Development: 55
2.4.1.1 Comparison of extraction buffer for L. stagnalis CNS 55
2.4.1.2 Determining degradation and concentration of protein during dissection 55
2.4.1.3 Determining the dynamic range of L. stagnalis protein on 2D PAGE gel 58
2.4.2 2D Difference in-gel electrophoresis: Cerebro-buccal Ganglia. 60
2.4.3 Identification of proteins using PEAKS 4.5 61
2.4.4 Highly regulated proteins with no assignable protein IDs 70
2.4.5 Summary of 2D DIGE of the aged cerebral and buccal ganglia 71

2.4.6 RESULTS (II): VALIDATION OF AGE-RELATED PROTEIN CHANGES 72

2.4.6.1 Method Development 72
2.4.6.2 Western Blot analyses of AChBP expression 72
2.4.6.3 Western Blot Analyses of α-tubulin expression 74
2.4.6.4 Western Blot Analyses of β-actin expression 75

***2.5.0* DISCUSSION: 76**

2.5.1 Cytoskeletal dysfunction in the aged CBG 76
2.5.2 Altered regulation of proteins involved in energy metabolism: 80
2.5.3 Altered regulation of protein synthesis in the aged CBG 82
2.5.4 Altered chaperone function in aged CBG 83
2.5.5 Altered cholinergic signalling in aged CBG 85

2.6.0 TECHNICAL CONSIDERATIONS DURING PROTEOMIC PROFILING 86

2.7.0 CONCLUSION & FUTURE DIRECTIONS 88

Chapter 3: ANALYSIS OF AChBP mRNA LEVELS AND GFAP PROTEIN LEVELS IN THE AGED *L. STAGNALIS* CBG 89

***3.1 BACKGROUND* 89**

3.1.1 An Introduction to cholinergic signalling: 90
3.1.1.1 Cholinergic targets: 90
3.1.1.2 Disruption of choline uptake at cholinergic synapses 91
3.1.1.3 Disruption to ChAT activity at cholinergic synapses 91
3.1.1.4 Cholinergic regulation by muscarinic acetylcholine receptors 92
3.1.1.5 Age-related changes in CNS nicotinic acetylcholine receptors 93
3.1.1.6 Neurotrophin receptor expression in cholinergic neurons 95
3.1.1.7 Cholinergic signalling in L. stagnalis 96

3.1.1.8 Functional Properties of AChBP 97
3.1.1.9 Molecular Properties Of AChBP 98
3.1.2 Gene expression profiling using quantitative RT-PCR 98
3.1.2.1 Relative quantification using the delta delta Ct method 100

3.2 OBJECTIVES: 102

3.3 MATERIALS AND METHODS 103
3.3.1 Immunohistochemistry 103
3.3.1.1 Paraffin sections 103
3.3.1.2 Dewaxing 103
3.3.1.3 Labelling method 104
3.3.2 Selection of L. stagnalis for RT-PCR experiment 104
3.3.3 RNA Isolation 104
3.3.4 Determination of RNA concentration in sample 105
3.3.5 Preparation of first-strand cDNA: 106
3.3.5.1 DNase-treated RNA 106
3.3.5.2 Reverse transcription (RT) 106
3.3.6 Real-Time RT-PCR Analysis 107
3.3.6.1 Primer Sequences for AChBP qPCR: 107
3.3.6.2 PCR amplification: 107
3.3.6.3 RT-qPCR data analysis: 108
3.3.7 Western Blot analysis: 108

3.4 RESULTS: 109
3.4.1 Immuno-histochemical labelling of AChBP 109
3.4.2 Method development - RNA extraction/ determination 110
3.4.3 DNase treatment 111
3.4.4 Annealing temperatures for each primer set 111
3.4.5 Optimisation of house-keeping gene GAPDH 112
3.4.6 Optimisation of house keeping gene Elf-α 114
3.4.7 AChBP mRNA expression profiling 118
3.4.8 GFAP expression in the aged CBG of L. stagnalis 124

3.5.0 DISCUSSION 125
3.5.1 Immunohistochemical analysis of AChBP in L. stagnalis 125
3.5.2 Transcriptional expression of AChBP in the young and aged CBG 126
3.5.3 GFAP expression in the young and aged CBG 127

3.6 CONCLUSIONS AND FUTURE DIRECTIONS 130

Chapter 4: dsRNA- AND siRNA-MEDIATED GENE SILENCING OF AChBP 132

4.1 BACKGROUND: 132
4.1.1 Mechanism of action of RNAi-mediated gene silencing 132
dsRNA mediated gene silencing 132
Step 1: The sense and antisense strands detach from each other 133
Step 2: The protein complex is attached to the antisense strand of the siRNA 134
Step 3: The protein complex is brought close to the mRNA 134
Step 4: The mRNA is cleaved 135
4.1.2 miRNA-mediated gene silencing 135
4.1.3 Activation of the interferon response 136

4.1.4 RNA-mediated silencing in L. stagnalis....137

4.2 OBJECTIVE: 139

4.3 MATERIALS AND METHODS 140

4.3.1 Nucleic acids: 140
4.3.2 AChBP dsRNA synthesis....141
4.3.3 Cloning AChBP into pGEM vector....141
4.3.3.1 cDNA synthesis and RT reaction....141
4.3.3.2 Primer Design and PCR....141
4.3.3.3 Vector ligation and sequence determination....143
4.3.4 Synthesis and purification of dsRNA....144
4.3.4.1 Addition of T7 promoter flanking the transcription region....144
4.3.4.2 In vitro transcription using Megascript synthesis kit (Ambion)...145
4.3.4.3 Synthesis of GFP dsRNA using Megascript kit:....147
4.3.4.4 Quantification of dsRNA....148
4.3.4.5 In vitro transfection of dsAChBP....148
4.2.5 Confocal imaging and electrophysiology....148
4.3.6 In vivo microinjection of dsRNA and siRNA in L. stagnalis 149
4.3.7 Behavioural assessment of dsRNA and siRNA mediated knockdown149
4.3.8 Statistics and data analysis....150

4.4 RESULTS 151

4.4.1 Method Development: transient transfection of siAChBP....151
4.4.1.1 Confocal microscopy shows siRNA transfection in whole CNS: .151
4.4.1.2 Desheathing of ganglia increases siRNA delivery into whole CNS 152
4.4.1.3 Identification of an appropriate incubation time and concentration of dsRNA/siRNA....153
4.4.1.4 Electrophysiological recording from whole CNS maintained in 20µl buffer 154
4.4.2 Assessment of RNAi using dsRNA in isolated CNS....155
4.4.3 Does stored AChBP in synaptic vesicles mask dsAChBP-mediated silencing?....157
4.4.4 dsRNA transfection in the intact animal....157
4.4.5 siRNA transfection in the intact animal....160

4.5 DISCUSSION....164

4.5.1 Targeting AChBP gene using dsRNA transfection....166
4.5.2 Off-target effects using dsGFP on AChBP protein expression....168
4.5.3 Modifying the concentration of the dsRNA/ or siRNA could improve transfection....171
4.5.4 Targeting AChBP using siRNA transient transfection....172
4.5.5 Does AChBP regulate feeding behaviour?....173

4.6 TECHNICAL CONSIDERATIONS:....175

5.0 GENERAL DISCUSSION....177

Declaration....182
Dated:
_____..182

APPENDICES 183
Western blot analysis of β-actin protein expression normalised to GAPDH 184
PEAKS 4.5 Protein sequence analysis from the cerebro-buccal ganglia 185
Peaks Protein Score 185
Validation of isoform differences in 14-3-3 protein 191
L. stagnalis cDNA alignment of 14-3-3 protein 193

Statistics: 195
Best-case values used for AChBP mRNA expression 195
Conservative Estimate for AChBP mRNA expression 195
Western Blot analysis of dsRNA-tranfected animals 48 hours post-injection 196
Western Blot analysis of dsRNA-tranfected animals 72 hours post-injection 196
Sucrose-evoked bites after 72 hours siRNA post injection 197
Sucrose-evoked bites after 96 hours siRNA post injection 198
Western Blot analysis of AChBP siRNA in vivo transfection after 72 and 96 hour post injection 199
References: 200

TABLE OF FIGURES

Figure 1: Schematic representation of a Ca^{2+} signalling at the synapse.....20

Figure 2: Representative light microscopy image of *L. stagnalis* whole CNS of a young animal with the left and right buccal ganglia enlarged in the photgraph. 29

Figure 3: Schematic representation of the neuropile and cell bodies of neurons in the buccal ganglia. 29

Figure 5: Schematic representation of the central pattern generator. 30

Figure 6 Neuronal circuit regulating the feeding rhythm in *Lymnaea stagnalis*.....31

Figure 7: Age-related changes in short-term feeding evoked by 0.01M sucrose stimuli. 54

Figure 8: Tissue extraction of young and aged *L. stagnalis* CNS show equal loading conditions 56

Figure 9: Protein extraction using different 2D-compatible extraction buffers show 2D Lysis buffer was suitable for solubilisation of *L. stagnalis* CNS proteins.....57

Figure 10: IPG strip pH 4-7 is optimal for visualising cerebral and buccal ganglia proteins.....59

Figure 11. 2D DIGE analysis young and aged cerebral-buccal ganglia 61

Figure 12A-Q: Average volume ratio of differentially expressed proteins 70

Figure 13: Schematic of total number of proteins identified using the combined proteomics workflow. 71

Figure 14 Western Blot analyses of AChBP expression in young and aged CBG show decreased AChBP protein expression. 73

Figure 15 α -tubulin protein expression in the young and aged cerebral and buccal ganglia. 74

Figure 16 Age-related changes in β-actin expression in the aged cerebral and buccal ganglia of *L. stagnalis*. 75

Figure 17 Schematic illustration of the function of AChBP at cholinergic synapses (Lopez, 2001). 97

Figure 19 AChBP labelling of left buccal ganglion with perforated commissure 109

Figure 20 Visualisation of Elf-α PCR product on a 2% agarose gel.....112

Figure 21 Dilution series for GAPDH 113

Figure 22 PCR amplification and melt curves for GAPDH in young and aged CBG 113

Figure 23 Dilution series for Elf-α to obtain the PCR reaction efficiency.....114

Figure 24 PCR amplification curves for Elf-α and NTC in young and aged CBG of *L. stagnalis* 115

Figure 25 PCR amplification melt curves for Elf-α and NTC in the young and aged CBG.....116

Figure 26 Dilution series of AChBP and Elf-α in young and aged CBG 117

Figure 27 Conservative estimate of ELF-α dilution series with correlation coefficient above 0.8.....119

Figure 28 PCR amplification curves for AChBP and NTC in young and aged CBG 120

Figure 29 PCR amplification melt curve for AChBP and NTC in young and aged CBG of *L. stagnalis* 121

Figure 30 AChBP mRNA expression in the CBG region of *L. stagnalis* 122

Figure 31 Conservative estimate of relative fold change in AChBP mRNA expression in the young and aged CBG of *L. stagnalis* 122

Figure 32 Western Blot analysis of Glial fibrilary acidic protein expression in the cerebral and buccal ganglia of *L. stagnalis*. 124

Figure 33 Schematic of the mechanism of gene silencing through siRNA (a) and miRNA (b) Cited from (Krulko *et al.*, 2009). Exogenous application (a) or endogenous synthesis (b) use the RISC to cleave complementary regions of the target mRNA and prevent the synthesis of the corresponding gene product. See text for details regarding the process of siRNA and miRNA-mediated silencing. 133

Figure 34 Selection of siRNA from AChBP mRNA coding sequence AF364899 140

Figure 35 Primer set designed for cloning of AChBP cDNA from *L. stagnalis* 142

Figure 36 Amplification of PCR products with T7 promoter.....144

Figure 37 In vitro transcription of AChBP dsRNA on 2% agarose gel. 146

Figure 38 In vitro transcription of GFP dsRNA using Ambion Megascript kit.....147

Figure 39 Time course study of fluorescent 21 mer scrambled siRNA in *Lymnaea* buccal CNS. 152

Figure 40 Desheathing the ganglia allow measurable uptake of fluorescently labelled siRNA after 17.5 hours 153

Figure 41 Intracellular recordings from a single *L. stagnalis* CGC cell in buccal ganglia.....155

Figure 42 AChBP dsRNA decreased AChBP levels in desheathed ganglia after 17.5 hour incubation.....156

Figure 43 Behavioural analysis of sucrose evoked feeding after 48 hour and 72 hour dsRNA-injection 158

Figure 44 dsRNA microinjection at Western blot analysis of CNS tissue at 48 and 72 hours. 159

Figure 45 Sucrose-evoked bites after 72 hour siRNA transfection 160
Figure 46 AChBP protein expression following siRNA transfection after 72 hours 161
Figure 47 Effects of siRNA injection on sucrose-evoked bites after 96 hour transfection 162
Figure 48 AChBP protein expression following siRNA transfection after 96 hour 163
Figure 49 Overview of experiments from the current study. 165
Figure 50 Schematic representation of the postulated off-target effect of GFP dsRNA on AChBP expression 171
Figure 51: AChBP Western Blot statistical analysis when normalised to GAPDH 183

INDEX OF TABLES

Table 1: In-gel rehydration and Isoelectric focusing. 48
Table 2: DIGE experimental design using fluorescently Cy Dyes 49
Table 3: Location and spot volume ratio of unidentified proteins 71
Table 4: Primer sequences used for real time PCR assays 107
Table 5: RT-PCR amplification cycle of AChBP and Elf-α 108
Table 6 Yield and purity readings from 3 RNA extraction methods. 111
Table 7: Relative AChBP mRNA expression in young and aged CBG 123
Table 8: Summary of published siRNA/dsRNA transfection in *L. stagnalis* 137
Table 9: Primers for AChBP and GFP with T7 promoter (underlined) 141

ACKNOWLEDGMENTS

First and foremost I would like to gratefully acknowledge my supervisor's Mark Yeoman, and Katrin Jennert-Burston for their patience, unwavering support and encouragement throughout my project. For Badr, Dominic, Kevin, Caroline and Tomader for being excellent listeners and drinking partners, and for Tim, my partner, who has to the best of his abilities calmed me down during times of panic and emotional unravelling - for this I am extremely appreciative and eternally grateful..

1D	one dimensional
2D	two dimensional
ACh	acetylcholine
AChBP	acetylcholine binding protein
APS	ammonium persulfate
CGC	cerebral giant cells
CID	collision induced dissociation
CNS	central nervous system
Cy 2	CyDye DIGE Fluor, Cy2 minimal dye
Cy 3	CyDye DIGE Fluor, Cy3 minimal dye
Cy 5	CyDye DIGE Fluor, Cy5 minimal dye
DIGE	difference in-gel electrophoresis
EST	expressed sequence tag
hTERT	human telomerase reverse transcriptase
IPG	immobiline pH gel
LC	liquid chromatography
LGIC	Ligand gated ion channel
LPS	*Lymnaea* physiological saline
mRNA	messenger RNA
MCI	Mild cognitive impairment
MS	mass spectrometry
MW	molecular weight
nAChR	nicotinic acetylcholine receptor
NCBI	National Centre for Biotechnology Information
NR	non-redundant
NHA	normal human astrocytes
PCR	polymerase chain reaction
PLG	phase lock gel
PAGE	polyacrylamide gel electrophoresis
PI	isoelectric point
PPM	parts per million
PTM	post translational modification
qRT-PCR	quantitative real-time PCR

ROS	Reactive oxygen species
RNA	Ribonucleic acid
RNAi	RNA interference
RPA	RNA protection assay
SDS	sodium dodecyl sulphate

Chapter 1: GENERAL INTRODUCTION AND BACKGROUND

The human population is ageing, particularly in the Western world where one in six people from the 60.2 million living in the UK are over the age of 65, a number which is set to increase (Office for National Statistics, 2007). Globally, this increase is ascribed to better healthcare, better lifestyle standards and dietary choices as well as the development of early diagnostic tests and medical equipment which detect potential age-related health problems before they become too serious.

In 2004, the disability-free life expectancy for men in the UK was shown to be an average of 62.3 years, and 64 years for women (Office for National Statistics, 2007). Behavioural changes that accompany old age include a decline in motor function, postural changes and postural reflexes that make the elderly prone to loss in motor coordination and balance making the older population more likely to use health care services and seek medical attention in the later stages of life (Office for National Statistics, 2007). In concordance, age-related problems such as cognitive decline, motor disturbances and incontinence represent a growing concern in healthcare. Therefore research into the basic biology of ageing is urgently required to reduce the overall burden on the UK economy through the cost of healthcare, hospital and nursing home care and drug treatments. In addition, the identification of common denominators of the ageing process will help to ensure a better quality of life for the aged and to provide them with a greater level of independence.

1.1 What is Ageing?

Ageing, the process of growing old can be defined as a progressive deterioration of all biological processes over time combined with an exponential increase in mortality with chronological age (Medawar, 1952). Strehler (1962) proposed five criteria to describe the ageing process as:

- Cumulative: the effects of age are a time-dependent process.
- Universal: evolutionarily conserved across species.
- Progressive: ageing is a series of gradual changes.
- Intrinsic: change occurs regardless of the environmental condition.
- Deleterious: biological function can be altered as a result of change during the ageing process.

Therefore two distinct sets of criteria can be used to define age-related changes in an organism. Firstly, the mortality rate of the organism increases with increased age. Secondly, characteristic phenotypic changes occur in organisms as a function of time (Arking, 2006). In humans, phenotypic changes relating to neuronal ageing manifest themselves in a marked decline in mental functions including a gradual loss of cognitive abilities which include memory loss (Akopian and Walsh, 2006) as well as disturbances in motor performance, e.g. a decline in hand motor function in elderly individuals (Scherder *et al.*, 2008).

1.2 Why we age – postulated mechanisms

Several theories of ageing have been suggested and refined over the years to explain the range of deficits observed during the ageing process. These theories could be broadly divided into two categories. Evolutionary theories predict the reproductive fecundity of an organism is a critical factor in determining the lifespan of an organism – whether it is through accumulated mutations which occur after an organism has reached sexual maturity; therefore mutations are not naturally selected against and eliminated from subsequent generations (accumulated mutation theory;(Medawar, 1952). Alternatively the selection pressure for genes may be such that genes which were selected to ensure reproductive success of the organism may be the same genes which are deleterious in later life (Antagonistic Pleiotropy Theory;(Williams, 1957). In contrast, in a more recent theory, ageing is thought to

occur due to a finite amount of energy reserves available to the organism (Kirkwood, 1977). Thus the distribution of metabolic resources required to ensure somatic cell functions such as DNA repair, protein turnover and antioxidant defences are compromised at the expense of reproductive success (Disposable Soma Theory;(Kirkwood, 1977).

Mechanistic theories on the other hand suggest that ageing could be the result of a gradual wear and tear and breakdown of biological processes over time and it is the organism's inability to adjust and maintain biological function that leads to the ageing process. Although no one theory has yet to explain the full range of deficits observed in neuronal ageing, mechanistic theories such as the free radical theory, the molecular inflammation theory, the calcium homeostasis theory, and the neurotrophic theory as well as genetic theories such as cellular senescence have gathered the most experimental support in their favour and will be discussed further.

1.2.1 Free radical theory of ageing

The application of the free radical theory can be directed to all organs in the body which are affected to varying degrees by the ageing process (Chung *et al.*, 2001). However the brain with the highest demand for oxygen is the most susceptible to oxidative damage according to the theory initially proposed by Denham Harman in 1956. His theory suggests free radicals (molecules with single unpaired electrons) that accompany the conversion of molecular oxygen into the highly charged superoxide anions ($O_2\cdot^-$) are capable of causing indiscriminate damage to cells in its vicinity (Harman, 1965). $O_2\cdot^-$ is an important progenitor to other free radical species such as the hydroxyl radical ($OH^\cdot$), peroxynitrite ($ONOO^-$) and nitric oxide radical ($NO^\cdot$) as well as non radical species such as hydrogen peroxide (H_2O_2) (Kourie, 1998). From an estimated 90% of cellular reactive species (RS) which are produced in the mitochondria (Balaban *et al.*, 2005), short lived RS like $O_2\cdot^-$ and $OH^\cdot$ are extremely unstable and produce the most damage; whereas relatively long-lived species such as H_2O_2, are freely diffusible or scavenged by enzymes such as glutathione perdoxidase and cytosolic catalase and converted into water and oxygen (Balaban *et al.*, 2005; Martin *et al.*, 2006). Thus, the mitochondria are both the leading source and prime target of damage by free radical species (Linnane *et al.*, 1992).

The premise of the free radical theory suggests disruption to complex 1 (NADH dehydrogenase) as well as complex III (ubiquinone–cytochrome c reductase) of the mitochondrial electron transport chain convert approximately 0.4% to 4% of oxygen into $O_2^{\cdot -}$ (Finkel and Holbrook, 2000; Kourie, 1998; Turrens, 1997). Disruption in mitochondrial function by RS lead to a disruption in the citric acid cycle and the inability of mitochondria within cells to generate ATP (Linnane *et al.*, 1992). The effects of ROS are further exacerbated by damage to mitochondrial DNA that can result in a cascade of events that gradually lead to a failure of ATP-dependent processes that compromise cellular function in aged animal (Linnane *et al.*, 1992).

Eukaryotes have developed intricate defence mechanisms against free radical damage through the endogenous release of antioxidant enzymes such as superoxide dismutase (SOD), glutathione peroxidase and catalase which all work together to maintain normal ROS levels (Martnez *et al.*, 2003). Genetic studies suggest that over expression of antioxidant genes, such as the SOD gene are able to increase longevity in three species: *D.melanogaster*, *mice* and *C. elegans*, presumably through the organisms elevated ability to breakdown ROS (Hu *et al.*, 2007; Martin *et al.*, 2006; Mitsui *et al.*, 2002). The ROS levels within the cell are therefore dependent on the homeostatic balance between ROS production and the antioxidant defence mechanisms which clear it. ROS leaking out of the mitochondria and into the surrounding cytosol causes indiscriminate damage to proteins, lipids, DNA, as well as altering second messenger pathways such as calcium signalling (Kourie, 1998; Korsloot *et al.*, 2004). Characteristic products formed during these reactions include: carbonyl groups in proteins, peroxidation products in lipids, and oxidised bases in DNA – all of which can be used to measure oxidative stress in the organism (Korsloot *et al.*, 2004).

1.2.2 Molecular inflammation theory of ageing

The premise of the molecular inflammation theory is based on two established findings: 1) altered REDOX homeostasis during ageing (free radical theory), and 2) disruption to the immune system with advanced age (Chung *et al.*, 2001). Both mechanisms lead to a systemic increase in inflammatory mediators, mainly through increased oxidative stress on the organism which can affect the lifespan of the organism (for review see (Chung *et al.*, 2009; Chung *et al.*, 2001). Age-related changes in glial cell function play an important role in the inflammatory process, including the secretion of pro-inflammatory mediators which are deleterious to neurons (see section 1.2.1.3). Pro-inflammatory mediators such as chemokines (IL-8 and RANTES), tumour necrosis factor (TNF –α and TNF-β), nuclear factor-κB (NF-κB) as well as inducible NOS synthase (iNOS) and cyclooxygenase (COX-2) are notable examples which are reported to increase in aged animals (Chung *et al.*, 2009).

Neuroinflammation, as an active process has the ability to change the substrate specificity of kinases and phosphatases that are central modulators that oversee protein turnover and degradation through phosphorylation and ubiquitination of proteins in aged animals (Lee *et al.*, 2000). Although the process of ubiquitination and phosphorylation are interrelated in many ways with respect to maintaining cellular homeostasis, there are critical differences. Whereas fluctuations in the protein phosphorylation state can enable cells to respond to the dynamic environment, this process is reversible and cells are able to return to their 'original' state (Nalepa *et al.*, 2006). Ubiquitination on the other hand marks proteins for degradation, a process which is non-reversible (Galvin and Ginsberg, 2005). Ubiquitination can result in the initiation of events such as programmed cell death or apoptosis (Mattson and Magnus, 2006). Conversely, an imbalance in ubiquitin-proteosome function can result in protein aggregates which are frequently associated with age-related neurodegenerative disorders such as Alzheimer's disease (ALZ) and Parkinson's Disease (PD) (Pickart, 2004; Kahle and Haass, 2004; Tuppo and Arias, 2005). Most notable are the accumulation of microtubule-associated proteins TAU protein and mutations in amyloid precursor protein-1 (APP1) in ALZ patients (Tuppo and Arias, 2005), and mutation in PARKIN gene in Parkinson's disease, where aggregation of substrate proteins ubiquitinated by the enzyme PARKIN lead to

degeneration of dopaminergic neurons in the substantia nigra (for review see(Kahle and Haass, 2004).

Thus chronic inflammation is postulated to be the causal link between normal ageing and the pathogenic changes which occur in age-related diseases such as arthritis, cancer, osteoporosis and dementia (Yu and Chung, 2006). Furthermore, the accompanying changes that are observed in the ubiquitin-proteosome system have led some researchers to suggest these alterations may preclude the disease process and are likely to be associated with advanced age (Mattson and Magnus, 2006; Farooqui and Akhlaq, 2009), i.e, the dysfunction of the ubiquitin-proteosomal pathway may be part of the natural ageing process.

1.2.3 The Calcium Theory of ageing

Besides energy production, mitochondria also serve to control intracellular calcium (Ca^{2+}). Age-related changes in mitochondrial function as observed through free radical damage (see free radical theory) can also impair Ca^{2+} signalling. Proposed in the early 1980's, the hypothesis states that alterations in Ca^{2+} homeostasis during ageing may affect Ca^{2+} signalling pathways and, consequently impair neurotransmission or lead to neuronal death (Landfield and Pitler, 1984).

Membrane associated oxidative stress causes the most damage to Ca^{2+} homeostasis through lipid peroxidation, impairing Na^{+}/ K^{+} ATPase, Ca^{2+}-ATPase, and glutamate transporter function reducing the ability of neurons to buffer the Ca^{2+} overload (Mattson, 2007; Mattson and Magnus, 2006) (also see Figure 1). Excessive levels of Ca^{2+} are excitotoxic to neurons which can lead to neurodegeneration in a process whereby glutamate receptors become over-activated (Mattson, 2007). Additionally, elevated calpains and caspases activated in response to Ca^{2+} influx degrade cytoskeletal proteins, and metabolic enzymes which are integral for synaptic transmission (Mattson, 2007).

Elevated Ca^{2+} levels result in an abnormal electrical activity in aged neurons – an event consistently observed as a delayed recovery of intracellular Ca^{2+} and increased amplitude/ duration of afterhyperpolarization (AHP) following stimulation (Terry and Buccafusco, 2003). Ca^{2+}-dependent potassium currents which mediate the AHP

and inhibit neuronal excitability are reported to be increased in aged animals (Terry and Buccafusco, 2003). Whereas the free radical theory offers an explanation of how the generation of ROS through the mitochondrial electron chain can cause indiscriminate damage, the calcium hypothesis suggests sustained levels in intracellular calcium concentration are likely to be a key component in the excitotoxic insult that lead to cell death in age-related neurodegenerative diseases (Thibault *et al.*, 2007; Duchen, 2000). The salient point here is that both theories are not mutually exclusive but a combination of the two factors are likely to coalesce and contribute to the ageing process (Toescu, 2005).

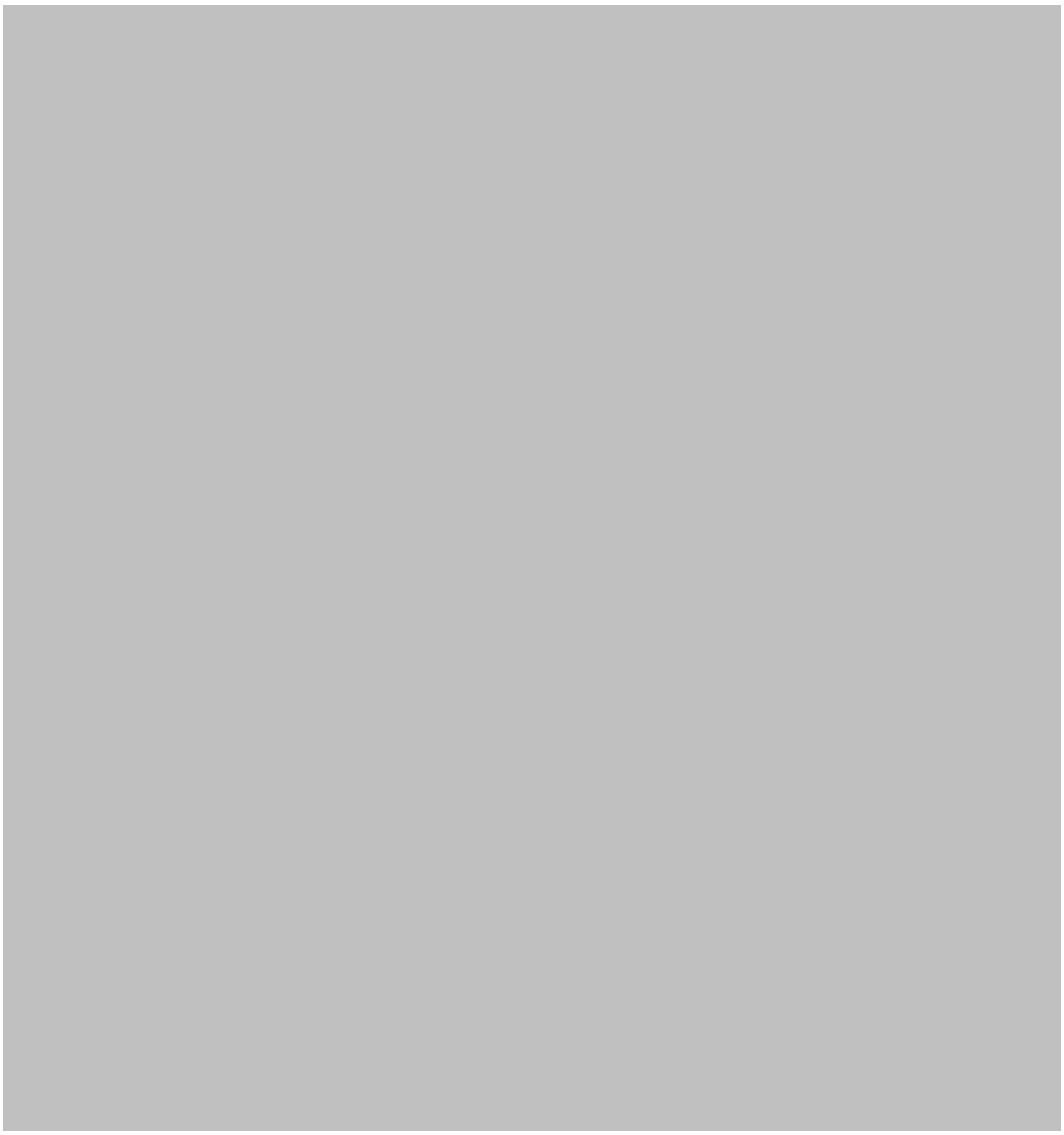

Figure 1: Schematic representation of a Ca^{2+} signalling at the synapse.

Mitochondrial dysfunction, disruption to voltage-dependent K+ channels, glutamate transport, as well as other Ca^{2+}-dependent processes that underlie normal biological processes are reported to be impaired with advanced age leading to elevated Ca^{2+} levels, and contribute to the Ca^{2+} theory of ageing (Mattson and Magnus, 2006).

1.2.4 Potential role of cellular senescence in brain ageing

With successive divisions mitotic cells undergo a phenotypic process termed 'cellular senescence' resulting in cellular growth arrest (Hayflick, 1965). The common features of the altered senescent phenotype in cells include impairment of one or more of the cell-cycle checkpoints including p16 upregulation (Alcorta *et al.*, 1996), and p53 induction (Shay *et al.*, 1991), and reduced telomerase activity (Evans *et al.*, 2003) which can be bypassed by immortalisation. The accumulation of senescent cells is thought to be an important component of the ageing process in mitotic cells (Hayflick, 1965). Senescence has been well studied in human fibroblasts (Coppe *et al.*, 2006), endothelial cells (Minamino *et al.*, 2002), vascular smooth muscle cells (Minamino *et al.*, 2003), and to a lesser extent in microglia and astrocytes (Flanary and Streit, 2004; Pertusa *et al.*, 2007; Evans *et al.*, 2003). Senescent cells are also able to up regulate growth factors, and pro-inflammatory cytokines that are secreted in order to mobilise the removal of degraded proteins. In doing so, increased expression of inflammatory mediators such as intracellular molecule-1 (ICAM-1) (Gorgoulis *et al.*, 2005) and growth factors such as vascular endothelial growth factors (VEGF) (Coppe *et al.*, 2006) can be detrimental to neighbouring cells.

One mechanism to activate senescence is the shortening of telomeres after repeated cell divisions (Harley *et al.*, 1990). Telomeres, which are highly conserved DNA repeat sequences at the physical ends of chromosomes are thought to prevent chromosomal degradation and DNA mutations from end to end fusion during cell division (Shay *et al.*, 1991). To delay the onset of senescence, cells could increase telomerase activity however acquisition of telomerase activity is also a critical step in maintaining malignant transformations (Hahn, 2001). Thus a reduction in the proliferative capacity through decreased telomerase activity in senescent cells are suggested to be a mechanism devised to reduce the risk of malignant transformations from occurring during the ageing process (Hahn, 2001; Stevens and Fields, 2002; Huschtscha and Reddel, 1999). Although the telomere lengths are species-specific, senescence is age-dependent and dependent on the number of cell divisions the cells have undergone, making measurement of telomere length a useful predictor of when a cell is likely to enter senescence (Hemann *et al.*, 2001; Flanary and Streit, 2004).

Neurons are largely regarded as post-mitotic, therefore senescence would be assumed to play a minor role in the nervous system, however glial cells are mitotic, and cultured normal human astrocytes (NHA) can enter senescence after 20 population doublings (pd) (Evans *et al.*, 2003). NHA cannot be immortalised by ectopic telomerase expression alone, and therefore telomere shortening does not play a major role in NHA senescence (Evans *et al.*, 2003). In the absence of telomere shortening, the induction of p53 that are considered to the predominant component in regulating senescence in NHA (Evans *et al.*, 2003). Moreover, if p53 is lost, NHA continue to proliferate, but enter growth arrest via a p16-dependent mechanism (Evans *et al.*, 2003).

Astrocytes are integral for neuronal survival and secrete antioxidant enzymes which are regarded as an integral defence mechanism to protect neurons against oxidative damage (Pertusa *et al.*, 2007). Astrocytes from aged animals show a significant reduction in mitochondrial activity following acute H_2O_2 treatment (Pertusa *et al.*, 2007). This is demonstrated in the MTT assay and show aged neurons have a reduced ability to protect themselves from oxidative damage (Pertusa *et al.*, 2007). The decreased mitochondrial activity in aged astrocytes are also accompanied by a marked increase in proteins such as GFAP, S100β protein levels that suggests aged astrocytes may be unable to maintain an appropriate level of antioxidant defence that are required to protect neurons against oxidative damage (Pertusa *et al.*, 2007).

Microglia on the other hand which are classically considered to be the first line of defence against neuronal injury up-regulate major histocompatability complex class II (MHC II) on their cell surface (Streit *et al.*, 1989), and in so doing provide a level of protection against neuronal injury (Streit, 2005). Although earlier evidence consistently reported microglial activation as offering neuroprotection during axonal injury, there is some debate as to whether these interpretations could be extended to microglial function in the aged CNS (Streit, 2005). Furthermore, there are several discrepancies that suggest subpopulations of microglia may be affected differently with age and in neurodegenerative diseases (Streit, 2005). For example, whilst some microglial cells show increased MHC-II activity in aged animals, other types of microglia increased in cell number or were enlarged (reactive gliosis); (Streit *et al.*, 1989; Streit, 2005). This view was also shared by recent papers demonstrating the secretome of activated microglia are able to up regulate pro-inflammatory mediators, antioxidants and neurotrophins that may be determental to the cell (Glanzer *et al.*,

2007). Secondly, morphological evidence suggest hypertrophy and cytoplasmic deterioration occur in the aged microglia (Streit *et al.*, 2004). What Streit *et al* (2004) propose this process may be the result of senescence. The observation that microglia lose their ability to proliferate over time through structural deterioration, suggest the altered secretome combined with the altered cell morphology may well impair the neuroprotective mechanism offered by microglia in aged animals (Flanary and Streit, 2004).

1.2.5 Neurotrophic Theory

None of the theories discussed so far have unambiguously accounted for why some cells remain healthy, whereas others are significantly impaired during the ageing process – a process termed 'selective neuronal vulnerability' (Cowen, 2002). Neurotrophins are a diverse family of proteins that influence multiple aspects of neuronal function ranging from cell survival to the regulation of synaptic activity to differentiation and neurogenesis (Gardiner *et al.*, 2009). The specificity of the effects of neurotrophins relies on their ability to activate receptor tyrosine kinase (Trk) family of proteins, or the p75 neurotrophin receptor ($p75_{NTR}$); (Friedman and Greene, 1999). The neurotrophic theory, (a modification of the antagonistic pleiotrophy theory) aims to address this, suggesting the function(s) of subsets of cells may be preserved at the expense of 'non-essential' physiological functions through its capacity to gain access to neurotrophic regulators to enable it to survive (Cowen, 2002).

Prominent examples in support of the neurotrophic theory include the identification that nerve growth factors (NGF) and brain derived neurotrophic factors (BDNF) work to up-regulate anti-oxidant proteins that protect neurons against oxidative damage (Gardiner *et al.*, 2009). Gardiner *et al*. (2009) suggest neurotrophins are able to up regulate anti-oxidants, but it is the loss of this positive feedback loop that deteriorates with age leading to increased oxidative damage. Experimental evidence suggests the selective loss of striatal dopaminergic neurons as experienced in Parkinson's Disease could be improved by application of application of BDNF or NGF that enhance components to increase protection against the oxidative damage caused by 1-methyl-4-phenylpyridinium (MPP++) (Kirschner *et al.*, 1996). The multiple component of signalling proteins that participate with the neurotrophin

signalling pathway have been well reviewed and the reader is referred to such publications for an in-depth coverage of the topic (Friedman and Greene, 1999; Gardiner *et al.*, 2009).

Examining molecular determinants that lead to increased lifespan in calorie-restricted provides convincing evidence that when an organism's survival is at stake, the organism is able to suppress physiological functions such as reproduction and growth in order to respond to environmental stresses to give it the cellular protection required to prolong its survival (Shimokawa *et al.*, 2008). Therefore neurotrophic factors that are involved in the regulation of the insulin signalling can directly regulate energy expenditure by regulating glucose metabolism (Shimokawa and Higami, 2001). As such, genes that participate in regulating insulin signalling could be considered the primary regulators of lifespan, even though the modifications occurring in mitochondrial REDOX signalling is an important component of this process (Shimokawa *et al.*, 2008).

The identification of at least 20 other longevity genes in the loss-of-function *C. elegans* dauer larva, suggest that the optimisation of the body's functional survival could be regulated by subsets of genes associated with nutrient sensing mechanisms, as well as those genes associated with mitochondrial regulation of REDOX signalling (Shimokawa *et al.*, 2008). Interestingly many of the nutrient sensing genes identified, such as the age-1 gene, a homologue of phosphoinositide 3-kinase (PI 3-kinase) can regulate longevity in *C. elegans* through its effects on insulin signalling (Hekimi *et al.*, 1998). Insulin signalling controls glucose metabolism through multiple metabolic regulators and the observation that insulin signalling can increase lifespan is encountered in other organisms such as *D.melanogaster* and rodents (Gems and Partridge, 2001; Avruch, 1998). Such observations suggest a degree of impairment in neurotrophic signalling could contribute to a reduction in lifespan of aged animals. Mutation of *daf*-2, a homologue of the insulin receptor could increase longevity *C. elegans* (Hekimi *et al.*, 1998), as well as mutation of the *Pdk*-1 gene, a homologue of phosphoinoside-dependent kinase, and mutation of *akt*-1, a homologue of Akt/ PKB by disrupting insulin signalling (Paradis and Ruvkun, 1998).

Conversely, despite evidence in favour of the involvement of neurotrophic signalling with the generation of ROS during normal ageing, only a small proportion of genes

have been identified to suggest genes which maintain ROS homeostasis could increase longevity. A longevity gene identified through the mutation of the *Clk*-1 gene (a homologue of the enzyme demethoxyubiquinone mono-oxygenase integral for ubiquinone biosynthesis), suggests that this component of the mitochondrial REDOX pathway could increase lifespan in *C. elegans* (Stenmark *et al.*, 2001). Additional studies have suggested that over expression of the anti-oxidant enzyme Thioredoxin (TXN), and SOD-2 could increase the level of resistance to oxidative stress in animals and contribute to lifespan extension in mice (Mitsui *et al.*, 2002; Hu *et al.*, 2007). However these findings alone do not support the notion that stress resistance alone is the primary factor in determining lifespan and that other factors may play a more central role to the regulation of lifespan.

Decreased insulin signalling in calorie-restricted animals is decreases leptin synthesis by fat cells (Shimokawa and Higami, 2001). Leptin interacts with its receptors in the CNS and peripheral tissues to regulate food intake and fat deposition and body weight (Shimokawa and Higami, 2001; Meier, 1995). Leptin also tonically inhibits the release of the food stimulating peptide, neuropeptide Y (NPY) levels within the hypothalamus (Shimokawa and Higami, 2001). Injection of NPY into the hypothalamus leads to increased food intake and increased body weight (Stanley *et al.*, 1986), suggesting the decreased NPY levels in the hypothalamus of calorie-restricted animals is a negative feedback signal designed to suppress expendable physiological functions to allow the animal to focus on metabolic and neuroendocrine adaptations to ensure its survival (Shimokawa and Higami, 2001). Although direct correlations into humans has not been conducted, calorie restriction has been shown to reduce morbidity and mortality in non-human primates (Hansen *et al.*, 1999). A comprehensive review of signals that regulate longevity genes is beyond the scope of this work however the reader is directed to (Shimokawa *et al.*, 2008; Shimokawa and Higami, 2001) for further information on longevity genes identified in calorie-restricted animals.

1.3.0 Age-related changes in invertebrate animal models

To examine age-related changes in animal models, rats and mice are frequently utilised to highlight age-related changes within the nervous system. For example, alterations to the cerebellum (Bickford, 1993), or disruption to dopaminergic system in the striatum are thought to contribute to age-related deficits in motor function (Joseph, 1992). However to examine such changes at the level of individual neurons which reside within a circuit requires the use of invertebrates which have the advantage of possessing relatively simple neuronal circuits compared to mammals, with reproducibly identifiable nerve cells.

In light of the relative complexity of the vertebrate nervous system, determining the precise cellular events which trigger or precede the observed age-related changes is at best difficult to interpret. The problems are confounded using vertebrates models that have a long lifespan and are difficult and costly to maintain for longitudinal studies. The relative complexity of the vertebrate neural network also makes it difficult to directly correlate behavioural changes with alterations at the neuronal level. Considerable progress has been made using surrogate invertebrate model species principally *Drosophila melanogaster* (Zou *et al.*, 2000), nematode, *Caenorhabditis elegans* (Li *et al.*, 2007), as well as *Aplysia californica* (Hansen *et al.*, 2004) and *Lymnaea stagnalis* (Yeoman and Faragher, 2001) in which age related changes can be measured from several different levels – ranging from behavioural changes to molecular biology approaches in a detail not currently achievable in the vertebrate systems.

Using forward genetics approaches, the ease of manipulation and short lifespan of the fruit fly, *Drosophila melanogaster*, can allow studies from multiple cohorts of animals with specific mutations to be studied (for review see (Melov, 2002)). Using this approach putative genes and proteins targets have been identified which are involved in the longevity of the organism (Zou *et al.*, 2000) . Although work on fruit flies benefits from their short lifespan, their nervous system is fairly inaccessible and determining potential neuron-specific changes becomes problematic.

Functional studies have relied on using *Caenorhabditis elegans* as test subjects for more detailed investigations on the role of specific genes in the ageing process (Pinkston-Gosse and Kenyon, 2007), or the contribution of proteins which are

differentially expressed in aged animals (Martin *et al.*, 2006). The ease of bacterial feeding used to induce RNAi in *C. elegans* for the purpose genome-wide screens for genes which confer longevity has made this organism instrumental in identification of novel molecular pathways which are altered during the ageing process (Lin *et al.*, 2001). Although the 302 neurons which make up the *C. elegans* nervous system makes it relatively simple compared to vertebrates (White *et al.*, 1986), neuron-specific changes are difficult to determine based on the localisation and ease of identification of individual neuronal subtype (Shaffer, 2006). Furthermore, electrophysiological recordings used to measure the activity of neurons within *C. elegans* has proven problematic due in part to the *C. elegans* proteinaceous hydrostatic skeleton which acts as a physical barrier to a recording electrode, but also the small size of the neuronal cell bodies (2-3μm in diameter) that makes such cells too difficult to record from (Shaffer, 2006). A high level of skill is therefore required not to damage constituent components of the organism during the loss of hydrostatic pressure from puncturing the tissue with an electrode (Shaffer, 2006).

To understand mechanisms of behaviour in detail, it becomes necessary not only to identify neurons responsible for the initiation of a particular behaviour but also their association within the framework of neuronal signals whose activity is responsible for generating that behaviour. Although *C. elegans* has proved instrumental in the understanding of behavioural genetics, its limitations in measuring neuronal activity has guided others to look towards other model organisms to assess age-related changes in a simple nervous system.

1.3.1 The L. stagnalis nervous system

The suitability of the gastropod *L. stagnalis* in assessing neuron-specific changes during ageing rely on its large, naturally pigmented neurons. The large neuronal cell bodies (20-150μm in diameter) (Joose, 1964), compared to 2-3μm in diameter in *C. elegans* (Shaffer, 2006), allow *L. stagnalis* neurons to be easily identified using a conventional light microscope. This has the distinct advantage over other systems of being able to reproducibly identify the same neurons between preparations and also in determining neuron-neuron interaction. The *L. stagnalis* CNS consists of a series of ganglia connected by connectives (between different ganglia) and commissures (between paired ganglia), whose activation can regulate specific subsets of

behaviours such as respiration and feeding (Benjamin and Rose, 1979). The development of a behavioural assay used as a marker of ageing in *L. stagnalis*, along with a detailed understanding of the signals regulating the behaviour *in vitro* (Elliott and Andrew, 1991), make this organism particularly suited for assessing neuron-specific behavioural changes. Molluscan models have been instrumental in the understanding the mechanisms underlying synaptic plasticity – the closest model we have at the cellular level of memory, as well as the understanding of hierarchical control of behaviours and sensorimotor organisation in the nervous system. For a review see (Yeoman and Faragher, 2001).

The *Lymnaea* nervous system contains approximately 20,000 nerve cells organised into a series of ganglia which form a central ring around the oesophagus of the animal (Elliott and Andrew, 1991) (see Figure 2). The neurons inside each ganglion are organised with the cell bodies facing outwards towards the periphery with their axons projecting inwards towards the centre – a region defined as the neuropile (see Figure 3). Electrophysiological recordings from cells in such a system is therefore made easier with minimal damage to other nerve cells during puncture with a recording electrode.

1.3.2 The feeding behaviour is regulated by the cerebral and buccal ganglia in L.stagnalis

Rhythmic behaviours in *L. stagnalis* such as feeding are well characterised and modelled onto neuronal networks called the central pattern generator (CPG). Of these, the rhythmic feeding behaviour shows age-related decline (Arundell M *et al.*, 2006; Patel *et al.*, 2006; Yeoman *et al.*, 2008). Neurons in the cerebral and buccal ganglia are responsible for the contraction of the buccal mass muscles which regulate the feeding movements (Elliott and Susswein, 2002; Elliott *et al.*, 1992).

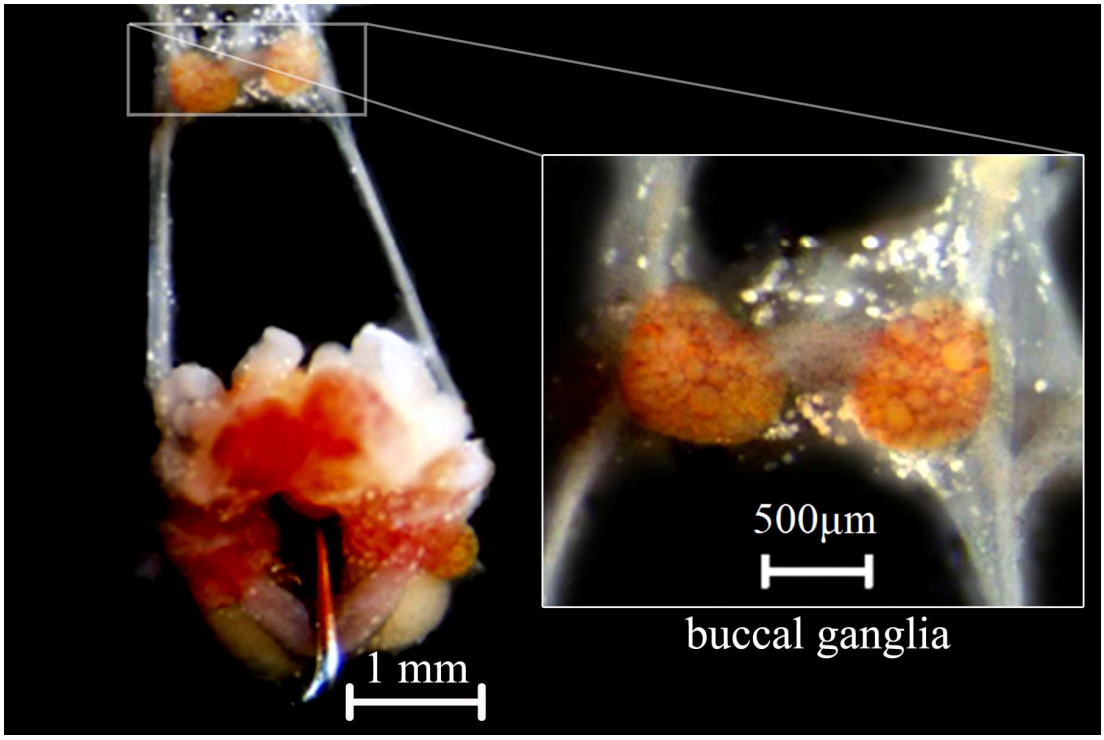

Figure 2: Representative light microscopy image of *L. stagnalis* whole CNS of a young animal with the left and right buccal ganglia enlarged in the photgraph.

The CNS is separated into series of ganglia grouped around a central ring. Light orange circles within the individual ganglia indicate neuronal cell bodies encased in a connective sheath. Individual neurons can be distinguished based on location, size and pigmentation of each neuron.

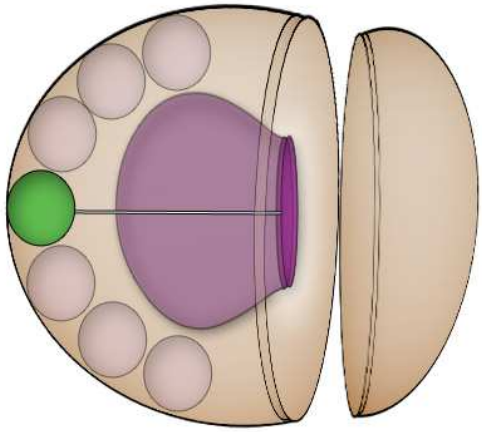

Figure 3: Schematic representation of the neuropile and cell bodies of neurons in the buccal ganglia.
Green circle represents a cell body located in the outside region of the ganglia; the neuropile axon-containing region (purple) is in the centre of the ganglia, adapted from (Joose, 1964).

1.3.3 In vitro modelling of the feeding behaviour in Lymnaea stagnalis

Three key pre-motor interneuron's, N1 (protraction), N2(rasp) and N3(swallow) fire sequentially to activate motor neurons which drive each phase of the feeding cycle (Figure 4 and Figure 5) (Rose and Benjamin, 1981; Elliott and Andrew, 1991). This patterned neural activity was recorded in isolated *in vitro* CNS preparations, a response referred to as 'fictive feeding reflex' (Elliott and Andrew, 1991; Rose and Benjamin, 1981). Results showed that a depolarising stimulus delivered to the slow oscillator (SO) interneuron initiated protraction (Rose and Benjamin, 1981; Kemenes and Elliott, 1994). Excitatory connections between N1 and N2 cells trigger the initiation of the rasp/ swallow phase to complete the feeding cycle (Kemenes and Elliott, 1994). Fine tuning of this circuitry through inhibitory feedback regulate the threshold required for N1 and SO cells to initiate an action potential and therefore the feeding cycle (Kemenes and Elliott, 1994) (see Figure 4 and Figure 5).

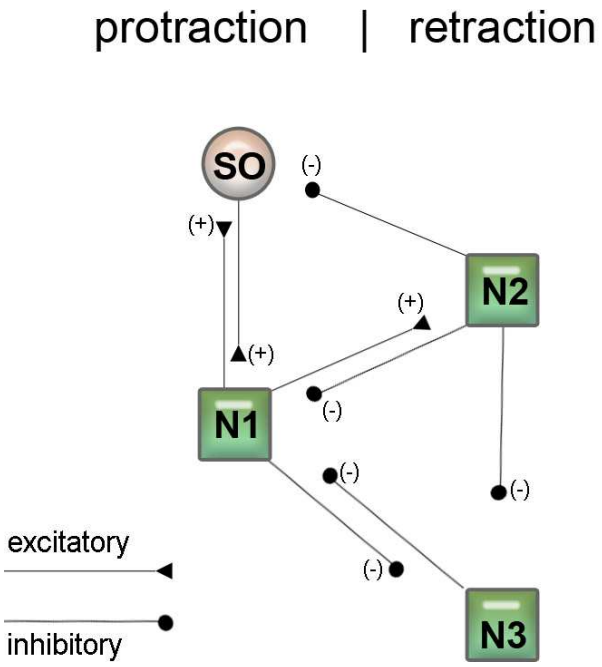

Figure 4: Schematic representation of the central pattern generator.
The central pattern generator consists of N1, N2 and N3 interneuron which are stimulated by the activation of the slow oscillator cell (SO). Reciprocal excitatory connections of N1 cells to SO and N2 cell initiate the rasp/ retraction phase of the feeding cycle, whereas the cycle is terminated through inhibitory feedback interneuron N2 which reduce the threshold of the N1 cells below the threshold required to initiate an action potential, adapted from (Kemenes and Elliott, 1994).

Figure 5 Neuronal circuit regulating the feeding rhythm in *Lymnaea stagnalis*. The feeding circuit comprising a three phase feeding reflex regulated by the same set of interneuron's and motor neurons. Active neurons and muscles are shown as filled circles. SO, N1M, N2v, N3t are interneuron's in the buccal ganglia. B1–B4, B6, B7 and B10 are motor neurons in the buccal ganglia which are activated and inactivated in a cyclic pattern to regulate different phases of the feeding rhythm (Elliott and Susswein, 2002).

1.3.4 Age-related changes to the feeding behaviour in L. stagnalis

Molluscs exhibit visible changes in behaviour with increased age. Chronological ageing is determined as the time at which a snail population exceeds 80 percent mortality rate (~10 months old). This end-point correlates with the Gompertz survival curve showing the decrease in feeding behaviour corresponds with populations which have reached approximately 80 percent mortality (Arundell *et al.*, 2006). As they age, the *L. stagnalis* feeding pattern (measured by the cyclic feeding movements of the radula) moves more slowly than the younger counterparts (Arundell *et al.*, 2006). Although a detailed mechanism through which this occurs is not precisely known, comparison of the feeding pattern between 3 month and 10 month naturally old molluscs showed a persistent decrease in the feeding reflex which has been successfully employed as a functional end point of ageing in snails

(Arundell *et al.*, 2006; Patel *et al.*, 2006; Yeoman *et al.*, 2008). This progressive impairment in the feeding cycle is followed by death.

1.3.5 Age-related electrophysiological changes in L. stagnalis

Many properties in molluscan neurons share a similar ancestral template to vertebrate neurons – their biophysical, biochemical and integrative properties are very similar. The main difference between molluscan nervous system and the vertebrate nervous system is at the level of functional organisation - the *L. stagnalis* nervous system is relatively simple. Based on the definition of ageing outlined in chapter 1, one might expect age-related changes in the nervous system to be uniform and result in the decline of cognitive, sensory and motor function with advancing age in all regions of the nervous system. However cells in the nervous system are differentially affected by age whereby some connections remain unaltered, while others are more vulnerable to the ageing process– a phenomenon coined 'selective neuronal vulnerability (Mattson and Magnus, 2006; Yeoman *et al.*, 2008).

Many studies have explored this aspect of ageing in a number of models, however the mechanism by which selective neuronal vulnerability occurs remain unknown. Structural examination reveals degradation of mitochondrial cristae and the formation of autophagosomes in aged of *Lymnaea* neurons (Frolkis *et al.*, 1984) These responses are accompanied by adaptive mechanisms in which aged neurons have increased nuclear membranes and hypertrophy of mitochondrial cristae (Frolkis *et al.*, 1984). Synapse-specific changes are also observed in the *L. stagnalis* nervous system (Yeoman *et al.*, 2008), however the mechanism by which molecular changes contribute to behavioural impairments in the animal is much less well understood.

Extensive work by Elliott and Andrew et al, 1991 demonstrated the rate of feeding (about 1s per phase) does not elicit a change in N2 neuronal cell firing regardless of the rate of the fictive feeding reflexes, however over 90% of the changes in the feeding cycle could be attributed to changes in the intrinsic firing of N3 (swallow phase) interneuron when stimulated with sucrose (Elliott and Susswein, 2002). This suggests that it is the N3 interneuron that can regulate the duration of the feeding cycle (Arundell *et al.*, 2006).

An examination of the physical properties of aged molluscan neurons revealed that many electrophysiological parameters in fact do not change with age, including the input resistance, and the amplitude of the action potentials, (Frolkis *et al.*, 1984; Yeoman *et al.*, 1993; Arundell *et al.*, 2006; Patel *et al.*, 2006). Therefore the threshold required to initiate an action potential remains unaltered in aged *Lymnaea* neurons (Arundell *et al.*, 2006). However, a significant increase in the amplitude and duration of the afterhyperpolarisation (AHP) phase of the action potential was reported in aged neurons (Arundell *et al.*, 2006). These changes are consistent with those reported in higher organisms (Landfield and Pitler, 1984).

At the level of the synapse, disruption to neuromodulators and endogenous signalling molecules which regulate cell to cell communication show selective vulnerability in the aged nervous system (Yeoman *et al.*, 2008). Pharmacological dissection of the feeding cycle through application of 10^{-5} M 5-hydroxytryptamine (5-HT) can actively initiate the feeding cycle through increased firing of N3 interneuron in the buccal ganglia (Kyriakedes and McCrohan, 1989). The ability of *L. stagnalis* to initiate the feeding behaviour was significantly reduced in the presence of *p*-chlorophenylalanine, the competitive inhibitor of the 5-HT synthesis enzyme tryptophan hydroxylase, suggesting that a reduction in 5-HT can result in the termination of the feeding rhythm (Patel *et al.*, 2005).

Recent work demonstrated a decrease in both the spontaneous firing rate and excitability of the serotonergic cerebral giant cells (CGCs) and their ability to communicate with the buccal ganglia in aged animals (Patel *et al.*, 2006). 5-HT-evoked depolarisation of B4 motor neurons was significantly attenuated in aged animals (Yeoman *et al.*, 2008). As B4 motor neurons are actively involved in the swallow phase of the feeding cycle, these results likely suggest that alterations in CGC signalling are responsible for the increase in the duration of the swallow phase seen in aged animals and the decrease in feeding frequency (Yeoman *et al.*, 2008).

By contrast, perfusion of 10^{-4} M dopamine initiated and increased the firing frequency of the feeding cycle (in N1, N2 and N3 cells) (Kyriakedes and McCrohan, 1989). However, the contribution of dopaminergic signalling the feeding cycle of aged animal has not yet been established. Application of 10^{-4} M acetylcholine (ACh) can also initiate firing in CGCs, and terminate the rhythmic activity in B3 and B4 motor neurons (Kyriakedes and McCrohan, 1989). Buccal motor neurons are

heavily innervated by cholinergic inputs that are regulated by ACh released in the protraction-phase of the feeding cycle in *L. stagnalis* (Elliott and Susswein, 2002). Neuronal membranes in aged molluscan neurons show increased sensitivity to ACh and 5-HT, suggesting a mechanism whereby at least in the *L. stagnalis* nervous system there is a selective and gradual impairment of neuronal function based on shift in responses of the CGCs to ACh and 5-HT signalling in aged animals (Frolkis *et al.*, 1984). Furthermore, these neuronal changes are precise whereby subsets of neurons remain unimpaired whereas others show age-related impairments with increased time (Yeoman *et al.*, 2008; Klaassen *et al.*, 1998).

Summary of the thesis

To identify proteins involved in regulating the feeding behaviour, **Chapter 2** describes the identification of brain-derived proteins that were altered between 3 month (young) and 10 month (old) gastropod *L. stagnalis*. A proteomics-based approach was applied for this purpose, using 2D DIGE to examine differences in protein expression as a function of age. Protein spots of interest were excised and the peptide digest mixture was run on an LTQ Orbitrap LC MS/MS. The fragment mass data was analysed in *de novo* sequencing PEAKS 4.5 software for homologous peptide sequences in the non-redundant database. Three of the proteins identified in the screen were validated using Western Blot analysis which included the proteins α-tubulin, β-actin, and the glial-specific protein, acetylcholine binding protein (AChBP).

In **Chapter 3**, using real-time reverse transcription polymerase chain reaction (RT-qPCR), changes in AChBP mRNA expression level between the young and aged animals were determined. To address the possibility that a reduction in AChBP levels was unrelated to age-related changes occurring in glial cells, glial acidic fibrillary protein (GFAP) antibodies were used to assess potential changes to astrocytes as a function of age, and validated using Western blot technique.

In **Chapter 4**, RNAi-mediated silencing of AChBP gene was performed to examine its potential role in regulating the feeding behaviour in *L. stagnalis*. In order to assess AChBP knockdown at the protein level, an *in vitro* whole CNS model was first used to optimise the transfection methods necessary to silence AChBP gene. To assess whether AChBP functionally contributed to the feeding behaviour, animals were microinjected with AChBP dsRNA and with AChBP siRNA duplexes at two time points. A behavioural assay was used to measure the number of sucrose-evoked bites in post-transfected and control animals prior to dissection of brain tissue and knockdown examined using Western blot analysis.

Chapter 5 offers recommendations and general discussion for future work.

Chapter 2: AGE-RELATED PROTEOMIC CHANGES IN THE CEREBRAL AND BUCCAL GANGLIA

2.1. BACKGROUND:

Proteomics involves the combined application of a number of separation technologies to identify proteins of interest. Based on the relative simplicity of the organism, invertebrate model systems such as *Lymnaea stagnalis* provide an ideal basis from which to examine how key proteins and signalling pathways may contribute to the ageing process. Monitoring gene expression changes using genomic approaches in model organisms such as *C. elegans* have extended the applicability of genome wide screens to examining pathways involved in the ageing process (Lin *et al.*, 2001). Such studies are however restricted to organisms which have their genome sequenced. For unsequenced organisms, like *L. stagnalis*, proteomic technologies are better suited to examine translational differences where protein sequences can be matched to proteins annotated from sequenced genomes.

The present study focussed on dissecting differences in protein expression in the feeding pathway by comparing young and old CNS samples. Specifically, the study concentrated on an examination of the cerebral and buccal ganglia which have previously been shown to be intimately involved in the regulation of feeding in *L. stagnalis* (see section 1.3.0 - 1.3.6). As the *L. stagnalis* genome is presently not sequenced, it is hoped that the present series of reports will contribute to the methodological developments in proteomics, as well as deepen our understanding of age-related proteomic differences in the *L. stagnalis* feeding system.

2.1.1 Expression profiling in aged animals:

Global analysis by DNA microarray of 6,347 genes profiled in the mouse neocortex and cerebellum suggested at least 1% (63) of the genes profiled were altered during the ageing process (Lee *et al.*, 2000). Together these regions in vertebrate models have received the greatest attention due to their inherent roles in regulating higher cognitive functions such as the modulation of sensory perception and the generation of motor commands, which are impaired with advanced age (see chapter 1). 20% of the genes whose expression is altered in the neocortex and 27% in the cerebellum are involved in regulating inflammatory processes, whereas 24% (16/63) in the neocortex and 13% (8/63) of the genes in the cerebellum could be assigned to genes involved in the stress response (Lee *et al.*, 2000). The two main conclusions that can be drawn from examining gene expression changes in the aged mouse brain are; 1) age-specific alterations are selective, and 2) aged animals are prone to an overproduction of ROS as well as the activation of inflammatory mediators (Bodles and Barger, 2004), (also see section 1.2.1.1). Upregulation of inflammatory mediators such as complement C4 and lysozyme C are observed in the aged neocortex and cerebellum (Lee *et al.*, 2000; Prolla, 2002). However, other inflammatory mediators such as the interferon-inducible (lfi-6-16 homologue) gene were selectively upregulated in the cerebellum (Lee *et al.*, 2000). The marked increase in stress-response mediated genes such as glial fibrillary acidic protein (GFAP), cathepsins as well as immediate early gene cFOS expression in the neocortex and cerebellum of aged animals are consistently observed and fit the framework of the free radical theory and inflammation theory (Lee *et al.*, 2000; Prolla, 2002) (also see section 1.2.1.1). Whereas other ontological groups identified suggest a concurrent decrease of growth/ trophic factors by 2 fold in the case of the zinc finger protein (Rfp) and 2.2 fold decrease for α-synuclein in the aged neocortex and cerebellum respectively (Lee *et al.*, 2000). Nerve growth factor (NGF) (Wehrman *et al.*, 2007), and brain-derived growth factor (BDNF) and its receptor tyrosine kinase B (TrkB) receptors are reported to decrease in the aged rodent hippocampus, suggesting a decline in neurotrophic support could be a key component in regulating synaptic plasticity (Gardiner *et al.*, 2009). This view is supported by Cerutti *et al.* (2000), who show administration of BDNF into the rat

brain could improve performances in spatial memory water maze task, suggesting a role of BDNF in regulating discrete types of memory function.

In contrast to the available microarray data, very few proteomic studies have explicitly examined age-related changes in the naturally aged brain directly (Sato *et al.*, 2005; Yang *et al.*, 2008; Carrette *et al.*, 2006; Poon *et al.*, 2006). Examination of the naturally aged mouse brain suggest at least 39 proteins are altered that participate in a wide variety of processes akin to those described earlier in the microarray data, in which metabolic proteins, cytoskeletal proteins, stress response proteins and apoptotic proteins are altered in the aged mice brain (Yang *et al.*, 2008). Similar findings were observed in the hippocampal synaptosomes of young and aged rats where at least 24 proteins belonging to a similar set of ontological groups are observed (Sato *et al.*, 2005). Poon *et al*. (2006) focussed attention on examining protein levels between young and aged mouse brains, and specifically correlated protein carbonyl values as an index of oxidative. These studies suggest β-actin and neurofilament 66 carbonyl values are significantly increased in the aged mouse brain and point to a process whereby cytoskeletal proteins show increased susceptibility to oxidative damage (Poon *et al.*, 2006).

Although the ontological groups between the microarray studies and proteomic studies were similar, there were a few discrepancies between the datasets in terms of the number of targets that were identified. Whereas a larger number of genes were identified as altered in the aged mouse brain (Lee *et al.*, 2000), only 39 proteomic changes were identified by Yang *et al*. (2008). These discrepancies are likely to be related to the limitations that arise during proteomic profiling in which high molecular weight or low abundance proteins are not fully represented on the PAGE gel, leaving open the possibility that the full repertoire of proteins that were altered in the aged brain could not be examined using these techniques alone (Yang *et al.*, 2008).

Bell *et al.* (2009) examined what has previously described as the 'interactome' (Sanchez *et al.*, 1999), in an attempt to crosslink the multiple protein interactions that conferred longevity in *C. elegans*, *D. melanogaster*, or *S. cerevisiae* either through mutation, knockdown or deletion of genes to its functional homologues in humans

(Bell *et al.*, 2009). The interactome could be defined as the assessment of all the molecular interactions that relate protein-protein and protein-DNA interactions within the cell (Sanchez *et al.*, 1999). Bell *et al.* (2009), suggest there could be as many as 175 homologous protein regulators that could be regarded as central 'hubs' that are key to either maintaining cellular function in aged humans, or are protein nodes that integrate with a number of other cellular components that coalesce to increase lifespan (Bell *et al.*, 2009). The proteomic studies and genome-wide screen in mice brain are consistent with the notion of the existence of 'hub' proteins that maintain mitochondrial homeostasis, and inflammatory mediated genes, as well as cytoskeletal dynamics as well as proteins involved in insulin signalling which are key mechanisms that are disrupted during the normal ageing process (Bell *et al.*, 2009; Lee *et al.*, 2000; Yang *et al.*, 2008). Other findings suggest at least 40% of the identified proteins that were disrupted in normal aged mouse brain were involved in protein metabolism (Yang *et al.*, 2008). Of interest has been the finding that calorie restriction can decrease the expression of inflammatory genes and stress-mediated genes while at the same time increase the expression of neurotrophic factors that can activate the antioxidant defences required to counteract oxidative damage in the aged animals (Lee *et al.*, 2000; Prolla, 2002) (also section 1.2.1).

2.1.2 Protein separation technologies

By analogy to the genome, the 'proteome' refers to an entire complement of proteins within a subset of tissues. Unlike gene expression analysis however which can be performed at a high throughput level using microarrays, parallel quantitative technologies are lacking for analysis of proteins due to protein turn over rates, and post translational modifications (PTMs) such as phosphorylation, glycosylation and methylation (Karp and Lilley, 2005).

Therefore a challenging task when examining age-related proteomic changes is to be able to isolate and differentiate individual proteins from within a complex protein mixture and examine the function of these proteins in relation to the tissue of interest. The *Lymnaea* nervous system is particularly suited to this type of study with its relatively simple but well defined neuronal circuitries (see chapter 1). A high level of information can therefore be obtained about functional circuits that control

behaviours such as feeding which have previously been reported to be altered in aged animals (Arundell *et al.*, 2006; Yeoman *et al.*, 2008) (also section 1.3.0).

Classical proteomics relies on three steps: 2D PAGE for protein separation, MS/MS analysis for confirmation of molecular weight of proteins, and bioinformatics for identification of proteins. To this end, protein separation techniques such as sodium dodecylsulphate-polyacrylamide gel (SDS-PAGE) that isolates proteins based on their molecular weight (MW) and isoelectric point (PI) is still the preferred method for quantitative proteomic analysis (Karp and Lilley, 2005). Intrinsic protein properties such as the molecular weight, PI, and hydrophobicity can be utilised to separate and simplify proteins of interest to resolve and array authentic proteins from a complex protein mixture (Karp and Lilley, 2005).

An example of use the use of 2D-PAGE analysis of proteins from fibroblasts of patients with progeria revealed a reduction in lamin levels compared to healthy controls (Robinson *et al.*, 2003). A reduction in lamin levels is consistent with Hutchinson-Gilford Progeria Syndrome patients, where a gene mutation in Lamin A is frequently associated with the premature aged pathology (Robinson *et al.*, 2003). Moreover 2D PAGE also revealed a shift ca. 0.3 units towards the basic PI in progeria samples which was consistent with a loss of a C-terminal phosphorylation site (Robinson *et al.*, 2003). This level of integration is difficult to obtain using comparable techniques currently used in quantitative proteomics (e.g. 2D-LC, iTRAQ) (Pasquali *et al.*, 1997).

The reliability and reproducibility of proteomic analysis has also been characterised by Chang *et al*. 2003. They concluded that a sample size of 10 animals would be sufficient to detect 100 percent difference in mitochondrial proteins from aged mouse skeletal muscle using 2D PAGE (Chang *et al.*, 2003). Although 2D DIGE is the most commonly used technique for expressional profiling, the method is labour-intensive and suffers several limitations such as the lack of resolution of highly acidic or basic proteins that are not resolved on the gel, as well as high molecular weight membrane associated proteins that are not represented on a PAGE gel (for review see Karp and Lilley, 2005). Therefore several attempts have been made to try and automate and use alternative high throughput methods for quantitative proteomic

profiling. Comparative quantitative methods include chromatographic separation tools such as reverse phase chromatography used to separate proteins based on the hydrophobicity of proteins whereas two-dimensional liquid chromatography (2D LC) can resolve proteins based on their PI and hydrophobicity (Pasquali *et al.*, 1997). However, these methods also suffer significant drawbacks. Although 2D-LC is relatively high throughput for quantitative proteomics, the detection of proteins significantly decreases with increased sample complexity. Therefore sample sets need to be simplified prior to 2D-LC. A review of the current separation methodologies can be obtained elsewhere (Pasquali *et al.*, 1997). This project utilised 2D PAGE separation to identify proteins of interest. Details of the technique are discussed below.

2.1.3 Proteomic profiling using 2 dimensional electrophoresis

For global protein expression profiling from a complex protein sample, the 2D-PAGE approach remains the most reliable technique currently on the market, followed by identification of the protein of interest by mass spectrometry. 2D PAGE has been used extensively for cells grown in culture, or in aged tissue where region specific proteomic differences can be assessed in young and naturally aged animals (Chang *et al.*, 2003; Vierstraete *et al.*, 2004).

Separation of charged proteins is achieved by passing an electric current through the gel until individual proteins within the complex mixture have reached their electrically neutral state (zwitter ion or PI) on an immobilised pH-gradient strip (Pasquali *et al.*, 1997). The gel strips are subsequently placed on top of a SDS-polyacrylamide gel and further separated so proteins migrate into the gel according to their molecular weight (Pasquali *et al.*, 1997). In doing so, the dynamic range of proteins within the proteome can be specifically visualised by altering the pH of the gel strip and therefore the PI of proteins within the sample, or by the molecular weight of the protein by altering the percentage of acrylamide in the gel (Pasquali *et al.*, 1997). The proteins within the gel can be visualised using silver stain, Coomassie or fluorescent stains – the choice of stain will vary depending on the cost or the dynamic range of the stain detection e.g. silver staining being more sensitive than Coomassie blue.

Although the 2D PAGE approach can resolve complex protein samples, a variation of this method 2D difference in-gel electrophoresis (2D DIGE), enables relative quantification between control and treatment groups by fluorescently tagging the proteins prior to the isoelectric focussing step (Karp and Lilley, 2005). Using 2D DIGE, the control and treatment samples are labelled with separate fluorescent tags and co-separated on a single gel (Karp and Lilley, 2005). An additional dye is used to label proteins to standardise against intra-gel variability (Karp and Lilley, 2005). The fluorescent dyes are charge- and weight matched to allow samples to co-migrate to the same point during electrophoresis. Proteins are labelled through nucleophilic substitution of the dye with the epsilon amino group on the lysine residue to form an amide during the labelling reaction (Pasquali *et al.*, 1997; Karp and Lilley, 2005). Keeping the ratio of dye to protein low proteins are labelled with a single dye molecule (Pasquali *et al.*, 1997; Karp and Lilley, 2005). Following 2D DIGE, proteins of interest are excised from the gel, digested by sequence-specific proteases such as trypsin and the peptides are eluted onto a mass spectrometer (Pasquali *et al.*, 1997; Karp and Lilley, 2005).

Using mass spectrometry, fragment masses or sequences of the peptides can be used to search against an *in silico* digestion of amino acid sequences from repository genomic or EST databases for positive identification of proteins of interest (Pasquali *et al.*, 1997). An analogous approach can also be applied to search for proteins of unsequenced organisms based on sequence homology matches to other genomes from sequenced organism using *de novo* sequencing PEAKS software.

2.2 OBJECTIVE:

As an initial series of experiments, the proteomic profile of the cerebral and buccal (CBG) was performed to determine the key proteins that may be altered and contribute to a reduction in feeding behaviour in aged animals. A combination of 2D DIGE, MS/MS sequencing and *de novo* sequencing was used to identify CNS proteins altered in the cerebral and buccal ganglia of 3 month (young) animals compared to 10 months (aged) animals that showed a reduction in sucrose-evoked bites.

2.3 MATERIALS AND METHODS:

2.3.1 Animals

Lymnaea stagnalis were bred under standard laboratory conditions at our in-house facility and maintained in groups of up to 600 in large circulating tanks at a stock density of approximately one snail per litre with continuous copper free water under temperature controlled environment (18-20 °C), under a 12 hour light/ dark cycle and fed lettuce or fish flakes (Tetra UK Ltd) *ad libitum* as described previously (Arundell *et al.*, 2006).

2.3.2 Chemicals and reagents

All chemicals used in the following experiments and assays were of reagent grade and unless stated otherwise purchased from Fisher Scientific. Buffer names are highlighted in **bold** text.

- ***L. stagnalis* physiological saline (Alcorta et al.):** 53 mM NaCl, 1.7 mM KCl, 4.1 mM $CaCl_2$, 1.5 mM $MgCl_2$, 5 mM HEPES, and adjusted to pH to 7.9 (NaOH) at 20 °C.
- **Tris Buffer:** 1 mM Sodium orthovanadate, 50 mM Tris, 1 protease inhibitor tablet (SIGMA*FAST*™ Protease Inhibitor Tablets, Sigma), 10 mM DTT
- **2D Lysis Buffer:** 7M Urea, 2M ThioUrea, 4%(w/v) CHAPS, 10mM DTT
- **1D Loading Buffer:** 62.5 mM Tris-HCl, pH 6.8, 25% glycerol, 2% SDS, 0.01% Bromophenol Blue. 500µl aliquots are stored at -20 °C and thawed before use.
- **12% Gel Cast (7cm): (Resolving Buffer)** For 2 gel casts 1mm thick, add protogel (Bis/acrylamide 30%) 3.3 ml, 1.5M Tris pH 8.8, 2.5 ml, 10% SDS 100µl, 10% APS 100µl, TEMED (Tetramethyl-Ethylenediamine) 14 µl, and made to 10 mls with distilled water.
- **12% Gel Cast (7cm): (Stacking Buffer):** For 2 gel casts 1mm thick, add protogel (Bis/acrylamide 30%) 1.7 ml, 1.5M Tris pH 8.8, 2.5 ml, 10% SDS 100µl, 10% APS 100µl, TEMED 14 µl and made to 10 mls with distilled water.
- **24cm 12.5% Gel Cast:** For 14 gel casts 1mm thick, add protogel (Bis/acrylamide 30%), 1.5M Tris pH 8.8, 10% SDS, 10% APS, TEMED 1.24 ml, Water 281 ml.

- **Displacement Solution:** 1.5 M Tris HCl pH 8.8, Glycerol 50 ml, Bromophenol Blue trace, DDI water 25 ml
- **Water-saturated butanol:** N or T butanol 50 ml, DDI water 50 ml
- **Rehydration Buffer:** 2% (w/v) CHAPS, 6M Urea, 2M ThioUrea. Stored in aliquots in -20°C. 0.5% IPG Buffer (GE Healthcare) added to rehydration buffer prior to before use.
- **Equilibration Buffer:** 50 mM Tris HCl pH 8.8, 6M Urea, Glycerol 30%(w/v), 2% SDS, was made and stored in 10 ml aliquots in -20°C. 40 mM DTT /10 ml were added to reduce proteins prior to use. 250mg Iodoacetamide /10mls was added to the buffer for protein alkylation prior to use.
- **Low Melting Point Agarose:** 0.5% (w/v) Agarose, 1 X SDS Running Buffer 25 ml, Bromophenol Blue trace. Agarose was gently heated with SDS running buffer in a microwave until agarose was completely in solution. Care was taken to prevent buffer from boiling. Aliquots were stored at room temperature (20 ºC).
- **10 X SDS Running Buffer:** Tris 30.25g, Glycine 144g, 0.2% (w/v) SDS 20g made up in 1L distilled water and stored at room temperature. 1 X Running buffer was made by doing a 1 in 10 dilution in distilled water.
- **Protein markers:** Precision plus proteinTM standards (Bio-Rad)
- **Coomassie Blue solution:** 0.1% Coomassie Brilliant Blue R250, 10% Acetic acid, 40%
- **Transfer Buffer**: 1.5g Tris base, 7.2g glycine, 100ml methanol made up to 500 ml with DI water
- Anti-rabbit α tubulin antibody (Dacocytomation Ltd)
- Anti-rabbit β actin antibody (Dacocytomation Ltd)
- Anti-rabbit GAPDH (Santa Cruz Biotech)
- Anti-rabbit conjugated to HRP (Dakocyomation Ltd)
- Anti-Lymnaea AChBP (kind gift from Pim Van Lierop, University of Vrije, Netherlands

2.3.3 Instruments:

Centrifuge	EBA 12 R (Hettich zentrifugen)
Electrophoresis equipment	Mini protean II system (Bio-Rad),
	Ettan DALT*twelve* system (GE Healthcare)
	Ettan DALT gel caster
Balances	FX-40 (Salter-AND)
Heat Block	QBT1 (Grant Instruments (Cambridge)
Isoelectric focussing	Ettan IPGphor system (GE Healthcare)
Orbital shaker	(Denley)
pH meter	(HANNA instruments)
Image scanner	Typhoon Scanner (GE Healthcare)
ChemiImager	(Alpha Innotech)
Stirrer	Heat stirrer SB162 (Stuart)
Waterbath	Grant Instruments (Cambridge) Ltd

2.3.4 Behavioural analysis of feeding in L. stagnalis:

A detailed method for this procedure has been reported previously (Arundell *et al.*, 2006). The feeding behaviour of chronologically young (3 month old) and old (10 month snails) were assessed upon presentation with a final concentration of 0.01M sucrose in dish. Snails were starved overnight prior to the experiment and placed in individual clear 15cm diameter Petri dishes containing 90 ml of copper-free water. 5ml water only (control) was carefully presented around the lips of the snail once the snails had emerged from the shell and the responses measured for 2 minutes prior to application of the sucrose stimuli. The measurements included the latency and duration of first bite, inter-bite interval, as well as the total number of sucrose-evoked bites were measured using an in-house software program over a 2 minute interval (Arundell *et al.*, 2006). Non responders were eliminated from the study, as were animals which responded to water alone with more than 10 bites per minute. Using this parameter, young snails responded to sucrose with a 20-30 bites per minute while the responses in the old was decreased to 10-15 bites per minute as has been described previously (Arundell *et al.*, 2006).

2.3.5 Tissue dissection

CNS was removed in LPS buffer as described previously (Benjamin and Rose, 1979). 80 young and 80 aged animals were behaviourally characterised and the CBG region extracted. 20 CNS extracts were removed and placed in pre-labelled tubes (Y1-4, O1-4) by Dr. Mark Yeoman. The ganglia were quickly removed (2-3 minute dissection time) and the excess LPS buffer was blotted on lint-free paper prior to storage of tissue in pre-chilled 1.5 ml microtubes which were placed on dry ice and then stored at -80°C until required.

2.3.6 Tissue Extraction in 2D Lysis buffer:

Microtubes containing 20 CNS tissue/ tube were removed from -80°C freezer and homogenised and solubilised 200µl in 2D Lysis buffer. Tissue extracts were dissociated with 20 full rotations using a plastic mortar fitting (VWR International) in a 1.5 ml microtube. Homogenisation was completed within 1 minute. Samples were centrifuged at 11,000 x g for 30 minutes in a pre-chilled centrifuge (EZ-2 Personal Evaporator, GeneVac) at 4 °C. A 100µl volume from each supernatant was removed to undergo an additional acetone precipitation step; the remaining 100µl was stored in 10µl aliquots at -80°C.

2.3.7 Acetone Precipitation

A tricholoroacetic acid (TCA)/ acetone precipitation method was used to prepare protein extracts from *Lymnaea* CBG. The protocol was adapted from the work of Dermerval *et al.* (1986) with some modifications. *Lymnaea* CNS tissue was dissociated and homogenized into a soluble suspension using 100µl - 200µl buffer. Acetone precipitation enabled the sample to be concentrated in a smaller volume following solubilisation of proteins without significant sample loss (Pasquali *et al.*, 1997), whilst maintaining the 10µg-15µg/µl sample to loading volume ratio required for 2D DIGE.

To precipitate samples, four volumes (400µl) of cold acetone/ 10% TCA were added to each (100µl) and reactions stored at -20 °C overnight (approximately 12-16 hours). Samples were centrifuged at 12,000 x g for 15 minutes in a pre-chilled centrifuge (EZ-2 Personal Evaporator, GeneVac) at 4 °C and the supernatant

(acetone/TCA) was removed. The process was repeated using an equivalent volume of 90% methanol (400µl) and the samples centrifuged (EZ-2 Personal Evaporator, GeneVac) for a further 15 minutes at 4 °C. Samples were left to air-dry until the methanol and acetone had evaporated from the sample. Samples were re-suspended in 50µl of either 2D Lysis buffer or Tris buffer and stored at -80°C.

2.3.8 Determination of protein concentration:

Protein concentration from the extracts was determined using a Quick Start™ Bradford Protein Assay kit (Biorad). Using a standard calibration curve fitted to five serial dilutions of the protein standard (bovine serum albumin), the unknown protein sample concentration was determined when the unknown sample concentration was within the linear range of the standard curve. The dynamic range for the unknown protein extracts was calculated using three dilutions of the protein extracts, prepared at 1:4, 1: 8, 1:16 dilution and the mixture briefly but vigorously mixed. 10µl of each diluted sample were added to 200µl reagent dye per well on a 96 well microplate and incubated at room temperature for 5 minutes. Optical density was determined using UV/visible microplate reader (Asys UVM340) at an absorbance reading of 595nm. As an additional setting parameter, the plates were shaken for 30 seconds in the microplate reader prior to being read to ensure sufficient mixing of samples. A blank reaction mixture containing the 2D Lysis buffer at the equivalent dilutions to the unknown sample served as blank reference during data analysis.

2.3.9 2D PAGE/ 2D DIGE

2.3.9.1 Large format gel casting

Proteins separated on large format (17cm X 24cm) 12.5% polyacrylamide gel required a 600µg protein load to visualize proteins using Coomassie blue stain. Gels were cast in Ettan Dalt Multi-Gel Caster as per manufacturer's instruction (GE Healthcare). A displacement solution was used to produce an even gel cast and reduce air bubbles within the gels during gel cast. Gels were overlaid with water-saturated butanol to produce an effective seal and barrier against gels dehydrating during the polymerization process.

2.3.9.2 First Dimension running conditions

2 different pre-cast immobilized pH gradient (IPG) strips (24 cm) were used. Initially pH 3-10 strips that were used during method development and subsequently, a narrower pH range of 4-7 was utilised. The strips were rehydrated in rehydration buffer containing 600µg protein sample and run for a total of 55-60 kVhrs using an 'active' in-gel rehydration method on an IPGphor system (Amersham Biosciences) which consisted of the following steps:

Procedure	Voltage	Hours
Step and Hold	30V	12 hours
Step and Hold	500V	500Vhr
Gradient	1000V	750Vhr
Gradient	8000V	13500Vhr
Step and Hold	8000V	40 000

Table 1: In-gel rehydration and Isoelectric focusing.
A constant 30 volts was applied during the 12 hour 'active' rehydration process, and proteins were focussed on each voltage step until proteins on the gel strip reached a total of 40,000 Volt hours.

2.3.9.3 Reduction and alkylation of IPG strips

To stop the formation of disulphide bridges and secondary protein structures, the IPG strips containing proteins were first reduced in equilibration buffer (see Chemicals and reagents section 2.2.2) containing DTT for 15 minutes followed by alkylation of the proteins in equilibration buffer containing Iodoacetamide for 15 minutes prior to the strips being run in the second dimension.

2.3.9.4 Second Dimension gel running condition

The second dimension was performed on Ettan™ Dalt twelve vertical system. IPG strips were implanted on top of the gel following the reduction and alkylation phase and sealed with low melting-point agarose. Gels were submerged in the rig with 1X SDS Running buffer in the bottom compartment and 2X SDS Running buffer in the top chamber to reduce SDS depletion during electrophoresis. The second dimension gel running conditions were calculated as 3W/gel for the first 30 minutes, followed by 17W/gel for 4-5 hours until the Bromophenol Blue dye front had reached the bottom of the gel. On completion of the second dimension, gels were placed in fixing solution, and stained with Coomassie blue stain solution as described previously.

2.3.9.5 2D DIGE experimental design

A minimal labelling Cydye™ kit obtained from Amersham Biosciences was used to identify differentially expressed proteins within our two sample set. The differential in-gel electrophoresis (DIGE) kit contained powdered cyanine dyes (5nmol/µl) which were diluted in anhydrous Dimethylformamide (DMF) (Aldrich) to 1000pmol/µl with 5µl DMF according to manufacturer's instructions (Amersham Biosciences). A working stock was made by diluting the 1000pmol/µl stock to 400pmol/µl using DMF and used to label 50µg of total protein per dye. The dyes were vortexed and centrifuged briefly and incubated with the sample on ice for 30 minutes in the dark. The labelling reaction was stopped by the addition of 1µl of 10mM lysine. The Cy2 flourophore was used as an internal pooled standard containing a 50:50 mixture of young and aged samples. This was used to normalise inter-gel variability during multiple gel analysis using DeCyder 6.0. The Cy3 and Cy5 dyes labelled the young (Y) and old (O) CBG homogenates which were matched to numerically labelled tubes i.e. Y1 to O1, Y2 to O2, Y3 to O3, Y4 to O4. Cy3 and Cy5 dyes were cross-labelled so the opposite samples were labelled to reduce intra-gel variability and false positive matches during DeCyder analyses. Incorporating this into the experimental design, 2 cross-labelled gels were made for each of 4 DIGE replicates (see Table 2). The experimental dataset was duplicated, producing 8 DIGE replicates in total.

	Fluorescent labelling of samples		
Replicate #	**Cy 2**	**Cy 3**	**Cy 5**
1	Pooled standard	Young 1	Old 1
2	Pooled standard	Old 1	Young 1
3	Pooled standard	Young 2	Old 2
4	Pooled standard	Old 2	Young 2
5	Pooled standard	Young 3	Old 3
6	Pooled standard	Old 3	Young 3
7	Pooled standard	Young 4	Old 4
8	Pooled standard	Old 4	Young 4

Table 2: DIGE experimental design using fluorescently Cy Dyes

2.3.9.6 Digitisation and analysis of 2D DIGE image

The DIGE gels were digitised using a Typhoon Scanner. Repeated scanning of a single gel generated three images corresponding to Cy 2, Cy 3, and Cy 5 labelled proteins. Protein expression analysis and statistics was performed within DeCyder 6.0. Protein spots were considered upregulated if a fold change above 1.10 fold threshold (i.e. 10% change) was detected. Conversely, downregulated proteins represented a fold change below -1.10 change in protein expression. Statistically significant changes in protein spot values were confirmed using ANOVA p value < 0.05.

2.3.9.7 Protein extraction from 2D PAGE gels

PlusOne™ Silver Staining Kit was used on eight preparative gels loaded with 500 µg protein to visualise and excise low abundant proteins. Identical proteins spots were excised from each gel and pooled into 1.5ml labelled microtubes. To minimise potential carryover from peptide digests from previously run samples during MS/MS data acquisition, successive gel plugs were excised from opposite ends of the gel and therefore had markedly different molecular weights and PIs.

2.3.9.8 Trypsin Digestion

Tryptic fragments of proteins were obtained as described by Shevchenko et al (1996). Briefly, the recovered peptides from the gel pieces were sequentially extracted in a series of solutions containing acetonitrile following reduction (10mM DTT in 25mM NH_4HCO_3 at 56°C for 1 hour) and alkylation (55mM Iodoacetimide in 25mM NH_4HCO_3 for 10 minutes) of proteins and the protein gel plugs incubated in 25ng/µl trypsin overnight at 37°C.

The supernatant from the overnight digest was recovered in a separate tube following a 20 minute centrifugation at 14,000 x g with 50µl 20mM NH_4HCO_3. Two further supernatant fractions were collected following the addition of 2X 50µl 5% formic acid and 50% acetonitrile to the gel plugs and centrifugation for 20 minutes. All collected fractions from the same protein samples were combined in a single tube and concentrated in a vacuum centrifuge (Speedvac SPD111V, ThermoFisher) at 10,000 x g to approximately 20µl volume and peptides stored at -20°C.

2.3.10 Mass Spectrometric Analysis Of Proteins

2.3.10.1 RP-LC fractionation of peptide digests

Trypsin-digested proteins from selected 2D gel plugs were analysed on a ThermoScientific LTQ Orbitrap hybrid Fourier Transform mass spectrometer (FT-MS). The machine was fitted with a nanospray ion source using stainless steel emitters (both Proxeon). Samples were fractionated on a reverse phase column (PepMap 100 C18, Dionex) using an ultimate nano-LC system (Dionex) equipped with a 20µl injection loop. The tryptic peptide fragments were separated using a linear gradient of 100 % solvent A (water, acetonitrile, formic acid; 97.9:2.0:0.1 v:v) and 0% solvent B (acetonitrile, water, formic acid; 90:9.9:0.1 v:v) to 60% Solvent B and 40% Solvent A at a flow rate of 350 nL/min and introduced directly into the FT-MS for analysis.

2.3.10.2 MS/MS spectral data acquisition from protein digest

Data was collected in the Orbitrap FT detector by sequential acquisitions of one full MS scan followed by MS/MS spectra of the top five most abundant precursor ions/scan (*m/z* range for both: 350-1800) over the duration of the eluting gradient. MS/MS spectra were generated by collision-induced dissociation (CID) using helium as the collision gas.

Implementation of a dynamic exclusion criteria enabled detected ions to be excluded from re-analysis for a 30 second period to allow MS/MS spectral data to be acquired for more as well as less-abundant ions series, and therefore increasing coverage of the protein.

2.3.11 De Novo Sequence Analysis of Protein Fragments

A more detailed description detailing the PEAKS algorithm can be obtained elsewhere (Ma *et al.*, 2003). For sequence comparison, the PEAKS scoring function related the intensity of all matched peaks to the detection of an ion series. By using the b- and y ion series, PEAKS computed the best possible sequences and assigned a score function on the best possible 'hits'. The derived peptide sequences were searched and matched to *in silico* digested proteins annotated in the non-redundant database. PEAKS results were accepted as those with a > 90% confidence score

assigned to a single protein ID, with at least 3 peptides matching to a unique protein and only after manual validation of the peptide sequence.

2.3.12 Western Blot analysis

2.3.12.1 Protein extraction and separation:

Cerebral and buccal ganglia extracts were dissected and homogenised as described previously. Samples (10 μg of total protein) were boiled for 5 minutes in denaturing SDS Loading buffer, separated on 12% 7.5 cm polyacrylamide SDS gels using a vertical gel electrophoresis unit (Protean II, Biorad, UK).

2.3.12.2 Gel transfer to PVDF membrane:

Gels were transferred to a polyvinylidene fluoride (PVDF) membrane using a wet transfer method using the Protean II system for 1 hour at 100 Volts submerged in transfer buffer. Heat was evenly distributed during the running of the electrophoresis unit by placement of an ice pack inside the chamber and circulating the buffer using a magnetic stirrer. PVDF membranes were blocked for 1 hour in 1 x phosphate buffered saline (PBS) with 0.1% Tween 20 and 10% skimmed milk powder at room temperature.

2.3.12.3 Antibody incubation

Membranes were incubated with primary antibodies overnight at 4°C. The antibodies used were guinea pig, anti-*Lymnaea* AChBP (1:10,000, gifted from Pim Van Lierop, Netherlands) and rabbit, anti-bovine GAPDH (Santa Cruz Biotech). The binding of the antibody was visualised by horseradish peroxidase-conjugated anti-guinea pig IgG (1:20,000) for AChBP and anti-rabbit IgG for GAPDH (1:1,000) (Santa Cruz Biotech).

2.3.12.4 Chemiluminescent detection

The membrane blots labelled with HRP-conjugated antibodies were detected using ECL™ plus kit (GE Healthcare) and exposed on Amersham Hyperfilm™ ECL, as per manufacturer's instruction. The blots (protein side up) were incubated with the ECL plus reagents and covered in Saran wrap (Aldrich) for 5 minutes. Excess reagents were removed and the blot placed in new saran wrap and fixed onto an x-ray film cassette with tape. The autoradiography film was placed on top of the blot, the

film cassette closed to a set exposure time in the darkroom. The exposure time varied depending on the concentration of the primary and secondary antibodies and the antibody being detected (see individual results section). The film was developed using an automatic X-ray film developer, Compact X4 (Xograph Imaging System). The developed immuno-reactive bands were scanned and digitised into ImageQuant software (GE Healthcare) for densitometric analysis. Proteins of interest were normalised to glyceraldehyde-3-phosphate dehydrogenase (GAPDH). As part of the glycolysis pathway, GAPDH proteins are highly homologous and ubiquitously expressed across tissue types, and were stable in the young and aged CBG.

2.3.12.5 Membrane stripping

Restore™ Western Blot stripping buffer (Pierce Biotechnology, US) was used to strip proteins from the blot. Membranes were placed in 20 ml stripping buffer solution and left on an orbital shaker for 15 minutes. The stripping buffer was removed and the membranes were washed with 1x PBS/ 0.1% Tween, and agitated for 10 minutes on an orbital shaker. The removal of the primary antibody was detected by performing the chemiluminescent detection step. The antibody was considered to be stripped from the blot when no corresponding band signals were detected on the blot.

2.3.13 Statistical analysis of data

Sucrose evoked feeding behaviour are represented as mean ± SEM. Statistical analysis on the sucrose-evoked feeding behaviour was performed using EXCEL spreadsheet where differences between the young and aged groups were examined using student t-test. Normalised protein expression in Western Blot analysis would be expected to deviate from a normal distribution, as indicated by a Kolmogorov-Smirnoff test using SPSS software (not shown). However the distribution appeared sufficiently symmetrical to be considered normal such that classical student t-test could be validly performed and considered significant if $p < 0.05$. Statistical analysis performed on differentially expressed protein spots using DeCyder 6.0 used one-way ANOVA.

2.4 RESULTS (1): DETERMINING PROTEOMIC CHANGES IN THE CEREBRAL AND BUCCAL GANGLIA OF L. STAGNALIS

Age-related changes in the feeding behaviour were examined using sucrose-evoked stimuli (Figure 6). As described previously (see Chapter 1), the principle component of the feeding cycle which showed a consistent decrease was the total number of sucrose-evoked bites over a 2 minute interval (Arundell *et al.*, 2006). Using the parameters outlined in Figure 6A, the number of sucrose-evoked bites significantly decreased in 10 month old animals when compared to 3 month old animals. Mean values for young was 32.14 ± 0.58 bites over 2 minutes, compared to 14.20 ± 0.97 in 10 month aged animals ($p < 0.05$). This data are comparable to those described previously (Arundell *et al.*, 2006).

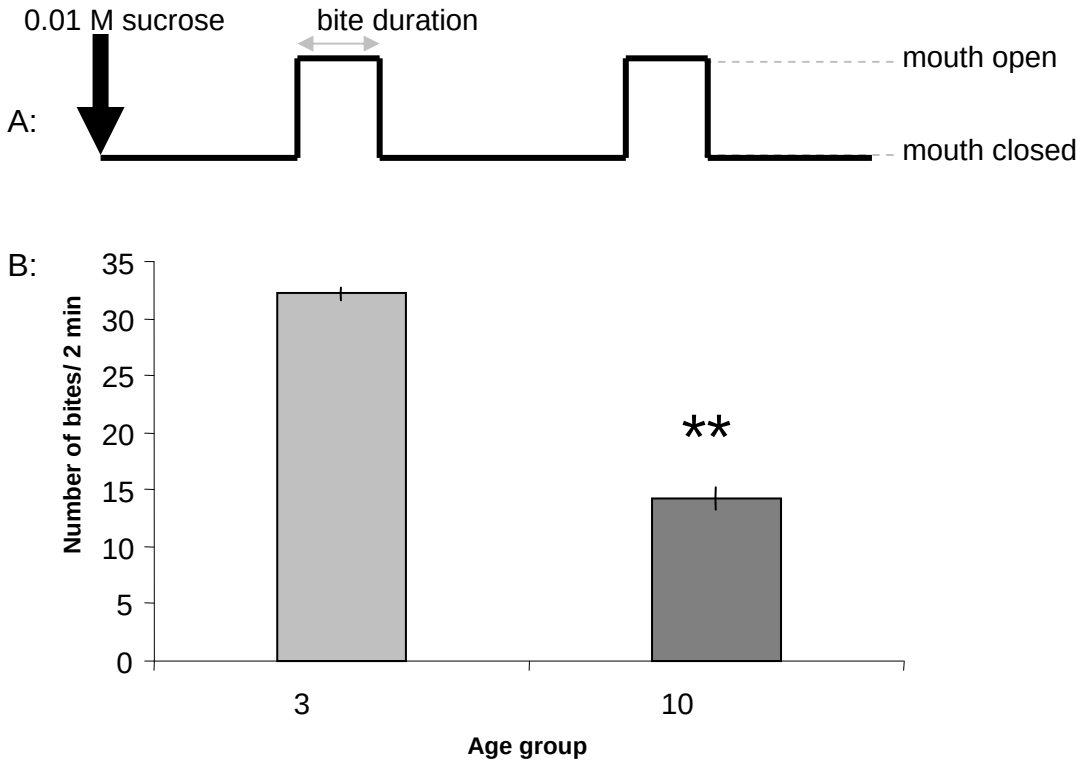

Figure 6: Age-related changes in short-term feeding evoked by 0.01M sucrose stimuli.
The feeding score for young and aged animals were obtained using the parameters outlined in the feeding trace (A) after the point of first emergence from the shell. The feeding traces were recorded in an in-house software for a total of 2 minutes per session, and the number of bites in 3 month snails and 10 month age groups (n=80/ group). Values represent mean **±** S.E.M (B). Significant differences were analysed using a student t-test, ** $p < 0.05$,

2.4.1 Method Development:

2.4.1.1 Comparison of extraction buffer for L. stagnalis CNS

2D-PAGE is a labour intensive process in which only a limited number of samples can be analysed at any one time. Limitations in 2D PAGE for proteomic analysis include loss of certain types of protein either through incompatibility of extraction buffers, the dynamic range of proteins or the resolution and abundance of proteins within the sample set (see discussion). Therefore protein samples needed to be completely solubilised, disaggregated and denatured to increase the dynamic range and the number of detectable proteins from within the *Lymnaea* nervous system. To ensure the extraction conditions were optimal for the CNS *Lymnaea* proteins, four different extraction media were compared.

A. Tris Buffer alone

B. Tris Buffer following acetone precipitation

C. 2D Lysis Buffer

D. 2D Lysis Buffer following acetone precipitation

The addition of an acetone precipitation step benefited from a complete buffer exchange. Tissue samples dissected in incompatible 2D PAGE buffers benefited from this additional step that enabled the samples to be separated using 2D PAGE, however salts and other contaminants were removed during the buffer exchange so that these would not interfere with LC MS/MS mass spectrometry and show contaminant peaks within the spectra.

2.4.1.2 Determining degradation and concentration of protein during dissection

A major concern when analyzing neuronal tissue (or any other complex biological sample) is the reproducibility and the integrity of polypeptides within the sample. To ensure the production of reliable and reproducible proteomic data, it is critical to set standards very high at the beginning of the experiment to ensure efficient extraction of proteins and avoid artificial losses and biases which may arise during sample collection. To avoid post mortem fragmentation of proteins, protease inhibitors was added to prevent the breakdown of proteins, and samples were snap frozen on dry ice

after dissection. Samples protein content was quantified using a modified Bradford method and visualised using Coomassie stain on a 1D gel by serial dilution of the protein sample from young and aged samples to determine protein load/ extraction was uniform between the two age groups (Figure 7).

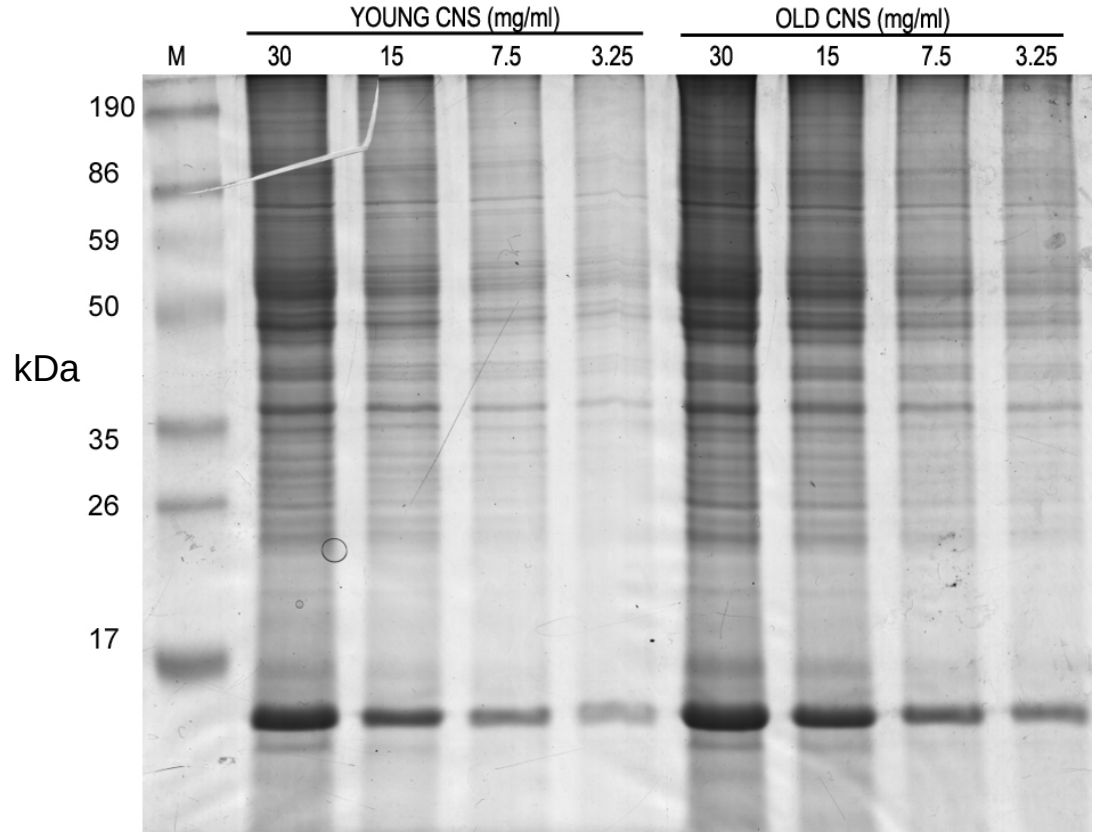

Figure 7: Tissue extraction of young and aged *L. stagnalis* CNS show equal loading conditions

Serial dilution of total protein lysate (mg/ml) from *Lymnaea* whole CNS were separated on a 12% 7cm SDS-PAGE and visualised using Coomassie Blue stain. Extracts from young and aged animals showed comparable protein load as determined using Bradford method and no protein degradation during the 2 minute dissection period. M = protein ladder (kDa).

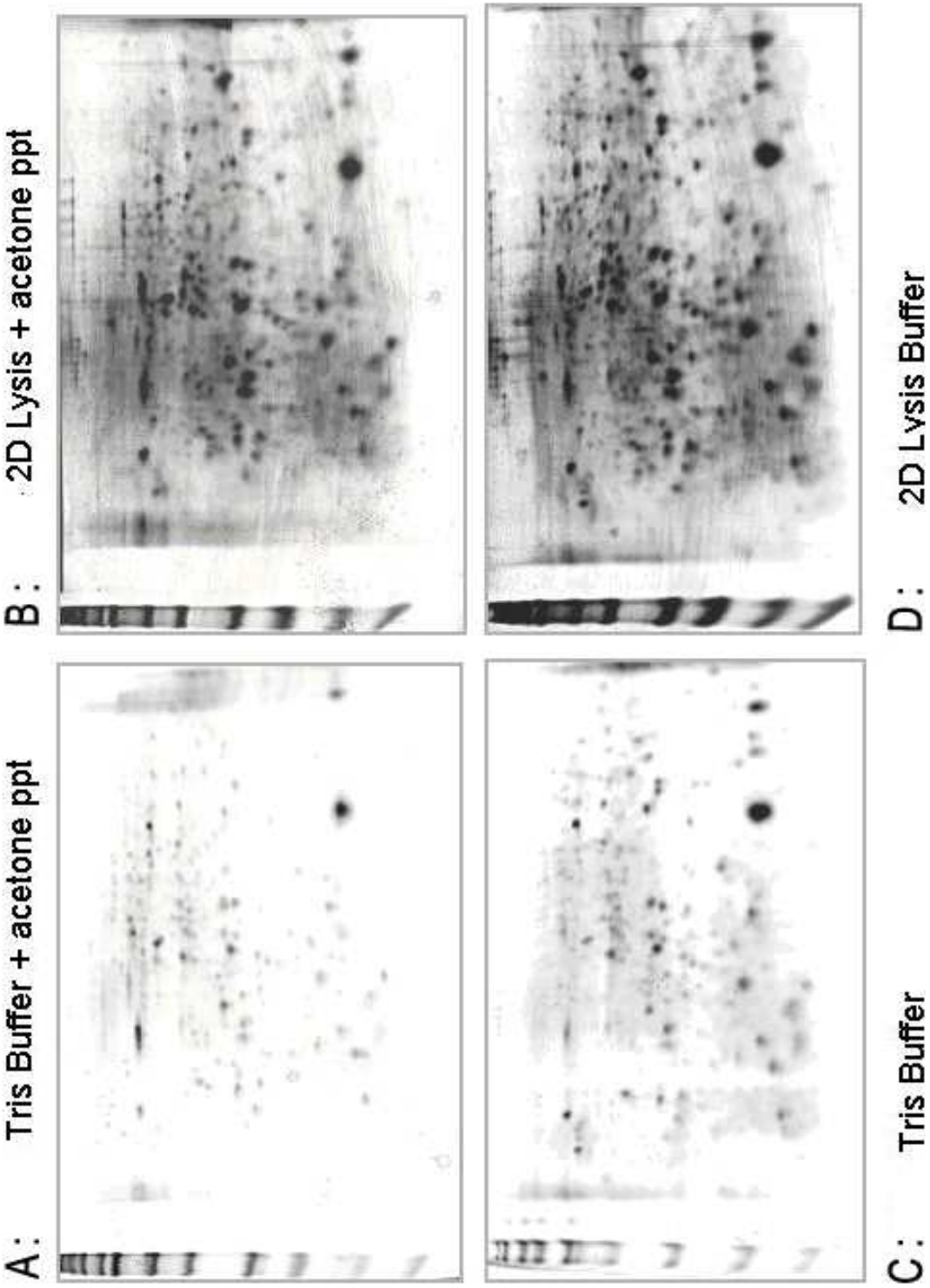

Figure 8: Protein extraction using different 2D-compatible extraction buffers show 2D Lysis buffer was suitable for solubilisation of *L. stagnalis* CNS proteins

2D lysis buffer following acetone precipitation showed minimal loss of sample compared to 2D lysis buffer alone. Both 2D lysis buffers were suitable for protein extraction compared to tris buffers when visualised on a 10% 7cm PAGE gels and scanned at the same expose settings.

Samples were subsequently run on 7cm 2D PAGE gels to compare the different 2D PAGE compatible extraction buffers used to suspend *Lymnaea*-specific CNS-derived proteins. Extraction in one of the two buffers was combined with an additional acetone precipitation step to give a total of four different extraction protocols (Figure 8). Proteins solubilised in Tris buffer alone or Tris buffer + acetone precipitation did not resolve the full complement of proteins on a gel (Figure 8). Fewer low molecular weight proteins were represented on gels containing proteins extracted in Tris buffer or Tris buffer alone + acetone precipitation (Figure 8 A,C) compared to two 2D Lysis extraction buffers (Figure 8 C,D). Thus, the Tris buffer was not a suitable extraction buffer for *Lymnaea* proteins, resulting in sample loss as all the proteins could not be solubilised and therefore represented on the PAGE gel. 2D lysis buffer on the other hand enabled detection of a broader range of proteins on the PAGE gel (Figure 8B, D). Sample loss was not observed when comparing 2D lysis buffer alone conditions to those combining the additional acetone precipitation step (Figure 8 D). The complete buffer exchange using the acetone precipitation method is chosen as this allowed the samples to be concentrated in a smaller volume as well as enabling a complete buffer exchange for removal of salts and other contaminants which are known to interfere with downstream analysis.

2.4.1.3 Determining the dynamic range of L. stagnalis protein on 2D PAGE gel

Next, the dynamic range of proteins able to be arrayed on a 2D PAGE gel was assessed using IPG strips of 2 different dynamic ranges (Figure 9). First, a linear gradient strip of pH 3 – 11 was used to assess the full complement of proteins present on a 2D gel (Figure 9A). The limits of the hydrophobic and hydrophilic regions which could not be visualised on the 12% 2D PAGE gels are denoted with (▼). ** indicates IPG strip loading error (Figure 9A). Most of the proteins were in the approximate range of pH 4 – 7. A narrow pH 4-7 gradient IPG strip was subsequently used to increase the resolution of the 2D PAGE gel (Figure 9B). Using a narrow pH gradient significantly increased the resolution of the protein spots (black dots) required for quantitative analysis. Therefore an IPG strip range of pH 4-7 was chosen for use for subsequent analysis.

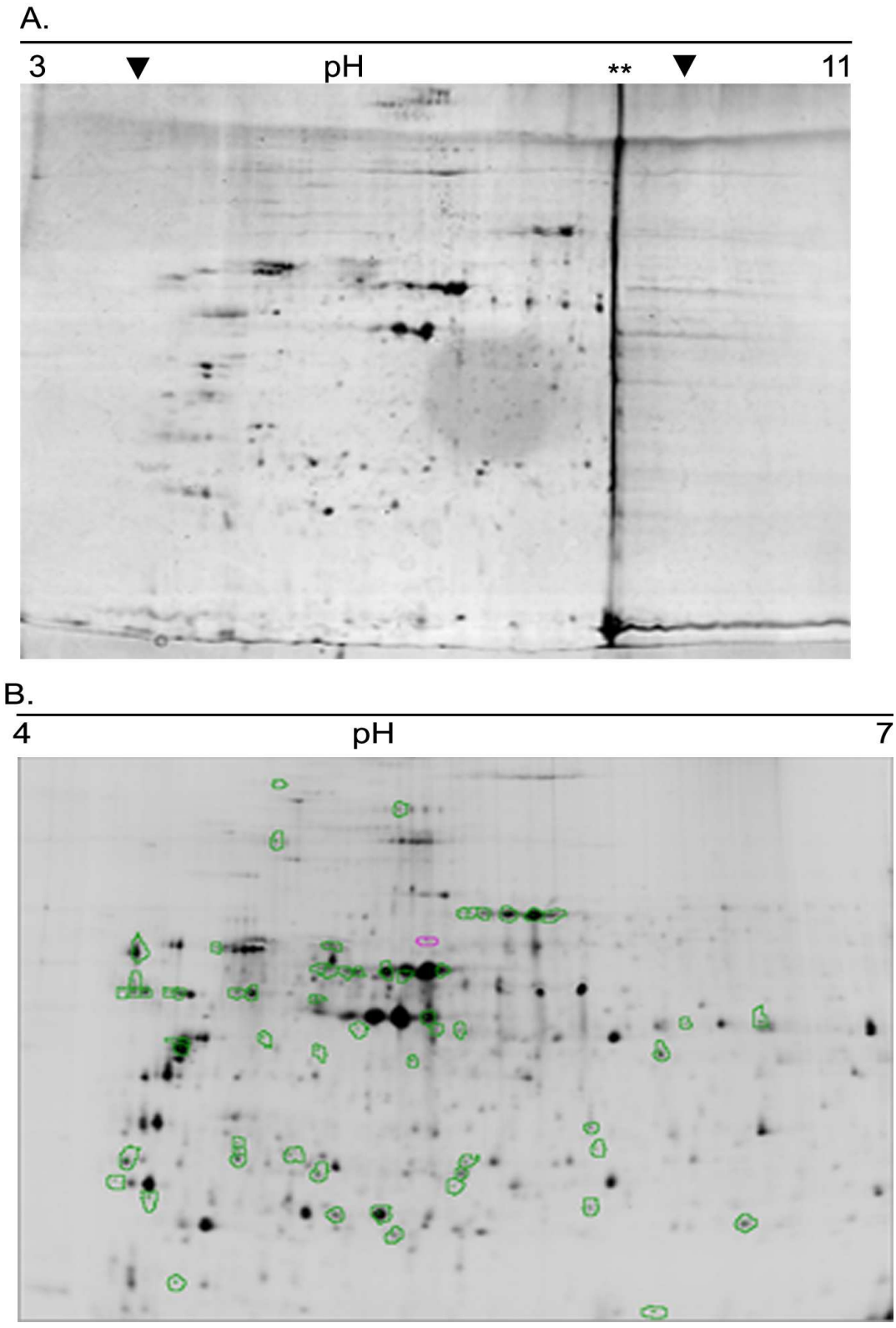

Figure 9: IPG strip pH 4-7 is optimal for visualising cerebral and buccal ganglia proteins

(A) IPG (pH 3-11) strips could not visualise proteins in the highly acidic or basic regions (denoted ▼). (B) IPG (pH 4-7) strip increased the dynamic range of proteins that could be resolved on a PAGE gel for quantitative proteomics. Green circles are proteins of interest. ** indicates with IPG during isoelectric focussing.

2.4.2 2D Difference in-gel electrophoresis: Cerebro-buccal Ganglia.

Figure 10 shows a representative 2D-DIGE gel of total protein examined from the cerebral and buccal ganglia using the experimental design outlined in section 2.2.9.5. Multi-gel analysis performed using DeCyder 6.0 (Amersham Biosciences) enabled detection of 1834 proteins with an assignable protein-spot boundary which are highlighted in green (Figure 10). Proteins were filtered to show an above 1.1 fold difference between the two groups and statistically compared using 95% confidence t-test and 1-way ANOVA analysis (Figure 11A-Q). 47 protein spots were identified as significantly different between the two groups (15 upregulated, and 32 downregulated). 30/47 protein spots could be stained and identified using either Coomassie blue stain or silver stain. The gel plugs containing the 30 proteins were excised from the gel and trypsin digested for MS/MS analysis, as summarised in proteomic workflow summarised in Figure 12.

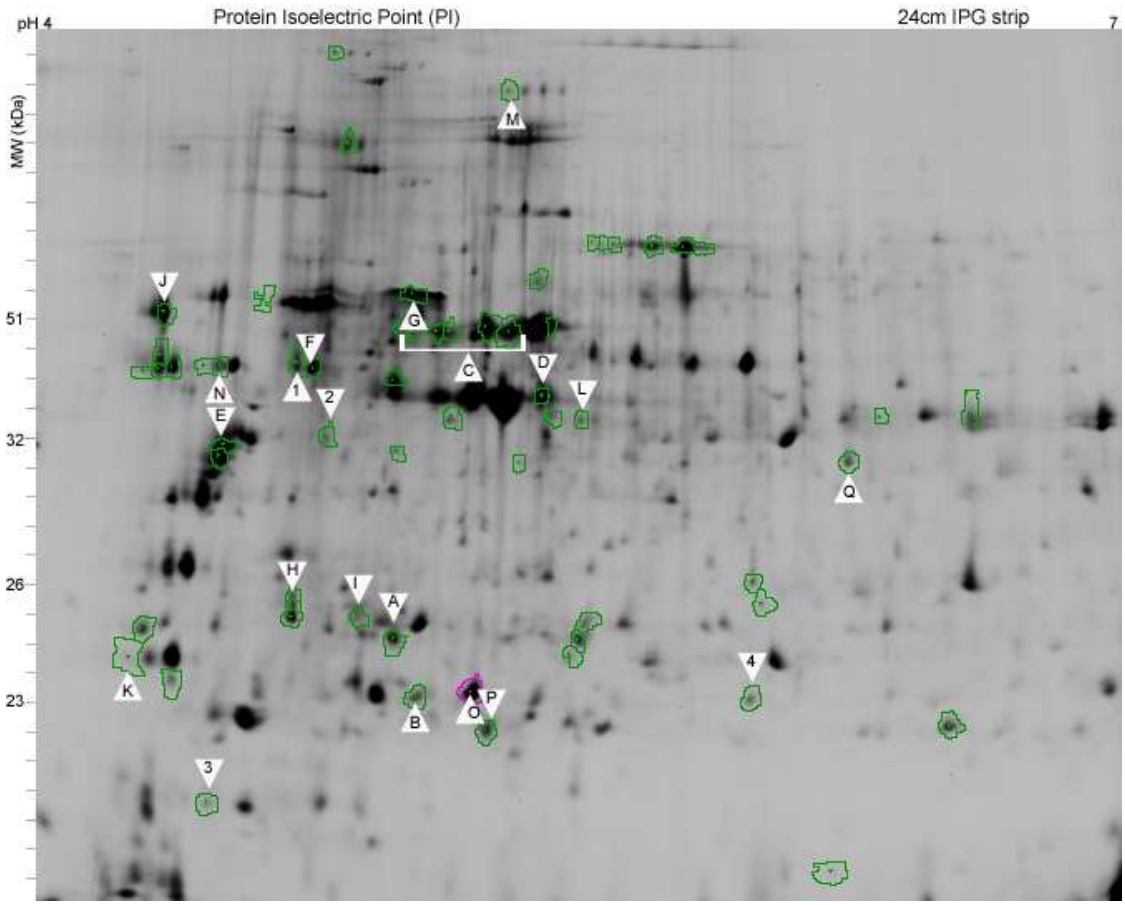

Figure 10. 2D DIGE analysis young and aged cerebral-buccal ganglia
Protein spots highlighted in green represent proteins differentially expressed between 3 and 10 month animals from 80 pooled CNS tissues. Triangles pointing upwards are proteins up-regulated, triangles pointing downwards represent proteins down-regulated. **A**: 14-3-3 protein; **B**: Glutathione-S-Transferase; **C**: Retrograde protein 51; **D**: β-actin; **E**: tropomyosin-2; **F**: Reductase; **G**: α tubulin; **H**: acetylcholine binding protein; **I:** probable reductase; **J:** Lysozyme; **K:** glycolate oxidase; **L:** cytoskeletal actin; **M:** Hypothetical protein; **N:** similar to 40S protein; **O:** HSP-90; **P:** kinesin-like protein; **Q:** arginine kinase; Proteins **1-4** could not be identified.

2.4.3 Identification of proteins using PEAKS 4.5

De novo sequencing of proteins was performed using PEAKS 4.5 (Bioinformatics solutions) on the MS/MS data acquired from the 30 protein spots. The majority of proteins identified were highly abundant proteins, showing a high degree of conservation (% protein coverage) to protein sequences already in the non redundant database (see Appendix). Unique proteins with highly confident peptide sequence but no homology match were classed as 'hypothetical proteins' for which sequence homology could not be assigned. 26/30 protein spots had assignable homologies to the NCBI non-redundant database proteins. 17 of the 26 proteins were independent proteins. The remaining 8 of the 26 proteins were possible modifications of the

proteins identified, and were therefore identified more than once or proteins for which no assignable homology was available.

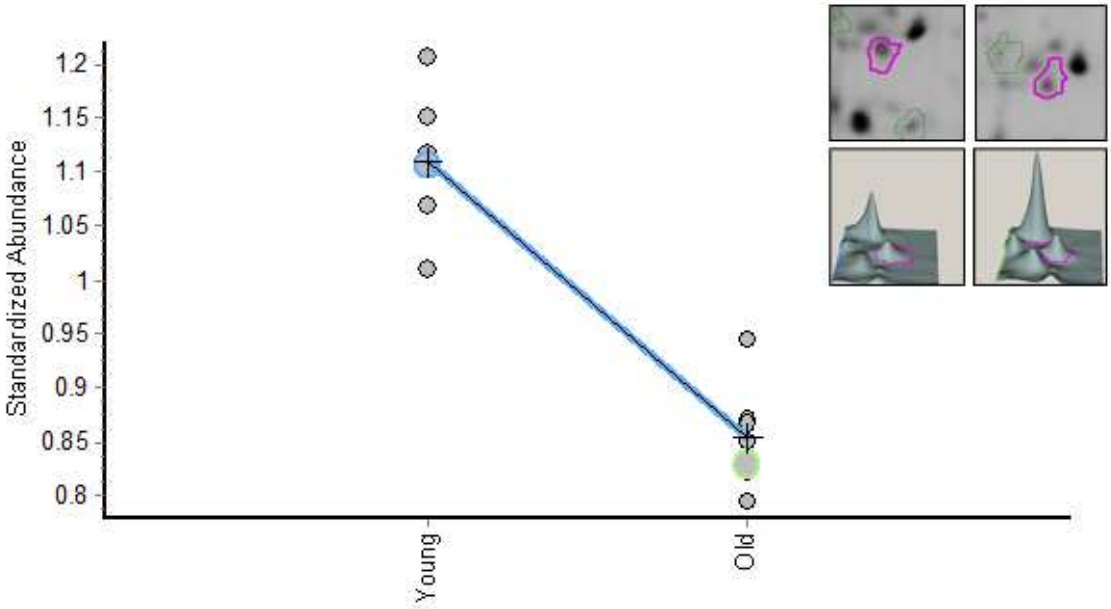

Figure 11A 14-3-3- like protein. -1.30 fold decrease in protein expression (p =1.3 E-06), accession number gi|112687

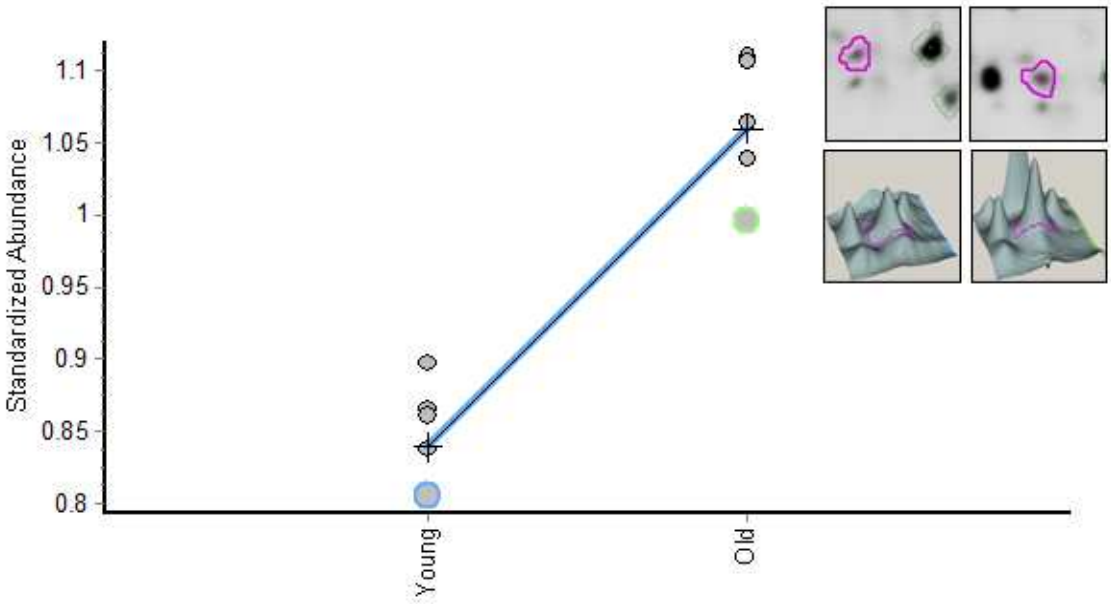

Figure 11B Glutathione-S-transferase. 1.26 fold increase in protein expression (p = 5.7 E-07), accession number gi|99109649

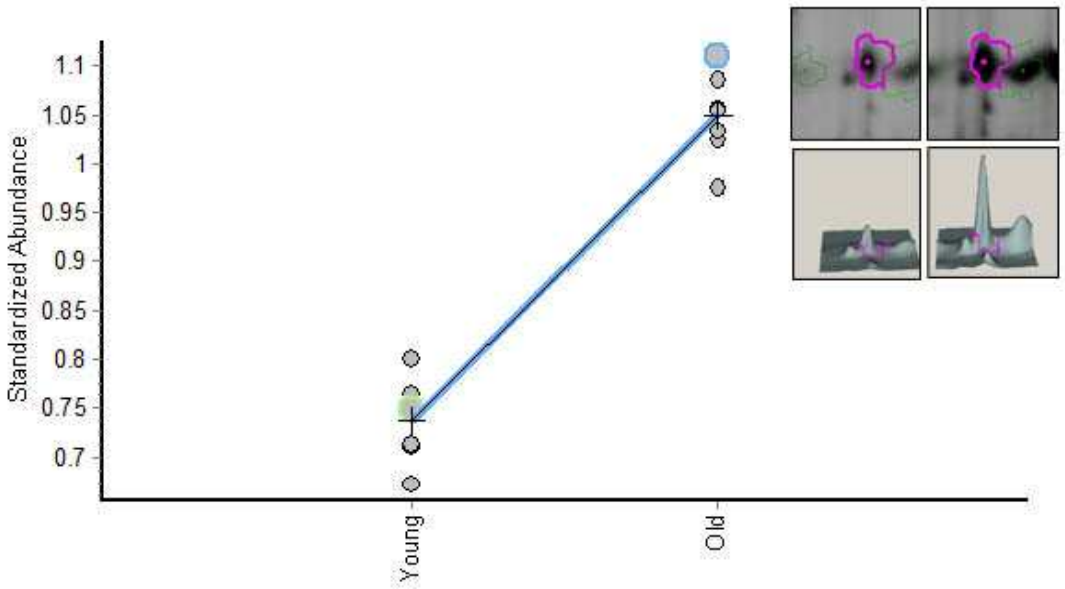

Figure 11C Retrograde protein 51 2.72 fold increase in protein expression (p = 1.18 E-07), accession number gi|468226

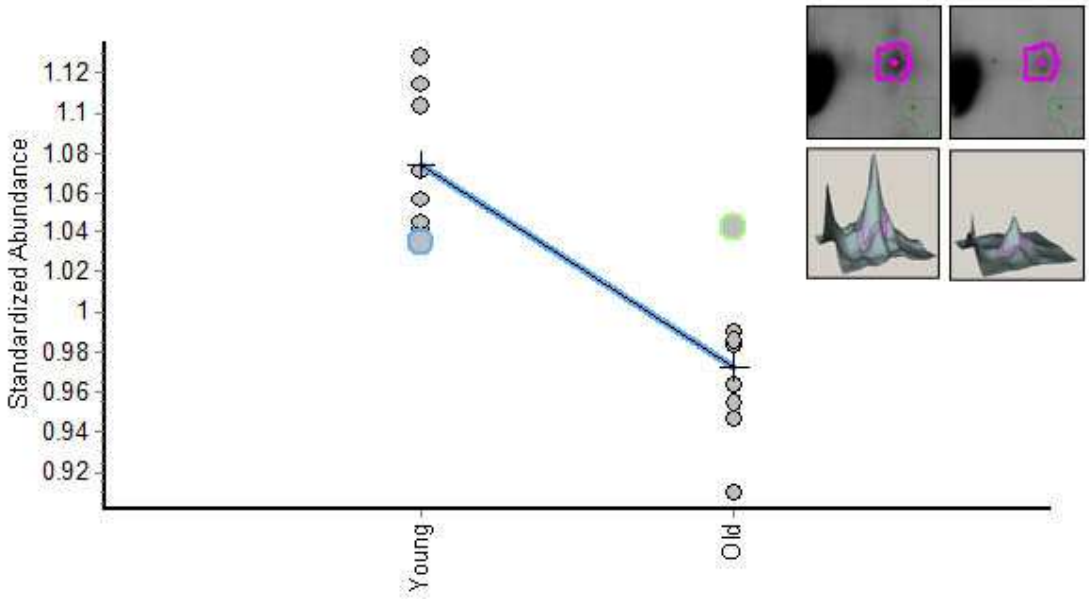

Figure 11D Beta-actin. -1.10 fold decrease in protein expression (p = 8.7 E-07), accession number gi|2724046

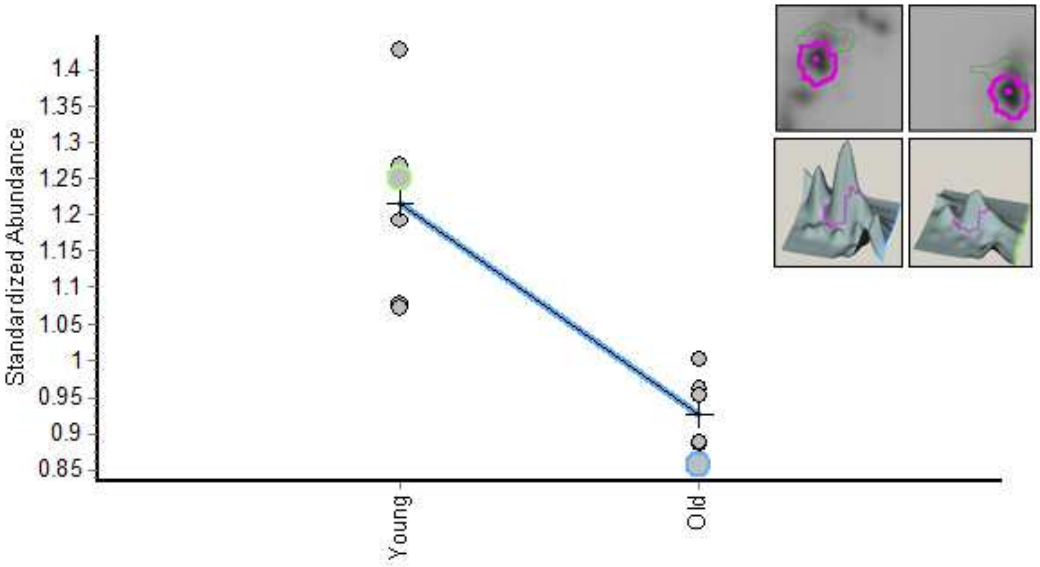

Figure 11E Tropomyosin-2 -1.31 fold decrease in protein expression (p = 8.7 E-06), accession number gi|174755

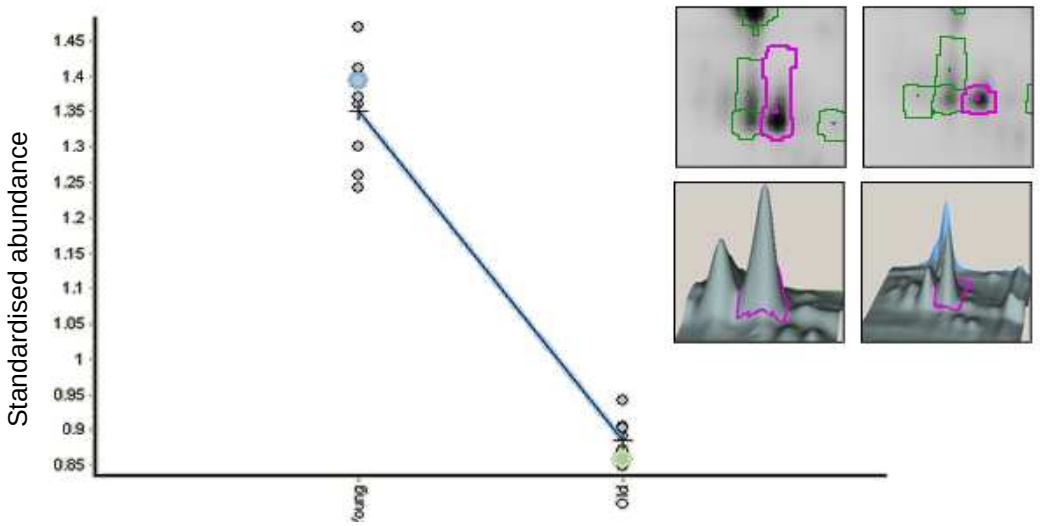

Figure 11F. Reductase. -1.53 fold decrease in protein expression. (p = 5.7 E-011) , accession number gi|71652882

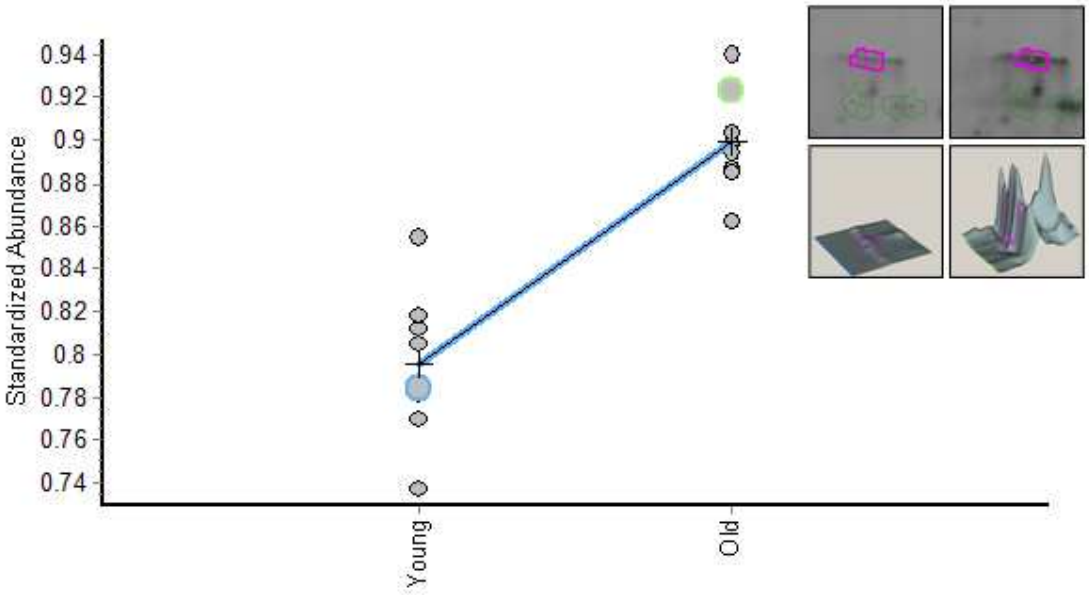

Figure 11G A-tubulin. 1.13 fold increase in protein expression (p = 8.6 E-07) , accession number gi|32967406

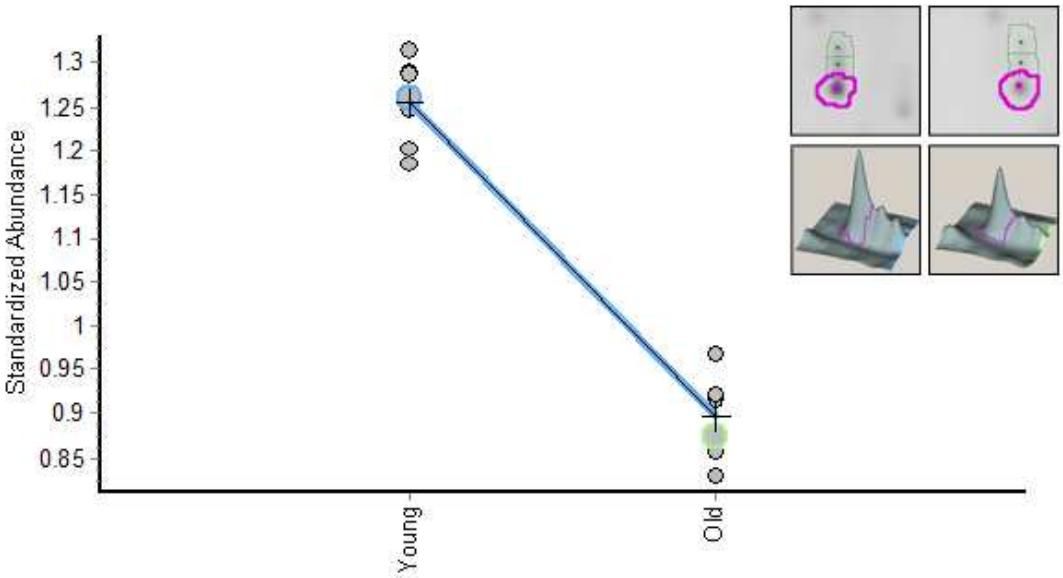

Figure 11H Acetylcholine binding protein. -1.71 fold decrease in protein expression (p = 1.43 E-08), accession number gi|47169297

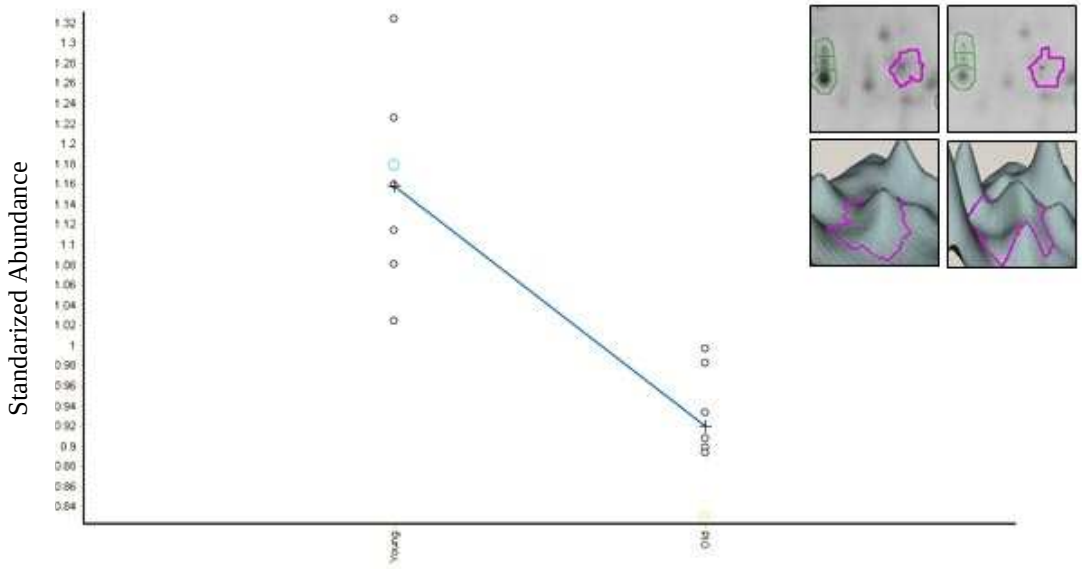

Figure 11I Probable reductase, -1.26 fold decrease in protein expression (p = 8.9 E-05), accession number gi|51105058

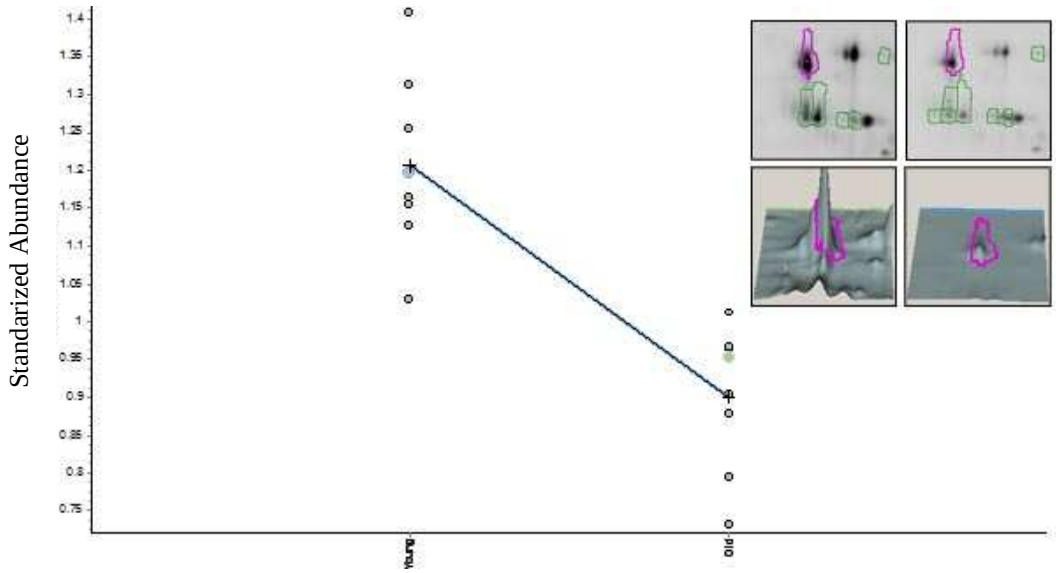

Figure 11J. Lysozyme – 1.34 fold decrease in protein expression (p = 5.9 E-05), accession number gi|2781273

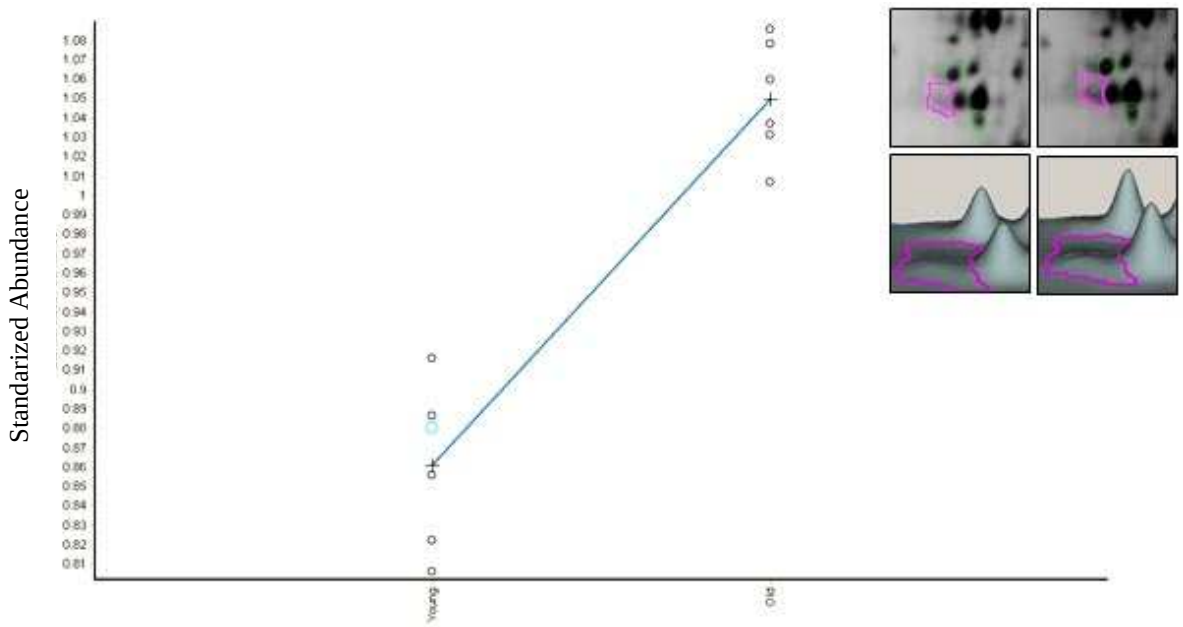

Figure 11K Putative glycolate oxidase 1.22 fold increase in protein expression (p = 5.9 E-06), accession number gi|78696405

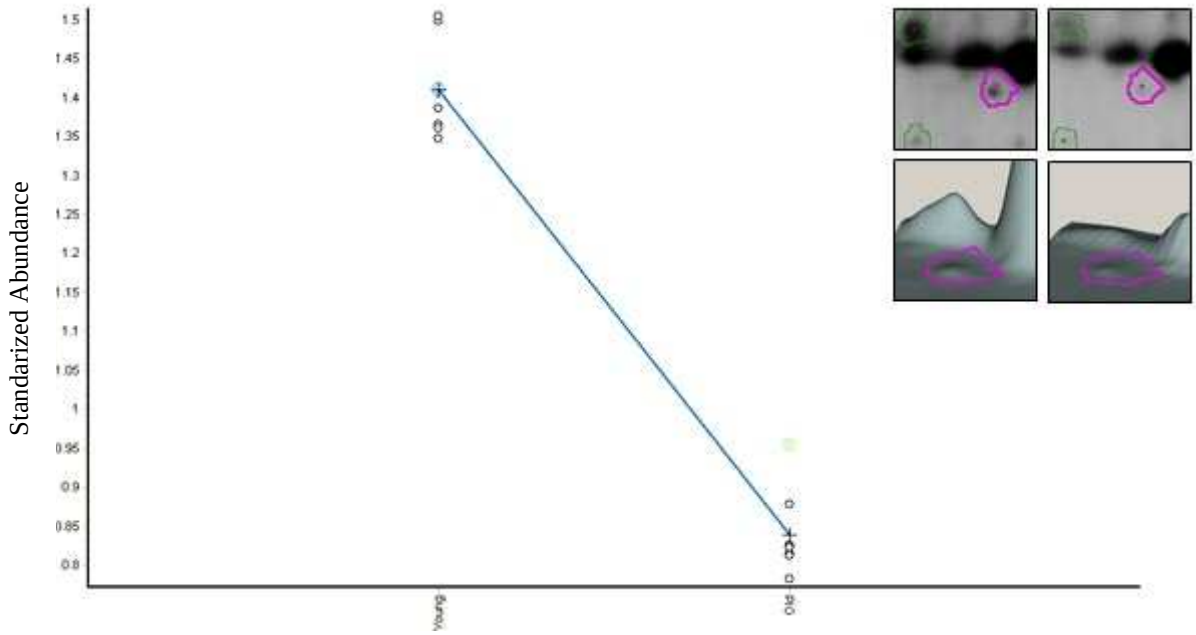

Figure 11L. Cytoskeletal actin. -1.68 fold decrease in protein expression (p = 1.3 E-11), accession number gi|47551035

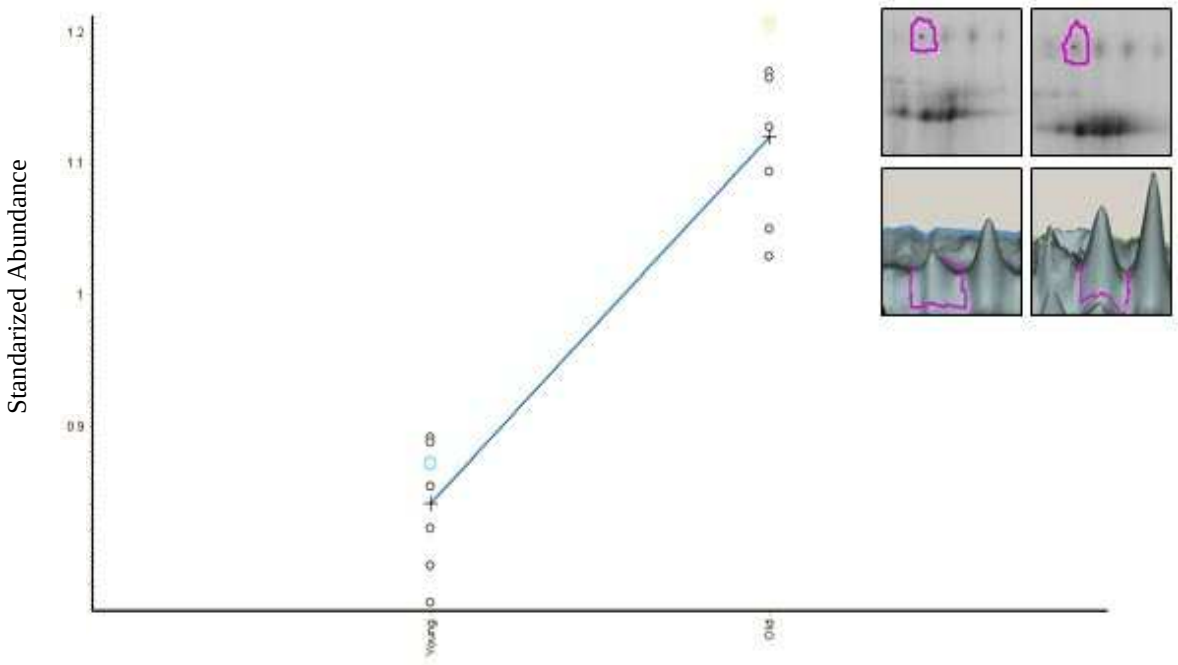

Figure 11M. Leishmania major strain Friedlin hypothetical protein LMJ_0952. 1.33 fold increase in protein expression (p = 9.4 E-07), accession number gi|72546785

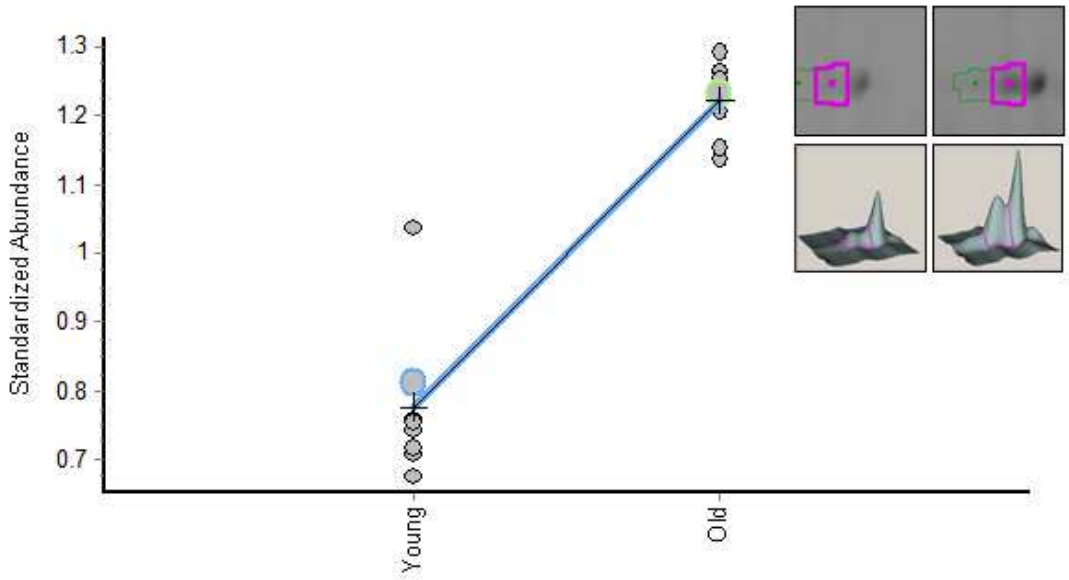

Figure 11N. similar to 40S ribosomal protein SA (p40) (34/67 kDa laminin receptor 1). 1.57 fold increase in protein expression (p = 2.1 E-07), accession number gi|109081713

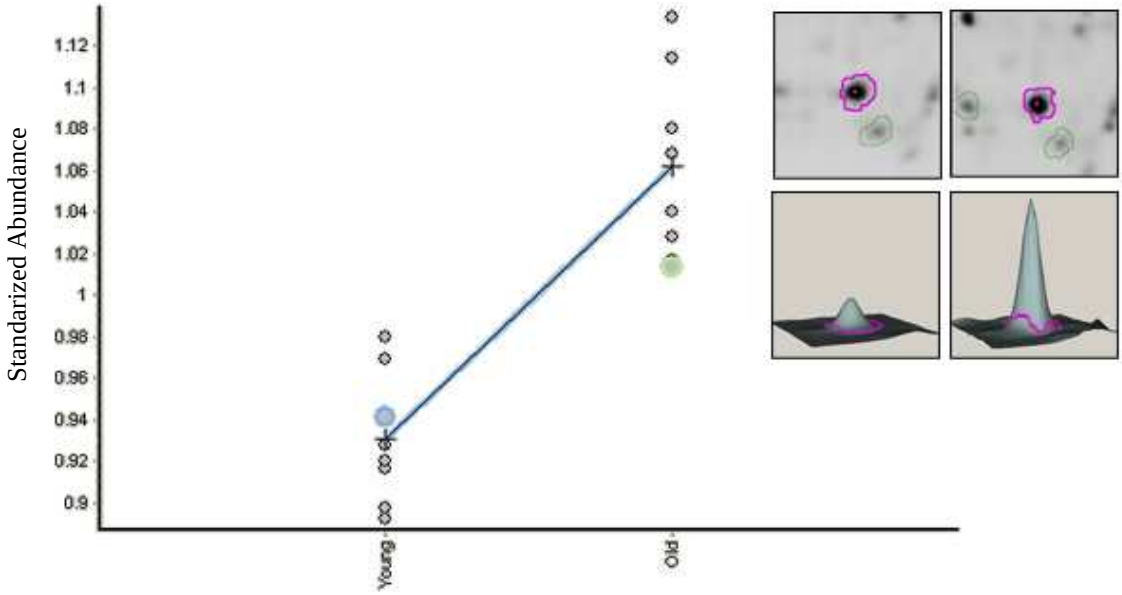

Figure 11O. HSP- 90. 1.14 fold increase in protein expression (p = 7.1 E-06), accession number gi| 28897595.

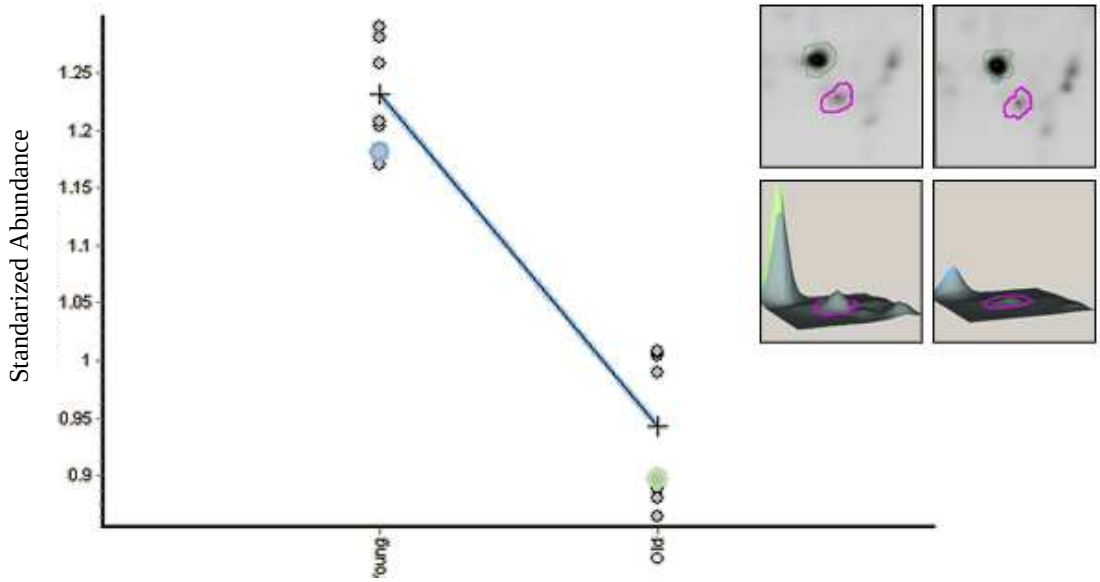

Figure 11P. Kinesin-like protein. -1.31 fold decrease in protein expression (p = 1.4 E-07), accession number gi|110773141.

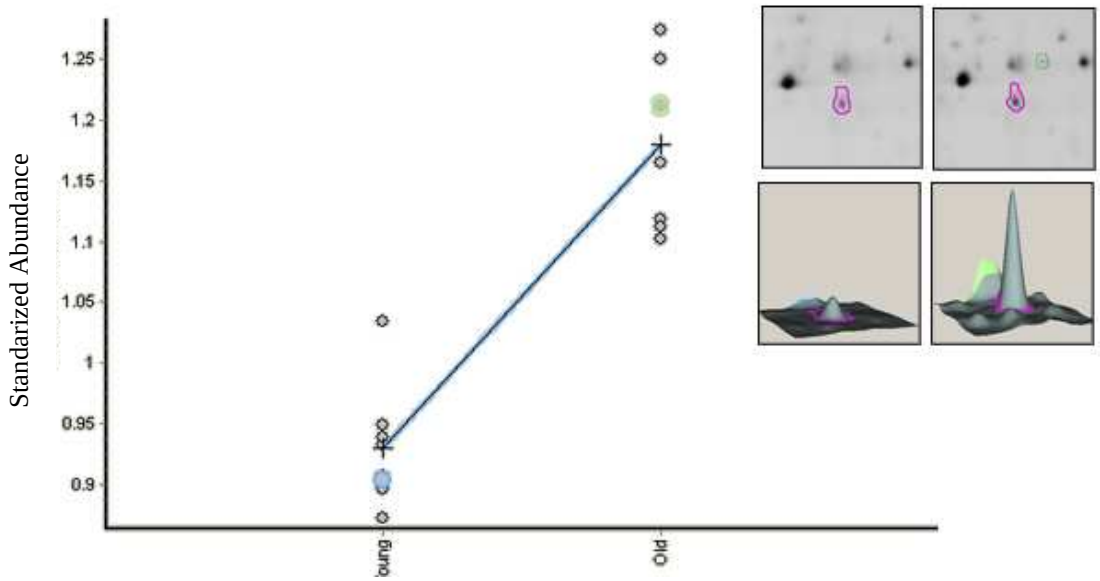

Figure 11Q. Arginine Kinase. 1.27 fold increase in protein expression (p = 4.0 E-07), accession number gi| 13647103.

Figure 11A-Q: Average volume ratio of differentially expressed proteins
Small circles represent individual replicates within the gels. Only proteins expressed in all eight replicate gels were considered during DIGE analysis. The fold change is expressed as a mean fold change between the two groups. The exact location of these proteins on the 2D DIGE can be seen in Figure 10. In the top quadrant panels, raw gel images of the protein spot are shown from young (left) and old (right) CBG. The bottom two quadrants are 3D intensity maps of the proteins in the above quadrants from young (left) and old (right) regions. Accession numbers of homologous proteins and statistical t-test (p-value) are presented.

2.4.4 Highly regulated proteins with no assignable protein IDs

Four proteins with no assignable homology were observed in the CBG. This is of interest as the levels of these proteins were significantly altered in the aged CBG. The location of each protein is denoted with placement numbers 1 - 4 represented in Figure 10. Table 3 provides more information about the average spot volume ratio and the statistical information about these 4 proteins.

Placement Number	P-value of fold-change (T-test)	Fold change (old vs. young)
1	1.7e-008	2.09
2	3.6 e-007	-2.22
3	1.0 e-007	-1.92
4	2.6 e-005	-1.14

Table 3: Location and spot volume ratio of unidentified proteins
Proteins which were differentially expressed but with no assignable homology were are denoted 1-4 in Figure 10, and annotated in DeCyder 6.0 with the corresponding Master gel identification number. Statistical significance is determined using student t-test, ($p < 0.05$).

2.4.5 Summary of 2D DIGE of the aged cerebral and buccal ganglia

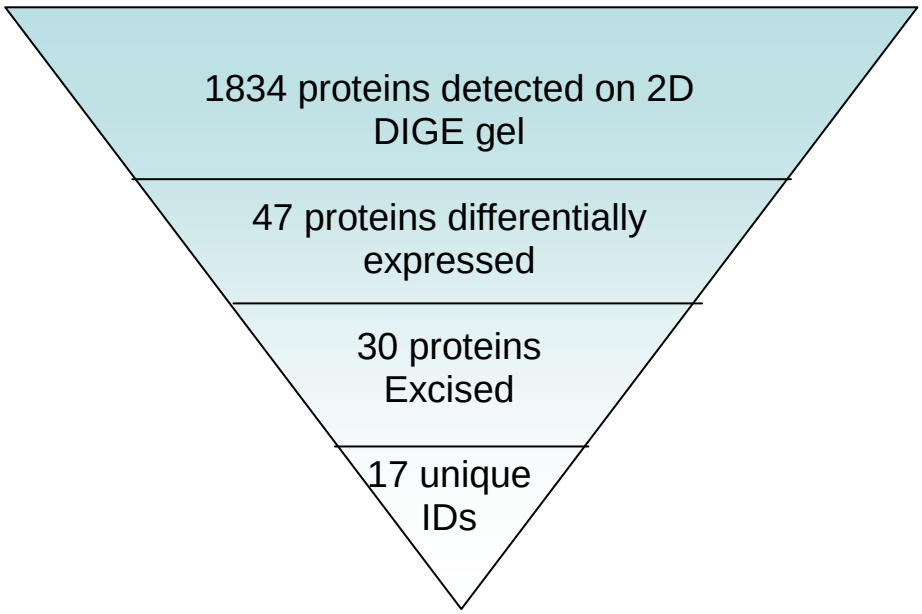

Figure 12: Schematic of total number of proteins identified using the combined proteomics workflow.
Of the 1843 unique protein spot boundaries that were assigned in the CBG proteome, 47 protein spots were differentially expressed following densitometric image analysis of the fluorescently labelled proteins using DeCyder 6.0. Spots from 2 different experiments were compared to a reference map containing a 50/50 mixture of the young and aged sample and labelled with Cy2 dye. Using MS, database search and subsequent gel matching, 17 unique proteins were identified which were altered in the aged CBG.

2.4.6 RESULTS (II): VALIDATION OF AGE-RELATED PROTEIN CHANGES

Validation of the proteins identified through proteomics is an integral component of the screening process to confirm that protein alterations are accurately represented during 2D DIGE analysis. Due to the limited commercial availability of some antibodies and out of an economic consideration, AChBP, α-tubulin and β-actin were selected for further confirmation by Western Blot analysis of proteins isolated from young and aged *L. stagnalis* CBG.

2.4.6.1 Method Development

The sample extraction procedure for Western blot analysis was the same as that describe for 2D PAGE. Samples were extracted in 2D Lysis buffer and acetone precipitated as described previously (see section 2.2.0).

2.4.6.2 Western Blot analyses of AChBP expression

For a 10 μg protein load/ lane, the primary anti-*Lymnaea* AChBP antibody was optimal at 1/10,000 dilution, whereas the secondary anti-Guinea Pig antibody conjugated to HRP was optimal at 1/20,000 dilution. The AChBP protein expression analysis confirmed a statistically significant decrease in the aged CBG compared to young CBG (43.81 ± 30.67%), when normalised to GAPDH ($p < 0.05$), $n = 4$ pools of 20 individuals (Figure 13). Statistical analysis was performed using standard t-test. Shapiro-Wilk test and Mann-Whitney U test was also used to allow for non-parametric variation of data. Both methods showed comparable significance in the data set (see Appendices).

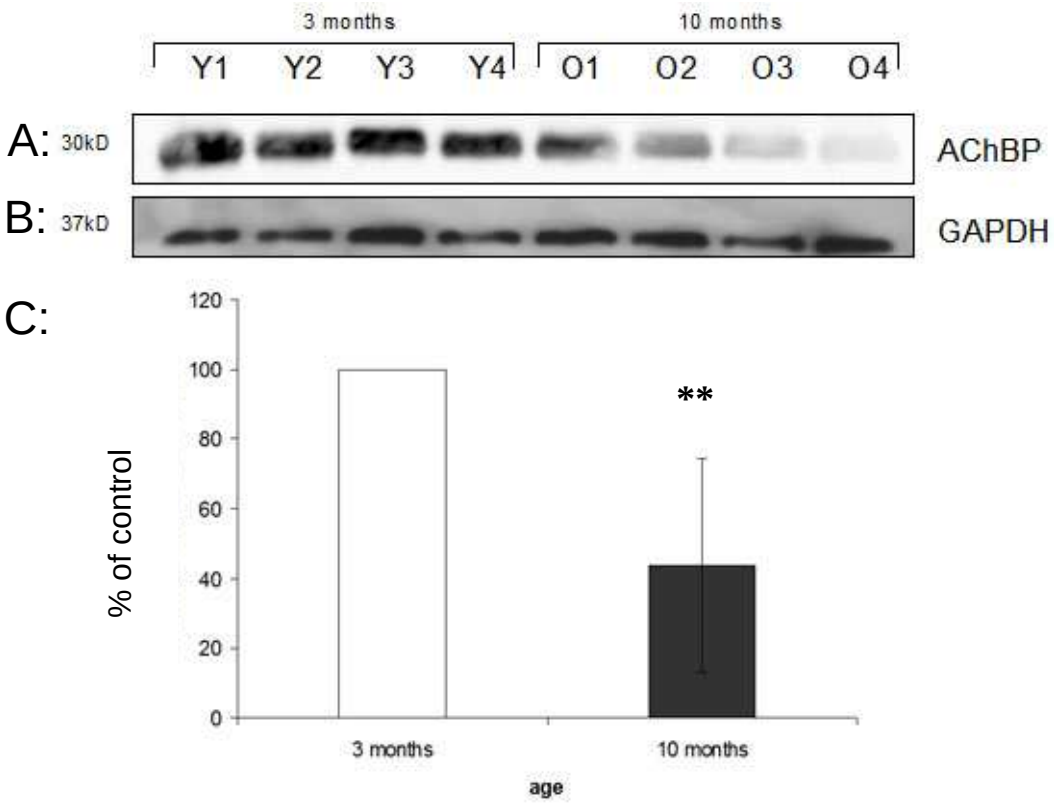

Figure 13 Western Blot analyses of AChBP expression in young and aged CBG show decreased AChBP protein expression.
Densitometry values of AChBP expression (A) were normalised against GAPDH (B) and expressed as a percentage of the young (C) (n=4). The data are represented as mean ± SEM, ** indicates statistically significant differences, $p < 0.05$.

2.4.6.3 *Western Blot Analyses of α-tubulin expression*

Anti-α tubulin antibody (Santa Cruz, sc-12462) was optimal at 1/200, and anti-goat secondary was optimal at 1/2,000 as per manufacturer's instructions. Western Blot analysis showed α-tubulin expression increased in the aged CBG compared to young CBG (110 ± 9.70%) when normalised to GAPDH ($p > 0.05$), n = 3 (Figure 14).

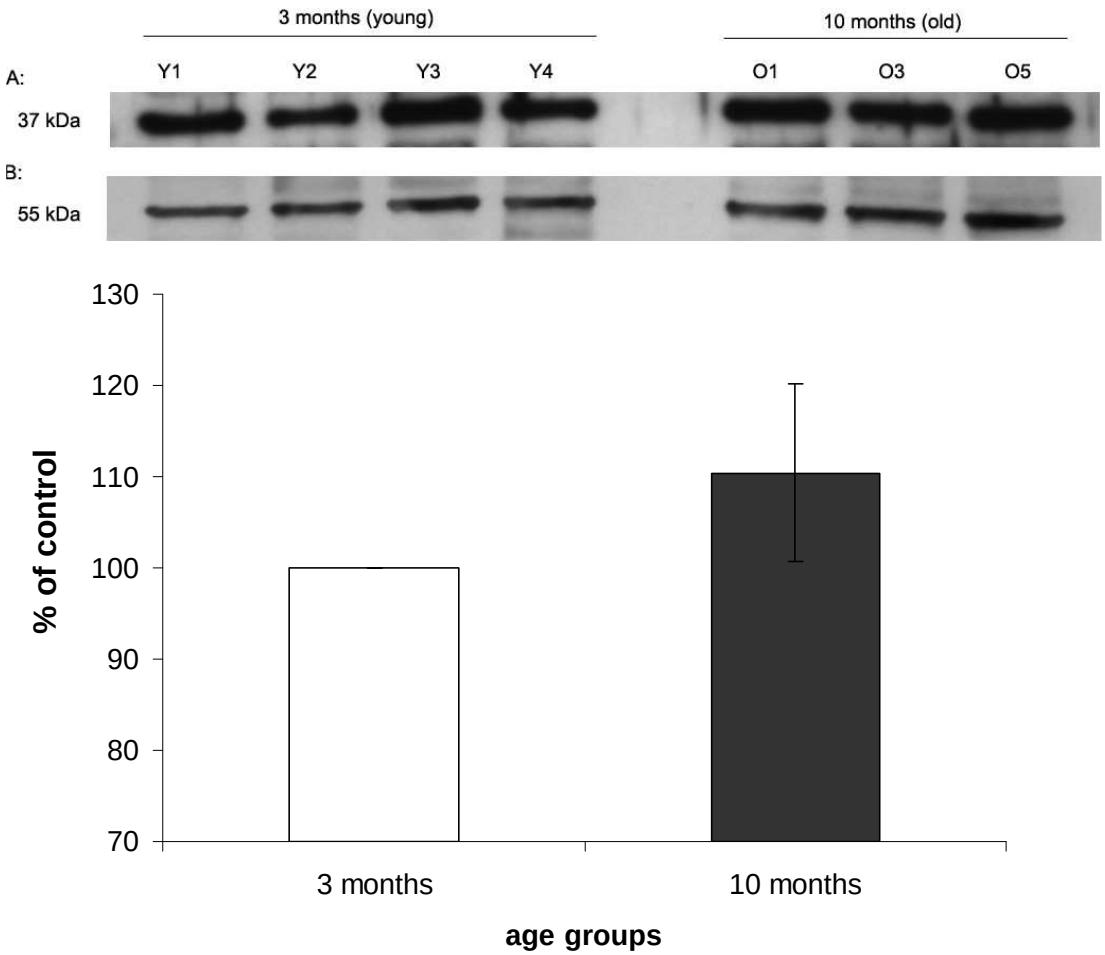

Figure 14 α -tubulin protein expression in the young and aged cerebral and buccal ganglia.
Tubulin protein expression densitometry values (A) were normalised against GAPDH (B) and expressed as a percentage of the young 3 month aged animals ((n=4). Membranes were probed with primary antibody 1/200 (Santa Cruz Biotech); secondary antibody 1/ 4,000 (anti-goat conjugated to HRP), and data are represented as mean ± SEM.

2.4.6.4 Western Blot Analyses of β-actin expression

Anti- β-actin antibody (Abcam, ab8226) was optimal at 1/1,000 dilution and a secondary anti-Guinea Pig antibody conjugated to HRP was optimal at 1/2,000 dilution. Western Blot did not show an age-related decrease in the β-actin expression in the aged CBG when compared to young (98.62± 9.13%) and normalised to GAPDH, n = 3 (Figure 15). Statistical analysis was performed using standard t-test and assuming unequal variance which failed to show a statistically significant difference ($p > 0.05$); (see Appendix section).

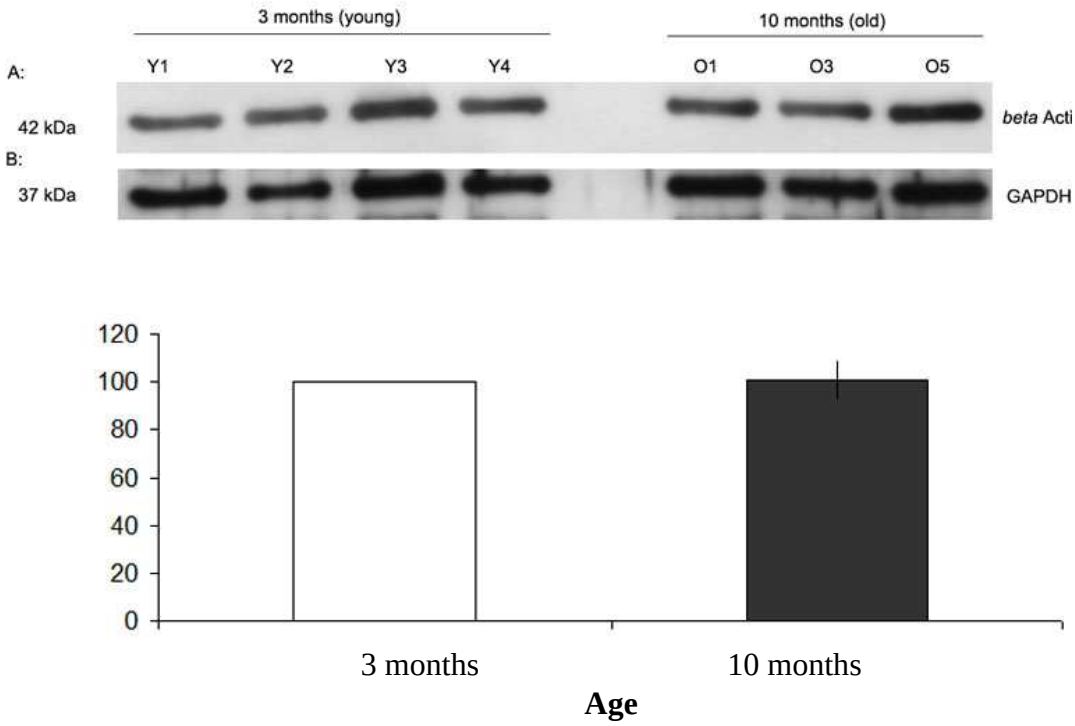

Figure 15 Age-related changes in β-actin expression in the aged cerebral and buccal ganglia of *L. stagnalis*.
β-actin protein densitometric values (A) were compared in 4 young and 3 old CBG and normalised to GAPDH (B) and expressed as a percentage of control. Data are represented as mean ± SEM, $p>0.05$.

2.5.0 DISCUSSION:

Ageing of the brain is an intricate process in which multiple cellular components that regulate neuronal function are affected as a function of time (Mattson and Magnus, 2006). In the *L. stagnalis* nervous system, the structural organisation of the CNS allows robust analysis of distinct populations of neurons that regulate the feeding behaviour in a manner that is not always possible in higher vertebrates. Benjamin *et al*. (1979) defined the subset of neurons that regulate the rasp, swallow and protraction phase of the feeding cycle which are regulated by neurons that reside within the cerebral and buccal ganglia (CBG) of *L. stagnalis* (also see chapter 1). Arundell *et al*. (2006) examined the feeding behaviour in chronologically aged animals and reported there was a significant reduction in the number of sucrose-evoked bites in the naturally aged 10 month (old) *L. stagnalis* when compared to 3 month (young) animals. However, the precise molecular events that participate in the reduction of feeding behaviour have not been clearly defined.

As a way of identifying protein candidates that participated in the age-related change in feeding pathway, the CBG of behaviourally characterised young (3-4 months) and naturally old (10-11 months) *L. stagnalis* were examined using 2D DIGE. Results indicated specific groups of proteins are altered as the animals' age, some of which have been previously reported to be altered in the other animal models of ageing.

2.5.1 Cytoskeletal dysfunction in the aged CBG

Comparison of proteins from young and aged CNS revealed cytoskeletal and cell signalling proteins as the top divergent categories. The frequent identification of intermediate filaments and cytoskeletal proteins is not altogether surprising considering these proteins are highly abundant and are therefore easily identifiable in proteomic assays. Secondly, cytoskeletal proteins are integral to the guidance and transport of signalling proteins along the cell and disruption to cytoskeletal function are a prominent feature in normal ageing (Chen *et al.*, 2003; Benuck *et al.*, 1996; Carrette *et al.*, 2006).

Actin, an abundant monomeric subunit of microfilaments which are present in both neurons and glial cells and participate in functions as diverse as cell signalling, to the

movement of vesicle along the axons (Arking, 2006), was decreased in the aged CBG (Figure 10D). DIGE analysis revealed β actin levels were downregulated by 10% in the aged CNS (Figure 10D), whereas a separate protein identified as cytoskeletal actin was downregulated by 1.68 fold in the aged CBG (Figure 10L). The actin-binding proteins such as tropomyosin-2, that can stabilise and regulate actin mechanics, was also downregulated by 1.31 fold in the aged CBG (Figure 10E). Proteomic analysis revealed that the gamma subunit of tropomyosin-3 was downregulated in the naturally aged mouse brain (Yang *et al.*, 2008). This view is shared by Sato *et al*. (2005), who suggest a reduction of β-actin levels in the aged hippocampus may contribute to impaired synapse formation and synaptic plasticity observed in aged neurons. Fountoulakis *et al*. 2000 also reported β-actin levels were reduced in the adult rat brain compared to neonates. Decreased β-actin expression in synaptic areas such as the pre-synaptic nerve endings and post-synaptic dendrites where β-actin are abundant may reflect synaptic alterations with increased age (Fountoulakis *et al.*, 2000). Synapse-specific alterations in serontonergic neurons was recently reported in the aged *L. stagnalis* (Yeoman *et al.*, 2008), and alterations in cytoskeletal dynamics through actin or actin-associated proteins are likely to contribute to this dysfunction.

The identification of motor proteins such as kinesins that participate in the recruitment of vesicles during Ca^{2+}-regulated exocytosis (Bi *et al.*, 1997), was also decreased in the aged CBG region (Figure 10F). Recent reports suggest actin expression can be attenuated during nerve injury in the *L. stagnalis* nervous system, suggesting a role of actin in retrograde signalling (Perlson *et al.*, 2004). A 1.10 fold decrease in β--actin expression observed in the proteomic study was not confirmed using Western Blot analysis. Increasing the sample size per treatment group in this case was not possible due to limited availability of aged protein sample from the CBG, leaving open the possibility that such a small difference in protein expression may not have been detected through Western Blot analysis.

Based on the above findings, it would be predicted that a down-regulation of actin, tropomyosin-2 and kinesin-like protein may significantly impair the transport and release which is regulated by Ca^{2+}-mediated stimuli. Such networks are likely to contribute to the higher inward Ca^{2+}-currents that are observed in aged *Lymnaea*

neurons (Frolkis *et al.*, 1991) (also section 1.3.0). The destruction of the actin cytoskeleton are also linked to the acceleration of apoptotic events through activation of caspases that can sever actin filaments in an unregulated manner (Kaji *et al.*, 2004), as well as the increased production of ROS within the mitochondria that can lead to cell death (Gourlay and Ayscough, 2005). As the *L. stagnalis* CBG contains a mixed population of cell types, it is difficult to speculate whether cells may be undergoing apoptosis during normal ageing, and further work is required to clarify the specific role(s) of cytoskeletal molecules in regulating this function.

The protein in Figure 10G was identified as 55kDa α-tubulin. α-tubulin subunit transportation is integral in axonal outgrowth to allow for the neuronal cytoskeleton to grow and shrink by loss or addition (dimerisation) of α-tubulin subunits to form microtubules (Miller and Joshi, 1996). Considerable evidence suggests disruption to calcium homeostasis which is a prominent feature of the ageing nervous system (see Chapter 1), are also impaired in the aged *L. stagnalis* nervous system (Frolkis *et al.*, 1991), and calpains, as activators of MAPK pathway can directly modify cytoskeletal proteins such as α-tubulin when neurons that are exposed to increased calcium influx (Kaji *et al.*, 2004; Benuck *et al.*, 1996). Our data suggests α-tubulin expression was increased in the aged *L. stagnalis* cerebral and buccal ganglia by 1.13 fold. However, further work is required to confirm α-tubulin expression levels, as this study failed to detect a statistically significant difference when the protein was validated using Western blot, $p > 0.05$. A possible biological role for increased tubulin expression may be a compensatory mechanism to recompense for increased calpain activation. However calpain activation has not been examined in the aged *L. stagnalis* nervous system, and further studies should examine this in conjunction with α-tubulin expression.

One of the more prominent features to suggest there are cytoskeletal impairments in the aged CBG was the identification of the *L. stagnalis*-specific intermediate filament, retrograde protein 51 (RP51) that was previously reported to be upregulated in axoplasms following nerve injury (Perlson *et al.*, 2004). Like the mammalian peripheral nervous system, neurons within the invertebrate CNS retain the ability to regenerate following nerve injury (Snider *et al.*, 2002). dsRNA targeted against RP51 caused a significant reduction in neurite outgrowth in *L. stagnalis* Pedal-A

neurons, suggesting RP51s are involved in the signalling events underlying regeneration of neurites in these neurons (Perlson *et al.*, 2004). From the current study, there was a significant upregulation of RGP51 expression in the aged CBG by 2.72 fold (Figure 10C). However, validation of RGP51 using Western Blot was not possible due to the lack of a commercially available antibody but the data presented here is of potential interest. Firstly, RP51 was annotated and present in the NCBI non-redundant database. Therefore *de novo* sequencing gave a highly confident match to the protein and false positive identification of the protein was therefore obviated as RP51 is a *Lymnaea*-specific protein. Secondly, the 2.72 fold increase observed aged neurons was well above the threshold required to discriminate altered expression using 2D DIGE (cut-off at 10%). Thirdly, spot C (Figure 10) was represented as at least 5 independent protein spots, each of which was confirmed independently as RP51. The pattern of expression of the multiple spots on the 2D PAGE gel is suggestive of a posttranslational modification of RP51 (horizontal streaking on PAGE gel), although it was not possible to examine the modifications directly using the current methodology.

Unlike nerve injury that resulted in the upregulation of the RGP51 as well as the detection of its cleavage products at 16kDa, 27kDa and 36kDa (Perlson *et al.*, 2004), no cleavage products were detected in the current study. Perlson *et al*.2004 used an *in vitro* cleavage assay to demonstrate ^{35}S-RGP51 could be cleaved in the axoplasm, but blocked in the presence of the calcium chelator EGTA or the calpain inhibitor, calpeptin (Perlson *et al.*, 2004). The conclusions derived from Perlson *et al*. 2004 study suggests calpain-mediated activation following nerve injury may participate in proteolysis of cytoskeletal accessory proteins such as RGP51 that may account for the increased RP51 expression following nerve injury. Although no cleavage products of RGP51 were detected in the present study, and indeed nerve injury may not be part of the normal ageing process in *L. stagnalis*, the reported observation that calpain mediated proteolysis may be inherently related to increased RGP51 levels suggests a similar mechanism may be occurring in the normally aged CBG of *L. stagnalis*.

2.5.2 Altered regulation of proteins involved in energy metabolism:

There is evidence to suggest the regulation of the mitochondrial respiratory chain which is heavily reliant on the relationship between reductase expression and REDOX metabolism, and thereby the regulation of free radical generation (Arking, 2006), are compromised in the aged CBG. Reductase, and oxidoreductase utilise the NAD+ substrate in the citric acid cycle to facilitate the reduction of FAD to phosphorylate ADP to ATP during ATP synthesis (Arking, 2006). The protein shown in Figure 10L was identified as the enzyme reductase which was down-regulated in the aged animals by 1.53 fold compared to controls ($p < 0.05$) (Figure 10). A separate protein, Figure 10P was also identified as the *L. stagnalis*-specific probable reductase. As important intermediates, and key controllers of the citric acid cycle, reductase enzymes play an important link in the generation of energy metabolism. Although the expression of reductase was not validated using Western Blot, the identification of two unique protein spots (one of which was *L. stagnalis*-specific) from the same protein family provide a level of confidence in the two datasets. A potential decrease in reductase levels in the CBG could impair the ability of mitochondria to generate ATP within the neurons. Dopaminergic cells for example in patients with Parkinson's disease show selective reductase deficiency that are key contributor's to dopaminergic cell death (Schapira *et al.*, 1992). Studies performed using the selective neurotoxin 6-hydroxydopamine suggests disruption to dopaminergic neurons is another mechanism which results in the reduction of feeding behaviour (Kemenes *et al.*, 1990). Thus in conjunction with the participation of reductase in the citric acid cycle, its reduction could also target dopaminergic neurons that contribute in the regulation of the feeding behaviour. It remains to be confirmed whether such an event reflects a global decrease in reductase expression or whether it could be isolated to subgroup of neurons within the ganglia that are more vulnerable to the ageing process.

The profiles observed of two enzymes, lysozyme and glutathione-S-transferase also suggest differential regulation of the REDOX homeostasis in aged animals. Spot K was identified as lysozyme protein (Figure 10). Lysozymes are one of the lesser known family of proteins called 'defensins' which are active in providing the host with increased defence against infection, including antibacterial activity (Liu *et al.*,

2006). In *C. elegans*, a knockdown of Lysozyme, Lys-8 can reduce the lifespan of the organism (Pinkston-Gosse and Kenyon, 2007). Conversely, increased insulin levels prevented ubiquitin-mediated degradation of lysozyme, suggesting decreased insulin signalling as experienced in calorie-restricted animals (see chapter 1) can alter the proteosome activity directed against lysozyme degradation in the aged animal (Bennett *et al.*, 2000). Explained by this line of argument, it is plausible that a reduction in lysozyme levels by 1.34 fold reflects a reduced ability of *L. stagnalis* to defend itself against infections in naturally aged animals. An alternative explanation is offered by Liu *et al.* 2006, who report lysozymes contain an 18 amino acid domain that are capable of binding to advanced glycation end products (AGE) which are known inducers of ROS (Liu *et al.*, 2006). This suggests a reduction in lysozyme activity may also accelerate the formation of ROS in the aged CBG. At the extreme end, elevated lysozyme levels are associated with accumulated fibrillar protein deposits in the extracellular space in diseases such as amyloidosis (Liu *et al.*, 2006), however this account may be disease-specific and not reflect lysozyme levels during the normal ageing process.

Glutathione-S-transferase on the other hand, represent a major group of mainly cytosolic enzymes that detoxify lipid peroxidation products that progressively accumulate in the aged organisms, and in so doing conjugate the electrophillic substrates to glutathione (Martnez *et al.*, 2003). Glutathione levels are reduced in a number of aged animals including rats and mice, that suggests there is a shift in the antioxidant homeostasis that is offered by glutathione into a pro-oxidant state (Rebrin and Sohal, 2008). Gopal *et al*. (2000), suggested GST enzymatic activity was significantly increased in 12 month aged rat cerebral hemisphere compared to 3 month young animals, and this correlated well with the level of lipid peroxidation in the tissue. As such, the 1.26 fold increased GST levels in the aged CBG may be indicative of the increased levels of lipid peroxidation products may have accumulated in the aged CBG (Figure 10B).

Glycolate oxidases are also part of the oxidoreductase family of proteins that was increased by 1.22 fold in the aged CBG (Figure 10K). Although glycolate oxidases are predominantly associated with plants and bacterial organisms in the glyoxylate cycle that facilitates in the conversion of fatty acids into carbohydrate, there is

limited information available on its role in higher organisms. Kohler *et al*. 1999 demonstrated that rat hepatoma cells were able to up regulate glycolate oxidase mRNA levels in response to iron salt, and suggest the iron regulatory protein (IRP) domain present in the both mammalian and spinach glycolate oxidase may enable it to regulate iron metabolism. Transition metals such as ferrous ion (Fe^{2+}) are able to convert H_20_2 non enzymatically into the more toxic superoxide ion and hydroxyl radical which can be detrimental to the cell (Schipper, 2004). Upregulation of glycolate oxydase in the aged CBG could therefore be used as a defence strategy against oxidative damage by reducing the production of more toxic and damaging forms of free radicals. Based on the sequence similarity of these domains, it would be anticipated that glycolate oxidase are involved in the detoxification of glycolate via oxalate synthesis as has been proposed by Kohler *et al*. 1999. However, the exact functional relevance of glycolate oxidase remains in the aged CBG is currently unclear.

Spot J, identified as arginine kinase (Figure 10) is a homologue of the vertebrate creatinine kinase which are involved in the transportation of the γ-phosphate group of ATP from the mitochondrial matrix to the mitochondrial interspaces where ATP is converted to ADP was increased by 1.27 fold in the aged CBG (Reddy *et al.*, 1992; Wyss and Kaddurah-Daouk, 2000). Experiments derived from 2 different mouse strains suggest creatinine kinase levels are up-regulated in normally aged vertebrate brains, although the presence of multiple isoenzymes within the vertebrate nervous system may represent a more complex and refined interaction (Yang *et al.*, 2008; Carrette *et al.*, 2006). Several explanations exist on how arginine kinase levels could modulate the rate of ATP production; however further upstream targets are required of the citric acid cycle to make conclusive comments on the role of arginine kinase in the aged CBG.

2.5.3 Altered regulation of protein synthesis in the aged CBG

Our data suggests the protein identified as 40S ribosomal protein, increased in expression by 1.57 in the aged CBG (Figure 10N). The 40S ribosomal proteins are encoded by the same gene as the 37kDa precursor of the 67kDa Laminin receptor, and are reported to have an evolutionarily conserved dual role (Ardini *et al.*, 1998), which along with its involvement in the translational machinery, steers and regulates

laminin-mediated migration during neurite growth (for review see Powell *et al*.1997; Plantman *et al*. 2008). Toda *et al*. 2007, suggest 40S ribosomal protein are upregulated in the human dopaminergic neuroblastoma cell line SH-SY5Y when exposed to oxidative stress conditions, suggesting 40S ribosomal protein may be upregulated in particularly vulnerable systems such the dopaminergic system during the ageing process. An alternative explanation was offered by Plantman *et al*. 2008, who reported exogenous application of laminin to mouse dorsal root ganglion could promote neurite outgrowth in culture. This suggests upregulation of 40S ribosomal protein as described here could serve a neuroprotective role. It is presently unclear whether 40S ribosomal protein expression suggests a general increase in protein translation, or whether it plays a neuroprotective role on particularly vulnerable neurotransmitter systems in the aged CBG.

2.5.4 Altered chaperone function in aged CBG

Whilst the recruitment of lysozymes has been shown to be associated with protein aggregation, chaperones such as 14-3-3 proteins are employed to offer a level of support to prevent unspecific aggregation of partially denatured proteins that are commonly observed in age-related diseases such as Alzheimer's Disease as well as in Parkinson's Disease (Söti and Csermely, 2002).

The existence of multiple 14-3-3 isoforms represented a potential problem during identification of the specific isoform that was altered in the aged CBG (Figure 10A). In *C. elegans*, the existence of two 14-3-3 homologues (*ftt-1* and *ftt-2*) have functionally distinct roles which work through DAF-2 dependent and DAF-2 independent-pathways respectively to promote stress resistance in the animal (Araiz *et al.*, 2008). The ability of 14-3-3 to regulate lifespan may be due to its ability to assist in the repair the proteotoxic damage that accumulates with advanced age (Nardai *et al.*, 2002). To mark this function, the major classes of chaperones use ATP-driven mechanisms to fold and re-fold damaged proteins to maintain a level of function whereby protein aggregation does not occur (Söti and Csermely, 2002). In order to maintain the conformational homeostasis of misfolded proteins, chaperones including crystallins, 14-3-3 proteins, small heat-shock proteins, Hsp-70, Hsc-70, and Grp 78, utilise a number of smaller co-chaperones such as Hsp-90 (Inoue T, 2006; Söti and Csermely, 2002). Impairment in protein folding can lead to alteration

in ubiquitin-proteosomal activation, in which misfolded proteins earmarked for degradation accumulate over time (see chapter 1).

Alignment of 14-3-3 clones from a *Lymnaea* cDNA CNS library revealed 3 possible isoforms present in *L. stagnalis*, one of which showed the highest homology to the mammalian epsilon subunit (see Appendix). Fountoulakis *et al*. 2000 reported 14-3-3 epsilon subunit was decreased in the aged rat brain compared to neonates, however its precise role in aged brains remains to be clarified. The protein sequence alignment of 14-3-3 across a number of different species suggested the majority of the amino acids of 14-3-3 were highly conserved across all species, with minor variations in the C terminal domain (see Appendices). The peptide fragments identified through MS/MS analysis matched regions that were identical in all three isoforms, therefore the exact isoform that was downregulated in the aged CBG could not be confirmed. Studies are now in progress in our laboratory to elucidate role and identification of the 14-3-3 like protein that was observed to be reduced by 30% in the aged CBG ganglia as represented in Figure 11A.

In contrast to 14-3-3-like protein, Heat-shock protein-90 (Hsp-90) expression increased (Figure 10I) in aged *Lymnaea* CNS highlighting potentially dynamic role(s) which chaperones play during the ageing process. Among the multi-functional role of HSP-90, it is inducible under heat stress conditions (Inoue *et al.*, 2006). However at physiological temperatures its involvement are diverse and depending on the formation of multiprotein complexes with other proteins, HSP-90 has been shown to be involved in the stability of cell cycle related protein kinases in *C. elegans* (Inoue *et al.*, 2006), to telomerase function and ageing regulation (Kim *et al.*, 2005). HSP-90 specifically binds to hTERT to promote telomerase activity (Kim *et al.*, 2005). Recent evidence suggests HSP-90 was downregulated in the aged mouse brain (Yang *et al.*, 2008). However, it is unclear whether this down-regulation was region-specific or globally decreased throughout the mouse CNS (Yang *et al.*, 2008). As HSP-90 has multi-functional roles, and the profiled CBG contains a mixed population of mitotic and post-mitotic cells, it is difficult to speculate on whether the increased HSP-90 levels represent a specific effect on a particular cell type, or whether it is in response to an increased level of oxidative stress in the CBG.

2.5.5 Altered cholinergic signalling in aged CBG

The data discussed so far suggests age-related reduction in mitochondrial function, alteration to REDOX signalling and protein synthesis may be compromised in the aged CBG. However additional changes were seen that did not fit this framework. Acetylcholine binding protein (AChBP) was identified to be downregulated by 71% in the aged CBG (Figure 10H). Glial cells which actively release this cholinergic mediator in an ACh-dependent manner are believed to regulate cholinergic transmission by binding to the neurotransmitter acetylcholine in the *Lymnaea* nervous system (see chapter 3) (Smit *et al.*, 2001). Given that other proteins may play an important role in the modulating the effects of feeding in *Lymnaea*, the close proximity of glial cells to neurons, represents the possibility that a reduction in AChBP levels in aged animals could directly alter neurotransmission, and influence the feeding behaviour. Mammalian systems lack a functional homologue of AChBP, therefore a direct functional comparison was not possible here. However, selectivity-based studies suggest AChBP pharmacologically resembles the α7 nAChR but lacks the pore forming domain or intracellular domain that typifies a nAChR (Smit *et al.*, 2003). Hence age-related reduction in α7 nAChR mRNA levels that are observed in the normally aged human frontal cortex (Utsugisawa *et al.*, 1999), can not be directly compared to functional changes that may be occurring in AChBP, as they are pharmacologically similar but functionally distinct proteins. However, it is plausible that components of cholinergic signalling in part through AChBP signalling may be altered in the aged CBG (also see chapter 3). Cholinergic abnormalities described through the cholinergic hypothesis suggest cholinergic dysfunction is an important component of the ageing process (for review see Terry *et al*. 2003). Understanding the divergent cholinergic role of AChBP herein may lead to a greater understanding of why some cholinergic pathways remain preserved whilst others are disrupted with advanced age. A high level of confidence was assigned to AChBP during *de novo* sequencing as the sequence was matched to an annotated *L. stagnalis* protein present in the nr database (Smit *et al.*, 2001). Validation of AChBP protein expression using Western Blot further confirmed the proteomic data showing a comparable reduction in AChBP reduction in the aged CBG (Figure 13). Further examination of this protein will continue in Chapter 3.

2.6.0 TECHNICAL CONSIDERATIONS DURING PROTEOMIC PROFILING

The proteomic workflow can be divided into 3 distinct stages; protein separation, peptide fragmentation and protein identification. In the first stage, proteins were solubilised in 2D Lysis buffer and resolved using 2D DIGE that allowed proteins to be separated according to their molecular weight and isoelectric point on a polyacrylamide gel but also enable detection of protein spots that were differentially expressed between the control and aged animals. High molecular weight proteins or highly acidic or alkaline proteins are not fully resolvable and therefore not represented on a PAGE gel. This left open key areas such as membrane-bound proteins which could not be examined using 2D DIGE (Tsugita *et al.*, 2000). However the reproducibility of the proteins that were represented on the PAGE gel was significantly enhanced by using fluorescent dyes (CyDye™) to tag an internal pooled standard containing a 50:50 mixture of young and aged CBG that was run in all gels to calibrate and account for inter-gel variability across all gels. Therefore the statistical power was significantly increased compared to conventional PAGE separation methods (Karp and Lilley, 2005). In the second stage, protein spots of interest were fragmented using a high-end LTD Orbit-trap to obtain the high mass accuracy for protein identification for *de novo* sequencing. *De novo* sequencing matched the peptide fragments against theoretical tryptic digests of protein homologues that were present in the non-redundant database. However, the search parameters used to identify peptide fragments which tolerated 1 missed tryptic cleavage, a carbamidomethyl modification of cysteine residues as well as possible mass shifts due to possible oxidation of methionine, or phosphorylation of serine, threonine or tyrosine, did not successfully assign a confident 'hit' to some proteins that were less abundant than the highly abundant contaminants such as keratin. Therefore, using an exclusion list designed to eliminate known contaminant masses from recurrent analysis, could not indentify low abundant transcripts with over 90 percent accuracy.

Secondly, isoenzyme differences with proteins such as 14-3-3 protein, and actin could not be distinguished due to the detection of residues that were not specific to a particular epitope. Alternative methodologies may be recommended such as digestion of the protein of interest using chymotrypsin instead of trypsin to obtain a

different fragmentation profile that may be specific for a particular subunit. However this trial and error approach is limited since the exact fragmentation pattern of the peptides can not be predicted in advance. Therefore, epitope-specific residues may not become obvious if for example the *L. stagnalis* proteins were not directly related to homologous proteins that are present within the nr database. Thus, without the aid of the *L. stagnalis* genome, the limitations in using a *de novo* sequencing approach as it currently stands mean that the identify of highly homologous proteins that are present in the nr database can be identified, but this process may not be able to distinguish organism-specific proteins or epitope-specificity residues unless the epitope-specific residues are detected during the fragmentation of the peptide.

2.7.0 CONCLUSION & FUTURE DIRECTIONS

In the *L. stagnalis* nervous system, the cerebral and buccal ganglia that regulate the feeding circuitry was assessed to examine proteins that were altered in the aged animal that could participate in the reduction in feeding behaviour. To this end, 2D DIGE was implemented to identify proteins that were differentially expressed in the aged CBG region. LC MS/MS and *de novo* sequencing was used in combination to deduce the identities of the proteins of interest. The findings in the current study are in line with the protein groups that were observed to be altered in the normally-aged mouse brain using proteomic profiling (Tsugita *et al.*, 2000).

Several recurrent findings of protein groups belonging to mitochondrial, cytoskeletal, and chaperone function were altered in the naturally aged CBG. The main ontological groups altered in the naturally aged *L. stagnalis* CBG region are well aligned with the themes highlighted in the free radical theory of ageing (see Chapter 1). Due to the limited commercial availability of antibodies for many of the proteins identified, only AChBP, tubulin and actin was validated in the current study. AChBP was successfully validated using western blot and therefore represented a validated target in which to pursue further investigation.

AChBP is of potential interest due to its proposed role in directly regulating cholinergic signalling in defined networks (Smit *et al.*, 2001). Cells within the CBG that participate in the feeding behaviour are heavily innervated by cholinergic neurons (Nierop *et al.*, 2006; Yeoman *et al.*, 1993). Our data suggests cholinergic signalling through AChBP may be impaired in the aged CBG. However, as a glial specific protein, it is presently unclear whether the reduction in AChBP reflects impairment in glial cells in the aged CBG. Furthermore, it is unknown whether a transcriptional decrease in AChBP regulated the decrease in AChBP protein levels. Finally it is unknown whether a decrease in AChBP expression can contribute to a reduction in feeding behaviour that is observed in the aged *L. stagnalis*. The subsequent chapters of this thesis will examine these questions in greater detail.

Chapter 3: ANALYSIS OF AChBP mRNA LEVELS AND GFAP PROTEIN LEVELS IN THE AGED *L. STAGNALIS* CBG

3.1 BACKGROUND

Cholinergic abnormalities in the nervous system are intrinsically related to how well neuronal cells respond to the excitatory neurotransmitter acetylcholine (ACh). Virtually all cell types including glial cells that make contact with synapses, respond to neurotransmission by an increase in cytosolic Ca^{2+} concentration, a key event observed when glial cells are co-cultured with neurons (Smit *et al.*, 2003). Ca^{2+} dysregulation in neurons of aged rodents have contributed to the formulation of the "Ca^{2+} hypothesis of brain ageing and dementia" (Landfield and Pitler, 1984). Proposed in the early 1980's, the hypothesis states that alterations in Ca^{2+}-dependent processes during ageing may affect Ca^{2+} signalling pathways and, consequently impair neurotransmission (Landfield and Pitler, 1984). Glial cells have the ability to release a variety of neuroactive molecules, including glutamate, ATP, nitric oxide and ACh which in turn can influence neuronal excitability (for review see(Karlin, 2001). This bi-directional signalling between glial cells and neurons represents a third active element together with the pre and postsynaptic signalling, referred to as tripartite synapse which makes the anatomical coupling and close proximity of glial cells to synapses ideal candidates to directly influence neurotransmission (Smit *et al.*, 2003).

Several subtypes of glial cells that are present in vertebrate species, have been identified in *L. stagnalis* (Kruatrachue *et al.*, 1999). However, in addition to neuronal activation of nAChRs, ACh stimulates the secretion of AChBP by *Lymnaea* glial cells (Smit *et al.*, 2003). Although ACh is hydrolysed by enzymatic degradation, ACh bound to AChBP is unable to cross into the postsynaptic cell (Smit *et al.*, 2001). The lack of esterase activity on AChBP suggests ACh bound to AChBP must be physically removed from the synaptic space in a mechanism that has yet to be defined (Smit *et al.*, 2001). In the molluscan central nervous system, glial cells are found throughout the brain, however their density and regional distribution differed significantly, leaving open the possibility that AChBP may selectively

mediate neurotransmission in localised networks of neurons (Smit *et al.*, 2003). Furthermore, the spatially segregated neurons which regulate the feeding pathway opened the possibility that AChBP may be able to regulate feeding in localised networks. Figure 16 represents a schematic of the function of AChBP at cholinergic synapses.

In addition, the glial cell within the nervous system of *L. stagnalis* was examined using the astrocytic marker glial acidic fibrillary protein (GFAP). Oxidative stress conditions that result in increased Ca^{2+} levels, also cause a concurrent increase in GFAP expression that are commonly associated with age-related alterations to glial cells. Western blot analysis was used to examine GFAP protein expression in the aged CBG compared to those of defined controls in *L. stagnalis* (see section 1.3.0 - 1.3.6).

3.1.1 An Introduction to cholinergic signalling:

3.1.1.1 Cholinergic targets:

In humans, the main cholinergic pathways run from the basal forebrain region to innervate the cerebral cortex and hippocampus. During normal ageing and in Alzheimer's disease these neurons undergo substantial degeneration (for review see (Giacobini, 1990). More recently, cholinergic dysfunction was associated with a loss of nAChRs, with no loss in cell numbers in post mortem aged human brain (Nordberg *et al.*, 1992). This suggests that an alteration in cholinergic signalling within areas such as the hippocampus and cerebral cortex that are important in regulating cognitive functions such as arousal, attention, learning and memory are receptor-specific and cognitive loss associated with receptor-specific decline could be improved by increasing cholinergic signalling (Giniatullin *et al.*, 2005). Evidence in favour of this hypothesis suggests clinical trials untaken to stimulate the cholinergic system using cholinomimetics such as donepezil, galantamine, and rivastigmine have shown symptomatic improvements by increasing the life cycle of ACh at the synapse (Pepeu, 2001). However, disruption to cholinergic signalling are evident on many levels including alteration to choline transport, acetylcholine release, nicotinic and muscarinic receptor expression, and decreased neurotrophin support which all contribute to cholinergic abnormalities and are recognised as key

participants in the progression of severe pathologies of the brain such as Alzheimer's Disease as well as normal brain ageing (for review see(Kelly *et al.*, 2006). Therefore simply elevating ACh levels alone is an ineffective means to increase cholinergic signalling due to unwanted side-effects through its actions on ion channels that may be unimpaired by the ageing process (for review see(Soreq and Seidman, 2001). For example, unwanted side-effects as a result of increased activation of muscarinic receptors can result in elevated parasympathetic responses such as increased sweating, secretion of glands in the digestive system, decreased heart rate, constricted pupils, and contraction of the smooth muscle of the respiratory, digestive and urinary systems (Eglen *et al.*, 2001).

3.1.1.2 Disruption of choline uptake at cholinergic synapses

Cholinergic cells use the enzyme choline acetyltransferase (Araiz et al.) to synthesise ACh from acetyl-coenzyme A, and choline (Bear *et al.*, 2006). Choline is derived from the diet and is one of the principle rate limiting steps in ACh synthesis. It is taken up into cells via a high affinity choline uptake (HACU) system (Yamamura and Snyder, 1972). When Brull *et al*. (2002) examined the kinetics of choline transport in aged rat hippocampus they reported that the ratio of the metabolites choline/ N-acetyl aspartate and choline/ creatine were increased *in vivo*, but creatine/ N-acetyl aspartate ratio was unaffected in the aged animals suggesting uptake of choline, as a precursor to the neurotransmitter ACh was increased in the aged hippocampus. This was in contrast to the finding that HACU was decreased in the aged rat hippocampus however there was a 3 fold increase in low affinity choline uptake in the cerebral cortex and hippocampus of aged rats, presumably to compensate for decrease in HACU and pointing to a mechanism whereby choline uptake was impaired in aged animals (Brull *et al.*, 2002).

3.1.1.3 Disruption to ChAT activity at cholinergic synapses

ACh synthesis relies on the enzymatic activity of choline acetyltransferase (Araiz et al.) in order for it to be synthesised on the ribosome's located in the soma of neurons and transported to the axon terminal (Eckenstein and Thoenen, 1982). Whilst ChAT activity was impaired in the cerebral cortex and hippocampus of aged Wistar rat, this

process was reported to be strain-specific, as the aged Fisher 344 rats do not show a the comparable decrease of ChAT in the aged hippocampus, but do show a significant decrease in ChAT in the aged cerebral cortex (Michalek *et al.*, 1989). In the cephalopod, *S. officinalis,* the superior frontal lobe, a region involved in motor behaviour and visual learning, age-specific reduction in ChAT activity was observed, suggesting cholinergic abnormalities may be part of the natural ageing process across all species (Bellanger *et al.*, 1997).

Once synthesised, ACh is concentrated into synaptic vesicles using the vesicular transporter (VAChT) (Weihe *et al.*, 1996). Depolarisation of the nerve terminal as a result of an action potential results in the release of ACh through exocytosis into the synaptic cleft (Terry and Buccafusco, 2003; Bear *et al.*, 2006). Once released, ACh produces a conformational change on two target classes of receptors, muscarinic (mAChR) and nicotinic (nAChR) receptors, both located pre- and postsynaptically (Bear *et al.*, 2006). The released ACh is subsequently inactivated by hydrolysis into the constituent acetic acid and choline by the enzyme acetylcholine esterase (AChE) and the choline is recycled back into the presynaptic nerve terminal (Giniatullin *et al.*, 2005). This mechanism is evolutionarily conserved, including in the mollusc *Lymnaea stagnalis* (Nierop *et al.*, 2006).

3.1.1.4 Cholinergic regulation by muscarinic acetylcholine receptors

ACh can act via mAChR which belong to a class of receptors that are G-protein coupled. The receptors are divided into a number of classes termed M1-M5 (Hulme *et al.*, 2003). In the brain, postsynaptic M1 and M3 receptors mediate the slow neuronal excitability via phospholipase C, which initiates phosphatidylinosotol turnover response and leading to increase in intracellular Ca^{2+} (Bonner *et al.*, 1987; Liles and Nathanson, 1987). The increase in Ca^{2+} regulates calcium-regulated potassium channels leading to the initiation of the after-hyperpolarisation phase of the action potential (Liles and Nathanson, 1987). In contrast, the M2 and M4 receptors inhibit adenyl cyclase activity through the activation of G-protein coupled potassium channels that lead to hyperpolarisation of the plasma membrane in excitable cells (Young *et al.*, 2005). The inhibition of neuronal firing observed

through M2 and M4 receptors are reported to participate in learning and memory (Young *et al.*, 2005). Moreover, there is a selective decrease in M1 and M2 nicotinic binding sites in the aged human cerebral cortex (Nordberg *et al.*, 1992). However M2 receptors were increased in the thalamic region compared to control, suggesting regional specialisation of subsets of mAChRs may contribute to contribute to cognitive decline in the aged brain (Nordberg *et al.*, 1992). The M5 mAChR in contrast were expressed at very low levels in the brain and its precise function has yet to be clarified. There is also an extensive loss of M1-subtype of mAChR experienced by patients with AD, thus compared to the other mAChRs, the M1 subtype of mAChR is the principal target in investigating age-related pathologies such as Parkinson's Disease and Alzheimer's Disease in which M1 agonists have shown symptomatic improvements (Langmead *et al.*, 2007). For a more detailed description of the involvement of mAChRs see Hulme *et al*. (2003).

3.1.1.5 Age-related changes in CNS nicotinic acetylcholine receptors

A diverse range of nAChRs have been classified in the mammalian CNS which specifically assemble into defined pentameric structures (reviewed in(Gotti and Clementi, 2004). Receptors composed of 5 structurally related subunits (homopentamers), or 5 structurally distinct subunits (heteropentamers) use combinations of α, β, γ subunits to form the pentameric structure of nAChR (Green, 1999).

In contrast to mAChRs, nAChRs are ligand-gated ion channels (LGIC's) organised around a central pore which elicit the rapid gating of ions by ACh binding to the extracellular domain of the α subunit interface (Sullivan *et al.*, 2002). The 200 amino acid residue of the α subunits consists of an N-terminal glycolipid region which possesses the ACh binding site and four hydrophobic regions that span the membrane. Nine α subunits have been cloned in total, along with four β subunits (reviewed in (Sullivan *et al.*, 2002; Gotti and Clementi, 2004). The C-terminal domain contains 4 transmembrane segment (M1-M4) that make up the channel pore component, and a 100 – 150 amino acid residues long intracellular cytoplasmic domain (Smit *et al.*, 2003). ACh, by binding to the extracellular site produces a

conformational change in the subunits to increase the transient flow of potassium or sodium ions through the channel (Giniatullin *et al.*, 2005).

Differentiation between the nAChR isoforms based on ligand binding affinity suggests heteropentameric nAChR such as the α4β2 subunit show a higher affinity to nicotine, whereas homopentamers structures such as the α7 nAChR show high affinity to α-bungarotoxin (Gotti and Clementi, 2004). Characterisation of the nAChRs based on the accessibility and affinity of different nicotinic ligands suggest the ligand binding affinity of nAChR is also dependent on its three distinct conformational states: basal or resting (closed, but rapidly activatable), activated (open), and desensitized (closed) state (Hansen *et al.*, 2005). Whilst it is unclear how the different nAChR subunits change during the normal ageing, *in vitro* evidence suggest nAChRs (especially α7) may control the development of neuronal architecture and stabilise synapse formation and neurite outgrowth (reviewed in (Gotti and Clementi, 2004). Accordingly, the two critical time points at which this process is most critical (i.e. during development and cellular degeneration during ageing) showed the greatest fluctuation in cholinergic signalling (reviewed in (Gotti and Clementi, 2004).

In aged animals, α7-dysregulation in the hippocampus is thought to be an important precursor to a number of age-related pathologies, including Alzheimer's Disease (reviewed in(Gotti and Clementi, 2004). Although α2 and α3 nAChR mRNA expression are selectively decreased in the aged rat hippocampus, no change was reported in α4 or α7-nAChR expression (Charpantier *et al.*, 1999). Other reports suggest whilst aged neurons show a selective loss of α7 and α4 nAChR, the expression of α7 receptors in astrocytes are increased (O'Neill *et al.*, 2002). Immunological and *in situ* hybridisation evidence suggests the highly expressed α7 nAChR within the hippocampus can activate presynaptic release of glutamate or GABA receptors (Alkondon *et al.*, 1997), which are important precursors to glutamate-mediated cytotoxicity that are assumed to be an important progenitor in cellular degeneration (Shimohama, 2009). In some cases, the selective activation of α7 and α4β2 nAChRs can signal the production of neurotrophic factors such as basic fibroblast growth factor (FGF-2) and brain-derived neurotrophic factor (BDNF) *in vivo*, suggesting differential regulation of α7 nAChR may be part of a

neuroprotective mechanism aimed at regulating glutamate-mediated toxicity (for review see (O'Neill *et al.*, 2002).

3.1.1.6 Neurotrophin receptor expression in cholinergic neurons

In 1963, Levi Montalcini and Angeletti first described the process by which nerve growth factor (NGF) (a member of the neurotrophin family) regulated the development and maintenance of noradrenergic peripheral sympathetic neurons – a finding that has now been extended to the several pathways within the central nervous system, including cholinergic signalling (Lewin and Barde, 1996). NGFs, which act through tyrosine kinase (trkA) receptors as well as the neurotrophin receptor p75 ($p75^{NTR}$) are increased in response to stimulation of the excitatory circuits connecting the dentate gyrus and the CA1 area of the hippocampus (Gall and Isackson, 1989). The activity-dependent release of NGF interacts with ChAT signalling in cholinergic neurons in the basal forebrain (Gustilo *et al.*, 1999). Intraventricular administration of NGF into basal forebrain neurons of adult rat brains prevented middle-aged animals from memory-related deficits (Klein *et al.*, 2000). The latter finding was correlated to increased in cholinergic cell size, suggesting NGF signals are able to modulate age-related memory deficits by regulating cholinergic signalling and therefore provide a means by which NGF signalling could directly participate in the regulation of cognitive functions such as learning and memory via its actions on cholinergic cells (Gustilo *et al.*, 1999; Lewin and Barde, 1996). This view is consistent with another report that showed a reduction in cell number and cell size of NGF/ ChAT positive cells in the aged rat basal forebrain showing morphological changes in cholinergic cells could be regulated through NGF signalling (Fischer *et al.*, 1992). Although disruption to NGF signalling are observed in the aged mammalian nervous system, the effects are not as obvious as those observed in AD where the retrograde transport of neurotrophins via trkA receptors are more pronounced (reviewed in (Frade and Barde, 1998).

3.1.1.7 Cholinergic signalling in L. stagnalis

Cholinergic signalling is an integral component of the feeding circuit in *L. stagnalis* (Yeoman *et al.*, 1993; Elliott *et al.*, 1992). Nicotinic acetylcholine receptors (nAChRs) residing in the central nervous system of *L. stagnalis* have been studied by a few authors. Most notably Smit and colleagues used degenerate primers to isolate 12 subtypes of nAChR subunit present in *L. stagnalis* CNS (Nierop *et al.*, 2005). Phylogenetic analysis of the derived sequences of the *L. stagnalis* nAChR (LnAChR) suggested the presence of cationic as well as anionic conducting properties in the LnAChR subtypes (Nierop *et al.*, 2005). Of the subtypes identified, LnAChR-A (cationic) and LnAChR-B (anionic) are the most abundant although oppositely expressed in the respective regions of the cerebral and buccal ganglia region, for example; LnAChR-A are highly expressed in the cerebral ganglia but lowly expressed in the buccal ganglia, whereas LnAChR-B are highly expressed in the buccal ganglia but lowly expressed in the cerebral ganglia (Nierop *et al.*, 2006). Functional expression of LnAChR-A and LnAChR-B in *Xenopus* oocytes suggests LnAChRs have evolved through a mutation of the ion pore channel (Nierop *et al.*, 2005). The presence of proline residue in the TM1-TM2 region in combination with the removal of charged residues nested within the intermediate rings are suggested to be the likely candidates for the conversion of cation to anionic ligand gated forms of ion channels (Nierop *et al.*, 2005). Although direct homologues to mammalian nAChRs have not been identified in *L. stagnalis*, pharmacological distinction between the subtypes suggest the presence of α-bungarotoxin sensitive and nicotine-sensitive nAChR in *L. stagnalis* central nervous system (Nierop *et al.*, 2005).

Morphometric analysis suggests synapse-specific alteration in cholinergic circuits at the *A. californica* neuromuscular junction where motor neurons L_7 are selectively vulnerable to ageing process compared to LDG1 neurons (Peretz *et al.*, 1984). However, age-related changes at cholinergic circuits in *L. stagnalis* have not as yet been addressed. For a detailed description on the effect of ACh on cholinergic neurons in the *L. stagnalis* feeding circuit see chapter 1.

3.1.1.8 Functional Properties of AChBP

Approximately 50% of glial cells in the *L. stagnalis* central nervous system (CNS) release the 25kDa AChBP in an ACh-dependent manner (Smit *et al.*, 2001). Along with acetylcholine esterase, the released AChBP is proposed to provide an additional mechanism by which to sequester ACh in the synaptic cleft resulting in an activity-dependent suppression of neurotransmission (Smit *et al.*, 2001) (see Figure 16). AChBP was also identified in the molluscs *Aplysia californica* (Hansen *et al.*, 2004) and in *Bulinus truncates* (Celie *et al.*, 2005). However orthologues of AChBP have not been identified in higher vertebrates, suggesting AChBP is a molluscan-specific protein.

Figure 16 Schematic illustration of the function of AChBP at cholinergic synapses (Lopez, 2001).
The AChBP pentameric structure with ACh binding sites at interfaces between the subunits are released in an ACh-dependent manner in close proximity to neurons. It is postulated the direct response from glial cells in close proxity to neurons could directly regulate cholinergic signalling via its ability sequester ACh released into the synaptic cleft.

3.1.1.9 Molecular Properties Of AChBP

AChBP currently represents the only model for examining the extracellular ligand-binding domain for the nAChR (Smit *et al.*, 2003), as well as other cys loop receptor family of proteins which include the GABAa,c and 5-HT-3 (Novere *et al.*, 2002). Like the ligand binding domains of other LGIC's, AChBP can form subunits of a single type subunit (homomeric) or by coexpression of α and β subunits (heteromeric) pentamers of related subunits analogous to the ligand-binding domain characteristics of nAChr's (Smit *et al.*, 2003). The functional amino acids forming the binding pockets of AChBP bind to ACh-receptor agonists such as ACh, nicotine, carbamylcholine, epibatidine and competitive antagonists such as (+)-tubocurarine as well as α-bungarotoxin, suggesting AChBP has a pharmacological profile similar to the α7-nAChR (Smit *et al.*, 2001).

3.1.2 Gene expression profiling using quantitative RT-PCR

Gene expression analysis can be performed using a number of different platforms, including microarray analysis, Northern Blot, RNA protection assay (Charpantier et al.) or RT-qPCR. However, the reproducibility, sensitivity and safety aspects of each platform can often be the determining factor as to which of these platforms are best suited for gene expression profiling in *L. stagnalis*. Microarrays are useful for examining thousands of genes on the same plate; however, as *L. stagnalis* genome is currently unsequenced, this was not a suitable platform. Northern Blot on the other hand utilises highly sensitive antisense RNA probes to target mRNA which are then visualised using autoradiography, following separation on an agarose gel and transfer to a membrane. However the method is restricted to detection of highly abundant transcripts as low abundant transcripts are not well represented using the Northern blot method. Furthermore, Northern blots are prone to RNA degradation which can significantly compromise quantitative expression analysis. Ribonuclease protection assay, on the other hand is more suitable it terms of its sensitivity and tolerance to RNA degradation over Northern Blot. RPA works by using a single stranded antisense RNA probe which is hybridised to its target in the RNA extract. The unhybridised RNA are then degraded using a mixture of nucleases. The hybridised RNA is then visualised using autoradiography after the sample has been run on an agarose gel. However, the antisense probes that are highly specific to the target

sequence are not tolerant to minor cross-species differences. Therefore, like microarray profiling, this platform was not suitable for examining gene expression changes in *L. stagnalis*. The high sensitivity of RT-PCR is currently the "gold standard" in terms of analysis of mRNA reverse-transcribed to cDNA due to its high sensitivity and ability to exponentially amplify cDNA from a much smaller starting material than either Northern blot or RPA (Pfaffl, 2001).

RT-PCR is a two-step process requiring reverse transcription of the RNA, followed by amplification of the cDNA in a PCR reaction. In the first step, RNA are reverse transcribed to cDNA using either random oligomers in which all combinations of 6-base oligonucleotides are present to reverse transcribe total RNA (Freeman *et al.*, 1999). Alternatively, reverse transcription can be achieved using selective oligonucleotides that contain deoxythymidine to anneal to polyadenylated 3' tail of mRNA from the total RNA pool (Freeman *et al.*, 1999). Alternatively gene-specific primers could be utilised to reverse-transcribe only the gene of interest from the total RNA pool (Freeman *et al.*, 1999).

In the second step, the cDNA is amplified in a PCR reaction when combined with a mixture of buffers, primers and DNA polymerase (typically *Taq* polymerase) and an accessory component, a DNA intercalating fluorescent dye such as SYBR Green that could be used to monitor the progress of the reaction (Freeman *et al.*, 1999). The PCR amplification in real time is monitored by plotting the fluorescence intensity against the number of PCR cycles, which translate to an initial linear ground phase in the reaction when there are insufficient products formed and the fluorescent signal has not yet arisen above background; an early exponential phase when amplicons double every cycle (also known as cycle threshold or Ct) and the final stage of the cycle when the reaction plateaus due to the depletion of nucleotides, and other PCR components as well as the decrease in polymerase activity (Freeman *et al.*, 1999; Pfaffl, 2001).

Plotting the fluorescence intensity as a function of temperature as the thermal cycler heats at the end of the PCR reaction, generates a melt curve that can be used to discriminate the specificity of the primers to the PCR product formed by relating the dissociation temperature of the PCR product to its estimated melting point from the

GC/AT ratio of the primers (Ririe *et al.*, 1997). A single PCR product will result in a single melt curve profile, however unwanted PCR products will affect the size and shape of the melt curves making it easier to detect (Ririe *et al.*, 1997).

3.1.2.1 Relative quantification using the delta delta Ct method

Several methods are available for quantification and analysis of a qPCR dataset, including relative quantification methods such as the standard curve method, delta delta Ct method and Pfaffl method or absolute quantification using a known calibrator (Pfaffl, 2001; Karlen *et al.*, 2007). Mathematical models that are used to derive absolute quantification of mRNA relate the PCR signal to the input copy number using a calibration curve and negate the need for a reference by assuming equal efficiency between the target gene and standard curve calibrator (Souazé *et al.*, 1996). In contrast, relative RT-PCR quantification methods normalise the expression levels of the target gene against a reference gene to take into account run-to-run or sample-to-sample variations that are inherent in a PCR experiment (Pfaffl, 2001). However, none of these methods are assumption-free, therefore variability in datasets exist depending on the type on quantification used to examine differences between two or more samples (Karlen *et al.*, 2007). Individual comparisons regarding the advantages and disadvantages of each method have been described in detail elsewhere (Pfaffl, 2001; Karlen *et al.*, 2007).

In the present study, the Pfaffl method was used to determine relative differences in AChBP mRNA expression in the young and aged CBG region. The Pfaffl method relies on the assumption that the amplification efficiencies of the housekeeping reference (HK gene) and target gene are similar but not necessarily equal. This is an important consideration to ensure that the reaction kinetics during the PCR reaction are taken into account as well as to compensate for any variances that may arise during RNA extraction, the PCR reaction or inter-experimental variation during subsequent PCR runs (Pfaffl, 2001; Karlen *et al.*, 2007; Freeman *et al.*, 1999). The expression of the HK gene by definition should be stable and its amplification should remain unaltered during the PCR reaction in both the experimental (old) and control (young) groups; however slight variations can be accounted for by examining the efficiency of both the control and HK gene in both conditions (Pfaffl, 2001).

The formula for this calculation is Efficiency = $[10^{(-1/slope)}]$ -1 (Pfaffl, 2001).

The efficiency of the reaction is obtained by performing a dilution series of the cDNA template from the experimental and control groups for both the target and reference gene on the same target plate to ensure identical experimental conditions. The Plot of the Ct as a function of log(amount of diluted cDNA) results in a linear regression of the amplicons with a negative slope that is used to estimate the efficiency of the reaction using the above equation. This is a critical validation step to ensure that the efficiency of both reactions are approximately equal (i.e. amplicons double every cycle) in order to make valid comparisons between the expression changes in the experimental and control groups. The target genes and reference genes are amplified from the same cDNA source per condition tested. In this set of experiments, cDNA from young 'controls' and aged 'experimental' were analysed as described above. As an additional quality control parameter, the specificity of the amplification product was examined on an agarose gel to reveal a single band of an appropriate size. The target samples, both control and experimental are each normalised to the reference gene by subtracting the Ct of the reference sample from the Ct value of the experimental sample that results in a 'delta Ct' value (Pfaffl, 2001). This process is repeated for the control sample (young). After normalisation to the reference gene, the 'delta-delta Ct value' is calculated by subtracting the delta Ct of the mean value for the control (young) from the delta Ct of the experimental group (old), which can be expressed mathematically as

Delta delta Ct = $(Ct_{experimental} - Ct_{reference}) - (Ct_{control} - Ct_{reference})$ (Pfaffl, 2001)

The relative mRNA expression between the control and experimental group are calculated by

$$\text{Pfaffl method for relative mRNA expression ratio} = \frac{[\text{Efficiency}_{(target)}]^{\text{delta delta Ct}}}{[\text{Efficiency}_{(reference)}]^{\text{delta delta Ct}}}$$

(Pfaffl, 2001)

3.2 OBJECTIVES:

The relative quantification of mRNA levels in young and aged *L. stagnalis* as described herein, provided an opportunity to determine whether a reduction in AChBP protein level was due to decreased gene transcription or whether other post translational factors such as the regulation of protein synthesis and turnover may have contributed to the reduction in AChBP protein expression in the aged CBG (refer to chapter 2). The stability of housekeeping genes GAPDH and elongation factor α (Elf-α) was determined in the cerebral and buccal ganglia. As Elf-α was the more stably expressed, the alterations in AChBP mRNA levels were normalised to elongation factor α (Elf-α) using the Pfaffl method during the reverse-transcription quantitative polymerase chain reaction (RT-qPCR).

3.3 MATERIALS AND METHODS

3.3.1 Immunohistochemistry

Immunohistochemistry was performed as described by(Boenisch *et al.*, 2001)and described in detail below.

3.3.1.1 Paraffin sections

L. stagnalis whole CNS was dissected as described previously (section 2.2.5) and pinned on a removable piece of sylgard square to give a flat sample. The tissue was submerged in 1% paraformaldehyde/ 1% acetic acid overnight at room temperature. Tissue was dehydrated using graded washes in 70%, 95%, 100% ethanol with 20 minute incubation per step. Alcohol was removed by washing tissue in xylene. Tissue was embedded in liquid paraffin wax at 55 °C, and cooled to room temperature. 5 μm sections of the whole CNS were obtained using a using Leica rotary microtome and floated on warmed slides coated with glycerine albumin solution, and slides then dried in 37 °C oven overnight. The sections were mounted on glass slides and air-dried overnight at 37 °C and placed in 100% ethanol:amylacetate mixture (1:1) for 30 minutes, then pure amyl acetate for 30 minutes, followed by warmed amyl acetate:wax (1:1). Samples in this mixture were transferred to 60 °C oven to keep wax molten. After 30 minutes, the amyl acetate:wax mixture was replaced with pure wax and left in oven for 60 minutes. The tissue was transferred to a pre-warmed wax-filled embedding trough and left to set overnight.

3.3.1.2 Dewaxing

Slides containing tissue sections were heated in the oven at 60 °C for 20 minutes to melt the wax, then placed in a bath containing xylene substitute and incubated for 20 minutes, then fresh solution of xylene substitute for another 20 minutes. Excess xylene was removed from the slide, and slides were placed in 100% ethanol for 20 minutes each, followed by 95% ethanol, and finally in 70 % ethanol. Sections were then placed in 1 x PBS.

3.3.1.3 Labelling method

A two-step indirect method was used to detect AChBP in the whole *L. stagnalis* sections. Slides were blocked with 4% goat serum in PBS for 1 hour, and replaced with 100µl anti-*Lymnaea* AChBP primary antibody at a dilution of 1/2000, 1/10,000 or 1/100,000 dilution in the presence of 10% skimmed milk or 10% BSA. A coverslip was placed on the tissue and left at 4 °C overnight. The tissue sections were washed three times with PBS (15 minutes per wash), and then incubated with 200 µl of anti-Guinea pig secondary conjugated to FITC at 1/10,000 dilution and left at room temperature for 1 hour in the dark. Tissue sections were washed three times with PBS in the dark (15 minutes per wash) and visualised using a confocal microscope.

3.3.2 Selection of L. stagnalis for RT-PCR experiment

Five microtubes containing 5 cerebral and buccal ganglia from adult young (3 month old), and five tubes containing 5 pooled cerebral and buccal ganglia from aged (10-11 month old) *L. stagnalis* were extracted to obtain sufficient quantities of RNA to evaluate AChBP mRNA expression using RT-qPCR. In order to further refine the effects of chronological and biological age of 10-11 month old *L. stagnalis*, aged molluscs were behaviourally classified as previously described (see chapter 2), resulting in the pairing of animals which exhibited the most severe deficit in feeding behaviour to healthy young snails which showed no impairment in feeding behaviour.

3.3.3 RNA Isolation

RNA purification from *L. stagnalis* CNS required a combination of TRIZOL™ reagent, a guanidinium thiocianate method, followed by phenol choloroform extraction and ethanol precipitation steps to achieve a level of RNA purity to confidently perform quantitative RT-PCR (see below). 5 cerebral-buccal ganglia from behaviourally tested animals were dissected and placed in 300 µl TRIZOL™ (Invitrogen) and snap-frozen on dry-ice before storage at -80 °C. Prior to extractions, samples were brought to room temperature for 5 minutes and homogenised using an RNase-free pestle. An additional 500 µl TRIZOL™ was used to wash the pestle of residual RNA. Samples were centrifuged at 4°C, 12,000xg for 20 minutes. The supernatant was carefully transferred into another microtube

containing 160 µl chloroform and vigorously shaken for 30 seconds prior to being transferred into a heavy phase lock gel (PLG; Eppendorf, UK) tube (previously centrifuged at 12,000xg for 2 minutes at room temperature). Samples were then centrifuged at 12,000xg for 10 minutes at 4°C.

The aqueous phase containing RNA was removed and transferred to a new tube containing an equal volume of phenol-chloroform-isoamyl alcohol (25:24:1 (v/v) and mixed vigorously by hand for 30 seconds. Samples were transferred into a second PLG tube (previously centrifuged at 12,000xg for 2 minutes at room temperature) and centrifuged at 12,000xg for 10 minutes at 4°C. The aqueous phase was then removed again and placed in a new tube containing an equal volume of isopropanol (400µl) and 1µl glycogen (20µg/µl) as a co-precipitant, shaken and left overnight at -20°C.

Samples were centrifuged at 12,000xg for 15 minutes, and the pellet was washed twice with 80% ethanol and spun for 10 minutes at 12,000xg each time. The pellet was left to dry at 65 °C for 7-10 minutes before being re- suspended in 50µl nuclease-free water and left on ice for 30 minutes. $1/10^{th}$ volume (5 µl) of 3M sodium acetate, pH 5.2 and 3 times volume of 100% ethanol (150 µl) was added and shaken briefly before being left to precipitate for 1 hour at -20°C. Samples were centrifuged for 20 minutes at 12,000xg, and the pellet washed twice with 80 % ethanol and centrifuged for 10 minutes at 12,000xg after each wash. Total RNA pellets were dried at 65 °C and re-suspended in 25µl nuclease-free water.

3.3.4 Determination of RNA concentration in sample

1µl of dissolved total RNA was diluted in 49µl nuclease-free water. The concentration of the total RNA was determined spectrophotometrically by averaging three replicate A_{260}/A_{280} absorbance ratios. The level of protein and solvent contaminants present within the sample was estimated using the A_{260}/A_{280} and A_{260}/A_{230} absorbance readings respectively. An absorbance reading above 1.60 for both readings was considered within acceptable range for quantitative RT-PCR. RNA was aliquoted in amounts of 2 µg RNA and stored at -80 °C.

3.3.5 Preparation of first-strand cDNA:

3.3.5.1 DNase-treated RNA

Removal of any potential DNA contaminant was achieved using a DNase-treatment prior to cDNA synthesis. Aliquots containing 2µg of total RNA were DNase treated using 1µl DNase buffer, 2 units (2µl) of Turbo DNase 1 enzyme (Ambion) and water making a total volume of 10µl. These were incubated for 30 minutes followed by addition of a further 2 units of Turbo DNase 1 enzyme (Ambion) and a further 30 minute incubation. 5µl stop solution was added to the reaction mixture and reaction incubated for a further 10 minutes at 65 °C.

3.3.5.2 Reverse transcription (RT)

Total RNA (2 µg) was subjected to random primed first strand cDNA synthesis (reverse transcription) in a 40 µl reaction volume. The first strand cDNA were used as template for the PCR reaction. A separate no template control (**NTC)** reaction was performed (minus the 1µl reverse transcriptase enzyme) that was used as a negative control. RNA was reverse transcribed using gene-specific primers as per manufacturer's instruction (iScript Select kit, Biorad 170-8896). Primer sequences are represented in

Table 4. The protocol consisted of an optimised proprietary mixture of Tris-HCl, KCl, DTT in the form of 5X iscript reaction mix (4 µl), gene-specific primers (GSP) enhancer solution (2 µl), and iscript reverse transcriptase (1 µl), RNA (1 µg), AChBP-specific primer (500nM) all made up to 20 µl final volume using nuclease-free water. The mixture was incubated at 42 °C for 60 minutes. The reaction was stopped by incubating tubes at 85 °C for 5 minutes to heat inactivate the reverse transcriptase. The resulting first strand cDNA was stored at -20 °C and subsequently used as template for PCR reactions. A separate **MOCK reaction** was also created as outlined above (minus the 1µl reverse transcriptase enzyme) which was used as a non-template PCR control.

3.3.6 Real-Time RT-PCR Analysis

3.3.6.1 Primer Sequences for AChBP qPCR:

The sequence of the primers for AChBP was a generous gift from Pim Van Neirop, Netherlands).

Gene	Forward primer (5´→ 3´)	Reverse primer (5´→ 3´)
AChBP	CAGGTTTCCGTGCCAATAAG	CCAGTTGCGGTGTAAGGAC
Elf-α	ACCACAACTGGCCACTTGATC	CCATCTCTTGGGCCTCTTTCT

Table 4: Primer sequences used for real time PCR assays

Predicted Tm for AChBP forward and reverse primers was 59.2'C and 60.5'C respectively and a product size of 91bp. Predicted Tm for Elf- α both forward and reverse primers was 62'C and product size of 85 bp.

3.3.6.2 PCR amplification:

Quantitative PCR amplifications were performed with SYBR Green labelled reactions on a thermal cycler (iCycler, Biorad) that was controlled by a Biorad iCycler software on a PC workstation. PCR reactions were performed in a 25 µl reaction volume according to Biorad guidelines (1 cycle at 95 °C for 3 minutes; 45 cycles at 95 °C for 10 s, 54.9 °C* for 49 s; 80 cycles at 55 °C for 10 s and increasing set-point temperature by 0.5 °C after cycle 2*); as summarised in

Table 5. In order to minimise variation in reaction volumes, a 'master mix' volume was determined by calculating the number of reactions required for each group + 1 extra surplus reaction for each group. For example, for 3 reactions, the master mix volume was prepared for 4 reactions worth of reagents. The master mix maintained the reaction volume ratio to 12.5 µl SYBR Green, 1 µl primer, 4 µl template, 7.5 µl RNase-free water making a total volume of 25 µl/ reaction.

Primers (forward and reverse)	Cycling conditions				
	Initial denaturation	Denaturation	Annealing	Extension	Dissociation curve
AChBP (F) AChBP (R)	95 °C 3 mins	95 °C 10 sec	54.9 °C 49 sec	55 °C 10 sec	Starting at 55 °C to 95 °C
		Repeated 40 cycles			1 cycle

Table 5: RT-PCR amplification cycle of AChBP and Elf-α

The threshold cycle (Ct) value for each gene was defined as the PCR cycle at which the emitted fluorescence rose above a background level of fluorescence and was set at 40.4 with cycles 2-17 selected as baseline cycles using software provided with the Bio-Rad iCycler. All samples were run in duplicate. Controls were run with water replacing the template to pick up primer dimers. Additional 'mock' templates were added to the plate to test for genomic contamination. The Ct value was obtained for each reaction and the ΔCt value was calculated by subtracting the target Ct value from the reference (elongation factor α) Ct values. ΔΔCt values were obtained by subtracting the mean ΔCt value of 'young' - ΔCt value of 'old'. Fold change was calculated by calculating the efficiency of the reaction (E) to the power of -ΔΔCt (i.e $E^{-\Delta\Delta Ct}$).

3.3.6.3 RT-qPCR data analysis:

Fold change of the gene expression was measured using the Pfaffl method as described previously with normalisation of the raw data to elongation factor (Elf-α) housekeeping (HK) gene.

3.3.7 Western Blot analysis:

In a separate set of experiments designed to examine how GFAP expression changes with increasing age, Western blot analysis was performed as has been described previously (see methods section, chapter 2.2.12). GFAP protein expression was compared in 3 month (young) and 10 months (old) CBG region. 10μg protein was loaded per well, and transferred to PVDF membrane. Protein levels in 10 month animals were expressed as a percentage of the 3 month age group. Membranes were probed with primary antibody 1/200 (Dako) overnight at 4°C; and secondary antibody at 1/ 2,000 dilution (anti-rabbit conjugated to HRP) and normalised with GAPDH primary antibody 1/200, secondary antibody at 1/4000 (anti-mouse

conjugated to HRP). The normalised intensity ratio of GFAP in the old was expressed as a percentage of young.

3.4 RESULTS:

3.4.1 Immuno-histochemical labelling of AChBP

Regulation of the feeding behaviour in *L. stagnalis* can be mapped to discrete sets of neurons that reside within the cerebral and buccal ganglia (Elliott and Andrew, 1991). In order to assess the possibility that glial cells release AChBP in localised networks that may participate in the feeding behaviour, 5µm histological sections of the whole CNS were incubated with 1/2000 dilution of anti-AChBP and visualised using FITC anti-Guinea Pig secondary antibody Figure 17 shows a representative section of the buccal ganglia that was labelled with anti-AChBP antibody. Figure 17 was re-scanned 12 hours after incubating the tissue in the secondary antibody as the signal intensity had saturated the entire tissue when the tissue was first scanned. No specific binding was observed with this antibody at any of the concentrations tested (Figure 17).

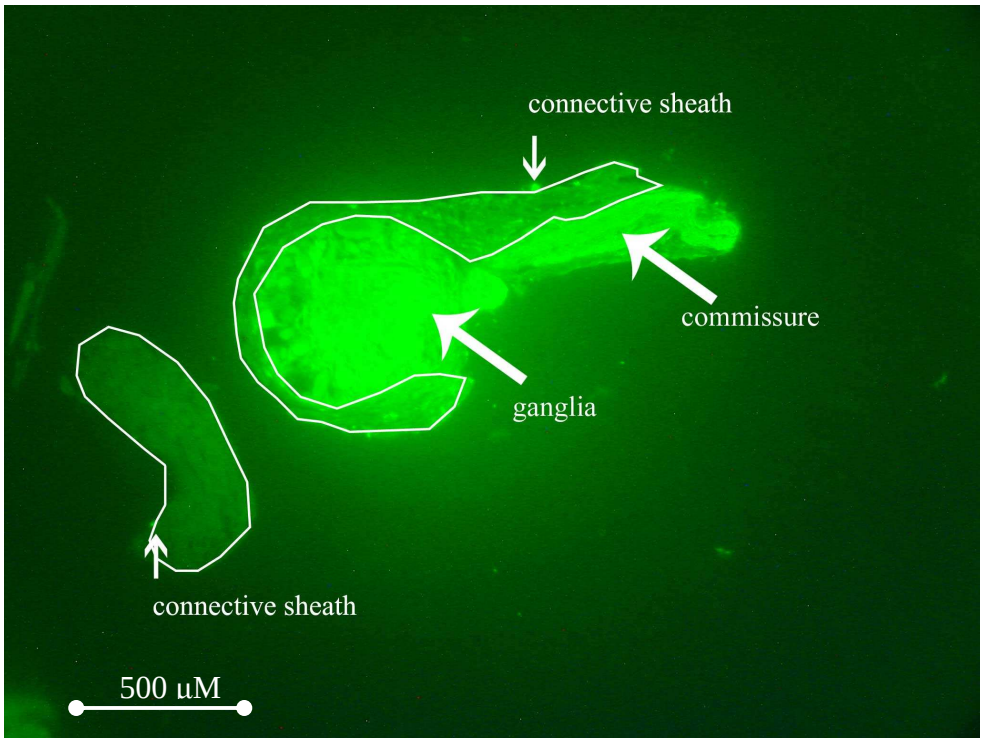

Figure 17 AChBP labelling of left buccal ganglion with perforated commissure

Sections were labelled with anti-AChBP (1:2000 dilution), and visualised using anti secondary anti-guinea pig antibody (1:10,000 dilution). Arrows indicate non-specific labelling of commissures, ganglia and connective sheath indicating the AChBP antibodies are not compatible in histological preparations.

3.4.2 Method development - RNA extraction/ determination

RNA quality was determined by detection of RNA using a UV spectrophotometer, and its relative purity examined by measuring the 260/280 and 260/230 absorbance ratio. A 260/ 280 ratio and 260/ 230 ratio in the region of 1.8 – 2 is generally considered ideal qPCR analysis (Fukunaga and Doudna, 2009). Using the QIamp kit, the RNA yield was considered too low to make sufficient cDNA. The TRIZOL™ method on its own was also not sufficient to produce quality RNA with the 260/280 ratio and 260/230 ratio below 1.8 from *Lymnaea* CNS (Table 6). A modification of the TRIZOL method was required for phenol-chloroform extraction, by using a two step phase-lock gel extraction process as well as changing the ethanol precipitation of samples to -20°C overnight instead of the recommended 1hour on ice improved both the quantity and quality of total RNA.

Two different methods were empirically compared to test which provided the highest quantity and quality of RNA required for RT-qPCR analysis. A guanidinium thiocyanate-phenol chloroform extraction (TRIZOL™, Invitrogen) was tested against the QIamp extraction kit (Qiagen). The QIamp columns produced relatively pure sample of total RNA as indicated by the 260/ 280 absorbance reading and 260/ 230 ratio; however the yield was much lower compared to the standard TRIZOL method (Table 6) and the RNA yield was considered too low to make sufficient quantities of cDNA. The TRIZOL™ method on its own, as outlined by the manufacturer (Invitrogen), was also not sufficient to produce quality RNA, with the 260/280 ratio and 260/230 ratio obtained from *Lymnaea* CNS considerably below 1.8 (Table 6). A modification of the TRIZOL method including a phenol-chloroform extraction, employing a two step phase-lock gel extraction process as well as changing the ethanol precipitation of samples to -20°C overnight instead of the recommended 1hour on ice, improved both the quantity and quality of total RNA. However, despite considerable optimisation, the 260/ 280 absorbance ratios typically achieved using this method were just below 1.8. Whilst this was not ideal, the low yield of the alternative approach made this the only feasible option.

Samples	N	Mean yield (µg/µl)	Standard deviation of yield	Mean $A_{260/280}$ ratio	Standard deviation of $A_{260/280}$	Mean $A_{260/230}$ ratio	standard deviation of $A_{260/230}$
A:	3	0.203	0.140	1.663	0.148	1.413	0.505
B:	1	0.04	n/a	2.15	n/a	1.89	n/a
C:	6	0.326	0.095	1.717	0.108	2.078	0.287

Table 6 Yield and purity readings from 3 RNA extraction methods.
A: standard TRIZOL extraction; B: QIamp extraction; C: modified TRIZOL extraction

3.4.3 DNase treatment

2µl (2U/ µl) DNase treatment was not effective at removing all DNA from the RNA sample. Additional steps were taken to incubate the samples twice with 2µl (2U/ µl) Turbo DNase each for 30 minutes.

3.4.4 Annealing temperatures for each primer set

Annealing temperatures for the primer set shown in
Table 4 were optimised to ensure there was minimal amplification of non-template controls (NTCs) or the negative control which only contained water. Where contaminants were present there was at least a 10 cycle difference between the actual sample and the NTC. This confirmed the contaminants were in low abundance. The sequences of the primers yielded a single product when run on a 2% agarose gel, confirming that there was no amplification of multiple transcripts (Figure 18).

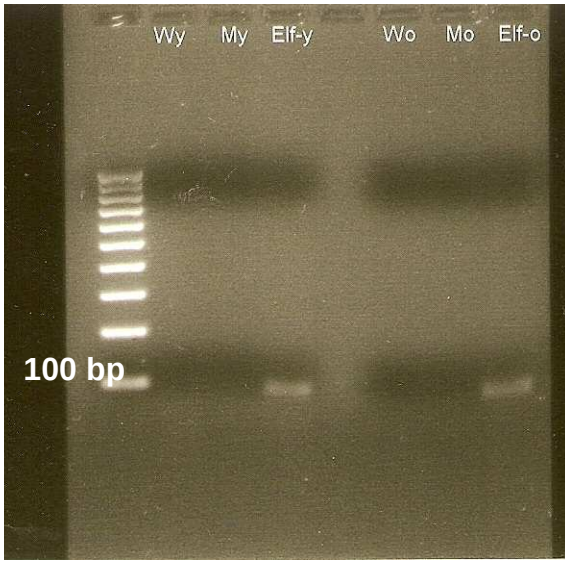

Figure 18 Visualisation of Elf-α PCR product on a 2% agarose gel
PCR products from RT-qPCR showed no product formation in the blank water sample (young (Wy) or old (Wo)); no contaminant amplification in the NTC in young (My) or old (Mo) CBG, and only a single band was detected at ~ 85 bp corresponding to Elf- α.

3.4.5 Optimisation of house-keeping gene GAPDH

In real time studies, differences in relative quantification of housekeeping mRNA levels can result in misinterpretation of real-time PCR data. According to Pfaffl (2001), standardised criteria for the use of an appropriate HK gene for normalization purposes include 1) HK gene are expressed at the same level as the gene of interest that do not differ by more than 1 cycle; 2) it is stable in the tissue of interest, 3) and unaffected by experimental conditions (Pfaffl, 2001).

Our initial studies examined the suitability of GAPDH as a suitable housekeeping control. The dilution series showed the reaction efficiency was 106.6% and within the acceptable 100% ± 10% range (Figure 19). There was no statistically significant difference between the young and aged samples ($p > 0.05$), however there was a large within-group standard error which showed that there was more than 1 cycle difference in GAPDH expression between the individual samples (Figure 20). This would equate to over a 2-fold difference of PCR product per amplification, hence, GAPDH did not meet the stringent requirements that a HK gene only vary between experimental groups by 1 cycle (or 2-fold) in a RT-qPCR experiment (Figure 20).

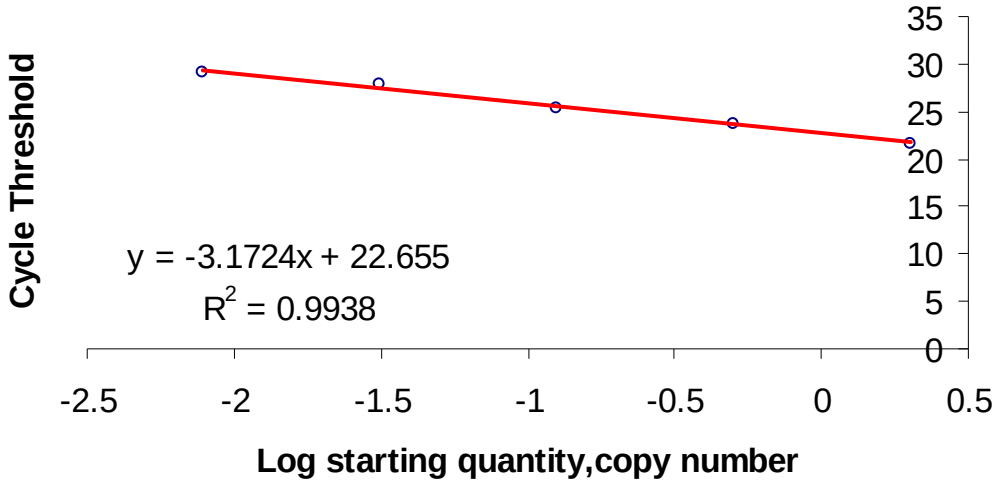

Figure 19 Dilution series for GAPDH
A dilution series for GAPDH was performed on the same target plate as the control and target genes. The efficiency of the reaction using GAPDH primers targeting the cDNA template showed a 106.6% efficiency in the CBG samples.

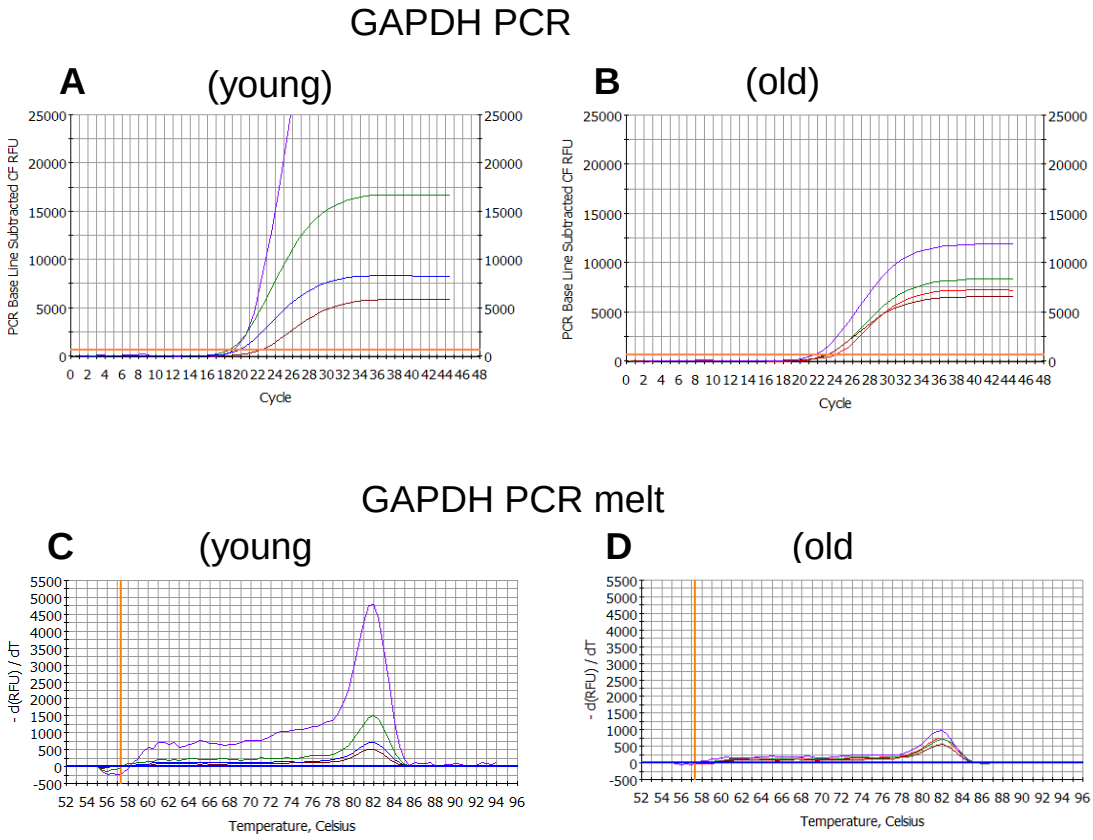

Figure 20 PCR amplification and melt curves for GAPDH in young and aged CBG
PCR amplification curve in young and old (A and B respectively) showed high inter-sample variability during PCR amplification; the melt curve profile showed only a single product was amplified in the reaction in the young and old CBG (C and D respectively) (n=4/ group).

3.4.6 Optimisation of house keeping gene Elf-α

Elongation factor α (Elf-α), a gene whose gene product is responsible for the enzymatic delivery of aminoacyl tRNAs to the ribosome was tested to assess its suitability as a reference gene in the aged *L. stagnalis* nervous system. A dilution series was performed as outlined previously for Elf -α to show the PCR efficiency of 101.6% (Figure 21). No difference was detected between young and aged Elf-α mRNA expression, meaning Elf-α was stably expressed between the two groups ($p > 0.05$); (Figure 22). After 36 cycles, there was some amplification in the non-template control reactions (Figure 22) which could also be observed in the melt curve profile (Figure 23). However, there were at least 10 cycle difference between Ct values of NTCs and samples. Furthermore, when the samples were visualised on a 2% agarose gel, these products did not generate a band in the NTC or water samples (Figure 18). As Elf -α was stable between the two age groups, and highly abundant, it was considered to be an appropriate HK gene for normalisation of mRNA expression in aged *L. stagnalis*.

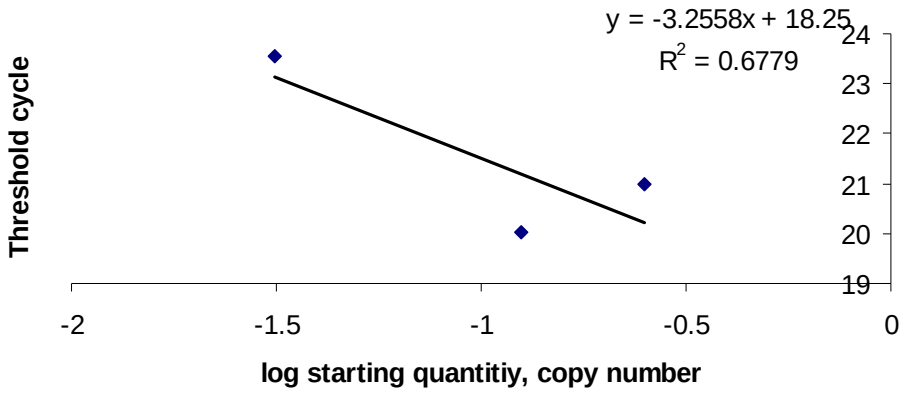

Figure 21 Dilution series for Elf-α to obtain the PCR reaction efficiency
A dilution series for Elf-α was performed on the same target plate as the control and target genes. The efficiency of the reaction using Elf-α primers targeting the cDNA template dilution series showed a 102.8% efficiency in young CBG samples.

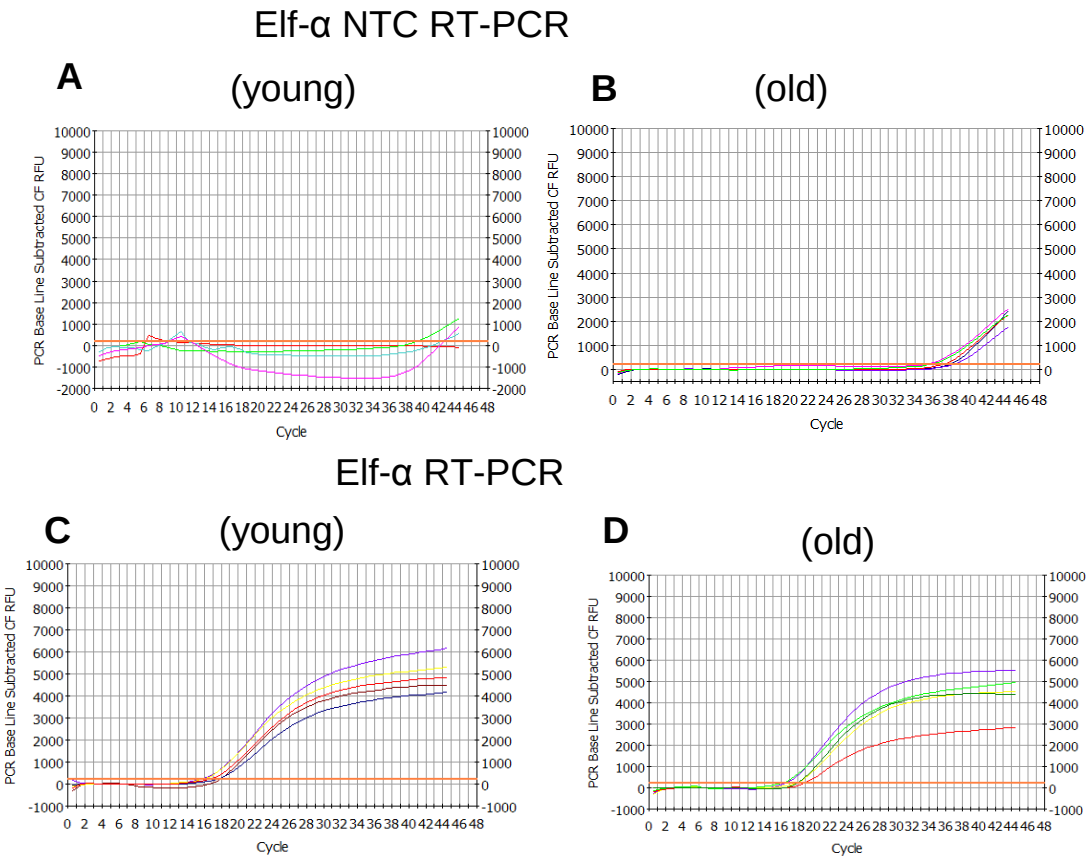

Figure 22 PCR amplification curves for Elf-α and NTC in young and aged CBG of *L. stagnalis*

Non template control (NTC) amplification curve in young (A) and aged (B) and cycle threshold of Elf-α in young (C) and aged (D) CBG. No differences was detected in threshold cycle in Elf-α in the cerebral and buccal ganglia of young 18.42 ± 0.35 cycles (n=4/ group), and old 18.45 ± 0.43 cycles (n=4/ group) *L. stagnalis*.

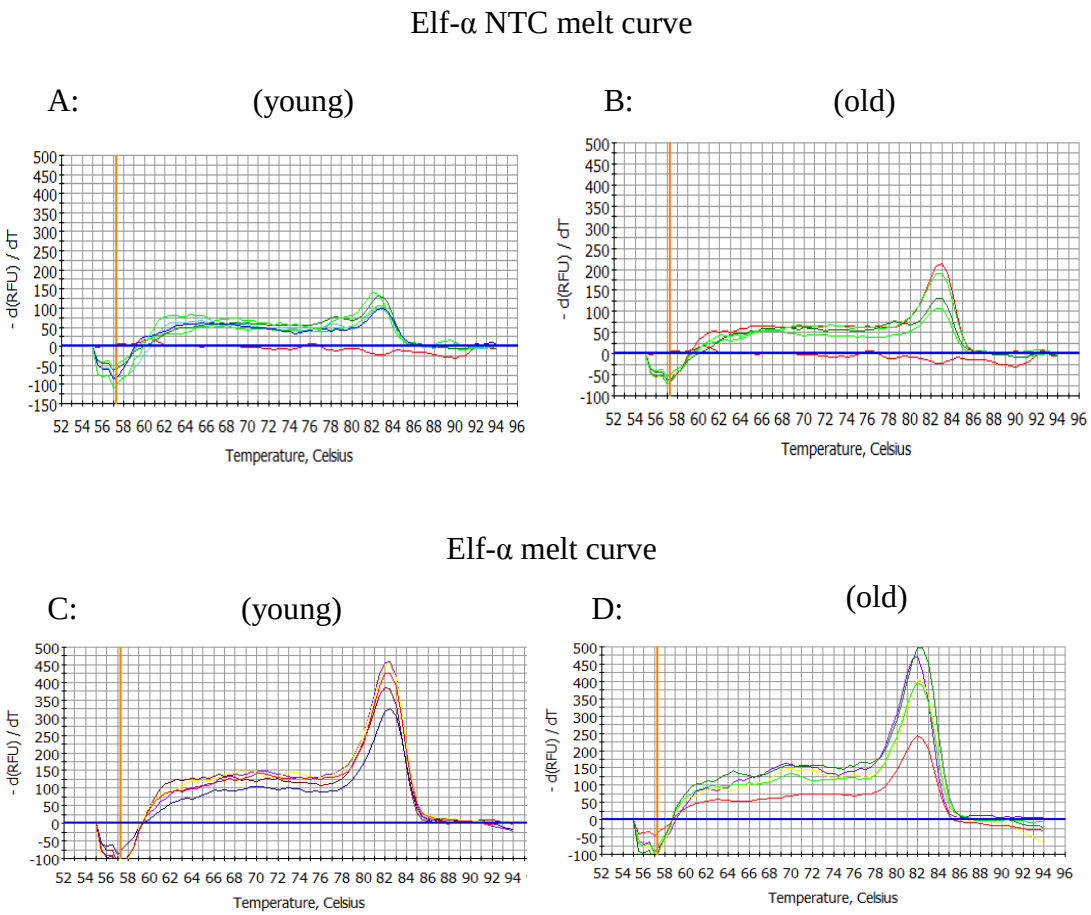

Figure 23 PCR amplification melt curves for Elf-α and NTC in the young and aged CBG.
Melt curve analysis was performed at the end of the PCR reaction in young (A) and aged CBG (B), Elf-α showed a single peak in the young (C) and old (D) samples, confirming a single product was generated during the reaction.

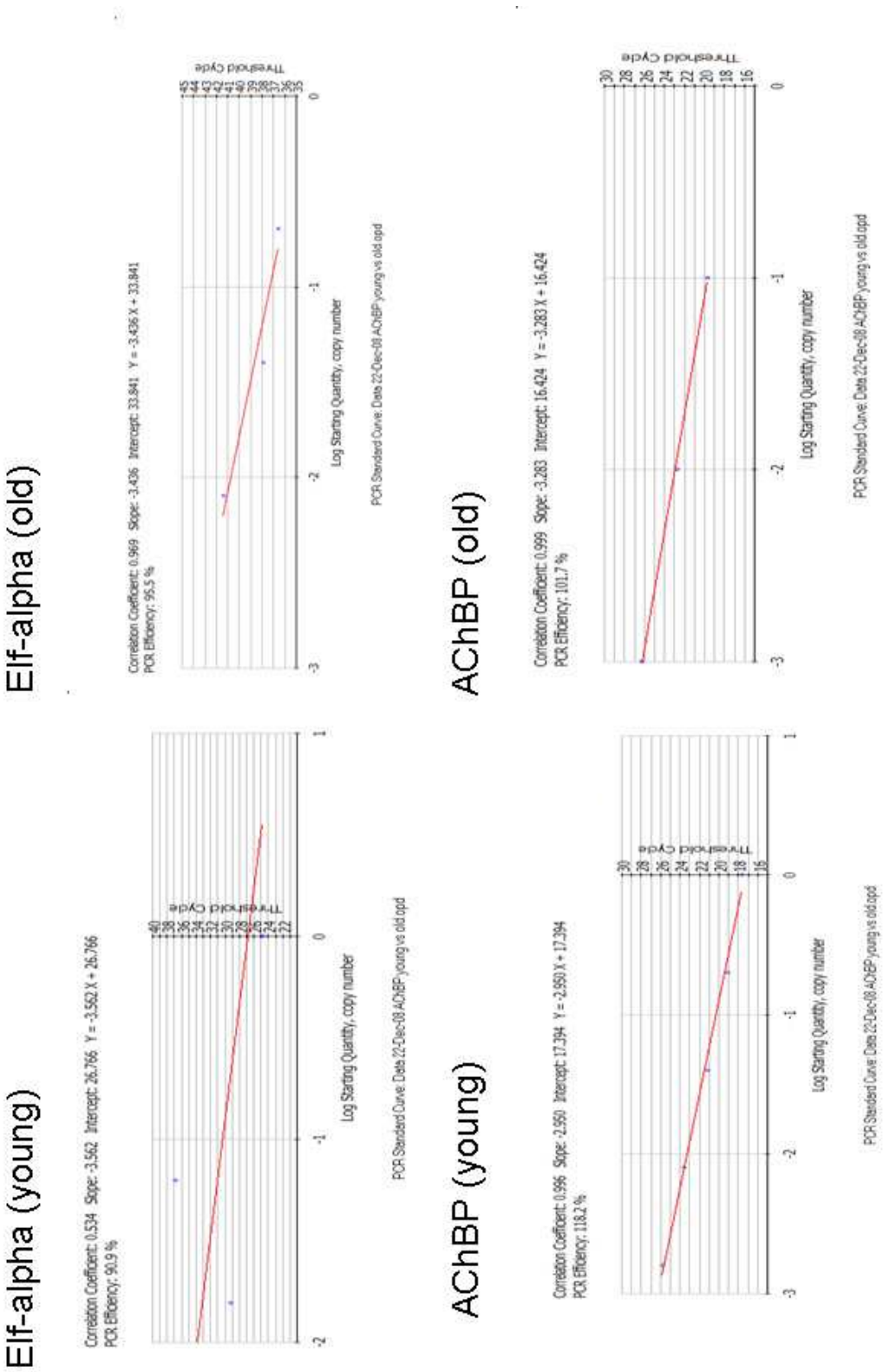

Figure 24 Dilution series of AChBP and Elf-α in young and aged CBG
Dilution series for AChBP and Elf-α was performed on the same target plate to estimate the efficiency of the reaction for the two transcripts. The efficiency of the reaction for young CBG using AChBP primers targeting the cDNA template dilution series showed a 90.9% efficiency in young and a 95.5% efficiency in old CBG samples. The efficiency of the reaction for young CBG using Elf-α cDNA template dilution showed a 118.8% efficiency in young and a 101.7% efficiency in old CBG samples.

3.4.7 AChBP mRNA expression profiling

To assess AChBP mRNA expression in the young and aged CBG of *L. stagnalis*, the Pfaffl method was used to normalise AChBP against Elf-α (
Figure 24). A prerequisite to obtaining meaningful expression data was to have the HK and target dilution series present on the same target plate as the samples of interest. PCR amplification curves for AChBP mRNA showed no amplification in NTC or product formation in the melt curve profile (Figure 26 and Figure 27 respectively). The dilution series used to obtain the efficiency of the HK and target genes are highlighted in (
Figure 24), and the relative fold difference in AChBP when normalised to Elf-α are represented in Table 7. When AChBP was normalised to Elf- α using the Pfaffl method, a significant reduction in AChBP mRNA expression was detected in aged *L. stagnalis* CBG relative to the young (0.104 ± 0.059, $p < 0.05$) (Figure 28); however, a sub-optimal correlation coefficient for one particular dilution series (ELF-α – young) was observed when the samples were run on the same target plate. Due to the limited amount of available aged samples, the entire experiment could not be repeated, having both dilution series on the same target plate as the samples. To calibrate for discrepancies that could account for poor reaction efficiency, the threshold cycle value was re-adjusted to give a correlation coefficient of above 0.8. This would account for a more conservative estimate of the relative fold difference in AChBP between the young and aged samples based on a 'corrected' ELF-α – young PCR reaction efficiency based on the following formula (Figure 25):

Efficiency = $[10^{(-1/\text{slope})}] -1$ (Pfaffl, 2001).

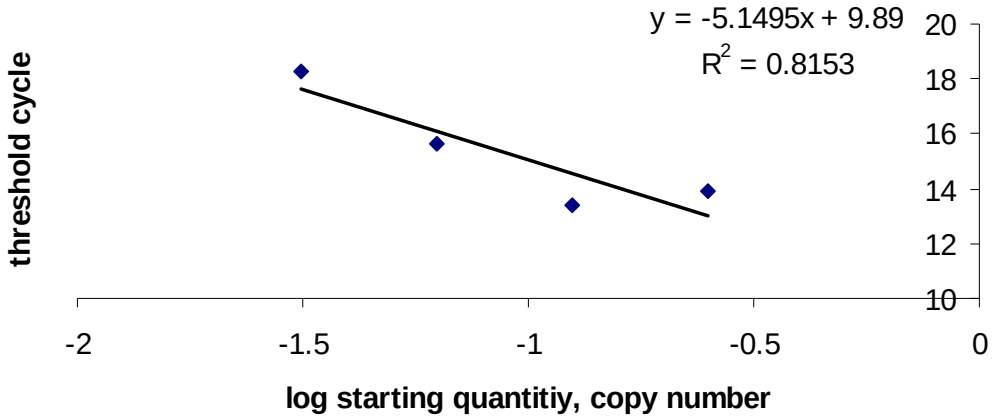

Figure 25 Conservative estimate of ELF-α dilution series with correlation coefficient above 0.8
A dilution series for Elf-α was performed to estimate the efficiency of the reaction using Elf-α primers. When the correlation co-efficient was adjusted to above 0.8, the PCR reaction efficiency of 52%.

When ELF-α was corrected for above 0.8 correlation coefficient, the efficiency of the reaction was calculated as 52.1%, i.e 1.521 fold PCR product amplification per cycle (Figure 25), instead of 1.909 as calculated previously (
Figure 24). Based on the new estimate, the conservative estimate of the relative fold difference in AChBP expression was 0.65 ± 0.37 relative to young and summarised in Table 7 shaded in grey, compared to 0.10 ± 0.05 as based on previous calculation in Table 7. Both graphs are represented in (Figure 29) and (Figure 28) respectively. Although a somewhat smaller decrease in AChBP mRNA expression was observed using the corrected value, the difference in expression between the two age groups was still statistically significant ($p < 0.05$).

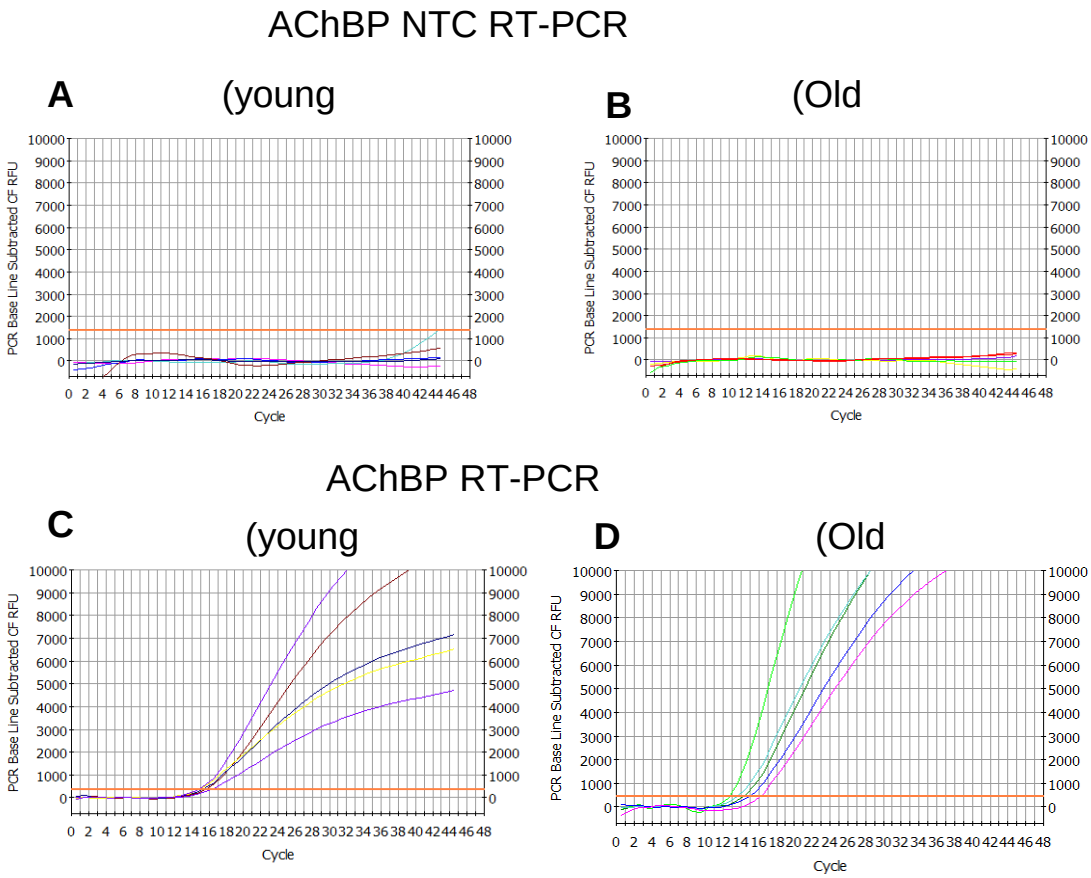

Figure 26 PCR amplification curves for AChBP and NTC in young and aged CBG

Non template control (NTC) amplification curve in young (A) and aged (B) showed no amplification and cycle threshold of AChBP in young (C) and aged (D) CBG showed differences in threshold cycle in the young CBG from 18.42 ± 0.35 cycles (n=4/ group), and old 18.45 ± 0.43 cycles (n=4/ group) *L. stagnalis*. PCR amplification of NTC showed no amplification in the young and aged CBG. AChBP mRNA amplification occurred from a cycle threshold of 12.

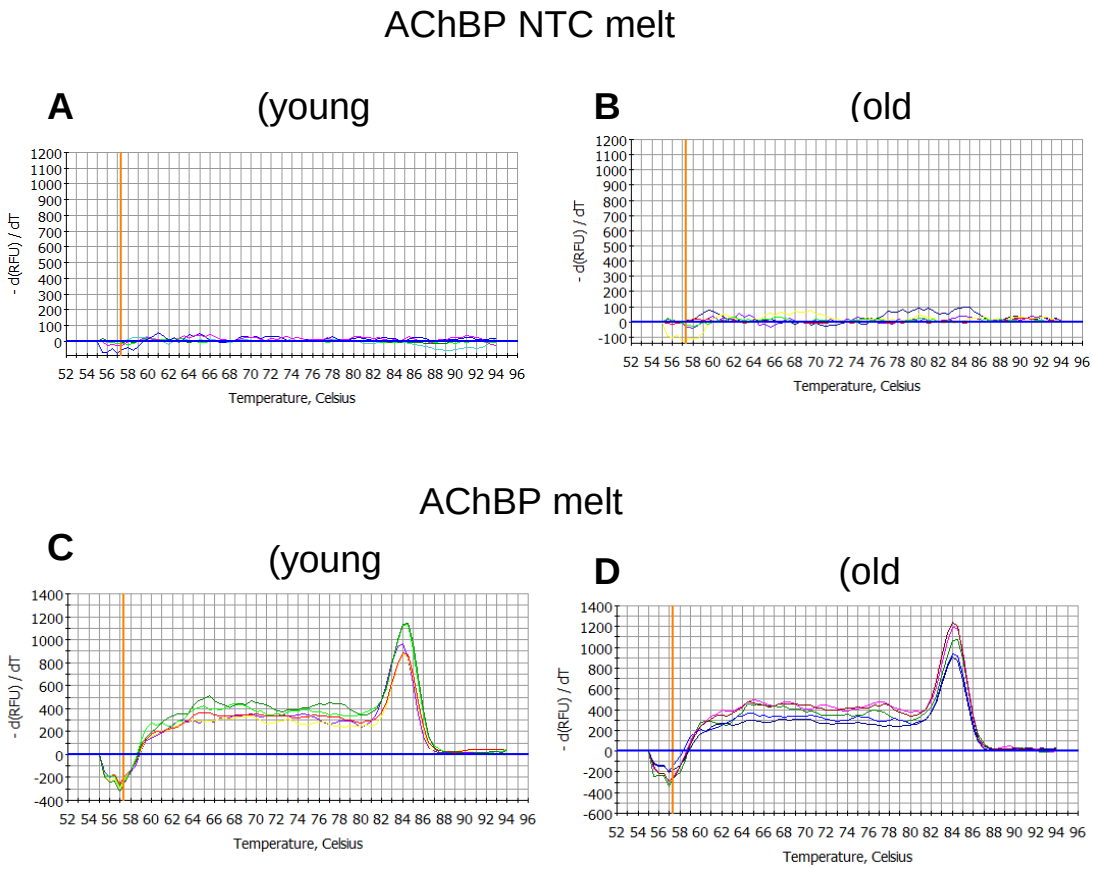

Figure 27 PCR amplification melt curve for AChBP and NTC in young and aged CBG of *L. stagnalis*

Non template control (NTC) showed no product formation during melt curve analysis following RT-PCR. A single product was observed in all young and aged CBG following melt curve analysis.

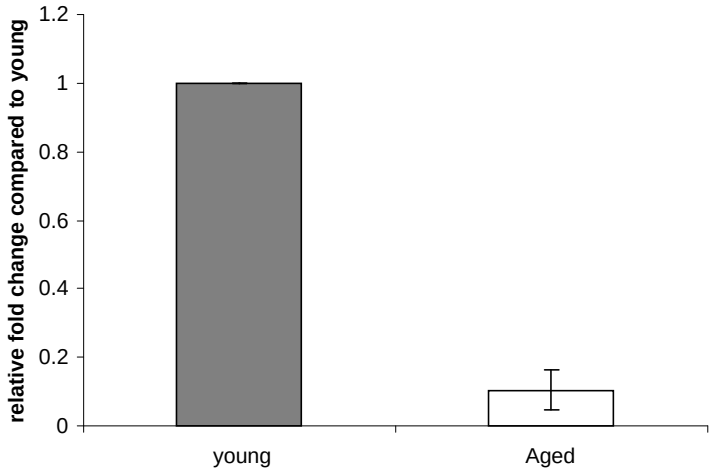

Figure 28 AChBP mRNA expression in the CBG region of *L. stagnalis*
The relative mRNA expression levels of AChBP when normalised to Elf-α showed a significant reduction in AChBP mRNA expression levels in 10 month (aged) animals 0.104 ± 0.059 compared to 3 month (control) animals ($p<0.05$); (n=4).

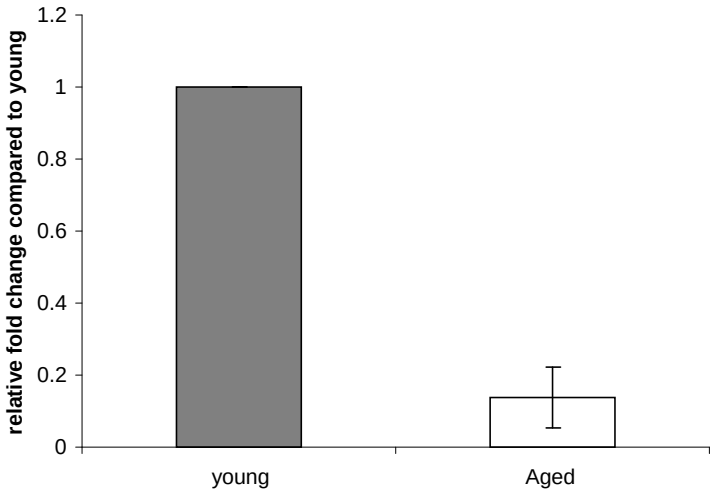

Figure 29 Conservative estimate of relative fold change in AChBP mRNA expression in the young and aged CBG of *L. stagnalis*
The relative mRNA expression levels of AChBP when normalised to Elf-α showed a significant reduction in AChBP mRNA expression levels, using a correlation coefficient of above 0.8 to estimate the efficiency of the reaction. 10 month (aged) AChBP mRNA expression levels were 0.137 ± 0.028 compared to 3 month (control) animals ($p<0.05$); (n=4).
(n=4).

Pfaffl method for relative mRNA	Young AChBP	Young Elf- α	Old AChBP	Old Elf-α	Ct Young-Ct Old for target gene	Pfaffl Equation Top Line		Ct Young-Ct Old For AChBP	Pfaffl Equation Bottom Line	Ratio Target Gene In Treated/ Control	
cDNA1	18.00	22.35	13.5	21.45	0.90	1.79	1.46	4.50	33.90	0.1	0.04
cDNA2	18.10	18.4	16.15	20.45	-2.05	0.27	0.42	1.95	4.60	0.1	0.09
cDNA3	18.85	19.65	15.20	20.95	-1.30	0.43	0.58	3.65	17.42	0.0	0.03
cDNA4	16.80	22.25	16.30	23.60	-1.35	0.42	0.57	0.50	1.49	0.3	0.38

Table 7: Relative AChBP mRNA expression in young and aged CBG
The AChBP expression was normalised to Elf-α and expressed as a ratio of young.
Grey columns provide a conservative estimate of Elf-α efficiency of 52.1%

3.4.8 GFAP expression in the aged CBG of L. stagnalis

To examine GFAP expression in the young and aged CBG, GFAP was validated using Western Blot analysis with 1/200 anti-GFAP antibody (Dako) and 1/2000 anti-rabbit secondary as per manufacturer's instructions. GFAP expression was increased in the aged CBG compared to young CBG (118 ± 7.10) when normalised to GAPDH, but failed to reach statistical significance ($p > 0.05$), $n = 3$, (Figure 30).

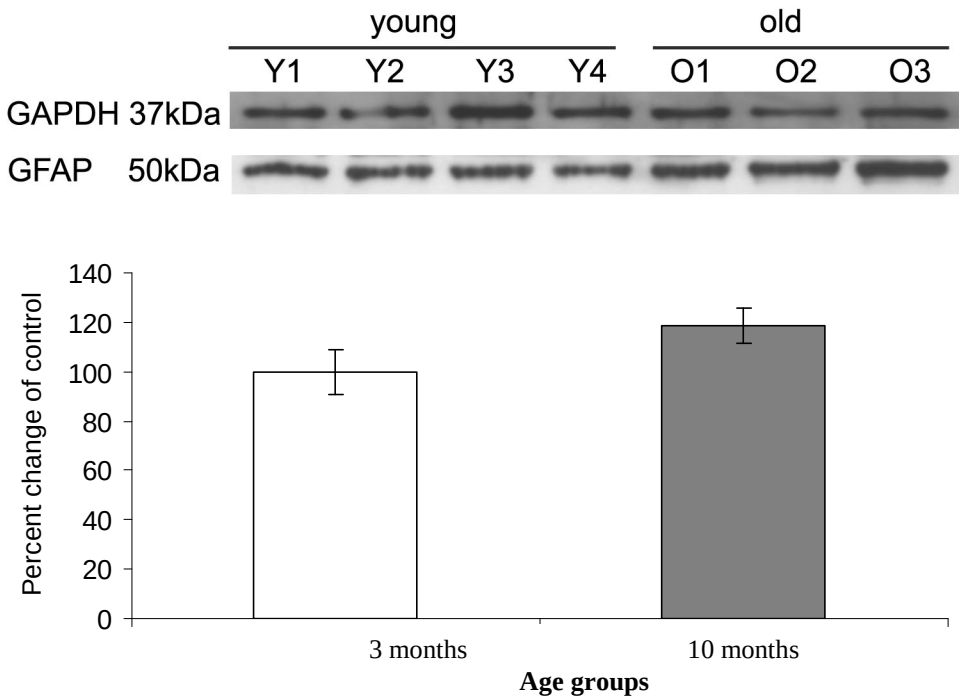

Figure 30 Western Blot analysis of Glial fibrilary acidic protein expression in the cerebral and buccal ganglia of *L. stagnalis*.
GFAP protein expression was compared in 3 month (young) and 10 months (old) CBG region. 10 μg protein was loaded per well, and transferred to PVDF membrane. 10 month were expressed as a percentage of the 3 month age group. Membranes probed with primary antibody 1/200 (Dako) overnight at 4°C; secondary antibody 1/ 2,000 (anti-rabbit conjugated to HRP) and normalised with GAPDH.

3.5.0 DISCUSSION

Cholinergic abnormalities in the nervous system have been observed consistently in aged animal models as well as in normal human ageing where disruption to choline transport (Brull *et al.*, 2002), receptor specific changes in nAChR expression (Court *et al.*, 1997) and decreased mAChR expression (Court *et al.*, 1997) are a prominent feature. In this study, proteomic profiling provided the first evidence that there may be cholinergic dysfunction mediated in part by a decrease in AChBP in the aged CBG of *L. stagnalis* (see Chapter 2). However, why the *L. stagnalis* nervous system utilises AChBP as an additional mechanism to regulate cholinergic signalling requires further clarification (Smit *et al.*, 2001); (also see Chapter 5).

Three preliminary experiments are outlined which aim to characterise the observed changes in AChBP expression in more detail, 1) Immunohistochemistry was performed to determine whether there are any changes in the localisation of AChBP in aged tissue; 2) RT-qPCR was performed to determine whether the changes in AChBP expression with age occurred at the level of transcription; and 3) GFAP was used to assess any changes in glial cells expressing GFAP in the young and aged CBG that could conceivably be responsible for changes in AChBP levels.

3.5.1 Immunohistochemical analysis of AChBP in L. stagnalis

To determine whether immunohistochemistry could be used to determine the localisation of AChBP in the *L..stagnalis* CNS and determine the relative expression in the young and aged CBG, 5µm sections of the whole *L. stagnalis* CNS were prepared and assessed using anti-AChBP antibody. The anti-AChBP antibody that was used to confirm the proteomic data on Western Blot failed to characterise the localisation of AChBP specifically, as the antibody was not suitable for immunohistochemistry preparations (Figure 17). Reducing the dilution or modification of the blocking buffer could not improve the resolution, and non-specific labelling was evidenced on the coverslips, and using a different antibody was also impossible as none were commercially available. Therefore immunohistochemistry could not address the question of AChBP localisation and its relative expression within subsets of neurons that regulate the feeding behaviour in *L. stagnalis*.

3.5.2 Transcriptional expression of AChBP in the young and aged CBG

Although significant changes in AChBP protein levels had been observed, it was unclear whether these were the result of an altered pattern of post translational modification or whether AChBP expression in the aged CBG was altered at the level transcription. A large number of post translational modifications that are observed during the ageing process, such as phosphorylation of proteins could alter the stability, specificity and lifespan of the protein (Rattan, 1996). In contrast, other modifications such as oxidation of proteins can transform particularly susceptible amino acids such as proline, arginine and lysine into their carbonyl derivatives which in turn can lead to protein aggregation, fragmentation and increased proteolytic susceptibility of the oxidised proteins (Rattan, 1996). Based on the 2D DIGE study (chapter 2), some resolved proteins showed multiple spots due to shifted PI, suggesting a high degree of PTM of these proteins (see chapter 2). However, shifts in PI were not detected for AChBP, leaving open the possibility that a reduction in AChBP protein levels was transcriptionally regulated.

To clarify whether transcriptional events were involved, AChBP mRNA expression was examined in the young and aged cerebral and buccal ganglia of *L. stagnalis* using semi-quantitative RT-qPCR analysis (Figure 28). Relative expression analysis of AChBP mRNA when normalised to Elf-α using the Pfaffl method showed AChBP mRNA was significantly decreased by 84.5% in aged animals when compared to young (Figure 28). However the normalised values relating to the Elf-α dilution series were not optimal. To provide a more conservative estimate of the relative AChBP mRNA expression, the slope of the dilution series for Elf-α was adjusted to give a correlation co-efficient of above 0.8 which showed a statistically significant decrease of 86% compared to the normalised control (Figure 25). The simplest explanation offered from this study suggests the reduced AChBP protein levels are transcriptionally regulated, however the precise mechanism by which mRNA reduction occurs would require further investigation. There are both gene specific as well as global changes that may be responsible for such expression changes in aged tissue. Nothing is currently known about the specific transcriptional regulation of AChBP locus. Unfortunately, specific transcription factors can be isolated (for example using an electrophoretic mobility shift assay) only once the DNA sequence

of the AChBP promoter region or ideally the full gene sequence has become available. Similarly, global or regional changes in chromatin conformation and other age-related epigenetic changes in DNA methylation or histone modification patterns may well play a role here (for a recent review see(Calvanese *et al.*, 2009)), but remain difficult to study in an unsequenced organism. Downstream mechanisms, such as pre-mRNA splicing may also be subject to age-related changes (Kar *et al.*, 2005). For example, alternative splicing of the tau gene lead to the formation of neurofibrillary tangles that are associated with Alzheimer's Disease (Kar *et al.*, 2005). Problems associated with polyadenylation, which as part of the process used to produce the mature form of mRNA used for translation via the addition of the Poly(A) could also contribute to a reduction in mRNA expression (Merrick, 1992). Such disruption to polyadenylation have been observed in Huntington's Disease that can result in variations in the length of the mRNA tail which are used to synthesise the protein (Lin *et al.*, 1993). However, more information about the AChBP gene is required if one is to take into account of possible variances that may be encountered as a result of intronic splice variation through disruption to spliceosome assembly. Alternatively, the multiple mechanisms that safeguard the integrity and stability of mRNA, such as the capping of 5' region, or polyadenylation that are key components of RNA transcription could also be impaired. The latter finding has been reported to be compromised in aged tissue (Meshorer and Soreq, 2002).

3.5.3 GFAP expression in the young and aged CBG

Likewise, it is conceivable that alterations in the abundance of *L. stagnalis* glial cells could be responsible for changes in AChBP protein levels, therefore a reduction in AChBP may be symptomatic of an impairment in glial cells with increased age. Unfortunately, it proved impossible to make a straightforward assessment of any changes in the number of AChBP-expressing glia due to the lack of an antibody suitable for immunohistochemistry. As the subtype of glial cells that release AChBP is currently unknown, it would have been necessary to examine all representative glial cell populations within the aged *L. stagnalis* CBG through cell counts. However, this was beyond the scope of the current study. An alternative method commonly used to examine potential alterations in astrocytes (the major glial cell component in higher vertebrate CNS) is to examine expression of the astrocyte-specific glial acidic fibrillary protein (GFAP) in the young and aged CBG (Figure 30). GFAP, as an intermediate filament is ubiquitously expressed in astrocytes in

the CNS in higher vertebrates. Reports that have examined GFAP expression in aged animals have reported its expression to be increased in the aged rat CNS (Nichols *et al.*, 1993), in humans (Nichols *et al.*, 1993) and in the hippocampal region of aged SAMP8 and SAMP1 accelerated-ageing mouse model (Wu *et al.*, 2005). Nichols *et al* (1993) further reported that increased GFAP expression is independent of gender in aged hippocampus and striatum of rat and human subjects, suggesting differences relating to GFAP expression are part of the normal ageing process. Increased GFAP expression is considered to be an important progenitor in the impairment of synaptic plasticity, and its increased expression in astrocytes is generally interpreted as a reflection of the hypertrophy of astrocytes in aged animals (Finch, 2003).

Examination of GFAP protein expression in the CBG in *L. stagnalis* has not been previously demonstrated, but the successful demonstration of its existence at the corresponding 55kDa molecular weight in the CBG of a related species, *M. abbreviatus* supports the notion that GFAP has a well conserved phylogeny *(dos Santosa et al., 2005).* Comparison of GFAP expression showed its expression increased in the aged CBG of *L. stagnalis* when compared to young and normalised to GAPDH, however this was not statistically significant ($p > 0.05$) (Figure 30). Due to limited sample availability of the 10 month old animals, increasing the sample size to increase the statistical power was not feasible in the current study. However an 18% increase in the aged CBG is suggestive that further clarification is necessary on age-related changes in aged *L. stagnalis* glial cells. However to obtain a more coherent view of the age-related changes in the nervous system, it is important to take into account of peripheral effects that may contribute to a reduction in AChBP in the aged CBG. To this effect, GFAP expression alone would not be able to rule out the possibility that AChBP protein levels are independently regulated by different glial cell subtypes, and it remains to be clarified whether AChBP and GFAP are colocalised.

There were several limitations to this study. Firstly, AChBP antibody labelling could not be used successfully to examine the localisation of AChBP using immunohistochemistry. This finding was unfortunate as the successful detection of AChBP in brain sections would have allowed identification of AChBP-releasing glial

cells that may be in close proximity to neurons that are involved in the feeding behaviour. However, whilst the anti-*Lymnaea* AChBP antibody which was a kind gift from Pim Van Lierop's (Netherlands) laboratory had been previously employed in Western Blot validations of AChBP (Sixma and Smit, 2003), it did not prove to be suitable for immunohistochemical studies. Binding specificity could not be improved upon by changing the dilution of the primary or secondary antibody, or by blocking the sections with 10% milk or BSA in order to reduce the background signal which labelled the coverslips as well as the tissue. The fluorescence detected here was unlikely to represent the ubiquitous expression of AChBP within the *L. stagnalis* CNS, but more likely the result of incompatibility of the anti-*Lymnaea* AChBP antibody. Therefore, the question of localisation of AChBP within the CNS could not be determined using this approach. Secondly, for reasons discussed above, GFAP expression could not be used conclusively to identify potential changes in the number of glials cell expressing AChBP.

Finally, the identification of an appropriate housekeeping gene for the purpose of normalisation represented a major obstacle in validating mRNA levels. HK genes should exhibit high abundance, and be stably expressed across a variety of experimental conditions and not vary between groups by more than one cycle (Livak and Schmittgen, 2001). In addition, the linear regression of the dilution series used to estimate the efficiency of the reaction should be within 0.8 – 1 for both the target and reference genes in order to make meaningful comparisons between the control and treatment groups (Pfaffl, 2001). The dilution series obtained for Elf-α from young cDNA was not optimal as the efficiency of the reaction was calculated based on a linear regression of below 0.8. Therefore the reliability of the mRNA expression data is to be considered with caution. However, a conservative estimate of the efficiency was calculated by re-adjusting the correlation coefficient to a value above 0.8 that provided a more realistic estimate of the reaction efficiency suggested there was a statistically significant difference between the two groups (Figure 25).

3.6 CONCLUSIONS AND FUTURE DIRECTIONS

In the present study, we could not rule out that disruption to glial cell accompany the reduction in AChBP levels that are observed in the aged CBG. Our conclusion was based on preliminary analysis of the astrocytic reporter GFAP that are widely used to detect the presence of astrocyte under a variety of conditions. The alternative would be to examine glial cell morphology in young and aged CBG, however this indirect measure is less labour intensive and costly and provided a convenient alternative to examine the commonly reported finding that astrocyte hypertrophy occurs in the aged CNS. One possibility for further characterising the glial cell subtype releasing AChBP would be *in situ* hybridisation experiments designed to detect the expression of AChBP and GFAP in order to examine their possible co-localisation.

Secondly, relative expression of AChBP as determined by RT-qPCR showed AChBP was decreased in the aged CBG, however caution was taken to avoid misinterpretation of the dataset due to sub-optimal reaction efficiency for one of the HK gene. Normalised against a HK gene relies on the HK being stable in both the control and treatment conditions in order to avoid misinterpretation of the dataset. The relative quantification of gene expression data generated from RT-qPCR between young and aged animals required the use of a suitable housekeeping gene to normalise the expression of target AChBP gene. However, the identification of an appropriate housekeeping gene for the purpose of normalisation represented a major obstacle in validating mRNA levels in aged tissue, as HK genes have been demonstrated to be altered in a tissue-specific way (Pfaffl, 2001). When using a HK for normalisation, the use of more than one reference is also recommended as the interpretation of the results can be falsely bias results when using a single gene (Livak and Schmittgen, 2001). However, assessment of multiple HK genes is not achievable in *L. stagnalis*, as very few routinely used HK genes are sequenced and this organism is not and even less is known about their expression patterns with age. The elongation factor α (Elf-α) isoform which is responsible for the enzymatic delivery of aminoacyl tRNAs to the ribosome (for review see Kapp and Lorsch, 2004) was used for RT-qPCR analysis. In the CBG region Elf-α was stably expressed with minimal variability between the two age groups and could therefore be considered a suitable HK gene. However as mentioned by Livak and Schmittgen, 2001 , using more than one HK gene would be the preferred option to

avoid variability in mRNA datasets. Regardless of whether single or multiple HK genes are used for normalisation, they should exhibit high abundance, and be stably expressed across a variety of experimental conditions and not vary between groups by more than one cycle (Livak and Schmittgen, 2001).

Chapter 4: dsRNA- AND siRNA-MEDIATED GENE SILENCING OF AChBP

4.1 BACKGROUND:

The post transcriptional silencing mechanism, originally outlined in *C. elegans* has become a useful method to actively regulate gene transcription (Fire *et al.*, 1998). Abbreviated RNAi, RNA interference is used by plant and animal cells to post transcriptionally silence genes through knockdown of mRNA in a sequence-specific manner, and thought to be a conserved antiviral defence mechanism (Jacobs *et al.*, 1998; Montgomery *et al.*, 1998). The high specificity of RNAi-based therapies has seen it used as a tool to identify gene products and elucidate gene function. It also may prove to be useful in the future as a therapy for silencing mutant genes involved in disease (Kamath *et al.*, 2003; Reynolds *et al.*, 2004). RNAi can be activated using a variety of different mechanisms, including micro RNA(miRNA) (Bartel, 2004), long double stranded RNA (dsRNA) and synthetic short interfering RNA (siRNA) (Bass, 2000). To help develop a better understanding of the functions of siRNA, this section contains a brief discussion on the biological background by which siRNA suppresses gene expression through mRNA destruction and dsRNA processing and highlights the applications of RNAi in the *L. stagnalis* nervous system.

4.1.1 Mechanism of action of RNAi-mediated gene silencing

dsRNA mediated gene silencing

RNAi works by cleavage of phosphodiester bonds through protein complexes or enzymes (Bass, 2000). The following series of steps describe the processing of double stranded (ds) RNA into intermediate siRNA fragments which are used in the regulation and expression of genes. A schematic of the known sequence of events is represented in Figure 31.

Figure 31 Schematic of the mechanism of gene silencing through siRNA (a) and miRNA (b) Cited from (Krulko *et al.*, 2009). Exogenous application (a) or endogenous synthesis (b) use the RISC to cleave complementary regions of the target mRNA and prevent the synthesis of the corresponding gene product. See text for details regarding the process of siRNA and miRNA-mediated silencing.

Step 1: The sense and antisense strands detach from each other

The silencing mechanism is initiated when the dsRNA fragment is processed into shorter small interfering RNAs (siRNAs) by the enzyme Dicer (Carmell and Hannon, 2004). The distinctive structure of the Dicer protein includes an Rnase III motif that specifically cleaves dsRNA into shorter 21-25 nucleotide fragments with a characteristic 2 nucleotide 3‘ overhang (Bass, 2000; Bernstein *et al.*, 2001; Sun *et al.*, 2005). As an initiation step to RNAi, the hydrogen bonds between the sense and antisense strand of the double stranded siRNA are broken (Bass, 2000). However the exact mechanism remains unclear. The unwinding of siRNA is believed to be an active energy consuming process, and most likely involves the DEXD/ H family of

RNA-unwindase enzymes (as reviewed in Sontheimer 2005). Yet, despite several ATPase/RNase helicase domains having been implicated in RNAi process, none have so far been unambiguously linked to the unwinding of siRNA (as reviewed in Sontheimer 2005). Dicer, which also contains a helicase domain at the amino terminal is a plausible candidate to separate the sense and antisense strand, although this has not been proven unequivocally (Bernstein *et al.*, 2001).

Step 2: The protein complex is attached to the antisense strand of the siRNA

In the 'effector' phase, the antisense strand from the cleaved siRNA is incorporated into a ribonuclease-inducing silencing complex (RISC); (Yan *et al.*, 2003). Efforts to try and understand the mechanism of action of the RISC complex have been hampered in part by the wide range of apparently different sizes observed within the RISC (from 106-550kDa) (as reviewed in Sontheimer 2005). Although, it is presently unclear whether these are genuine differences or whether the discrepancies are due to technical variations. A common theme among the effector RISC are its association with the Argonaut-2 family of proteins (Sontheimer, 2005). Other proteins which bind to RISC include species-specific proteins such as Dcr1, Dcr2, R2D2 and Tsn in *D.melanogaster* as well as AGO1, Gemin3 and Gemin4 in humans (reviewed in Sonheimer 2005). Given that Dicer also associates with Ago-2, suggests Dicer may have an as-yet unknown but additional role beyond dsRNA cleavage (as reviewed in (Sontheimer, 2005)). The characteristic two nucleotide 3' overhang produced by Dicer resembles breakdown products in *E.coli* through RNase III-like digestion (Bass, 2000). In *D.melanogaster*, the two nucleotide 3' overhang of the siRNA was shown to bind to the highly conserved N-terminal PIWI Argonaut Zwille (PAZ) domain of the Ago-2 protein (Cerutti *et al.*, 2000). The suggested role for these domains include the guidance and orientation of RISC-bound siRNA complex to the complementary strand of the target mRNA (Song *et al.*, 2004).

Step 3: The protein complex is brought close to the mRNA

The RISC-incorporated siRNA is able to recognise the target mRNA by siRNA-mRNA base pairing (Sontheimer, 2005). The active antisense strand is able to form hydrogen bond to the complimentary target on the mRNA. It must be noted that in the absence of the guidance mechanism provided by RISC to the complementary mRNA target, siRNA can act as primers for RNA-dependent RNA polymerase

(RdRP) and generate further siRNA (Sijen *et al.*, 2001). Therefore only a small amount of dsRNA is required to degrade a much larger population of mRNA (Fire *et al.*, 1998). The dsRNA is subsequently cleaved by the Dicer enzyme to create further sequence-specific siRNA which can activate RNAi (also see Figure 31). Evidence that RdRP can act as a catalyst during endogenous amplification of siRNA and that this process is integral for induction of RNAi was found in *C. elegans* where a mutation in RdRP renders the organism incapable of switching on systemic RNAi (Sijen *et al.*, 2001). RdRP-dependent siRNA amplification has so far been observed in plants and in *C. elegans*, however this kind of amplification has not been demonstrated across all species. Currently, there are no identifiable RdRP homologues in mammalian systems that could be examined in a comparable manner. Furthermore, RNAi activation in mammalian systems has been observed independently of RNA-dependent RNA polymerase (Stein *et al.*, 2003; Martinez *et al.*, 2002).

Step 4: The mRNA is cleaved

At the centre of the PIWI domain of the Ago-2 protein, there are three highly conserved carboxylates: Asp-558, Asp-628 and Glu-635 which are homologous to other members of the RNase H family of enzymes (Song *et al.*, 2004). This suggests PIWI may be an RNase H domain, and the catalytic component of RISC which specifically cleaves the mRNA complex causing post transcriptional silencing (Cerutti *et al.*, 2000; Yan *et al.*, 2003). Site-directed mutagenesis where the aspartate was swapped with alanine residue within the PIWI domain of the human Ago-2 demonstrated that, in the absence of the PIWI domain, siRNA are still capable of forming a complex with RISC (via the unaltered PAZ domain) (Liu *et al.*, 2004). However, the RISC-incorporated siRNA was unable to cleave the target mRNA suggesting the PIWI domain may play an active role in the cleavage of mRNA targets (Liu *et al.*, 2004).

4.1.2 miRNA-mediated gene silencing

The naturally occurring miRNAs can also down regulate the target mRNA either through translational repression, mRNA cleavage, or deadenylation in a manner summarised in Figure 31, (Krulko *et al.*, 2009). miRNAs have been identified with their own promoters, however the majority of the miRNAs are considered to reside within the small non-coding intronic regions of the pre-mRNA gene, and as such

share their regulatory elements during transcription (Bartel, 2004). As a precursor step to obtaining the mature form of miRNA (21-25nt), genes encoding miRNA are first transcribed by RNA polymerase II into smaller ~70nt fragments called 'pri-miRNA'. This process enables the pri-miRNA to be folded into stem-loop structures and exported from the nucleus to the cytoplasm using the karyopherin exportin-5 and Ran-GTP complex (Bartel, 2004). Within the cytoplasm, pri-miRNA are recognised and cleaved by the RNA polymerase III enzyme DICER to generate a 21-25nt miRNA and incorporated into the RNA inducing silencing complex (RISC); (Bartel, 2004). While the mechanism of miRNA unwinding and miRNA-mRNA target complementarity parallel that described for siRNA, however, there is one distinction compared to siRNAs. Endogenously released miRNA show only partial complementarity to the target mRNA, and this action is likely to contribute to transcriptional repression rather than complete gene silencing as can be observed using siRNA (Bartel, 2004). For a more detailed information regarding miRNA biosynthesis and structural pre-requisites involving partial complementarity, the reader is directed elsewhere (Bartel, 2004).

4.1.3 Activation of the interferon response

Infections from viruses which contain dsRNA or dsDNA molecules commonly activate the interferon regulatory factor (IRF) family of proteins to prevent viruses from entering the organism (Jacobs and Langland, 1996). At the core of the IRF superfamily is a homologous DNA-binding domain at their N terminus containing the DNA sequence (GAAA) which is typically embedded in a more complex DNA regulatory domain (Cheng *et al.*, 2006). However the C terminal end is highly divergent allowing for site-specific interactions with several transcription factors (Cheng *et al.*, 2006). IRF-3 activation plays an important role during viral infection and activates the type 1 interferon response (Cheng *et al.*, 2006). Cells initiate the interferon response through activation of serine kinases as well as toll-like receptors (TLR) which both phosphorylate IRF-3 from a latent form ubiquitously expressed within the cytoplasm to an active form which accumulates in the nucleus in response to a viral attack (Cheng *et al.*, 2006).

A major difference between activation of RNAi in invertebrates such as *C. elegans*, or *D.melanogaster* and mammalian cells is that dsRNA administration into mammalian cells activates a type 1 interferon response (Jacobs and Langland, 1996).

This has not been observed in invertebrates. Furthermore, administration of a 21-25nt synthetically synthesised siRNA does not elicit an interferon response in invertebrate or mammalian systems (Heidel *et al.*, 2004).

4.1.4 RNA-mediated silencing in L. stagnalis

RNAi has been used successfully to knockdown proteins in *L. stagnalis*, allowing us to deduce that the RNAi machinery is in fact present in this organism. The ability to introduce long *in vitro* transcribed dsRNA into *L. stagnalis* rather than chemically synthesised siRNAs make it a particularly suitable and cost effective model for assessing gene function without the risk of activation of the interferon response. A list of studies that have utilised RNAi to examine functional changes in the *L. stagnalis* nervous system are detailed below (for summary see Table 8).

Authors	Amount	Time points	Monitor RNAi	Gene silenced	Administration
Fei *et al*.2007	1000ng	2-8 days	WB,VB, CI	Hsp-70	MI*
Korneev *et al*. 2002	500ng	3,24,48 hrs	R,E,VB	nNOS	MI*
Spafford *et al*. 2003	10μM	3 days	Y, E, P	CASK	T,C
Perlson *et al.*, 2004	10pM	72 hrs	VB	RGP51	T,C
van Diepen *et al.*, 2005	300ng/ml	24-96 hrs	I	L-TRIM	T,C
van Kesteren *et al.*, 2006	300ng/ml	0-72hrs	I,PVB	β-thymosin	T,C

Table 8: Summary of published siRNA/dsRNA transfection in *L. stagnalis*
RNAi was demonstrated by examining a variety of different techniques after administration with siRNA and dsRNA **C**: incubated in cell culture; **CI**: co-immuno precipitation; **E**: electrophysiology; **I**: *in situ* hybridisation; **MI**: microinjection; **R**: RT-PCR, **T**: transient transfection; **VB**: Visual Behaviour; **WB**: western Blot, **Y**:yeast 2 hybrid assay. The 'amount' of dsRNA or siRNA differed depending on the experimental conditions used to monitor the effects of RNAi. The time points denote the duration of time point to effect measurement. * denote studies undertaken in the intact animal.

A small number of studies have applied RNAi techniques to the whole animal, using various phenotypic outcome measures. Fictive feeding refers to the pattern of neuronal activity recorded in neurons of the isolated CNS. This pattern of activity is believed to mimic what occurs during normal feeding in the whole animal (Benjamin and Rose, 1979). Examination of this behaviour has generated interest in examining the role of nitric oxide synthase (nNOS) gene in the regulation of the feeding behaviour (Korneev *et al.*, 2002). Microinjection of 500ng dsRNA targeted against *L. stagnalis* nNOS through the animal blood space (haemocoel) directly under the foot caused a decrease in nNOS levels (Korneev *et al.*, 2002). These decreases correlated with a reduction in the fictive feeding behaviour compared to controls (Korneev *et al.*, 2002). This suggests the neuronal isoform of nNOS gene could participate in the feeding behaviour of *Lymnaea stagnalis* (Korneev *et al.*, 2002).

Other studies have utilised the cell culture models with either dsRNA microinjection into identified neurons or incubation in media containing siRNA to address the participation of epidermal growth factors influencing axotomised and injured *L. stagnalis* neurons (Spafford *et al.*, 2003; Perlson *et al.*, 2004). This process has proved the particularly versatile as time course assessment (see Table 8) of axonal regeneration can be directly correlated with changes in protein levels to assess the participation of other proteins involved in retrograde nerve injury (Perlson *et al.*, 2004).

Induction of RNAi in *L. stagnalis* however is not as easily accomplished compared to the *C. elegans* model system in which RNAi could be initiated through multiple mechanisms e.g., feeding bacterial colonies containing dsRNA, bathing in media containing dsRNA or siRNA or through direct microinjection. Despite the absence of a reliable RNAi delivery mechanism, the accessibility of large neurons has made *L. stagnalis* an attractive model in understanding neuronal function. To achieve gene silencing, microinjection into *L. stagnalis* has been the favoured option (Korneev *et al.*, 2002; Fei *et al.*, 2007), although transient transfection can be appropriately used in culture (Spafford *et al.*, 2003). See Table 8 for a summary of techniques used to assess RNAi in *L. stagnalis*.

4.2 OBJECTIVE:

RNAi was used to knockdown AChBP *in vitro* as well as *in vivo* in the nervous system of the pond snail *L. stagnalis* to determine whether a reduction in AChBP levels contributed to the decrease in feeding behaviour observed in aged animals. Since AChBP activity can regulate ACh at cholinergic synapses, I hypothesised that a reduction in AChBP protein expression may be part of the network of proteins participating in the regulation of feeding behaviour in *L. stagnalis*.

The suitability of AChBP-mediated knockdown was tested in an *in vitro* model using AChBP dsRNA in the presence and absence of 10μM ACh and assessed using Western Blot analysis. AChBP dsRNA and two different AChBP siRNA duplexes targeting different regions of the AChBP gene were used to attempt to knockdown AChBP gene *in vivo*, at two different time points. The animals feeding score was assessed after each time point and the extent of knockdown was determined using Western blot analysis on AChBP expression in the CBG.

4.3 MATERIALS AND METHODS

4.3.1 Nucleic acids:

siRNA duplexes against AChBP (siAChBP1, and siAChBP2), and a non-targeting scrambled siRNA (siScrambled) with no sequence homology to proteins present in the non-redundant database and siScrambled fluorescently labelled siRNA (Allstars Neg siRNA AF546) were purchased from Qiagen (Figure 32). siRNA came purified and pre-annealed by the manufacturer. The two siRNA duplexes were selected by Qiagen based on the BIOPREDsi algorithm licensed from Novartis (http://www.biopredsi.org/start.html) together with a proprietary homology analysis tool (see discussion). siAChBP1 and siAChBP2 was reconstituted as per manufacturer's instruction using the 1ml siRNA suspension buffer. Tubes were heated to 80°C for 1 minute, then incubated for 60 minutes at 37°C and stored at -20°C.

The sequences for siAChBP1 and siAChBP2 were as follows:

```
  1 CTCATCTAAC TGTATTTCGG GGGTGCTGAT AAAAATATCA AAATGCGTCG AAACATTTTC
 61 TGCCTTGCTT GTCTCTGGAT CGTGCAAGCG TGTCTAAGCT TGGACCGGGC AGACATCTTG
121 TACAACATAC GTCAGACATC GAGACCGGAT GTGATTCCCA CACAGCGAGA TCGCCCAGTG
181 GCGGTGTCCG TCTCTTTGAA GTTCATCAAC ATCTTGGAAG TGAATGAAAT AACCAATGAA
241 GTGGACGTGG TCTTTTGGCA GCAGACGACA TGGTCGGACA GGACCCTCGC CTGGAACAGT
301 TCTCACTCAC CAGATCAGGT TTCCGTGCCA ATAAGCTCTT TGTGGGTGCC TGACCTCGCT
361 GCATACAACG CCATCTCGAA ACCTGAAGTC CTTACACCGC AACTGGCCAG GGTCGTATCC
421 GATGGTGAAG TGCTGTACAT GCCGAGTATC CGCCAGCGGT TCTCCTGCGA TGTATCGGGT
481 GTCGATACGG AGTCCGGTGC TACATGTCGG ATCAAAATTG GTTCCTGGAC CCACCACAGT
541 AGAGAGATTT CTGTAGATCC CACGACAGAA AATAGTGATG ATTCTGAATA CTTCTCCCAA
601 TACTCTCGCT TTGAAATCTT GGACGTCACA CAGAAGAAGA ACTCGGTTAC CTACTCTTGC
661 TGTCCGGAGG CATACGAGGA CGTTGAAGTG AGTCTCAATT TCCGGAAGAA GGGACGCTCC
721 GAAATTCTTT AGTCAAGCGT TTATGTCCCG ACTGATATCC TAAGCACATC ATTTAAGGAA
781 GAAATGAATC CTCATGGATA GAATTCTTGT CTAACATTTT AAAAAAAATT TATACAGCTA
841 TTAGCCATAT TTTTTAAATT ATTTTTTAAA AATTGATTTT GTTTGCTCTG ATATTTTATT
901 TTTTTCTATT TTGCAGTATA TTGATGTAAA ATATTTAAGT TTAAGAGTTT GATAATATAT
961 AAATACATTT GTAAAAATTG
```

siAChBP1 targeted region: GTG AAT GAA ATA ACC AAT GAA
sense r(GAA UGA AAU AAC CAA UGA A)dTdT
antisense r(UUC AUU GGU UAU UUC AUU C)dAdC
siAChBP2 targeted region: CAG GGT CGT ATC CGA TGG TGA
sense r(GGG UCG UAU CCG AUG GUG A)dTdT
antisense r(UCA CCA UCG GAU ACG ACC C)dTdG

siScrambled +/- flourophore: Allstars Neg siRNA AF546 (proprietary sense and antisense strand) Modification: sense 3'-alexaFlour546

Figure 32 Selection of siRNA from AChBP mRNA coding sequence AF364899
AChBP siRNA was designed by Qiagen using BIOPREDsi algorithm and a proprietary homology analysis tool.

4.3.2 AChBP dsRNA synthesis

dsRNA synthesis is a multi-step process requiring the cloning of AChBP gene into a vector, PCR amplification of the forward and reverse strand of the gene with a T7 promoter overhang, *in vitro* transcription of the gene product into ssRNA, and annealing the two separate strand into a dsRNA. The following steps were used to produce dsRNA specific to AChBP, as well as to green fluorescent protein (GFP) which was used as a negative control. The sequences for AChBP and GFP dsRNA are summarised in Table 9.

Product	Forward primers	Reverse Primers
AChBP antisense template	5'-CGGGGGTGCTGATAAAAATA-3'	5'-**TAATACGACTCACTATAGGG** AGTCGGGACATAAACGCTTG-3'
AChBP sense template	5'-**TAATACGACTCACTATAGGG** CGGGGGTGCTGATAAAAATA-3'	5'-AGTCGGGACATAAACGCTTG-3'
GFP antisense template	5'-TAAACGGCCACAAGTTCA-3'	**5'TAATACGACTCACTATAGGG** CTTTACTTGTACAGCTCGTC-3'
GFP sense template	**5'TAATACGACTCACTATAGGG** TAAACGGCCACAAGTTCA-3'	5'-GCTTTACTTGTACAGCTCGTC-3'

Table 9: Primers for AChBP and GFP with T7 promoter (underlined)

4.3.3 Cloning AChBP into pGEM vector

4.3.3.1 cDNA synthesis and RT reaction

Total RNA was isolated from 3 month old *L. stagnalis* CNS in a manner described previously (see section 2.3.1 - 2.3.2.1). The mRNA was reverse transcribed using Oligo(dT)15 primers (Promega) using a 2:1 ratio of RNA concentration versus primer concentration and reverse transcribed using Superscript II (Invitrogen) according to manufacturer's instructions (Invitrogen).

4.3.3.2 Primer Design and PCR

AChBP cDNA cloned into a plasmid vector was a kind gift from Preet Sian and Katrin Jennert Burston. Forward and reverse primers for the dsAChBP were designed for the *L. stagnalis* AChBP (accession number AF364899) using

Primer3Plus (http://www.bioinformatics.nl/cgi-bin/primer3plus/primer3plus.cgi). Forward and reverse primers were size-matched to 20 nucleotides in length, located at positions 195 and 961 of the cDNA sequence (accession number AF364899); (Figure 33).

A:

```
  1 CTCATCTAAC TGTATTTCGG GGGTGCTGAT AAAAATATCA AAATGCGTCG AAACATTTTC
 61 TGCCTTGCTT GTCTCTGGAT CGTGCAAGCG TGTCTAAGCT TGGACCGGGC AGACATCTTG
121 TACAACATAC GTCAGACATC GAGACCGGAT GTGATTCCCA CACAGCGAGA TCGCCCAGTG
181 GCGGTGTCCG TCTCTTTGAA GTTCATCAAC ATCTTGGAAG TGAATGAAAT AACCAATGAA
241 GTGGACGTGG TCTTTTGGCA GCAGACGACA TGGTCGGACA GGACCCTCGC CTGGAACAGT
301 TCTCACTCAC CAGATCAGGT TTCCGTGCCA ATAAGCTCTT TGTGGGTGCC TGACCTCGCT
361 GCATACAACG CCATCTCGAA ACCTGAAGTC CTTACACCGC AACTGGCCAG GGTCGTATCC
421 GATGGTGAAG TGCTGTACAT GCCGAGTATC CGCCAGCGGT TCTCCTGCGA TGTATCGGGT
481 GTCGATACGG AGTCCGGTGC TACATGTCGG ATCAAAATTG GTTCCTGGAC CCACCACAGT
541 AGAGAGATTT CTGTAGATCC CACGACAGAA AATAGTGATG ATTCTGAATA CTTCTCCCAA
601 TACTCTCGCT TTGAAATCTT GGACGTCACA CAGAAGAAGA ACTCGGTTAC CTACTCTTGC
661 TGTCCGGAGG CATACGAGGA CGTTGAAGTG AGTCTCAATT TCCGGAAGAA GGGACGCTCC
721 GAAATTCTTT AGTCAAGCGT TTATGTCCCG ACTGATATCC TAAGCACATC ATTTAAGGAA
781 GAAATGAATC CTCATGGATA GAATTCTTGT CTAACATTTT AAAAAAAATT TATACAGCTA
841 TTAGCCATAT TTTTTAAATT ATTTTTTAAA AATTGATTTT GTTTGCTCTG ATATTTTATT
901 TTTTTCTATT TTGCAGTATA TTGATGTAAA ATATTTAAGT TTAAGAGTTT GATAATATAT
961 AAATACATTT GTAAAAATTG
```

B:

Property	Forward Primer	Reverse Primer
Bp position from start codon of full length cDNA	-27	813
Nucleotide Length	20	20
Melting temperature (Tm)	59.79 °C	60.13°C
% CG content	45.0	50.0
Sequence	5'-CGGGGGTGCTGATAAAAATA-3'	5'-AGTCGGGACATAAACGCTTG-3'

Figure 33 Primer set designed for cloning of AChBP cDNA from *L. stagnalis*
Forward and reverse primers were designed to target 760bp of AChBP cDNA shown highlighted in the box (A). Optimal annealing conditions for forward and reverse primers targeting AChBP (AF364899) (B).

For each PCR reaction 1/40th (1 µl) of the AChBP cDNA reaction was amplified in a 25 µl reaction volume containing 0.5 µM of each primer. The PCR reaction was performed using the iCycler thermal cycler (Biorad). Initial PCR conditions were as follows: denaturation at 94°C for 2 minutes, 45 cycles at 94°C for 30 seconds, 47.3°C for 30 seconds, 72°C at 45 seconds, then final extension at 72°C for 5 minutes.

The buffers used in the reaction vessel were as follows: 1 x Accurase™ buffer (Biogene), 1.5mM $Mg(OA)_2$ (Invitrogen), 1pmol/µl forward and reverse primers, 0.2 mM dNTPS, *L. stagnalis* cDNA, 0.5u/µl Accurase™ (Biogene). The samples were loaded on a 2% agarose gel prepared with 1 x Tris-acetate-EDTA (40mM Tris, 20mM glacial acetic acid, 1mM EDTA, pH 8) (Aldrich) and 0.2µg/ml ethidium bromide (Cambridge Bioscience). AChBP positive bands visualised on a 2% agarose gel corresponding to a single product at the correct molecular weight was excised and cDNA was recovered using Zymoclean Gel DNA recovery kit (Zymo Research).

4.3.3.3 Vector ligation and sequence determination

AChBP cDNA was cloned using pGEM-T vector systems (Promega) as per manufacturer's instructions by Katrin Jennert-Burston and Preet Sian, with the following alterations.

a) 250µl SOC medium was added to the prepared JM109 cells instead of the recommended 950µl.
b) Cells were incubated at 37°C for 1 hour instead of the recommended 1.5 hours.

Individual colonies positively transformed with pGEM-T harbouring the AChBP gene were selected using blue/ white screen selection (16 hour incubation time). Positive clones (white) were picked out and isolated from LB agar containing IPTG (0.5mM), X-Gal (80µg/ml) and ampicillin (100µg/ml) and incubated in liquid broth medium (prepared with 5ml LB Broth containing 100µg/ml ampicillin).

DNA was extracted and purified using Promega Wizard *plus* SV Miniprep DNA purification system. DNA was ethanol precipitated and the dried pellet was sent for

sequencing (MWG Operon, Germany) to confirm the successful ligation of AChBP cDNA into the vector.

4.3.4 Synthesis and purification of dsRNA

4.3.4.1 Addition of T7 promoter flanking the transcription region

AChBP and GFP full length cDNAs were amplified using a primer tailed with a T7 consensus promoter sequence. The T7 promoters are required to in vitro transcribe each strand of the dsRNA molecule (Dekker *et al.*, 2004). Although this could occur in a one-step reaction, in our case flanking the T7 promoter for both the forward and reverse strand in a single reaction did not result in product formation (data not shown). Therefore a combination of a T7-tailed primer on one side of the amplicon with an ordinary non-tailed primer on the other side was used during PCR amplification. This process was repeated for GFP. The primer combinations for the forward and reverse amplification are described in

Table 9. The schematic representation of a T7 promoter-tailed primer combined with a reverse primer which does not contain a T7 overhang and vice versa is shown in Figure 34.

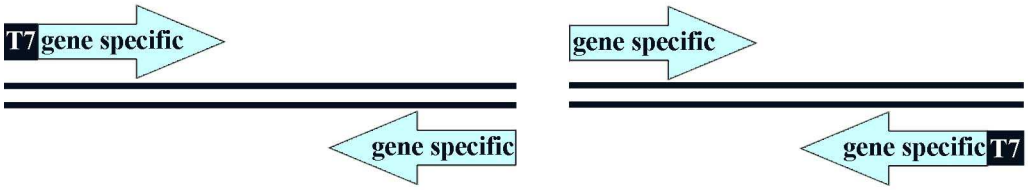

Figure 34 Amplification of PCR products with T7 promoter

Sense and anti-sense AChBP and GFP strands were amplified separately with one primer containing a T7 promoter as represented in Figure 34. The PCR reaction contained 1 X PCR Buffer (Invitrogen), 25mM $MgCl_2$, dNTPs (10mM), 20µM forward and reverse primers each, 0.25µl Invitrogen Taq (10 u/µl) and 0.5µl pEGFP-N1 (5.56µg/µl) template (Invitrogen) for GFP gene and 0.5µl pGEM-T-AChBP 12 ng/µl) for AChBP. The PCR amplification steps included denaturation at 94 °C for 2 mins, followed by 45 cycles at 94 °C for 30s, 50 °C for 30s, 72 °C for 60s, then final extension at 72 °C for 10 mins, with the following modification to the annealing

temperature – for AChBP primers the annealing temperature was optimal at 45°C for 30s and for GFP primers the annealing temperature was optimal at 57°C for 30s. The PCR products were visualised on a 1.5% agarose gel (see optimisation of dsRNA section).

4.3.4.2 In vitro transcription using Megascript synthesis kit (Ambion)

dsRNA was synthesised using Megascript kit (Ambion) as per manufacturer's instructions. For the *in vitro* transcription reaction, 1µg of each template containing a T7 promoter flanking the transcription region was transcribed in separate tubes with 2µl 10X T7 Reaction buffer, 2µl each of 75mM solutions of ATP, CTP, GTP, and UTP and 2µl T7 enzyme mix made up to a volume of 20µl with nuclease-free water. Forward and reverse ssRNA were synthesised over a 16 hour period at 37°C. Sense and antisense strands were combined and incubated at 75°C for 5 minutes and cooled to room temperature to anneal into dsRNA. Nuclease digestion was performed to remove ssRNA from the cooled mixture using 2µl Dnase1 and 2µl Rnase, 5µl 10X Digestion Buffer with the 20µl ssRNA and made up to a volume to 50µl with nuclease-free water and digested at 37°C for 1 hour.

To remove proteins, degraded nucleotides and free nucleic acids from the dsRNA mixture, proprietary binding columns (MEGAscript kit, Ambion) were used to bind dsRNA and elute contaminants from the mixture. 100µl of dsRNA was combined with 100µl of 10X binding buffer, 300µl nuclease-free water and 250µl ethanol in a microtube and gently pipetted to ensure the solutions were mixed. 500µl of dsRNA binding mix was pipetted into the binding column which was placed on top of a collection cartridge. The sample was centrifuged at 12,000xg for 2 minutes. The flow through was discarded, and replaced with a new collection tube. dsRNA was recovered from the column using 500µl of the wash solution provided and the sample centrifuged as described above.

Two different annealing temperatures were tested to establish the optimal conditions required for amplification of AChBP dsRNA template with forward and reverse primers containing a T7 promoter. The AChBP template could not be amplified using the forward and reverse primers tailed with T7 overhangs in opposing

directions in the same tube. This is likely due to the length of the AChBP primer and the length of the T7 overhang which may likely self-anneal during amplification (see Table 9). Therefore the sense and anti-sense templates were amplified in separate reaction tubes and ssRNA annealed after separate in vitro transcription of sense and anti-sense RNA. The optimal annealing temperature for both forward and reverse primers was 45°C (see Figure 35).

Following annealing of ssRNA strands into dsRNA, a series of 50 µl fractions were collected using a wash solution provided by the manufacturer (MEGAscript kit, Ambion) and centrifuged for 2 minutes at 14,000 x g. A modification of the recommended protocol was the elution buffer was heated to 90°C and added to the column and a series of fractions collected in labelled microtubes (Figure 35C). In total, 5 fractions were collected to ensure any residual dsRNA bound to the binding column was eluted in the wash solution. The five fractions were visualised on a 2% agarose gel, showing AChBP dsRNA amount decreasing after the 4th fraction (Figure 35C) All the dsRNA fractions were combined and quantified using spectrophotometer at the 260nm absorbance readings as 0.5 µg/µl.

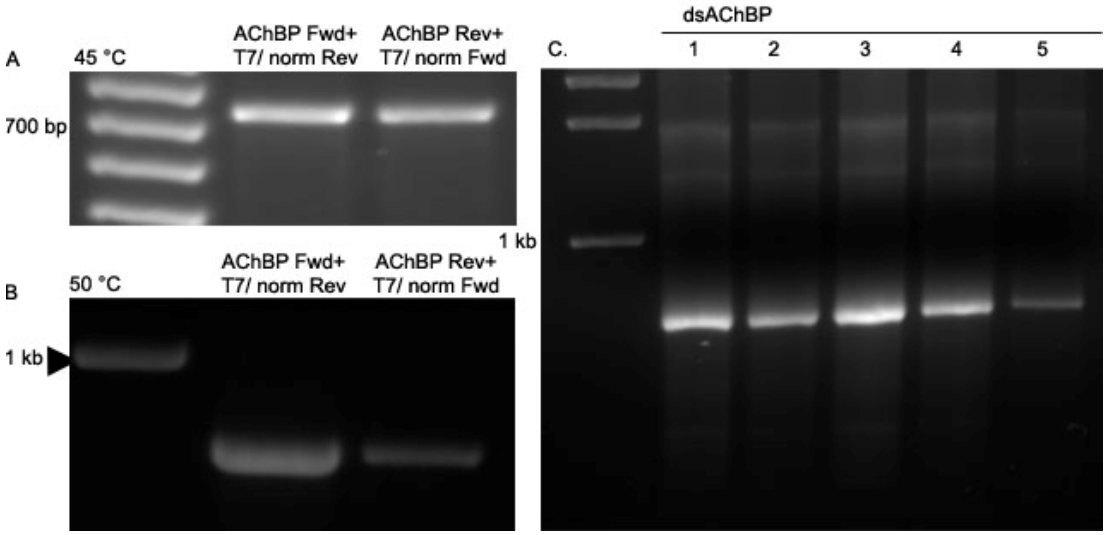

Figure 35 In vitro transcription of AChBP dsRNA on 2% agarose gel.
PCR amplification of AChBP gene with T7 overhang at 45° annealing temperature (**A**) and 50°C annealing temperature (**B**) showed 45°C was the preferred annealing temperature for AChBP gene. 5 dsRNA fractions were collected using 50µl of wash solution (**C**) as described previously (see methods section).

4.3.4.3 Synthesis of GFP dsRNA using Megascript kit:

Two different annealing temperatures were tested to establish the optimal conditions required for amplification of GFP dsRNA template with forward and reverse primers containing a T7 promoter. The selection of the annealing temperature was based around the recommended annealing temperatures provided by Primer3plus. The predicted temperatures for the primers with T7 overhangs were higher (65°C for GFP forward primer + T7 overhang, and 68°C for GFP reverse primer + T7 overhang) compared to 48°C for 'normal' GFP forward primer and 53°C for 'normal' GFP reverse primer without T7 overhang. 50°C and 57°C were chosen for a PCR reaction only one of the strands with a T7 overhang. As described previously, the elution buffer was heated to 90°C and added to column and the series of fractions collected in labelled microtubes (Figure 36C). More dsGFP came off in the second elution, and less in subsequent elutions (Figure 36C). Samples were quantified spectrophotometrically at the 260nm concentrations of all samples were in the region of 400ng/µl. 1/400th of the sample was run on a 2% agarose gel to visualise the level of purity of single product amplification (Figure 36C).

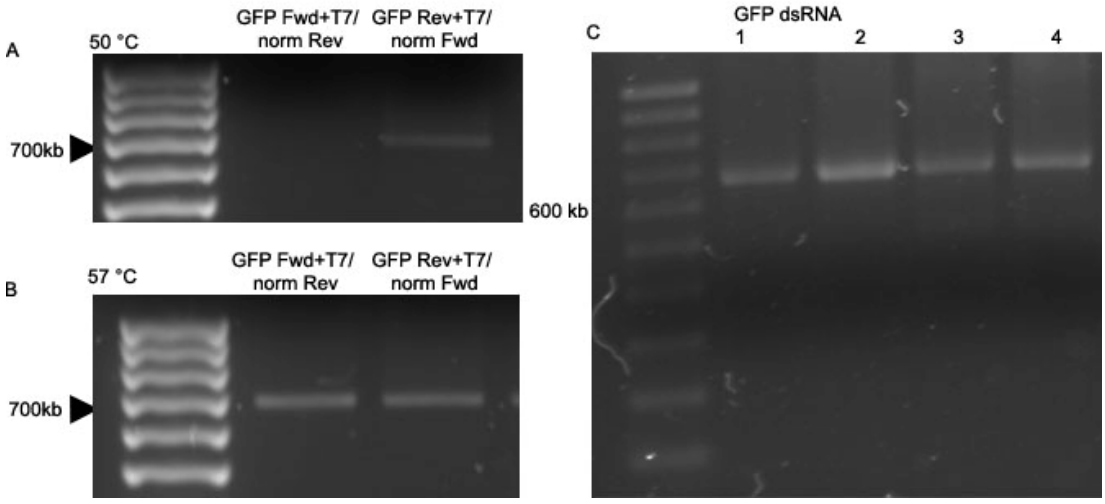

Figure 36 In vitro transcription of GFP dsRNA using Ambion Megascript kit

A. 50°C annealing temperature was not optimal for either the forward or reverse strand. **B**. 57°C annealing temperature produced forward and reverse strands in both directions. **C**. Annealed GFP dsRNA (lanes 1-4) were eluted using elution buffer from the Megascript kit showed a single band corresponding to the molecular weight of GFP as described in text.

4.3.4.4 Quantification of dsRNA

1µl of dissolved total dsRNA was diluted in 49µl nuclease-free water. The concentration of the total RNA was determined spectrophotometrically by averaging three replicate A_{260} absorbance ratios. The level of organic solvent and protein contaminants present within the sample was estimated using A_{260}/A_{230} and A_{260}/A_{280} absorbance readings according to Warburg-Christian calculations (Warburg and Christian, 1942). An absorbance reading above 1.60 for both readings was considered within acceptable range. RNA was aliquoted to a concentration of 2 µg RNA and stored at -70 °C. $1/400^{th}$ of the dsRNA was run on a gel to confirm the level of purity of AChBP dsRNA and GFP dsRNA (see dsRNA method development section).

4.3.4.5 In vitro transfection of dsAChBP

The whole CNS was dissected as described previously (see section 2.2.1) in RNase-free LPS. To improve transfection efficiency, the connective tissue surrounding the CNS was also removed. To avoid user bias, animals were kindly dissected by Dr M Yeoman, which were placed in pre-coded microtubes containing 20µl of RNase-free LPS medium. Upon completion of all dissections, the RNase-free buffer was removed and exchanged with either saline only, 20µl of 125ng/µl dsGFP, or 20µl of 125ng/µl of dsAChBP each dissolved in LPS solution and the tissue incubated at 19°C for 17.5 hours in the dark. The transfected tissues were washed with RNase-free media, and homogenised and acetone precipitated in a manner described previously (see section 2.2.2).

4.2.5 Confocal imaging and electrophysiology

A confocal microscope (Leica TCS SP5) was used to determine the transfection efficiency of fluorescently labelled 21mer siRNA into the whole CNS and correlated with electrophysiological recordings (see method development section) to confirm the integrity of neuronal connections in the cerebral and buccal ganglia. The images were scanned at an 8 bit resolution (1024 x 1024px) from the surface of the tissue and obtaining digital images moving into the middle of the tissue to visualise the level of penetration of siRNA into the ganglia. The PMT was set at a bandwidth of 551nm - 618nm at a scan speed of 400Hz, and objective set at an aperture of 0.50.

4.3.6 In vivo microinjection of dsRNA and siRNA in L. stagnalis

5µl microinjection needles (Hamilton) were used to inject dsRNA and siRNA into the foot of *L. stagnalis*. Care was taken to minimise user bias and stress on the animals. Animals were anesthetised with Listerine (Johnson & Johnson) and injected through the base of the foot of the snail into the interstitial fluid surrounding the CNS as has been described previously (Fei *et al.*, 2007). To minimise user bias, all injections were conducted by the same investigator with vials containing the dsRNA or siRNA that were coded by another investigator. To avoid stress to the animals, the base of the foot of *L. stagnalis* was gently teased until the animal had retracted into the shell prior to being injected with either 5µl HEPES saline, 5µl scrambled siRNA, 5µl AChBP1, 5µl AChBP2, 5µl dsGFP, 5µl dsAChBP, all at a concentration of 0.5µg/ µl.

4.3.7 Behavioural assessment of dsRNA and siRNA mediated knockdown

Behavioural assessment included the assessment of the number of sucrose-evoked in all treatment groups as described previously (see methods section, Chapter 2.2.8) with the following modifications.

Age-matched animals (6 months old) were starved overnight prior to transfection. Two time points were chosen based on the *in vitro* experiments that examined the transfection of fluorescently labelled siRNA into the cerebral and buccal ganglia. AChBP-dsRNA mediated transfection was measured at 17.5 hrs and 48 hours to measure the:

1). level of knockdown of AChBP protein at these time points, and

2). whether loss of AChBP correlated with a decrease in feeding behaviour.

Previous work has shown that application of ACh to isolated *L. stagnalis* glial cells could significantly decrease AChBP levels (Smit *et al.*, 2003; Smit *et al.*, 2001). Application of AChBP dsRNA or siRNA should block the ability of the glial cells to re-make this protein. In order to try to mimic this situation *in vivo*, animals were placed in clean copper-free water and fed on fish flakes and lettuce for 6 hours *ad libitum* after injection. As ACh forms a key neurotransmitter for both the slow

oscillator (SO) and N1 interneuron and for some of the motor neurones, activation of feeding should increase ACh, which in turn should activate glial cells and deplete them of AChBP. Animals were placed in clean water after the 6 hour period to remove residual food and placed in another tank containing copper-free water. Animals were starved again for the remaining 11.5 hours and 42 hours respectively. The top of the shells of each snail was marked with the respective code with which it was injected. The sucrose-evoked feeding measurements were performed as normal (see section 2.1.2.) at 17.5 hour and 48 hour post injection.

4.3.8 Statistics and data analysis

Sucrose evoked feeding behaviour are represented as mean ± SEM. Statistical analysis on the feeding behaviour was performed using EXCEL spreadsheet where differences between the control and treatment groups were examined using student t-test. Normalised protein expression in Western Blot analysis would be expected to deviate from a normal distribution, as indicated by a Kolmogorov- Smirnoff test using SPSS software (not shown). However the distribution appeared sufficiently symmetrical to be considered normal such that classical t-test could be validly performed and considered significant if $p < 0.05$.

4.4 RESULTS

4.4.1 Method Development: transient transfection of siAChBP

4.4.1.1 Confocal microscopy shows siRNA transfection in whole CNS:

Direct visualisation of the transfection efficiencies was performed using fluorescently labelled scrambled 21mer siRNA (Qiagen) with no sequence homology in the nr database. Assessment of transfection efficiency was performed in whole CNS with the transfection efficiency of the duplex assayed at 3 time points: 2 hours, 4 hours and 24 hours. Although this may seem a long time for endocytosis to occur, no reports to my knowledge had previously examined the length of time required to transfect siRNA duplexes into the whole *Lymnaea* nervous system in culture.

Examination of transfection into the whole CNS for less than 4 hours revealed fluorescence only in the cells in the connective sheath surrounding the CNS (Figure 37A and B). Transfection efficiency into the peripheral regions of the buccal ganglia increased after 24 hour incubation, however transfection did not occur inside the centre of the ganglia, which can be seen as a distinct dark circle (Figure 37C). As the regions differ in terms of thickness, transient transfection into the entire CNS is likely to be a time-dependent but dependent on the permeability of the connective tissue sheath to the siRNA. We did not observe fluorescent particles in the cytoplasm or nuclei in any of the ganglionic cells after 2 or 4 hours of treatment (Figure 37A, Figure 37B). Fluorescent particles could cross the connective tissue after 24 hours incubation but this failed to penetrate the ganglia (Figure 37C).

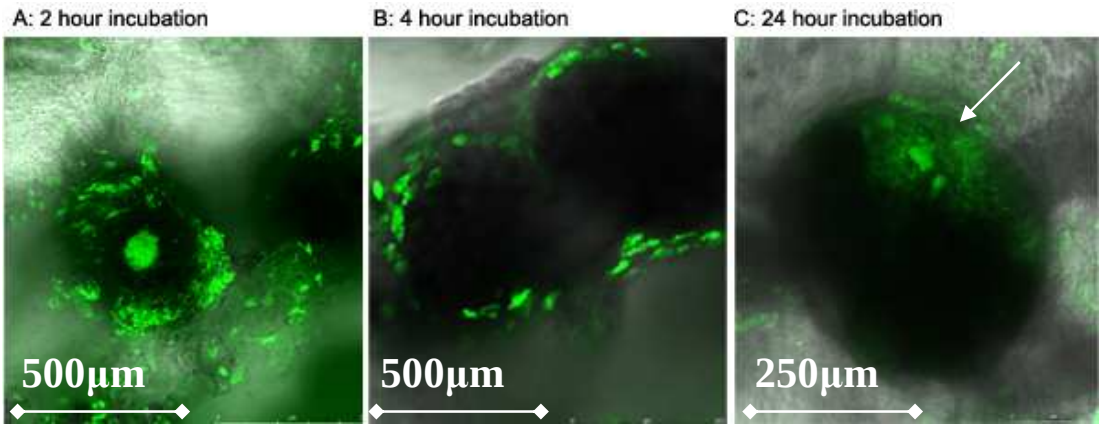

Figure 37 Time course study of fluorescent 21 mer scrambled siRNA in *Lymnaea* buccal CNS.
The buccal ganglia outlined as dark circles are the thinnest part of the whole CNS and most likely to show transfection (n=3). The fluorescent labelling at 2 hours (A) s showed high labelling on the outside of the ganglia, but no transfection occurred inside the buccal ganglia (**A**); labelling of cells in the connective tissue became more apparent after 4 hours but not inside the ganglia (**B**); some peripheral regions of the CNS (top right arrow) showed fluorescent labelling penetrating the tissue after 24 hour incubation (**C**).

4.4.1.2 Desheathing of ganglia increases siRNA delivery into whole CNS

To explore the implications of removing the connective tissue surrounding the CNS on siRNA transfection, cerebral and buccal ganglia from whole CNS were desheathed and transfected for 17.5 hours using fluorescently labelled siRNA (Figure 38). The siRNA uptake into cells could be visualised by the cytoplasmic labelling of cells inside the buccal ganglia (Figure 38A) as well as in the cerebral ganglia (Figure 38B). Furthermore, there was a marked increase in fluorescence in desheathed ganglia compared to the buccal ganglia at 24 hours which had its connective tissue intact. This suggests the connective tissue surrounding the ganglia was acting as a physical barrier to prevent transient transfection of siRNA into the ganglia. This process was also independent of the thickness of the tissue in desheathed ganglia which showed more consistent internalisation of the fluorescently labelled siRNA in thick tissues such as the cerebral ganglia (see Figure 38B).

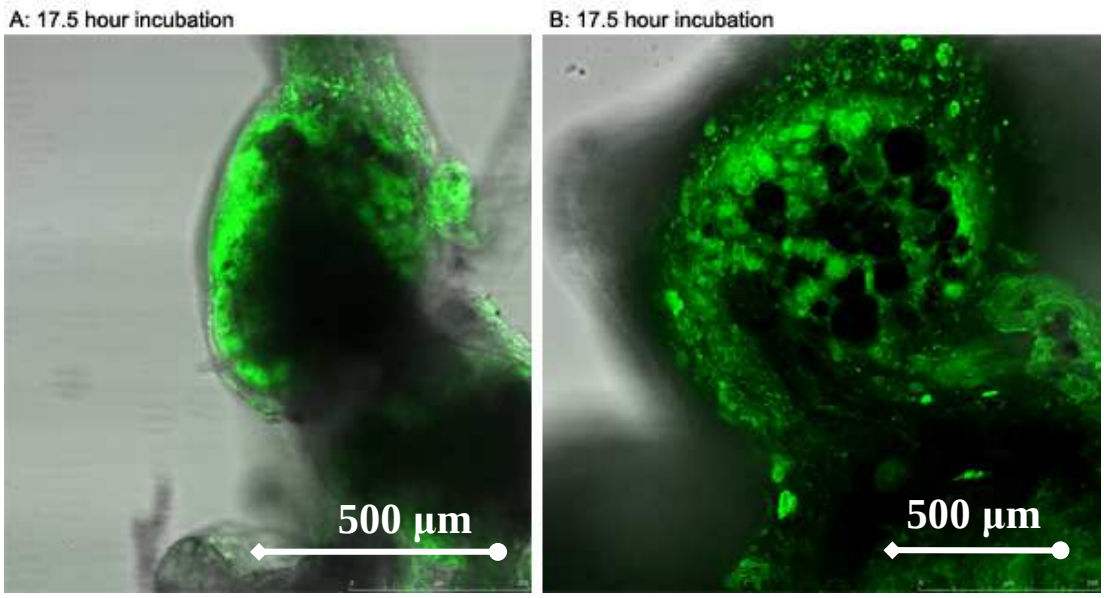

Figure 38 Desheathing the ganglia allow measurable uptake of fluorescently labelled siRNA after 17.5 hours
Scrambled siRNA of similar size to the siAChBP duplex was incubated in 20 µl Rnase-free HEPES saline with desheathed cerebral and buccal ganglia. Transfection observed as an increase in fluorescence in the cytoplasm after 17.5 hours showed successful transfection in the buccal ganglia (**A**) and in the cerebral ganglia (**B**).

4.4.1.3 Identification of an appropriate incubation time and concentration of dsRNA/siRNA

The concentration of AChBP dsRNA, and AChBP siRNA was determined by examining other reports where RNAi was successfully achieved in the *L. stagnalis* CNS. The review of the studies summarised in Table 8 includes the time points used to measure RNAi, the amount of dsRNA/siRNA duplex, and the assays performed to measure RNAi. The reported amount of dsRNA administration in *L. stagnalis* varied markedly between groups and depended on whether transfection was induced in isolated cells, where the concentration of the duplexes were relatively low compared to those studies in which RNAi was performed in the intact animal where the amount of dsRNA injected was higher (see Table 8). Based on the findings highlighted in Table 8, a 24 hour time point was chosen to assess AChBP knockdown at the protein level in the isolated CNS model. In order to observe an effect, the maximal amount that could be delivered to the intact animal from the purchased siRNA was 2.5µg of total siRNA (n=5). Thus the dsRNA was maintained at the same concentration.

4.4.1.4 Electrophysiological recording from whole CNS maintained in 20µl buffer

To submerge whole CNS in media containing 2.5 µg of AChBP dsRNA, the minimum volume that the dsRNA could be prepared was a 20µl volume. There was no evidence in the literature to suggest that this volume of saline could maintain the whole *Lymnaea* CNS tissue physiologically active for 24 hours, in the absence of culture medium containing antibiotics to prevent bacterial contamination.

To determine whether the whole CNS could remain physiologically active after incubation in 20µl RNase-free HEPES saline for 24 hours, electrophysiological recordings were undertaken from the CGC cell in the cerebral ganglia (Figure 39). The CNS tissue was first submerged in RNase-free HEPES saline in 1.7ml eppendorf tubes and the integrity of the tissue determined by measurement of the resting membrane potential (RMP) after 24 hours. At the end of this time point, there was clear evidence of tissue degradation (data not shown). The tissue had become opaque and discoloured and bacterial contaminant was evident from the odour of the tissue suggesting the tissue had degraded at the 24 hour time point in the 20µl volume. We were also unable to produce any trace recordings from tissue confirming the tissue was electrically dead.

However, when the whole CNS tissue was maintained in Rnase-free HEPES saline for 17.5 hours (i.e. overnight) and placed in a 200µl microtube instead of a 1.7ml microtube to ensure all nerves and tissue were fully submerged in the 20µl volume, we were able to obtain electrophysiological trace recordings from the tissue. Two HEPES saline solutions were prepared; 1) contained a solution made up in milliQ water; 2) contained a solution made up in RNase-free water. To determine potential differences between the two solutions, the resting membrane potential of the CGC cells in the buccal ganglia were measured after 17.5 hour transfection (Figure 39). The tissues were monitored for discolouration and signs of degradation. At 17.5 hours, there was no obvious discolouration and cells maintained the red-orange hue with no obvious odour emanating from the tissue. There a 17.5 hour time point was used for transfection into organ cultured CNS instead of the previously described 24 hours.

Electrophysiological trace recordings confirmed there was no difference in the resting membrane potential of CNS incubated in MilliQ HEPES saline (Figure 39A) and Rnase-free HEPES saline (Figure 39B) and both were within the normal RMP (-50mV - -60mV) of *Lymnaea* CGC neurons after 17.5 hours. These results are comparable to previous work on the CGC cells, suggesting no difference between the two samples (Nikitin *et al.*, 2006).

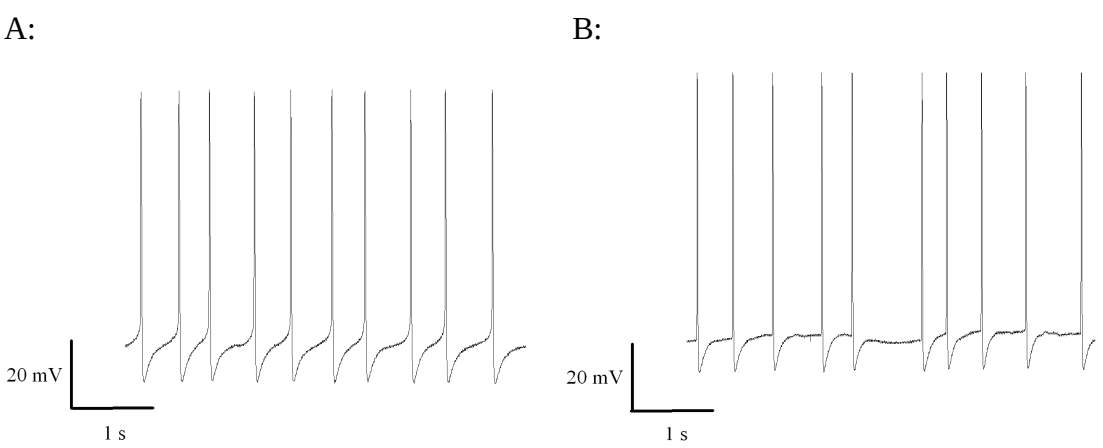

Figure 39 Intracellular recordings from a single *L. stagnalis* CGC cell in buccal ganglia
(**A**) 17.5 hour submersion in 20 µl HEPES saline made from milliQ water, and (**B**) recordings from CGC cells incubated in 20 µl Rnase-free HEPES solution. Trace recordings were kindly completed by G.Scutt (gs59@brighton.ac.uk).

In conclusion, *Lymnaea* whole CNS organ could not be maintained at room temperature for 24 hours in 20µl RNase-free HEPES saline in the absence of antibiotics. The whole CNS tissue could remain electrophysiologically active for a period of 17.5 hours in RNase-free HEPES saline and MilliQ HEPES saline with no discolouration and without the need for antibiotics at room temperature.

4.4.2 Assessment of RNAi using dsRNA in isolated CNS

Three different incubation media were tested to examine RNAi in desheathed whole CNS for 17.5 hours: 1) incubation in RNase-free HEPES saline (control); 2) incubation in 125ng/µl dsGFP (negative control); 3) incubation in 125ng/µl dsAChBP (Figure 40) and replicated in 5 animals/ group. At 17.5 hours, dsAChBP transfection in desheathed CBG ganglia failed to show a decrease in AChBP levels compared to saline controls or GFP (Figure 40A).

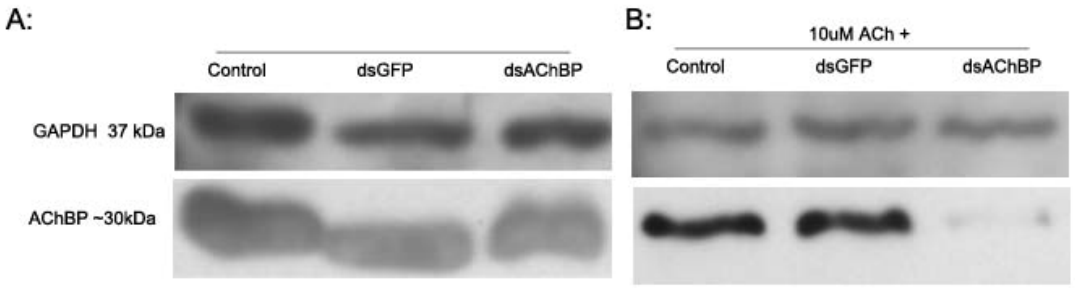

C:

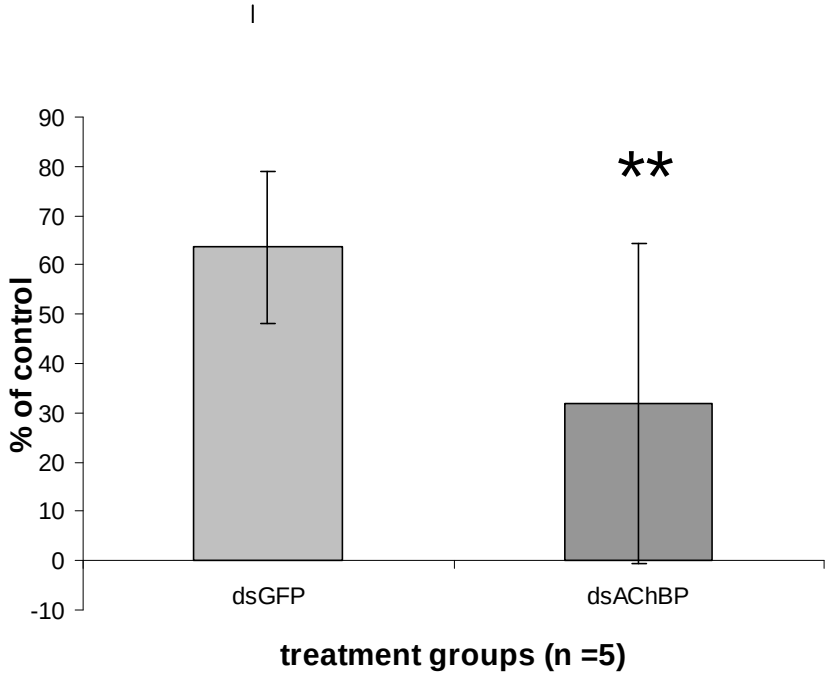

Figure 40 AChBP dsRNA decreased AChBP levels in desheathed ganglia after 17.5 hour incubation

Western Blot analysis showed no change in AChBP protein expression in dsRNA, transfected whole CNS compared to controls after 17.5 hours in the absence of 10μM ACh (A). In the presences of 10 μM ACh, there was a significant decrease in AChBP expression (B). All transfections in the presence of 10 μM ACh were compared to HEPES-treated saline control and represented as mean ± SEM normalised to control (C). ** $p < 0.05$. AChBP levels after 2.5μg GFP dsRNA incubation were not significantly different compared to control, n = 5 samples per group.

4.4.3 Does stored AChBP in synaptic vesicles mask dsAChBP-mediated silencing?

To address the possibility that the AChBP dsRNA was blocking protein expression at the 17.5 hour time point, but masked in whole cell protein lysates due to the presence of pre-synthesised AChBP, the previous dsRNA transfection was replicated in the presence of 10μM ACh, which has been previously reported to stimulate the release of AChBP at cholinergic synapse (Smit *et al.*, 2001).

Figure 40B shows a representative Western Blot analysis of CNS treated with AChBP dsRNA, in the presence of 10μM ACh. There was a statistically significant reduction in AChBP release in dsRNA-transfected CNS compared to HEPES-treated control groups (31.90 ± 32.55, $p < 0.05$). Incubation with GFP dsRNA caused a 36% decrease in AChBP levels in the CBG, which was not statistically different from controls, $p > 0.05$.

4.4.4 dsRNA transfection in the intact animal

Using the assumption that transient transfection of siRNA would be comparable to the dsRNA, young animals (3-4 months old) were injected with either 5μl 500ng/μl dsGFP or dsAChBP or saline through the foot of the animal into the haemocoel. As there are currently no published data available regarding knock down of AChBP in *L. stagnalis*, the incubation time was based on the observation that 17.5 hour transient transfection in desheathed ganglia was sufficient to see a decrease in AChBP protein levels (Figure 40). Given that desheathing cannot be carried out *in vivo* and tissue penetration may take considerably longer, it was decided to look at incubating the animal for 48 hours and 72 hours, and monitored for the first 24 hours using a video camera to ensure no toxicity-mediated deaths had occurred with dsRNA injections and if they did, the time of toxicity would be known. No deaths were detected after 24 hours,

Sucrose-evoked bites measured at 48 hours and 72 hours post injection were not significantly different in AChBP dsRNA treated animals compared to both sets of controls ($p > 0.05$; $n=5$); (Figure 41).

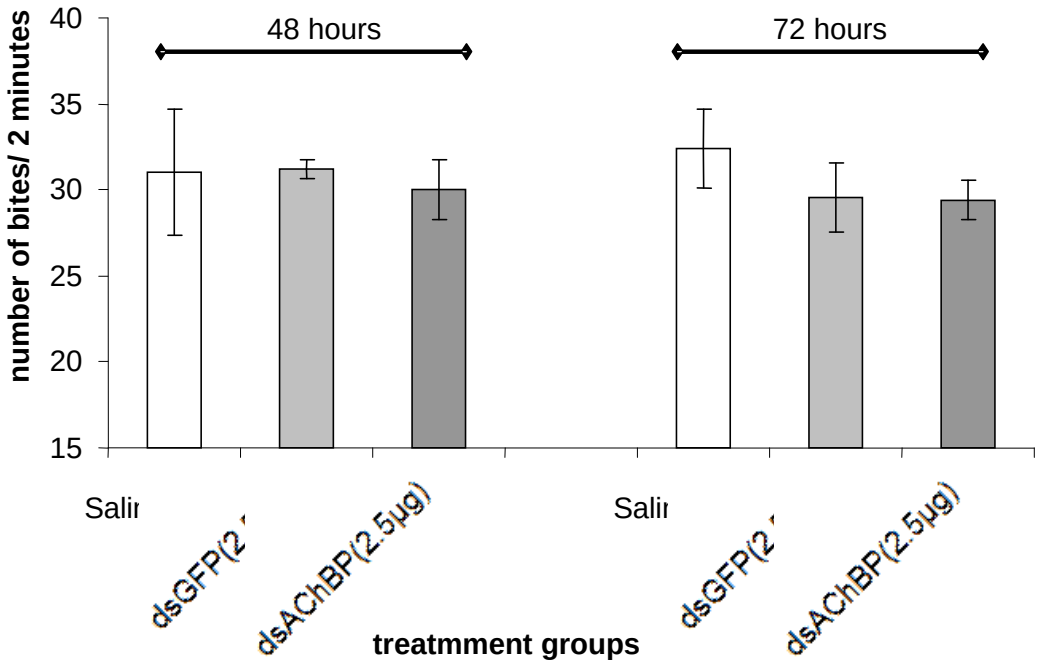

Figure 41 Behavioural analysis of sucrose evoked feeding after 48 hour and 72 hour dsRNA-injection
Lymnaea stagnalis were injected with either HEPES saline only (n=5), 2.5µg GFP dsRNA (n=5), or 2.5µg AChBP dsRNA (n=5) through the foot of the animal and into the bloodstream. After 48 and 72 hours post injection, animals were presented with sucrose stimuli to detect the number of sucrose-evoked bites for 2 minutes. Injection of both dsRNA failed to significantly alter sucrose-evoked bites at both 48 hours and 72 hours. The CNS of the animals was removed, and stored in -20°C ready for protein extraction. All transfections are compared to saline control and represented as mean ± SEM.

Western blot analysis was used to assay relative protein levels of AChBP in the whole CNSs of animals injected with dsRNA at the corresponding time points with the blots normalised to α-tubulin signal as a loading reference. α-tubulin was selected as it was highly abundant that should not be altered in the same age group (young) that was injected with dsRNA. It was also a different molecular weight from AChBP such that both these proteins could be visualised more easily. 10 µg of total protein was loaded in each lane and probed using Anti-AChBP antibody. No difference in protein levels was detected after 48 hour or 72 hour transfection. (Figure 42).

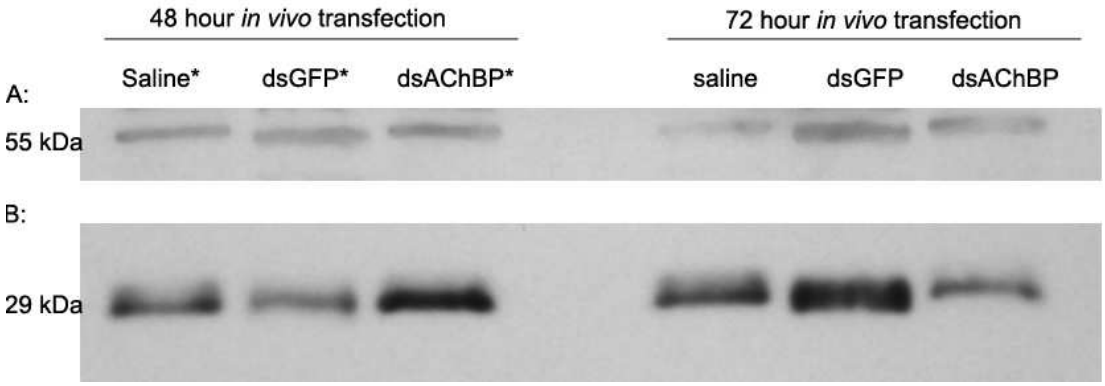

C:

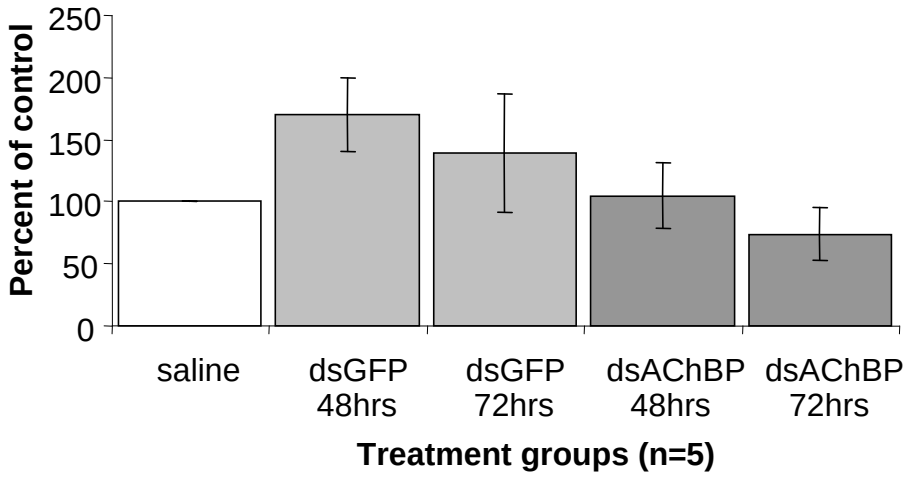

Figure 42 dsRNA microinjection at Western blot analysis of CNS tissue at 48 and 72 hours.

Sample Western blot taken from a saline, dsGFP and dsAChBP injected animals 48 hours (A) and 72 hours (B) post injection. Band at 29kDa shows AChBP protein. The band at 55kDa represents α-tubulin which was used as an internal standard. (C) Bar chart showing relative changes in AChBP expression following injection of dsRNAs for 48 and 72 hours. No significant change was seen in protein levels in dsAChBP-transfected animals ($p > 0.05$), (n=5)

4.4.5 siRNA transfection in the intact animal

AChBP siRNA was used to increase the specificity of RNAi to the AChBP message, and reduce the potential for off-target effects. Animals were monitored for potential signs of toxicity-mediated deaths within the first 24 hours after micro-injection of the siRNA duplexes in a manner described previously for dsRNA-injected animals, and sucrose-evoked bites measured at 72 hours and 96 hour post injection, following by examination of AChBP levels in the CBG using Western Blot analysis. At the 72 hour time point, AChBP siRNA duplex 1 (siAChBP1) transfected animals showed a statistically significant decrease in sucrose-evoked bites per 2 minutes (22.75 ± 1.60 bites) when compared to HEPES saline-treated controls (30.25 ± 2.50 bites), $p < 0.05$); (Figure 43). AChBP siRNA duplex 2 (siAChBP-2) transfected animals also showed a significant decrease in sucrose-evoked bites (18.00 ± 3.63 bites), compared to saline treated controls (30.25 ± 2.50 bites); (Figure 43), ($p < 0.05$). Examination of AChBP protein levels using densitometric intensities following Western Blot from individual animals failed to show a statistically significant decrease in either siAChBP1 or siAChBP2 transfected animals compared to saline-treated controls (Figure 44).

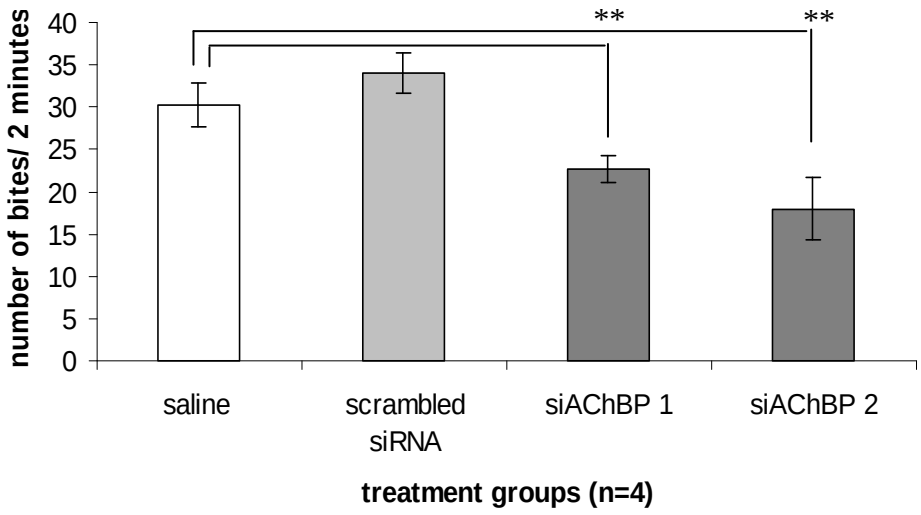

Figure 43 Sucrose-evoked bites after 72 hour siRNA transfection
L. stagnalis were injected with either HEPES saline only (n=4), 2.5µg scrambled siRNA (n=4), or 2.5µg siAChBP-1 (n=4), or 2.5µg siAChBP-2 (n=4) through the foot of the animal and into the bloodstream. Animals were monitored for the first 24 hours for toxicological effects and fed *ad libitum* on lettuce. After 72 hours from point of first injection, animals were presented with sucrose stimuli to measure the number of sucrose-evoked bites after 2 minutes. Both the siAChBP1 and siAChBP2 injected animals had fewer bites compared to control (** $p < 0.05$).

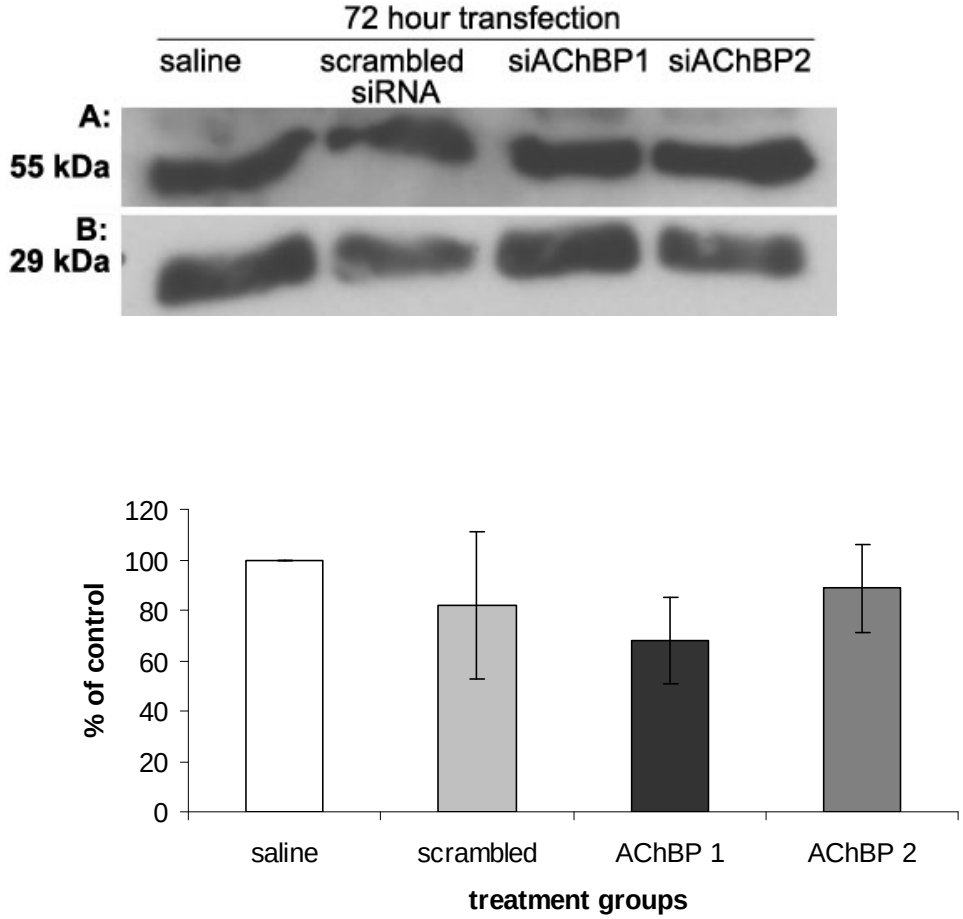

Figure 44 AChBP protein expression following siRNA transfection after 72 hours

Assessment of AChBP protein levels in the brains of young *L. stagnalis* following micro-injection with 2.5µg siAChBP duplexes (500ng/µl) or 2.5µg scrambled siRNA. (A) Typical Western blot showing bands at 29kDa (AChBP) and at 55kDa (α-tubulin) for 4 different animals injected with either saline, scrambled siRNA, siAChBP1 or siAChBP2. (B) Bar graph showing change in AChBP expression as a percent of control saline injected animals. Bars represent mean ± SEM. No significant changes were observed, $p > 0.05$.

Sucrose-evoked bites after 96 hour transfection showed a significant decrease (20.75 ± 3.77), compared to control (31.75 ± 1.89, $p < 0.05$) in siAChBP1-treated animals (Figure 45). Sucrose evoked bites in siAChBP2-transfected animals were decreased (28.00 ± 5.05) compared to control (31.75 ± 1.89, $p > 0.05$); (Figure 45). Densitometric intensity analysis of AChBP protein expression in Western blot failed to show a statistically significant difference in either siAChBP1 or siAChBP2-treated animals when compared to saline control (Figure 46, and Appendices).

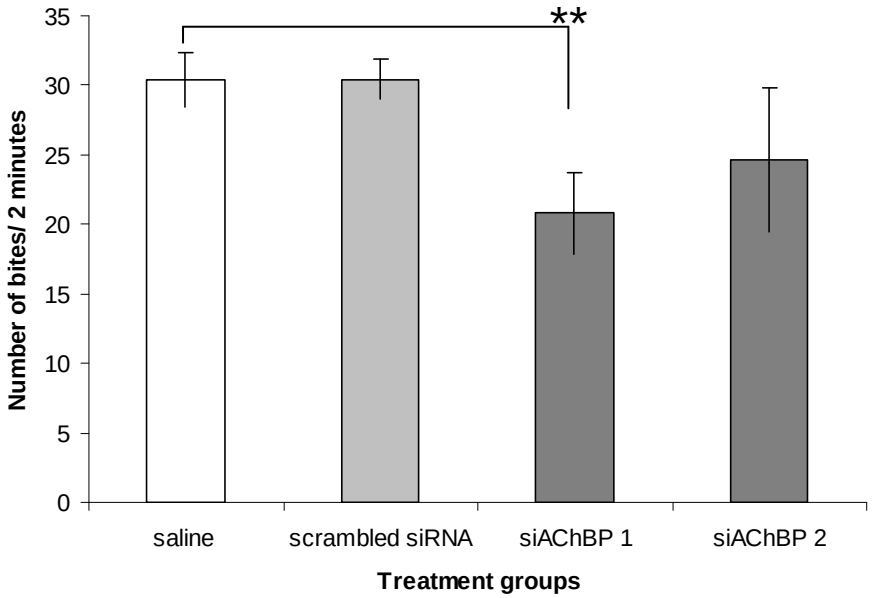

Figure 45 Effects of siRNA injection on sucrose-evoked bites after 96 hour transfection

L. stagnalis were injected with either HEPES saline only (n=4), 2.5µg scrambled siRNA (n=4), or 2.5µg siAChBP-1 (n=4), or 2.5µg siAChBP-2 (n=4) through the foot of the animal and into the bloodstream. Animals were monitored for the first 24 hours for toxicological effects and fed *ad libitum* on lettuce. After 96 hours from point of first injection, animals were presented with sucrose stimuli to measure the number of sucrose-evoked bites after 2 minutes. Both the siAChBP1 and siAChBP2 injected animals had fewer bites compared to control (** $p < 0.05$).

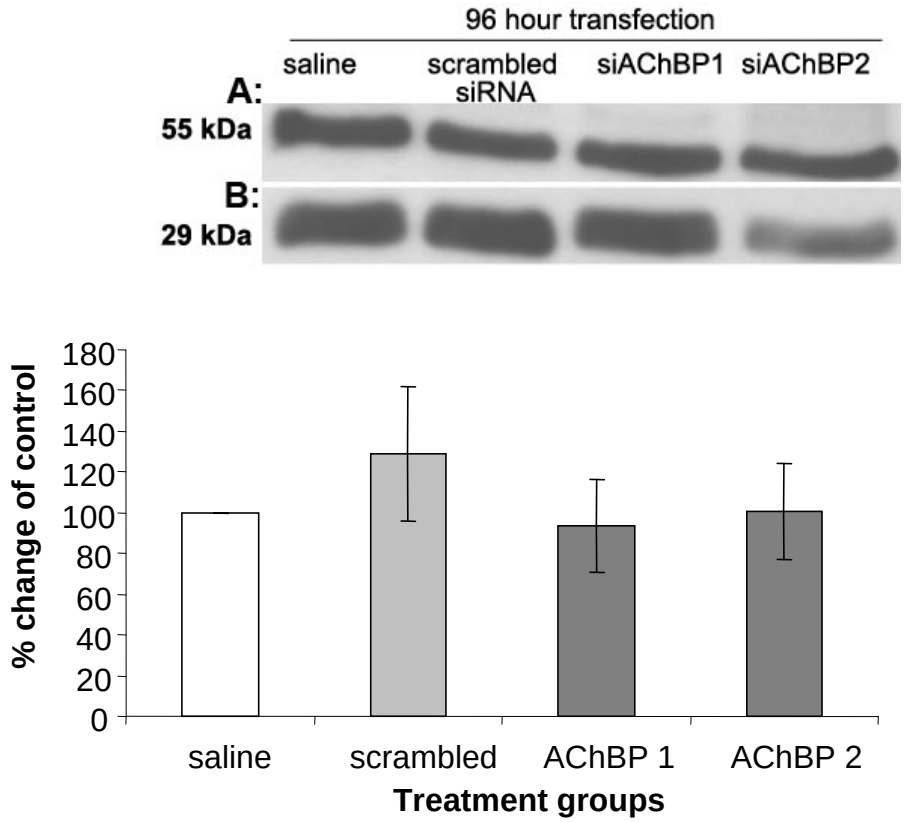

Figure 46 AChBP protein expression following siRNA transfection after 96 hour

Assessment of AChBP protein levels in the brains of young *L. stagnalis* following micro-injection with 2.5µg siAChBP duplexes (500ng/µl) or 2.5µg scrambled siRNA. (A) Typical Western blot showing bands at 29kDa (AChBP) and at 55kDa (α-tubulin) for 4 different animals injected with either saline, scrambled siRNA, siAChBP1 or siAChBP2. (B) Bar graph showing change in AChBP expression as a percent of control saline injected animals. Bars represent mean ± SEM. No significant changes were observed, $p > 0.05$.

4.5 DISCUSSION

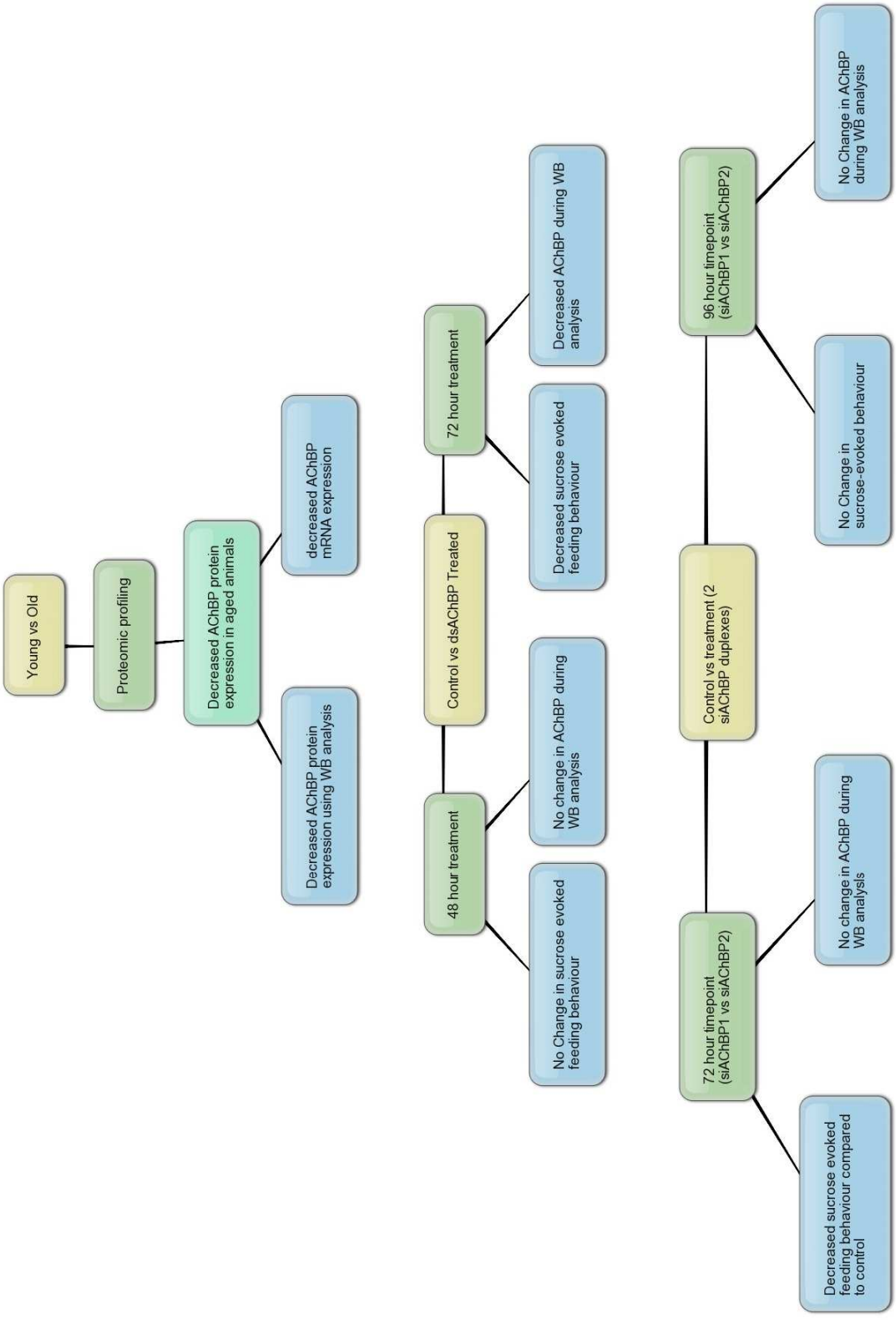

Figure 47 Overview of experiments from the current study.
Proteomic profiling demonstrated a decrease in AChBP in aged *L. stagnalis*. AChBP is involved in the regulation of ACh activity and regulates synaptic transmission; therefore we hypothesised that decreased AChBP contributed to a reduction in feeding behaviour that is associated with the aged *L. stagnalis* phenotype. Transient transfection of dsAChBP at 48 hours showed no change in protein expression using Western blot (Hekimi et al.), or a correlation in the number of sucrose evoked bites. 72 hour transient transfection showed decreased protein expression correlated with decreased sucrose-evoked bites, suggesting longer time points may be required to show an effect. siAChBP transient transfection at 72 hours showed decreased sucrose evoked bites were not correlated with decreased AChBP protein expression. siAChBP transient transfection at 96 hours did not show decreased AChBP protein expression correlated with sucrose-evoked bites.

Cholinergic signalling is altered at many levels during the ageing process, ranging from alteration in choline transport (Brull *et al.*, 2002), to receptor specific changes in nAChR expression (Court *et al.*, 1997) and mAChR expression (Court *et al.*, 1997). Our data provided the first evidence to suggest AChBP protein expression declined in the aged CBG (see Chapter 2), one of the major centres of the *L. stagnalis* nervous system involved in the regulation of feeding behaviour in *L. stagnalis* – and a process which is attenuated in the aged animal (Yeoman *et al.*, 2008; Yeoman and Faragher, 2001; Arundell *et al.*, 2006). To assess the possible contribution of AChBP to the feeding network in *L. stagnalis*, the current study evaluated whether AChBP repression could mimic the biological effect of age on feeding behaviour in the *L. stagnalis*. A schematic of the study is represented in Figure 47.

4.5.1 Targeting AChBP gene using dsRNA transfection

In the first instance, dsRNA targeting AChBP gene was constructed by *in vitro* transcription from a plasmid vector. Unlike mammalian cells which are unable to withstand long dsRNA without activation of type 1 interferon response (Geiss *et al.*, 2001), the *L. stagnalis* nervous system like other invertebrates do not accompany non-specific interferon-mediated response by dsRNA administration. It is widely accepted that dsRNA combinations activate the ribonuclease inducing silencing complex (RISC), working through Ago-2 to mediate cleavage followed by sequence-specific degradation of RNA (Bernstein *et al.*, 2001; Li *et al.*, 2006; Liu *et al.*, 2004). In order to examine knockdown of AChBP, the size of dsAChBP was constructed at a length of 760bp which spanned almost the entire length of AChBP gene (Figure 33). The length of dsRNA was in line with previously reported duplexes that were successfully used in *L. stagnalis* nervous system (Korneev *et al.*, 2002; Perlson *et al.*, 2004; Fei *et al.*, 2007). dsRNA targeted against the bioluminescent green fluorescent protein (dsGFP) which have not been demonstrated to be present in anything other than coelenrates were constructed and used as a negative control (Chalfie, 1995).

With respect to identifying a functional role of AChBP in *L. stagnalis* nervous system, AChBP dsRNA administered to the isolated CNS decreased in the level of AChBP. However in the intact animal, microinjection of the AChBP dsRNA failed to cause a significant decrease in AChBP levels at both the 48 hour and 72 hour time

point or alter the feeding behaviour. The differences observed between the *in vitro* and *in vivo* results may be due to a number of reasons. Firstly, AChBP dsRNA caused a significant reduction in AChBP levels in the *in vitro* model, but only in the presence of ACh suggesting depletion of synaptically stored AChBP was necessary in order to observe a reduction in AChBP protein levels. Animals injected with AChBP dsRNA showed a small reduction in feeding behaviour at the 72 hour time point ($p > 0.05$), however this was not correlated with a reduction in AChBP protein levels due to the high level of variability at the protein level in the transfected group. Therefore even though some animals had reduced AChBP levels, this was not demonstrated in all n=5 / AChBP dsRNA treated group. Furthermore, if activity-dependent depletion of synaptically stored AChBP was required in order to observe a decrease in AChBP at the protein level, then comparable paradigm to that used in the *in vitro* study could not be accomplished in the intact animal as overproduction of ACh are likely to lead to toxicity mediated death of the animal. Examples of overproduction of ACh are used in insectides such as those observed when AChE gene is silenced in *Helicoverpa armigera* that leads to increased mortality (Kumar *et al.*, 2009). We could not conclude conclude therefore that AChBP knockdown was achieved in the intact animal from the Western blot data, or confirm that the reduction in feeding behaviour was primarily due to an effect on AChBP knockdown using dsRNA.

If AChBP are involved in the feeding behaviour, transfection in sub regions of the ganglia, such as the buccal ganglia may have occurred that could have contributed to the observed reduction in feeding. However in order to maintain consistency with the proteomic data, individual regions of the cerebral and buccal ganglia were not examined separately. In line with this speculation, the protein expression may have been masked as the extracts were taken from the combined regions of the cerebral and buccal ganglia, however the buccal ganglia for one example, is physically thinner and smaller than the cerebral ganglia, and more amenable to transfection than in the cerebral ganglia which may require a longer transfection time point. Fei *et al*. (2007) for example demonstrated the effects of hypoxia on Hsp-70 levels could be observed for up to 8 days in *L. stagnalis* (see Table 8), therefore a longer transfection time point may increase the chances of detecting a reduction in AChBP protein expression from the intact animal. The fluorescently scrambled siRNA data

presented here are in support of the view that transfection into the CNS depended in part on the ability of the siRNA to enter the tissue, and on the thickness of the tissue and connective tissue surrounding the ganglia.

As the buccal ganglia comprises mainly motor neurons that innervate the buccal mass that contain the muscles for the opening and closing of the mouth of the animal, a reduction in behaviour via a reduction ACh levels through AChBP knockdown in this region could be a plausible candidate for the observed reduction in feeding. However, a single buccal ganglia was too small to acquire sufficient protein quantities to examine AChBP protein levels on a region per region basis. Based on the assumption that partial transfection may have occurred in the buccal ganglia but not the cerebral ganglia, follow-up experiments may benefit from examining regional differences in AChBP mRNA expression following RNAi instead, to make use of the sensitivity of this approach in assessing knockdown in the intact animal.

4.5.2 Off-target effects using dsGFP on AChBP protein expression

A common problem experienced using long dsRNA to induce RNAi are the increased incidence of off-target effects based on sequence similarity of the siRNA or short motifs to mRNA not intended to be knocked down. Great care was taken to minimise the risk of an off-target effect during the selection process for an appropriate negative control. The GFP gene which is not expressed in *L. stagnalis* was chosen as it would activate the RISC complex without having any known effect in *L. stagnalis*. However, the results derived from the current study suggest dsGFP may have had an off-target effect by increasing AChBP expression level at both the 48 hour and 72 hour time point which could be quantified at the protein level (Figure 42).

From a transfection point of view, this data suggests that both the selected time points could be used to successfully transfect the animal with dsRNA. However GFP may be targeting factors upstream of AChBP signalling to increase AChBP expression and in so doing producing an off-target effect. In the aforementioned scenario, if transfection into the intact animal with GFP dsRNA could significantly

increase AChBP expression, then it stands to reason that the lack of response observed with AChBP dsRNA was unrelated to transfection, and perhaps more to do with the localisation of AChBP, or the selectivity of the AChBP dsRNA to AChBP message (Figure 42; $p < 0.05$).

In silico evaluation of GFP dsRNA transcript was performed prior to transfection to determine whether GFP was a suitable choice as a negative control in *L. stagnalis*. The results suggested that 21mer permutation that could be generated from GFP dsRNA could be a partial match to regions of the AChBP gene. However without prior knowledge of an initial RISC cleavage site, a large number of 21mer siRNA permutations could be generated from any single long dsRNA (Bass, 2000). Therefore *in silico* evaluation using FASTA alignments alone may not necessarily differentiate between the most appropriate negative control for a dsRNA as the alignment algorithm are biased towards finding a best possible matches (Jackson *et al.*, 2003). Hence *in silico* evaluation of dsRNA could not provide a definitive answer when determining the likelihood of an interaction between two dsRNAs (Jackson *et al.*, 2003). Partial sequence identity as low as a 14-15 nucleotides to the central region of the target siRNA have been reported sufficient to see off-target effects from control genes (Jackson *et al.*, 2003). Prominent examples include the silencing of *hif-1α* gene in which siRNAs containing the 7 nucleotide (AGGCAGT) motif could not only silence the target gene but other mRNAs containing the same sequence (Lin *et al.*, 2005). Thus the identification of an appropriate negative control for dsRNAs could at best therefore rely on an initial screening of an appropriate gene with no sequence homology to the target gene and only through experimental evaluation (Jackson *et al.*, 2003).

As GFP dsRNA increased AChBP expression, it is unlikely the effects are mediated by its action on the AChBP gene, but more likely to occur from sequence complementarity to genes which may induce AChBP activation. Candidates for partial complementarity for the GFP dsRNA could be any number of molecules that act upstream of AChBP. However, with the 21 nucleotide *in silico* permutations suggesting a potential match of GFP dsRNA to AChBP, it is possible that nAChRs that are partially homologous to AChBP could be targets for GFP dsRNA (Smit *et al.*, 2001). Explained by this line of argument, it could be speculated that if GFP

dsRNAs actions increased ACh levels directly, then this would lead to elevated levels of AChBP as observed in the study. However, this view was not supported from the *in vitro* study which showed that AChBP levels actually decrease the presence of 10μM ACh when transfected with GFP dsRNA (Figure 40). Given that the effects of GFP dsRNA could be manipulated by ACh, it stands to reason that both excitatory (cationic) and inhibitory (anionic) nAChRs which are present in the *L. stagnalis* nervous system and co-activated in the presence of 10μM ACh, could be candidates for partial complimentarity of GFP dsRNA. A partial knockdown of cationic subtype of nAChRs, for example could reduce ACh levels and over activation of anionic receptors that could serve to decrease AChBP levels in support of the data presented here (Figure 40). Although direct experimental evidence are lacking to support this view, mRNA expression analysis for the most highly abundant nAChR A and nAChR B transcripts could be profiled in the cerebral and buccal ganglia to examine this in greater detail (Nierop *et al.*, 2006)

A further source of confusion was that the most abundant cationic and anionic forms of nAChR are not ubiquitously expressed in the cerebral and buccal ganglia but the anionic nAChR-B are highly abundantly expressed in the buccal ganglia, but not in the cerebral ganglia, whereas the cationic nAChR-A are highly expressed in the cerebral but not in the buccal ganglia (Nierop *et al.*, 2005). This view also supports our initial speculation that AChBP may show regional knockdown contributing to a reduction in feeding behaviour in the intact animal.

Although the effects of GFP dsRNA on nAChR is currently speculative, GFP dsRNA as a choice for a negative control showed it could increase AChBP protein expression in *L. stagnalis*. The recently reported finding that siRNA targeting of GFP in HEK and HeLA cells decreased GFP mRNA levels along with other genes such as RAB21, NUDT3, TCF4, CLYD, and SOAT, demonstrate for the first time that off-target effects from unrelated sequences could occur from GFP siRNA fragments (Tschuch *et al.*, 2008). Figure 48 represents a schematic of the possible effects of GFP dsRNA could have on AChBP expression. A possible GFP dsRNA interaction with cationic and anionic forms of nAChR could be pharmacological dissected using electrophysiological parameters outlined in a report using

methyllycaconitine (MLA) to selectively block nAChR-B, whereas nAChR-A are selectivity blocked by α-conotoxin-IMI (Nierop *et al.*, 2005).

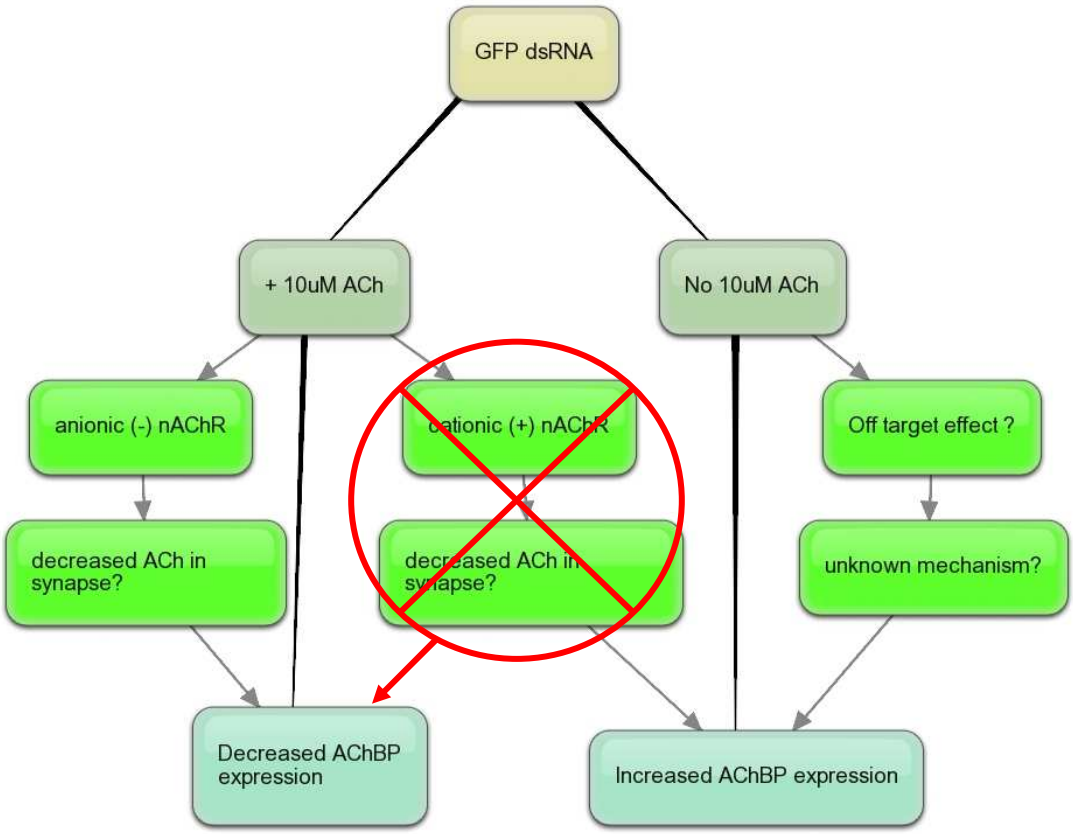

Figure 48 Schematic representation of the postulated off-target effect of GFP dsRNA on AChBP expression
In vitro studies using 10μM ACh could reduce AChBP levels in GFP dsRNA-treated animals. A plausible mechanism could be partial complementarity to cationic subunits of nAChR (marked in cross) which would lead to a reduction in AChBP levels.

4.5.3 Modifying the concentration of the dsRNA/ or siRNA could improve transfection

Off-target effects could also be the result of an elevated siRNA concentration (Tschuch *et al.*, 2008), suggesting that a reduction in the concentration of dsRNA and siRNA concentration may minimise this risk. Due to economic considerations a single maximal concentration was tested with AChBP siRNA based on earlier studies in *L. stagnalis* (see Table 8). Future work may benefit from reducing dsRNA concentrations in order to minimise potential off-target effects. This was in contrast to other reports that suggest the outcome of off-target effects could not be eliminated

in its entirety by decreasing the siRNA concentration alone as off-target effects are also determined by the sequences surrounding the complementary region, the position of the mRNA and the copy number of the complementary region (Lin *et al.*, 2005). The results here show as proof-of-principle that knockdown following dsRNA microinjection could occur *in vivo* in *L. stagnalis*, however a more stringent criteria is required in the selection of an appropriate negative control when using dsRNA, as GFP dsRNA as reported here was not a suitable negative control in the *L. stagnalis* nervous system. These results also demonstrate for the first time that dsGFP can bind to targets that increase AChBP expression which can be detected at the protein level.

4.5.4 Targeting AChBP using siRNA transient transfection

To reduce any bias associated with the composition of the negative control when using dsRNA, a 21mer scrambled negative control siRNA was selected to examine AChBP protein knockdown. This was compared against two 21 nucleotide siRNAs targeting AChBP gene with incubations lasting 72 hours and 96 hours in the intact animal. In *D. melanogaster*, 21 nucleotide siRNA subunits paired with a 2 nucleotide 3‘ overhang have been demonstrated to be the most efficient trigger of mRNA degradation (Elbashir *et al.*, 2001). Based on the dsRNA transfection, a 96 hour time point in addition to the 72 hour time point was used to increase the dynamic range of the time points used in this study. The scrambled negative control siRNA (proprietary sequence) purchased from Qiagen, was previously screened to have no significant homology to the entire nr nucleotide database and screened by microarray expression profile against the human and mouse genome to show no off target effects in those organisms. However, as the *L. stagnalis* genome sequence is not known and gene expression profiling in *L. stagnalis* cannot be carried out, we cannot be absolutely confident that there would be no off target effects when using the scrambled negative control. The selection criteria used for the two siAChBP duplexes have been outlined in detail elsewhere (Elbashir *et al.*, 2001), including regional targeting, asymmetric pairing, and maintaining a 45-55% GC content. The results presented outline 2 siRNA duplexes, siAChBP1 (GTG AAT GAA ATA ACC AAT GAA) and siAChBP2 (CAG GGT CGT ATC CGA TGG TGA) used to silence AChBP gene (Figure 32). siAChBP1 targeted the 5‘ region of AChBP gene whereas siAChBP2 gene targeted the centre of the AChBP gene (Figure 32). Both duplexes induced a significant reduction in sucrose evoked bites at 72 hours compared to

saline-treated control, or to scrambled siRNA controls (Figure 43). However there was a failure to detect a reduction in AChBP protein levels in either treatment groups.

As demonstrated earlier in the dsRNA study, a failure to detect a reduction in protein level may not be have been due entirely to transfection issues as the GFP dsRNA was able to increase AChBP at both time points tested. Alternatively, the reduced selectivity may be in part due to siRNA:mRNA pairing and the selection of the appropriate siRNA targeting region. Problems with siRNA:mRNA pairing could occur if the AChBP mRNA target were inaccessible due to the formation of mRNA secondary structures (Heale *et al.*, 2005), and may be altogether unrelated to the transfection process per se. Although controlling the GC content could be used to estimate the mRNA thermodynamic stability and local folding of substructures which may prevent the siRNA from interacting with the target mRNA, this process is by no means completely understood or reliable (Heale *et al.*, 2005). Comparison of the ability of both siRNA duplex to induce RNAi suggests siAChBP1 which targeted the 5' region may have been moderately more effective at inducing RNAi than siAChBP2 which targeted the centre of AChBP message (Figure 44).

4.5.5 Does AChBP regulate feeding behaviour?

From the current series of experiments, there is incomplete evidence to suggest AChBP has a role in regulating the *L. stagnalis* feeding circuits. If a reduction in AChBP protein levels were involved in decreasing feeding behaviour, such reductions when emulated using siRNA would be speculated to correlate with a reduction in feeding scores. Using the two siRNA duplexes showed a reduction in sucrose-evoked bites in AChBP siRNA transfected animals at 72 hours, but this was not correlated with a reduction in the AChBP protein. This difference may mean that differences do not exist between the treatment and control groups or that the differences were obscured by the large biological variation observed both at the behavioural and at the protein level. The possibility that the siRNA had toxicity-related side effects in the intact animal that affected the feeding behaviour could also not be ruled out (Figure 43; Figure 45).

First, if AChBP regulated cholinergic signalling by altering ACh levels at the synaptic level, then disruption to ACh levels are likely to alter the entire cholinergic

framework which constitutes approximately 10% of neurons within the *L. stagnalis* nervous system (Nierop *et al.*, 2006). Second, if the function of AChBP was as fundamental to synaptic signalling as originally hypothesised (Smit *et al.*, 2001), then the spectrum of effects observed would be more akin to disruption in ACh esterase (AChE) levels. AChE inhibitors that are commonly used in insecticides to control pests for example lead to increase mortality, larval growth arrest, and increased malformations (Kumar *et al.*, 2009). In either of the aforementioned scenarios, the interdependence on AChBP signalling would likely have a profound effect on cholinergic signalling and on the *L. stagnalis* feeding network. The question then must be asked – how important is AChBP in regulating cholinergic signalling? A very recent report on the localisation of AChBP revealed some important findings (Banks *et al.*, 2009). 1) Immunohistochemical analysis revealed distinct 'oval-shaped' populations of AChBP-positive glial cells, approximately 3-6μm wide and 5-12μm long reside in the *L. stagnalis* CNS. 2) 74% of AChBP positive cells were localised to the periphery of the ganglia between the cell bodies of neurons (Banks *et al.*, 2009). 2) 12% of AChBP positive cells were expressed in the neurite-specific centre of the ganglia, a region called the neuropile which contain neurites (see chapter 1); (Banks *et al.*, 2009). The localised expression of AChBP suggest AChBP regulates ACh levels between adjacent neuronal cell bodies (i.e. non-synaptic sites) and less likely at neurite:neurite or axosomatic synapses as was previously hypothesised (Smit *et al.*, 2001).

In light of this evidence, AChBP may have a more temporal control over cholinergic signals in that glial cells that release AChBP are likely to regulate cholinergic signalling between adjacent neuronal cell bodies, but unlikely to regulate synaptic signalling as has been previously postulated (Smit *et al.*, 2001). The effects of cholinergic signalling in *L. stagnalis* are further complicated by the presence of anionic and cationic nAChRs that are distributed differentially in the CBG. The cationic nAChR-A for example is highly abundant in the cerebral ganglia, but relatively low in the buccal ganglia whereas the anionic nAChR-B is highly expressed in the buccal ganglia, but in very low abundance in the cerebral ganglia (Nierop *et al.*, 2005). Given the significant variation in the nAChR subtype within these two regions, disruption to AChBP levels may likely affect cholinergic signals in a region-specific manner. (Nierop *et al.*, 2005). It could be speculated therefore,

that a reduction in AChBP levels may be a compensatory mechanism to enhance cholinergic signalling at non-synaptic cholinergic sites in the aged CBG.

4.6 TECHNICAL CONSIDERATIONS:

There are numerous challenges that are required to be overcome in order to create a non-viral delivery system that combine the power of RNAi to examine gene-specific attributes without suffering losses that are the result of its integration. Examples of the detrimental effects off-target effects already exist: as shown, GFP dsRNA can alter the feeding behaviour as well as increase AChBP mRNA gene expression. The key issue is to develop delivery systems that can provide the appropriate level of loss-of-function in the behaviour. Early examples of these systems do exist in *L. stagnalis*, where detectable phenotypes of RNAi could be measured in the form of neurite growth, that are directly monitored in culture conditions (Perlson *et al.*, 2004). However direct measurement of an observable phenotype in the intact animal are lacking apart from only a few notable examples (Fei *et al.*, 2007; Korneev *et al.*, 2002). The reason for this are particularly evident when examining phenotypic changes as complex as feeding that are not a reliable indicator of loss of function without taking into account of toxicity-mediated effects that could be observed in the intact animal.

In addressing the question of whether AChBP was involved in the regulation of feeding behaviour, an alternative approach could be employed, using electrophysiological parameters to assess changes in the *in vitro* semi-intact lip-CNS preparation designed to measure the fictive feeding rhythm (see chapter 1) (Korneev *et al.*, 2002). Furthermore, the contribution of nNOS gene to the fictive feeding rhythm was monitored for up to 24 hours following micro-injection into the ganglia (Korneev *et al.*, 2002). Due to limitations in time, these additional experiments could not be carried out in conjunction with the RNAi work presented here, however future studies attempting to identify elements of the AChBP pathway as part of the ageing process, may benefit from perturbing each component of the system in culture using the fictive feeding reflex prior to examining its effect in the intact animal.

A recent study suggests a number of other neurobiological parameters could also be assessed RNAi in the *L. stagnalis* CNS, including the righting reflex and *L. stagnalis*

sensitivity to light (Fei *et al.*, 2007). Although details of the neuronal mechanisms regulating these behaviours have not been characterised with respect to the ageing phenotype, examining these behaviours in this context may broaden the applicability of the loss-of-function phenotype in the intact *L. stagnalis*.

5.0 GENERAL DISCUSSION

If aging has many causes, then the problem for aging research is to identify and characterize the most important drivers of decline that affect the aged animal. For the most part, this project remains a work in progress. In *L. stagnalis*, the phenotypic reduction in sucrose evoked bites that occur in animals towards the end-stage of their life was used to determine the causal or predisposing elements that regulate the "healthspan" of the organism. To test whether this phenotypic signature (a risk-factor associated with increased mortality in *L. stagnalis*) could be used to identify groups of proteins that are required for common processes and to give a biological insight into the network of proteins that are likely to contribute to the reduction in feeding behaviour, **Chapter 2** of this thesis utilised 2D DIGE, LC MS/MS and *de novo* sequencing platforms to highlight the groups of proteins that were aberrant in the aged cerebral and buccal ganglia. Profiling techniques allowed us to address not only the pattern of protein expression but also single factors that may be contribute to the normal ageing process in *L. stagnalis*. The proteomic study revealed three key groups of proteins; those involved in regulation of cytoskeletal function, energy-dependent processes, and chaperones that were significantly altered in the aged CBG.

As one of the most extensively studied groups of proteins, cytoskeletal dysfunctions are frequently associated with pro-apoptotic events that lead age-related neuropathological condition such as Alzheimer's Disease and amylotropic sclerosis (Akopian and Walsh, 2006). However, the emerging view that unlike age-related neurodegenerative diseases that are accompanied by extensive cell death, normal neuronal ageing involves a selective alteration to only subset of proteins are consistently observed across a number of different species, including flies, nematodes, molluscs, mouse, and in humans. Coined 'selective neuronal vulnerability', this phenomenon points towards a mechanism whereby core groups of proteins or 'nodes' that are integral to the healthspan of the animal become progressively impaired and eventually become detrimental to the organisms survival (antagonistic pleiotropy) (Cowen, 2002; Bell *et al.*, 2009; Williams, 1957). The benchmark of the current proteomic study highlighted that key groups of proteins that were impaired in the aged CBG, corresponded with similar findings undertaken in the aged mouse brain (Poon *et al.*, 2006), as well as in human aged brain (Chen *et*

al., 2003). This suggests age-related changes specific to the CBG in *L. stagnalis* may be encountering a similar set of biochemical challenges as those experienced in higher vertebrates.

Attempting to solve the problems associated with improving the biochemical paradox that affects the healthspan of aged animals is the ultimate goal in gerontology research. However, we are a long way away from obtaining a coherent view of which factors are the predisposing causes of the problem compared to those that are altered to redress the balance and enable the animal to survive into old age. Chemical signatures that are intrinsically related to a patterned response that parallel the biological age of the animal have been demonstrated in many systems, and at many levels. For example, evaluation of the rat brain provides compelling evidence that selective neuronal vulnerability could occur from targets sensitive to increased Ca^{2+} levels, especially those in areas such as the hippocampus and cortex where Ca^{2+} levels are markedly increased in aged animals (Murchison and Griffith, 2007).

Problems associated with increased Ca^{2+} signalling manifests itself in a number of different ways, but are together related to the ability of the cell to regulate Ca^{2+} (Murchison and Griffith, 2007). In the CBG, the results showed increased cytoskeletal disruption in α-tubulin and β actin expression, decreased tropomyosin-2 and kenesin-like protein expression and RP51 expression that was significantly increased in the aged animal. Earlier studies have highlighted the relationship between increased calpain-activation and Ca^{2+} signalling and suggest an age-related activation of calpain-mediated proteolysis underlay cytoskeletal abnormalities (Toescu, 2005). Tubulin degradation for example are highly susceptible to calpain-mediated proteolysis, but relatively unaffected by cathespin D in the aged rat kidney (Benuck *et al.*, 1996). Parallel studies need to be undertaken in the aged CBG to confirm whether the changes observed herein reflect elevated levels of calcium-mediated proteolysis. The consequence of alteration to cytoskeletal dynamics may mean components that regulate neurite outgrowth such as growth cone motility and neurite elongation that are reliant on different cytoskeletal systems are likely to not only contribute to cognitive decline as experienced in higher vertebrates (Toescu, 2005), but disrupt motor function through a reduction in motor proteins such as kenesin, that are the driving force in the axonal transport of proteins and vesicles into

the cytoplasm which could impair muscle contraction such as those responsible for the reduction in feeding behaviour.

With ageing, and in disease, increased Ca^{2+} levels are likely to result from a sustained disruption to proteins related to mitochondrial function, as well as to the protein synthesis machinery, such as those highlighted in this study, that work together to maintain biological processes. However an additional but frequently unappreciated observation involve the elevated inflammatory mediators that accompany the increased oxidative damage and reflect the decreased ability of the animal to repair itself with advanced age (Vasto *et al.*, 2007). Among the key pathways perturbed during an inflammatory response, the phosphorylation and ubiquitination pathways that oversee protein turnover and degradation are disrupted in aged neurons (Lee C.K, 2000). Prior studies have observed accessory proteins to 40S ribosomal protein such as ribosomal protein S3 (rpS3) are able to function as independent polypeptides to modulate protein synthesis via a non-ribosomal mechanism (Zimmermann, 2003). This bi-functional role can allow rpS3's to associate with chaperones such as Hsp-90; which if blocked using Hsp-90 inhibitor, Geldanamycin, can lead to the destabilisation of rpS3 and the subsequent activation of ubquitin-proteosome pathway (Kim *et al.*, 2006). Given that both 40S ribosomal protein and Hsp-90 were up-regulated in the aged CBG, these patterned protein responses could be examined in the broader context of age-related changes occurring in protein synthesis pathways that relate the phosphorylation of proteins to its activity. Interrelated pathways that activate protein kinase *target of rapamysin* (TOR) for example can reduce the substrates required for protein synthesis (Wullschleger S, 2006). Several pathways are phosphorylated through the activation of the TOR pathway, however the mechanism by which TOR pathway directly regulates lifespan is currently unclear (Tavernarakis, 2008). Data suggests TOR signalling could be regulated by insulin as well as other stimuli which induce site-specific phosphorylation of ribosomal protein S6 (S6K1) and 4E-BP (Proud, 2004) – key components in the initiation of protein translation, and it is plausible that calorie-restriction experiments which extend lifespan through a reduction in insulin signalling may in fact be affecting lifespan by regulating protein synthesis (Syntichaki *et al.*, 2007) (see Chapter 1). The results presented in **Chapter 2** therefore represent a hypothetical sequence of events that are likely contribute to the

normal ageing process in CBG that coincide with the observed reduction in feeding behaviour.

From the list of protein candidates identified, priority was given to AChBP due to its apparent role in regulating cholinergic signalling, and changes in ACh signalling were common among many aged species. So far, AChBP homologues have only been identified in the invertebrate *A.californica* (Bourne *et al.*, 2005), and *B.truncatus* (Celie *et al.*, 2005). To examine the associated notion that impairment in cholinergic signalling in part through AChBP may be disrupted in the aged CBG, **Chapter 3** first highlighted a reduction in AChBP mRNA in the aged CBG using RT-qPCR, suggesting the reduction in AChBP at the protein level was transcriptionally regulated. However, our findings that reduced AChBP mRNA and protein expression in the aged CBG do not nullify the hypothesis that AChBP participates in the feeding pathway. To draw firm conclusions from these observations, **Chapter 4** determined quantitatively the effects of AChBP knockdown on the CNS, and correlated the finding with the feeding behaviour. Two different RNAi approaches were tested however both failed to show a statistically significant difference in AChBP knockdown *in vivo*. There was some evidence to suggest a reduction in feeding behaviour had occurred in siAChBP1-transfected animals after 72 hours, but without the paralleled reduction in AChBP at the protein level, these studies could not unequivocally relate the reduction of AChBP gene with the reduced feeding phenotype. **Chapter 4** therefore allowed us to address the important issue of reproducibility and the reliability of using RNAi in the intact animal, even when analysis was restricted to the CBG region in *L. stagnalis*, and recommendations were offered to improve the detection of RNAi when assessing the feeding behaviour.

However, we should be wary of over committing ourselves to a strict hierarchy of function to AChBP protein in the aged animal as it is equally likely that changes in AChBP expression are independent of the proteins that are involved in the feeding behaviour. Equally likely is the possibility that disruption to AChBP may be the consequence but not the determining factor in age-related reduction of the feeding behaviour. It is also clear from the proteins identified that were disrupted in the aged CBG, that no one factor could solely determine the healthspan of the animal, and it is the culmination of all these events that lead to the animals decline. In view of the

finding that AChBP was primarily localised to non-synaptic regions of the *L. stagnalis* CNS, the participation of AChBP in regulating cholinergic signalling requires further clarification (Banks *et al.*, 2009). To examine the possibility that a reduction of AChBP was symptomatic of an alteration accompanying glial cells rather than intrinsically related to transcriptional or translational events regulating AChBP per se, **Chapter 3** directed attention to possible changes that may be occurring in glial cell GFAP expression with increased age. The results from the young and aged CBG although not statistically significant, point towards increased GFAP expression in the aged animal; however as this data failed to reach statistical significance despite the 20% increase in GFAP expression in the aged CBG. It is highly likely that this may be due to the limited sample size (n=3) of the aged groups tested for GFAP expression, and increasing the sample may show significance.

Changes in protein expression are strongly dependent on the type of proteome under investigation, the stage and duration of the impairment, as well as the age of the animal. Our results represent protein changes occurring during mid- to end stage of the life span of the mollusc. Due to the stage of animal ageing studied here, it may not be altogether surprising that some of the results presented here differed from those suggested in the published literature. In addition, it is important to note that only 17/ 47 proteins (Figure 12) were successfully identified, leaving open the possibility that other targets more relevant to the feeding pathway may not have been identified in the current study. As described in this thesis, ageing is a multi-factorial process, and a number of factors that were identified are likely to control a fundamental biological process such as feeding in *L. stagnalis*. It is not altogether surprising that the reduction in feeding behaviour in the RNAi studies was at best modest, and may represent only a small component of the feeding behaviour. However, in addition to the work concerning AChBP expression in the aged CBG, this thesis opens up the possibility of using *de novo* sequencing to refine the *L. stagnalis* model to examine neuron-specific changes to identify potential regulators of AChBP signalling as well as other regulators of the ageing process. This thesis indicates that AChBP, as a novel cholinergic regulator, was impaired in the aged CBG and this could be a useful predictive tool to assess old age in *L. stagnalis*. However further studies are required to provide more direct insight into AChBP function and the implications of its reduction during the ageing process.

Declaration

I declare that the research contained in this thesis, unless otherwise formally indicated within the text, is the original work of the author. The thesis has not been previously submitted to this or any other university for a degree, and does not incorporate any material already submitted for a degree.
Signed

Dated: _____

APPENDICES

Figure 49: AChBP Western Blot statistical analysis when normalised to GAPDH

Blot 2 - GAPDH probe

Black is 0, White is 255

#	IDV	% AREA	AVG	BACK	
1n	181757790	6255	29058	0	
2n	186674220	6255	29844	0	
3n	189976860	6255	30372	0	
4n	136233900	6255	21780	0	
5n	152953515	6255	24453	0	
6n	153610290	6255	24558	0	
7n	183177675	6255	29285	0	
8n	136471590	6255	21818	0	

IDV=Integrated D s=stan dard
* based on Integ Value

Blot 2 AChBP probe

Black is 0, White is 255

#	IDV	% AREA	AVG	BACK	
1n	18240677	20111	907	0	
2n	14479920	20111	720	0	
3n	16289910	20111	810	0	
4n	14419587	20111	717	0	
5n	10859940	20111	540	0	
6n	7722624	20111	384	0	
7n	4062422	20111	202	0	
8n	2513875	20111	125	0	

IDV=Integrated D s=standard
* based on Integ Value

	% GAP
young	3.121344
young	2.412545
young	2.66693
young	3.292011
old	2.208318
old	1.563645
old	0.689773
old	0.572921

	avg value	**SEM**	**% change**	**% SEM**
3 months	3.569135	0.334502	100	9.372067209
10 months	1.735715	0.305414	48.63125	17.59586358

Anova: Single Factor combined result

SUMMARY

Groups	*Count*	*Sum*	*Average*	*Variance*
young	8	28.55308	3.569135	0.895131022
old	8	13.88572	1.735715	0.746221747

ANOVA

Source of Variatio	*SS*	*df*	*MS*	*F*	*P-value*	*F crit*
Between Groups	13.44571	1	13.44571	**16.3836945**	0.001198689	**4.60011**
Within Groups	11.48947	14	0.820676			
Total	24.93518	15				

Western blot analysis of β-actin protein expression normalised to GAPDH

#	IDV	% AREA	actin AVG	GAPDH AVG	actin/GAPDH	avg (actin/GAPDH
1n	58846095	3465	16983	31445	0.54008586	
2n	61108740	3465	17636	24851	0.70966963	
3n	90235530	3465	26042	35975	0.72389159	
4n	66212685	3465	19109	27686	0.69020444	0.665962881
5n	73967355	3465	21347	35831	0.59576903	
6n	71042895	3465	20503	34290	0.59792943	
7n	101115630	3465	29182	37571	0.77671608	0.656804846

IDV=Integrated I s=stan dard
* based on Integ Value

		SEM actin/GAPDH
young	0.665963	0.04252322
old	0.656805	0.05995886

% change compared to young

		SEM
young	100	0
old	98.62484	9.12887

t-Test: Two-Sample Assuming Unequal Variances

	Variable 1	*Variable 2*
Mean	0.665963	0.656805
Variance	0.007233	0.010785
Observations	4	3
Hypothesized M	0	
df	4	
t Stat	0.124587	
P(T<=t) one-tail	0.45343	
t Critical one-tail	2.131847	
P(T<=t) two-tail	0.906861	
t Critical two-tail	2.776445	

PEAKS 4.5 Protein sequence analysis from the cerebro-buccal ganglia

Table 3 shows *de novo* sequence of proteins identified from the cerebral-buccal ganglia. Unique proteins with highly confident peptide sequence but no homology matches were classed as 'hypothetical proteins' for which sequence homology could not be assigned. None of the proteins identified in this screen were unique with no sequence homology in nr database.

Peaks Protein Score

	PEAKS SCORE			
Protein ID	**Acc No**	**Peaks score %**	**% pr coverage**	**# peptide matches**
Glutathione S transferase	Gi|66534655	99	16	4
Retrograde protein 51	Gi|468226	99	69	75
Beta–actin	Gi|2724046	99	26	8
Glial acidic fibrillary protein	Gi|251802	94	7	6
Tropomyosin-2	Gi|174755	99	80	81
Acetylcholine binding protein	Gi|47169297	99	35	15
14-3-3 like protein	Gi|112687	99	22	5
A-tubulin	Gi|3745821	99	19	9

Table 3: PEAKS 4.5 identification of protein spots in the young and age in cerebro-buccal ganglia region in Lymnaea *stagnalis*. Confidence score (Peaks % score) correlate number of correctly identified peptides to the number of peptides matching a particular protein. Overall score of 90% or above was used for each protein identification, with a minimum of 3 peptides matching to a particular protein. % protein coverage = the percentage of peptide matching a protein.

Accession	Mass	Display	Score (%)	Coverage (%)	Query matched	Description
gi|13647103	39,328		99	15	6	arginine kinase [Aplysia kurodai]

```
1    MEQEAERLYE LLKKDTNCKS LLSKALTPER VKELKAKKTK FNGTLADCIR
51   SGCENTDSGV GVYASDPEAY TTFAPLLDAV IKDYHKVDTL NHPNPDFGDV
101  DKLDFGDLDP SGNVIVSTRV RVGRSHDSYG FPPVISKEDR VDMEKKTVAA
151  LAKLDGELKG TYHPLTGMSK ETQTQLTEDH FLFNNSDRFL EAAGGYKDWP
201  TGRGIYFNNN KTFLVWVNEE DHLRFISMQK GGNLKEVYVR LVKAIRALET
251  SGLSFAKRDG LGYLTFCPSN LGTTLCVSVH IKIPKLAASP DFKAFCDKLN
301  IQARGIHGEH TESVGGVYDI SNKRRLGLTE IQAIQEMRKG VEAVIAEEKK
351  LAGN
```

Accession	Mass	Display	Score (%)	Coverage (%)	Query matched	Description
gi|78696405	107,099		90	4	2	putative glycolate oxidase [Bradyrhizobium sp. BTAi1]

```
1    MPNAKAGPSR LEQKLRAEIT GDVFFDRFNR GRYATDASFY QVIPAGVVVP
51   RTMDEALRAL AIARDDGRIV TPRGGGTSQC GQTVNEGIVV DFSKHLNRIV
101  SLDVAGRTCV VEPGIVLDDL NRQLKTHGLW FPVDVSTASR ATIGGMAGNN
151  SCGGRSLRYG TMRDNTIAID AALADGTQAR FAEVPRDLAD VNAPDKARAL
201  FRDMLALGER EAAEIGDRFP KVQRRVGGYN LDALTPRNAA NNLAHLLVGS
251  EGTLAFSTRI ELKLWPLIRN KVLGVCHFGS FYEAMDAAQH LVKLKPIAVE
301  LVDRTMIGLG RDIAMFQPVI AAAVRGDPDA ILVVEFAEET VDANLAKLKL
351  LSELMGDLGF SWTNEPRKWG GVVEISEPAL QTAVADFRAA GLNVMMSMKE
401  AGKPVSFVED CAVPLPHLAD YTARLNEVFA RHGTRGTMYA HASEGCLHVR
451  PVLNLKLEKD VKAMRAIAEE AFAMVREYKG SHSGEHGDGI VRSEFHEQMF
501  GSRIVADFEE VKQRFDPANV LNPGRIVDPP RMDDRSLFRY PPDYRIDDIK
551  TVLDWSAYPG AAGGFQGAVE MCNNNGACRK LDGGVMCPSY RATRNEKDVT
601  RGRANTLRLA ISGQLGPGAL SSDEMMETLK LCVSCKACRR ECPTGVDMAK
651  MKIEVLAARA TSHGLILRDR IVAYLPRYAD LAARFAPLAN LRNHSAPLRA
701  LMERVAGISA KRKLPAFRSD TFRVDAEAFG PENGREVVLF GDTFNRIYER
751  ENLDAALRVL IAGGYRVYVP RPVDGGRALC CGRTFLSAGL VDEAKSELQR
801  LVETYAPFAA RGVPIIGLEP SCLLTLRDEL LSLRSDAKAR TISAHALLLE
851  EFLAREAESG RLALPLGPLP GKALLHGHCH QKSFAAFKPV EQVLRLIPEL
901  EVETIESSCC GMAGAFGYGA DTYEVSLQMA EASLLPAVRK ADSTTFIVAD
951  GTSCRHQIQD GAARGAVHAA QLLAMSLERT QASQ
```

Accession	Mass	Display	Score (%)	Coverage (%)	Query matched	Description
gi|83286456	289,424		90	1	4	chromodomain-helicase-DNA-binding protein, CHD-1-related [Plasmodium yoelii yoelii str. 17XNL]

```
1    MHGNFYPYMT NGFYGMSSTN CFKPTSTNIP NNNNTNTTNN NNTSMNSFNQ
51   INGSFPYDNT IRSGVGPSAP PGGVNNAISS NSNNNNNNNS NFVNNLNSVN
101  YGDNINCNSI NNILNKDSEN LDKSSQIKSL SNNMNVNNLN MGHHVNNTAI
151  TSGTNNNSNN NGINSNVKDN MTKMANNNFK GIGSICNNIP PYRINSDQQL
201  DKQHNSIDDN NNNNNNNTRY HPMNMYNRME YVIVITSNLL GDNKTNASIS
251  KIRKGNNKDG VIGDNNGNSN GLINNDSDGY KQYKNEVDGN HNKMKDGTDG
301  MIKDPKLNDS VNSNGNNSYA MFPNYNLKYP MNMNMFNNIN HFNMNNKNGI
351  NNIGGVSNMN VEGGNYQSFN LINNMSDLNS AYNNMNKLPN VNNYNMMNIY
401  SDNRYNNNNT NIPVGVNNNI INMNNYNNMN YMNMRLLNSR NIPNNMNNSD
451  LNTNYMTDGM GNRIVNHDMN NNMNDGNLNN GNKYVRKTGI GKQYVNNNVT
501  SGSMKKKNET QKDKKKKRKK KNENNIPESD DEEDNDLYIN SYVKKSAPKN
551  SNGNKSWLQY DSLDDKYTEK MKRNEKNDIF VSPNIGAVGG RTNLRERKRV
601  YNYAQIDNYY ETDEEDKKVD EEKNLLRQEK QSMGGIDRVI HHRKIKDWDI
651  INSIKNNPFL FINRKKPEQG ENANGDANEN ANENGDTNGD SKKNENLIGS
701  TEMSSDSLNA TETAGTDGAP DVSCHKILGG VENNEDPALD DFYEEEDIVD
751  VNEVEFLVKW IGKSHIHNFF CTYEYLRYFN GVKKVDNYIK KIRLSFQKRK
```

```
801  YMTADEIEQE KIYSEIKKQI EMDSIHAERI ITHRKCEITN EQLFLVKWTS
851  CAYDQCTEET KQTLLDHNFG KLIDEYFDRE SKIYGPKALS SIWNRGPLTA
901  TKFDPYNETP SYLHGKKLRA YQLTGLNWMV SRMKRNLSVL LADEMGLGKT
951  VQTIAVVGHM LYKEKLIGPY LVLVPQSTVD NWLNEFKNWL PQANVVCYHG
1001 NAVSRELIRT YELKKVYVQN RGYRYKFDVC ITTPSILNSV SDVELLKRIP
1051 WQLMVVDEAH QLKNRQSKRF IELKQFMAES KLLLSGTPLH NNLEELWTLL
1101 HFLNPQQYTY YEAFQKKYNE IENTSLIGEA KQKQLMQLQH ELHEVILRRV
1151 KKDVEKSLPN KVERILRVEL SPIQIEYYKN ILTKNYEQLA KASGGAKNSL
1201 QNICMELKKV CNHPFLCCEP IDKDEYRERL VYSSGKICLL EKLLIRLKER
1251 GNRVLIFSQM VKMLNILSEY LTLRGFKHQR LDGTMTKEMR KKAMNHFNSK
1301 NSDDFVFLLS TKAGGLGINL TSADTVIIYD SDWNPQNDLQ AGARAHRIGQ
1351 TKTVQIYRLV TKDSIEQTIL ERAKVKMVLD TLVVQGLNKK QNDNVNFIGG
1401 EGSNSSNGFT REELSKILKF GSQKLWEKNS SKYSPQDGED GKNIIKGVDV
1451 DLDKILEEAE ANENTNNANK DINSELNSLQ NGAASNFFNT NTNLFGNGVS
1501 GNGVNNIGGG IADDLLSSYN NITEFKYEPP ENLKSNILYN DSTKQGELDV
1551 EENDKDFWDK TIPLEERLKL KKMKEEELLV HGPRKTRTRD ARYNQGLYYD
1601 GGAHNNNSEG DDSDEFTIKY TDKYNKNLNK KKRKRRTSTH ITEKDKFRLY
1651 RSLLKFGNPT LRLDDIQFDS KLMKVDRNVI LTELNIIVDT CKEIVEKVAK
1701 EGNNTNGQQP GLATQNVKTD NDDQTEYNNE ECNTTNANSV NVKSNDMGVE
1751 VKEENDQQAE DINDENDKNK RGKRGVRTTA TPSTGENVEA TEVSKKEEAN
1801 NNDNDNNSGG GDGGGFFSKF MKFTKGSTGA KREDEIEGKG IKAKTEDDGV
1851 KDELDDDIVK DELNDESDNN NKTKGERGRK IDAYTFYIGT NKANALDLCH
1901 RLQLFKSLHD FIKEQNNDNE YSFRLPLKPP QTNPNNEIVN NDNVVDSVVE
1951 NVEVNNKSVV KNDKIKNKKD EVEGAGATTT TADVEEEATL NLTTTSETKQ
2001 EGKTSNECEA TESSMVVVGG NPSDDYLKLK LPNYIFDHLR DLSTKDVKAW
2051 TKEDDENLIK GIYIYGFGSF NEICVDVNLN LEHMKNIKWD KIKMRCIKIL
2101 KMIEEYTSNN KEGTPGKKRR RARGKNKNHD EIKEEYDNGN NNTSIKSEGT
2151 GGINKSNSIN GRHSINNYGR RSSERVKAIY SQEDKENGGI LKKRVVSSRK
2201 GERDNKNNST HLGSNGTSSK LENVYDINNK GGENTLLSSS TLDKRRRRGI
2251 SSKSSNVTLK NEKTNSKCII ESSECSSSNE QKSNGSDDDD DEEEDDEINT
2301 NIVKRSGRSG SNRSSRMNSY ENYKLTRRRS TRTRRGGGND SIVGSECVNS
2351 IDPDGDDEYH NDSNDRKKLK KKKKKKKKLT DEEIIEIIKN SNLREMDQHS
2401 INKLTKKPLK KYKKLLKIVK KVLSSKTNEL GQAEEQVSDD IRKKTDELIF
2451 YIGNYIGKFF DHCVDSECKD ILNNSGWEYI SNFVNETSEN LKEKYEKFKS
2501 SNLKDSDNAD ITEENIISFF YSKKCSGLLC PEDDPDDVMD E
```

Accession	Mass	Display	Score (%)	Coverage (%)	Query matched	Description
gi|47551035	41,832		99	14	4	cytoskeletal actin CyIIIb [Strongylocentrotus purpuratus]

```
1    MCDDDVAALV VDNGSGMVKA GFAGDDAPRA VFPSIVGRPR HQGVMVGMGQ
51   KDSYVGDEAQ SKRGILTLKY PIEHGIVTNW DDMEKIWHHT FYNELRVAPE
101  EHPVLLTEAP LNPKANREKM TQIMFETFNS PAMYVAIQAV LSLYASGRTT
151  GIVFDSGDGV SHTVPIYEGY ALPHAIIRLD LAGRDLTDYL MKILTERGYS
201  FTTTAEREIV RDIKEKLCYV ALDFEEEMQT AASSSSLEKS YELPDGQVIT
251  IGNERFRCSE TLLQPSFIGM ESAGIHETCY NSIMKCDVDI RKDLYANTVL
301  SGASTMFPGI ADRMQKEIVA LAPPTMKIKI IAPPERKYSV WIGGSILASL
351  STFQQMWISK QEYDESGPSI VHRKCF
```

Accession	Mass	Display	Score (%)	Coverage(%)	Query matched	Description
gi|51105058	40,595		99	14	4	probable reductase [Lymnaea stagnalis]

```
1    MSSLVLITDA TNFTSAHIIK QLQEEGYQVR GTVTSLQDED ARIKQLQELV
51   PEAKFKLEIV EADPAKPETW EEAIKEVQYV IHAVKPVAAL PPAAEGEAPV
101  QPAVEAVQNI FKASVKSTSV KRIILTSSFQ AITAGPTAAT DKVFTEADWA
151  DAETADPLVK SLILAEKSAW DFIKELTDSD KIDLVVMNPT LALGPPLLDA
201  QQDVVKMLLD RGITGCPRVS YSVVDVRDVA AAHVKALLLD NVSGNRHILH
251  GGNLWMKDIA LALAKEFKPQ GYSIHTMSIP NVALWGLSLF NKTAKTFLPI
301  VGKQSQFDNT RMKDVLGITP KDVKETVVEE ANVLIEKGLV KKPKRVRCQG
351  GAAAAEGEAK AEDGSEKKEG ESEE
```

Accession	Mass	Display	Score (%)	Coverage(%)	Query matched	Description
gi|57903365	45,260		98	16	8	α-tubulin [Pavlova lutheri]

```
1    GPQVGNACWE LFCLEHGIQP DGQMPSDKTI GGGDDAFNTF FSETGSGKHV
51   PRTVFIDLEP TVIDEVRTGT YRQLFHPEQL ISGKEDAANN YARGHYTVGK
101  EIIDLVLDRI RKLADNCTGL QGFLVFNAVG GGTGSGLSSL LLERLSVDYG
151  RKSKLTFTIY PSPQISTAVV EPYNTVLSTH SLLEHSDVSF TVDNEALYDI
201  CRRNLDIERP TYTNLNRLVA QIISGLTASL RFDGALNVDL TEFQTNLVPY
251  PRIHFVLSSF APIISAEKAY HEQLSVAEIT NAVFEPASQL VKVDPRHGKY
301  MSCCMMYRGD VVPKDVNAAI ATIKTKRTIQ FVDWCPTGFK CGINYQPPTV
351  VPGGDLAKVM RAVTMEANST AFAELYSRID HKFDLMYAKR AFVHWYVGEG
401  MEEGEFSGP
```

Accession	Mass	Display	Score (%)	Coverage (%)	Query matched	Description
gi|10908171 3	73,077		95	4	4	PREDICTED: similar to 40S ribosomal protein SA (p40) (34/67 kDa laminin receptor) (Colon carcinoma laminin-binding protein) (NEM/1CHD4) (Multidrug resistance-associated protein MGr1-Ag) [Macaca mulatta]

```
1    MSGALDVLQM KEEDVLKFLA AGTHLDGTNL DFQMEQYIYK RKSDGIYIIN
51   LKRTWEKLLL AARAIVAIEN PADVSVISSR NTGQRAVLKF AAATEATPIA
101  GRFTPGTFTN QIQAAFREPR LLVVTDPRAD HQPLTEASYV NLPTIALCNT
151  DSPLRYVDIA IPCNNKGAHS VGLMWWMPAR EVLRMRGTIS REHPWEVMPD
201  PYFYRDPEEI EKEEQAAAEK AVTKEEFQGE LTSPAPEFTA TQPEVADWSE
251  GVQEALLIAL PKHVLACALL SPGWRGVGTS AAPLPSSLLN STPGGYTPYP
301  NYHLVGLICF PGFCPHPWSK HLAKPNLVIS SAPESEGANG LCPSGVLAIS
351  GSTMASVMPP RGSIDSLPGG GSVSSFGSAL APRGSASVAL DSYSQALHRI
```

```
401  PCSEMMEPSS LLDVTCLHAL LMRVPAGIST LPAPPPSMLS FTHKVLSYRP
451  PTPADQLPPH GILLRLFDDK SMSFSSAALE DASSDDNSAA PLPPPGPRGL
501  WSSDMQMFLC FLPWFWRSFL LKNLPPLLHQ WKHCAFLKDQ TKNTLLLAAS
551  PGSSEPASPW PWAGAIRAAM VQVSCRLPGD IGLSGPTFWK GNKQGLTGMM
601  EIEIASDRGA QEAGPGKAQT GSLSPQIYSC DLEQARTVRG QGGIRGLGAL
651  QRTDTDNHAS KSLTSQNRVA LGTHIYM
```

Accession	Mass	Display	Score (%)	Coverage (%)	Query matched	Description
gi|71652882	37,146		97	14	5	reductase [Trypanosoma cruzi strain CL Brener]

```
1    MRVVVSFAAG LLAALLHRPV DDAFPAECYR SIENALHFRN KKRDGEVFSQ
51   RYEPYQLGEV IPITHDTALF RFLLHADEEF NLKPCSTLQA CYKYGVQPME
101  QCHRFYTPVT ANRTKGYFDI IVKRKNSGLM TTHLFGMHVG DKLLFRSVTF
151  KVQYKPNKWN HVGMIAGGTG FTPMLQIIRH SLMEKWNDGS VDNTKLSFLF
201  CNRTEKHILL KGLFDDLAER YSNRFKVYYT VDQPVEPENW KHFVGYVSKE
251  MVQQTMPAPD EKKIIMLCG PDQLLNHVAG TPMGTMSAMS SGMNIQPLAP
301  DLNNLVSLGG ILGELGYKND DVYRF
```

Accession	Mass	Display	Score (%)	Coverage(%)	Query matched	Description
gi|1174755	32,683		99	59	49	Tropomyosin-2 (TMII)

```
1    MDAIKKKMLA MKMEKENAID RAEQMEQKVR DVEETKNKLE EEFNNLQKKF
51   SNLQNDFDTA NEGLTEAQTK LEASEKHVAE LESDTAGLNR RIQLLEEDLE
101  RSEERLQSAT EKLEEASKAA DESERGRKVL ESRSLADDER LDGLEAQLKE
151  AKYIAEDAER KYDEAARKLA ITEVDLERAE ARLEAAEAKI IELEEELKVV
201  GNNMKSLEIS EQEASQREDS YEETIRDLTQ RLKDAENRAT EAERTVSKLQ
251  KEVDRLEDEL LAEKERYKSI SDELDSTFAE LAGY
```

Accession	Mass	Display	Score (%)	Coverage(%)	Query matched	Description
gi|28897595	72,161		90	19	19	heat shock protein 90 [Vibrio parahaemolyticus RIMD 2210633]

```
1    MSETVSQNKE TRGFQSEVKQ LLHLMIHSLY SNKEIFLREL ISNASDASDK
51   LRFQALSNPD LYEGNADLGV KLSFDESANT LTISDNGIGM SRNDVIEHLG
101  TIAKSGTAEF FSKLSEEQSK DSQLIGQFGV GFYSAFIVAD AVTVRTRAAG
151  LPADEAVQWH SAGEGEYTIE NITKESRGTD IILHMRDEGK EFLNEWRLRD
201  VISKYSDHIG IPVSIQTVVR DEDGKETDEK KWEQINKAQA LWTRNKADIS
251  DEEYQEFYKH VSHDFADPLV WSHNRVEGKN DYTSLLYIPS KAPWDMMNRD
301  HKSGLKLYVQ RVFIMDDAEQ FMPSYLRFVR GLIDSNDLPL NVSREILQDN
351  KVTQSLRNAC TKRVLTMLER MAKNDEEKYQ SFWKEFGLVL KEGPAEDFAN
401  KEKIAGLLRF ASTEVDSAEQ TVGLASYVER MKEGQDKIYY LTADSYAAAK
451  NSPHLEQFKA KGIEVILMFD RIDEWLMNYL TEFDGKQFQS ITKAGLDLSK
501  FEDEADKEKQ KETEEEFKSV VERTKSYLGD RVKDVRTTFK LASTPAVVVT
```

```
551  DDYEMGTQMA KLLAAAGQAV PEVKYIFEIN PEHELVKRMA DEADEEAFGR
601  WVEVLLGQAM LAERGSMEDP TQFLGAINKL LTKV
```

Accession	Mass	Display	Score (%)	Coverage(%)	Query matched	Description
gi|47169297	23,839		99	29	9	Chain A, X-Ray Structure Of Acetylcholine Binding Protein (Achbp) In Complex With Carbamylcholine

```
1    LDRADILYNI RQTSRPDVIP TQRDRPVAVS VSLKFINILE VNEITNEVDV
51   VFWQQTTWSD RTLAWNSSHS PDQVSVPISS LWVPDLAAYN AISKPEVLTP
101  QLARVVSDGE VLYMPSIRQR FSCDVSGVDT ESGATCRIKI GSWTHHSREI
151  SVDPTTENSD DSEYFSQYSR FEILDVTQKK NSVTYSCCPE AYEDVEVSLN
201  FRKKGRSEIL
```

Accession	Mass	Display	Score (%)	Coverage(%)	Query matched	Description
gi|112687	24,731		99	11	4	14-3-3-like protein

```
1    RNLLSVAYKN VVGARRASWR IISSIEQKEE SRGNEDHVSV IRDYRSRIEK
51   ELSDNCDGIL KLLDTKLVPA ASSGDSKVFY LKMKGDYHRY LAEFKTGAQR
101  KEAAESTLTA YKAAQDIANA ELAPTHPIRL GLALNFSVFY YEILNSPDRA
151  CNLAKQAFVE AIAELDTLGE DSYKDSTLIM QLLRDNLTLW TSDMQDEAAD
201  EITEEAAKQQ KAVNNNKIAY
```

Accession	Mass	Display	Score (%)	Coverage(%)	Query matched	Description
gi|66534655	17,700		99	16	4	PREDICTED: similar to Glutathione S transferase S1 CG8938-PA, isoform A, partial [Apis mellifera]

```
1    TPFGQVPVLD VDGKKIAQSV AISRYLAKKS GLAGKDDWEA LEIDSIVDTI
51   HDVRARLAAF HYEENEEIKA AKRKIADEVV PYYLERLDAQ VKNNGGYFVG
101  GALSWADLSF VALLDYLNFM NGSDLIEKYD NLKQLKEKVL NLPAIKSWLD
151  KRPHSDF
```

Validation of isoform differences in 14-3-3 protein

Due to the lack of antibodies specific for AChBP initially, we progressed with validating one of the candidate proteins, the 14-3-3-like protein which was identified through *de novo* sequencing PEAKS 4.5. However, we were unable to attain more specific information from the peptides recovered in the collision induced dissociation (CID) spectra with regards to the epitope uniquely homologous in *Lymnaea* (Figure 9).

Figure 9. **Cross species analysis of sequence homology of 14-3-3 protein.** Homologous amino acid residues are highlighted in blue. De novo sequence of peptides shows >90% confidence in red.

Antibodies directed against 14-3-3 β subunit failed to show specific differences in young, middle aged and old snails in the cerebrobuccal ganglia region (Figure 10). In addition, two bands were detected, instead of the single band as expected. Although dimerisation of this protein is possible, it is unlikely here, as the mass difference between the two bands are not double units apart. It is possible more likely that we have detected the presence of more than one analogue of 14-3-3 having an identical moiety to the β-subunit specific antibody.

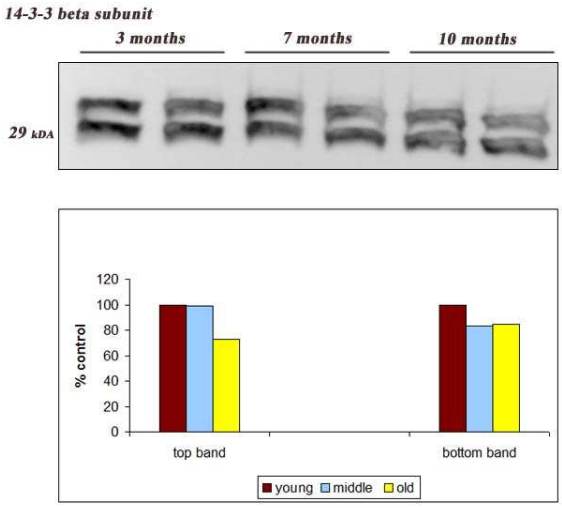

***Figure 10*. Western Blot analyses of 14-3-3- β expression in pooled (n=70) cerebro-buccal ganglia region of 3 month, 6-7 month, and 10 month old Lymnaea stagnalis CNS** (n=2). Samples were normalised to total protein content of homogenates. Membranes probed with primary antibody 1/500 (K-19, sc-629, Santa Cruz Biotech Inc overnight at 4°C; secondary antibody 1/ 4000 (HRP labelled anti-rabbit conjugated to HRP. 8 µg protein Detection of proteins achieved on proteins being transferred to PVDF membrane. 7 month and 10 month groups are expressed as a percentage of the 3 month age group.

Expression analyses of the 14-3-3-γ subunit revealed a single band; however this showed an increased expression in aged animals (Figure 11). These characteristics are in disagreement with the previous proteomic finding (Figure 8A), suggesting the identity of the 14-3-3 protein specifically downregulated in *Lymnaea* remains illusive and has yet to be characterised with a subunit specific antibody.

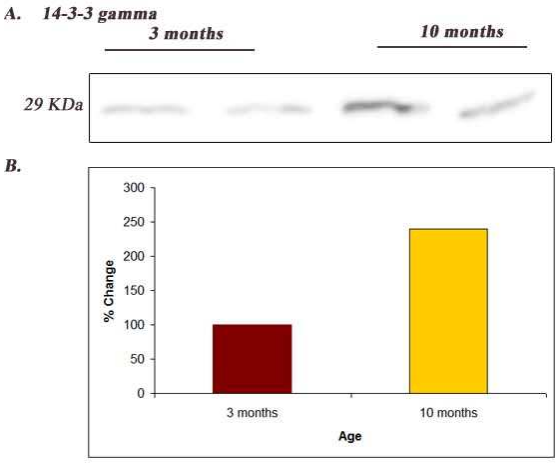

***Figure 11*. Western Blot analyses of 14-3-3- γ expression in pooled (n=70) cerebro-buccal ganglia region of 3 month and 10 month old Lymnaea stagnalis CNS** (n=2). **A.** Membranes probed with primary antibody 1/800 (sc-731, Santa Cruz Biotech Inc overnight at 4°C; secondary antibody 1/ 4000 (HRP labelled anti-rabbit conjugated to HRP. 8 µg protein load. **B.** relative change in protein expression of the above fluorescence intensity expressed as a percent change compared to 3 month (control) (n=2).

Alignment of 14-3-3 cDNA clones present in *Lymnaea* showed the 14-3-3-ε subunit to be the closest evolutionary homologue within *Lymnaea* (Figure 13). Whilst the possibility exists that a number of epitopes are functionally behaving in opposite directions, without a *Lymnaea* -specific antibody directed against the 14-3-3 protein, this question could not be addressed directly.

L. stagnalis cDNA alignment of 14-3-3 protein

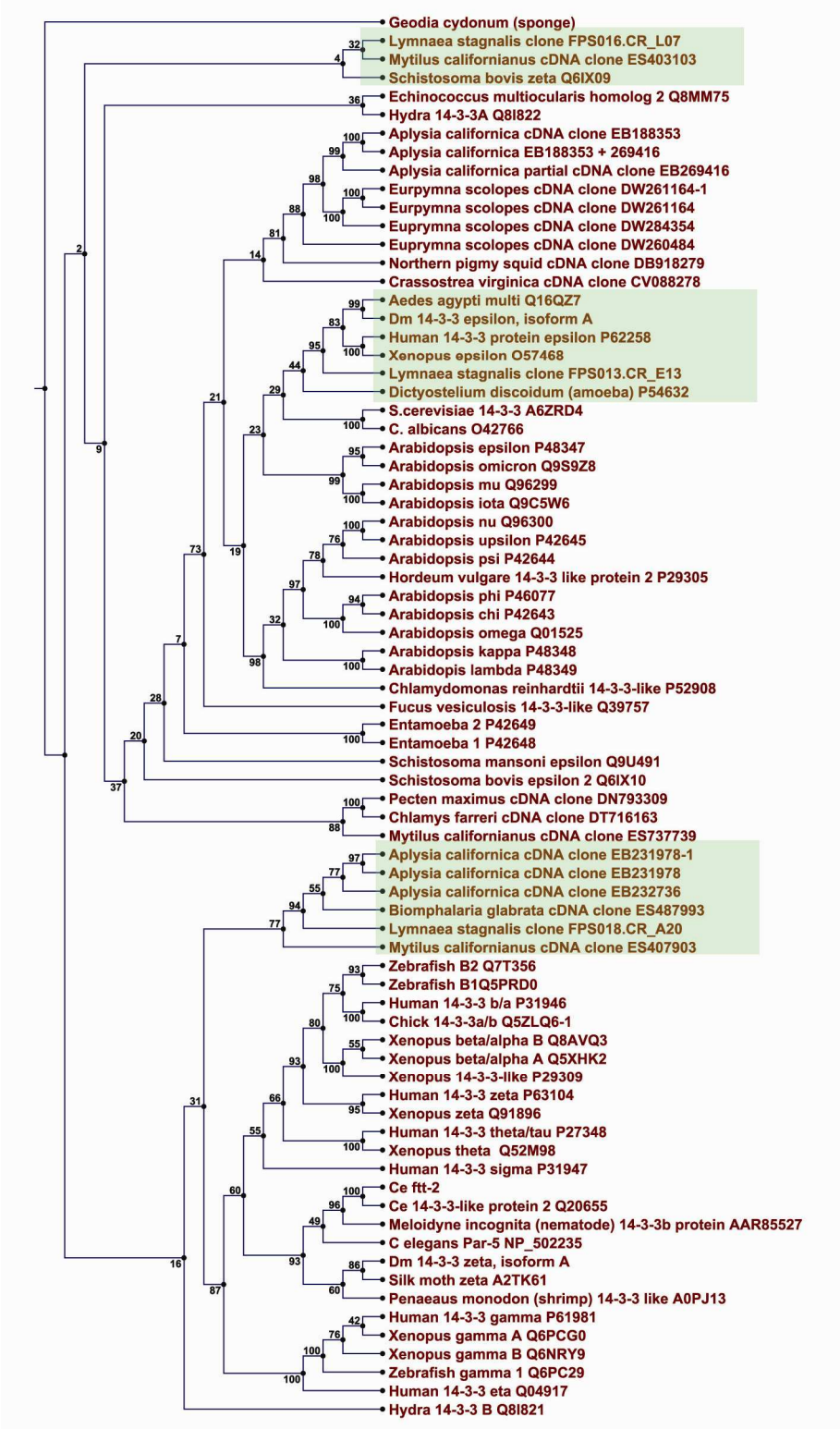

Figure 13. Phylogenetic comparison of the partially identified 14-3-3 protein from whole CNS cDNA library. Clones FPS016.CR_L07 and FPS018.CR_A20 form divergent clusters with no sequence homology to other 14-3-3 proteins. Clone FPS013.CR_E13 forms part of a sub tree most closely related to 14-3-3-epsilon-like subunit.

Analysis of 14-3-3-ε subunit in young and aged groups showed a decrease in subunit expression in aged groups (Figure 12), supporting the proteomic data.

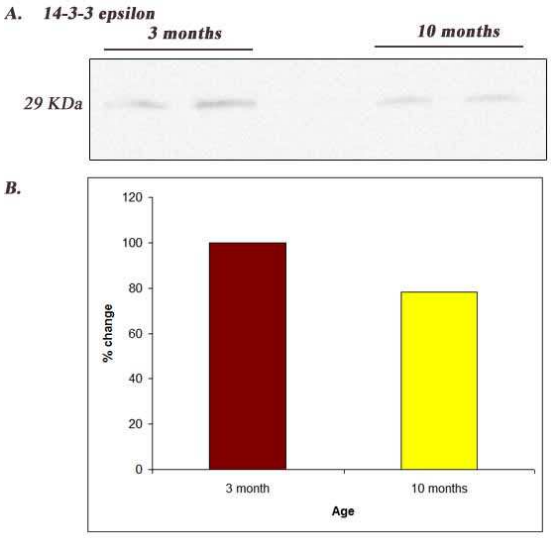

Figure 12. **Western Blot analyses of 14-3-3- ε expression in pooled (n=70) cerebro-buccal ganglia region of 3 month, and 10 month old Lymnaea stagnalis CNS** (n=2). **A.** Membranes probed with primary antibody 1/800 (sc-731, Santa Cruz Biotech Inc overnight at 4°C; secondary antibody 1/ 3000 (HRP labelled anti-rabbit conjugated to HRP. 10 µg protein load. Groups were confirmed in replicates. **B.** relative change in protein expression of the above fluorescence intensity expressed as a percent change compared to 3 month (control) (n=2).

We have recently obtained a *Lymnaea* specific AChBP antibody (gifted from Pim Van Leirop, Netherlands). As the protein is specifically raised against *Lymnaea* AChBP, validation of this protein should prove less problematic than that evidenced with the 14-3-3 protein.

Statistics:

Best-case values used for AChBP mRNA expression

t-Test: Two-Sample Assuming Unequal Variances

	young	*Aged*
Mean	1	0.104418
Variance	0	0.014292
Observations	4	4
Hypothesized Mean Difference	0	
df	3	
t Stat	14.9827	
P(T<=t) one-tail	0.000323	
t Critical one-tail	2.353363	
P(T<=t) two-tail	0.000645	
t Critical two-tail	3.182446	

	Best case	
	young	Aged
cDNA 1	1	0.052785
cDNA 2	1	0.057711
cDNA 3	1	0.024762
cDNA 4	1	0.282415
avg	1	0.104418
SEM	0	0.059774
		57.24517
	1	-0.89558

Conservative Estimate for AChBP mRNA expression

t-Test: Two-Sample Assuming Unequal Variances

	young	*Aged*
Mean	1	0.13801
Variance	0	0.027509
Observations	4	4
Hypothesized Mean Difference	0	
df	3	
t Stat	10.39436	
P(T<=t) one-tail	0.00095	
t Critical one-tail	2.353363	
P(T<=t) two-tail	0.0019	
t Critical two-tail	3.182446	

	conservative estimate	
	young	Aged
	1	0.043023
	1	0.091948
	1	0.03327
	1	0.383797
	1	0.13801
	0	0.082929
		60.08896
		-0.86199

Western Blot analysis of dsRNA-tranfected animals 48 hours post-injection

ANOVA: Single Factor 48 hours

SUMMARY

Groups	*Count*	*Sum*	*Average*	*Variance*
Column 1	5	500	100	0
Column 2	5	849.7224	169.9445	4417.696
Column 3	5	523.3277	104.6655	3447.325

ANOVA

Source of Variation	*SS*	*df*	*MS*	*F*	*P-value*	*F crit*
Between Groups	15292.22	2	7646.112	2.9165	0.092841	3.885294
Within Groups	31460.08	12	2621.674			
Total	46752.31	14				

Western Blot analysis of dsRNA-tranfected animals 72 hours post-injection

ANOVA: Single Factor 72 hours

SUMMARY

Groups	*Count*	*Sum*	*Average*	*Variance*
Column 1	5	500	100	0
Column 2	5	695.8794	139.1759	11354.56
Column 3	5	369.9076	73.98151	2368.036

ANOVA

Source of Variation	*SS*	*df*	*MS*	*F*	*P-value*	*F crit*
Between Groups	10770.03	2	5385.014	1.177259	0.341315	3.885294
Within Groups	54890.38	12	4574.198			
Total	65660.41	14				

Sucrose-evoked bites after 72 hours siRNA post injection

	72 hour transfection			
	saline	scrambled s	siAChBP 1	siAChBP 2
	23	29	20	8
	33	38	25	18
	34	31	20	21
omitted	30	34	19	24
	31	38	26	25
avg	**30.25**	**34**	**22.75**	**18**
% control	**100**	**112.39669**	**75.2066116**	**59.504132**
± SEM	2.50	2.35	1.60	3.63
± % SEM	**8.25**	**6.90**	**7.04**	**20.16**
	30.25	34	22.75	18

siAChBP 1

t-Test: Two-Sample Assuming Equal Variances

	saline	*siAChBP 1*
Mean	30.25	22.75
Variance	24.91667	10.25
Observations	4	4
Pooled Variance	17.58333	
Hypothesized Mean I	0	
df	6	
t Stat	2.529447	
P(T<=t) one-tail	0.022357	
t Critical one-tail	1.94318	
P(T<=t) two-tail	0.044713	
t Critical two-tail	2.446912	

siAChBP2

t-Test: Two-Sample Assuming Equal Variances

	saline	*siAChBP 2*
Mean	30.25	18
Variance	24.91667	52.66667
Observations	4	4
Pooled Variance	38.79167	
Hypothesized Mean	0	
df	6	
t Stat	2.781518	
P(T<=t) one-tail	0.015966	
t Critical one-tail	1.94318	
P(T<=t) two-tail	0.031933	
t Critical two-tail	2.446912	

Sucrose-evoked bites after 96 hours siRNA post injection

	behavioural assay 96 hour transfection			
anti-AChBP	saline	scrambled	siAChBP 1	siAChBP 2
1	37	32	18	36
3	31	27	17	15
5	28	28	32	36
22	25	35	21	11
24	31	30	16	25
	31.75	**29.25**	**20.75**	**28**
	104.9587	**96.69421**	**68.59504**	**92.56198**
	1.89	1.11	3.77	5.05
	5.94	**3.79**	**18.18**	**18.03**

siAChBP 1

t-Test: Two-Sample Assuming Equal Variances

	saline	*siAChBP 1*
Mean	31.75	20.75
Variance	14.25	56.91667
Observations	4	4
Pooled Variance	35.58333	
Hypothesized Mean Difference	0	
df	6	
t Stat	2.607861	
P(T<=t) one-tail	0.020118	
t Critical one-tail	1.94318	
P(T<=t) two-tail	0.040236	
t Critical two-tail	2.446912	

siAChBP 2

t-Test: Two-Sample Assuming Equal Variances

	saline	*siAChBP 2*
Mean	31.75	28
Variance	14.25	102
Observations	4	4
Pooled Variance	58.125	
Hypothesized Mean Difference	0	
df	6	
t Stat	0.695608	
P(T<=t) one-tail	0.256351	
t Critical one-tail	1.94318	
P(T<=t) two-tail	0.512702	
t Critical two-tail	2.446912	

Western Blot analysis of AChBP siRNA in vivo transfection after 72 and 96 hour post injection

Anti-AChBP 1/20,000 primary and secondary

		72 hour transfection				96 hour transfection			
		saline	**scrambled siRNA**	**AChBP 1**	**AChBP 2**	**saline**	**scrambled siRNA**	**AChBP 1**	**AChBP 2**
AChBP	blots								
	1	10279	9287	6412	8696	8367	8443	9888	14529
	3	7490	9050	4326	12087	9204	12703	13432	20801
	5	20451	14286	19231	14241	18403	20799	21068	13910
	22	17512	20183	11268	19326	30333	30394	27427	23503
	24	16655	17267	14980	19705	15708	12171	13674	13786
tubulin	blots								
	1	3677	4982	5010	5797	8341	4101	10353	10346
	3	15300	11095	8138	11144	8659	17045	17509	21113
	5	26891	24428	23485	20019	17862	14862	17205	18478
	22	4676	3446	3956	4854	5698	7181	7803	7081
	24	38702	42088	36939	29327	37203	36353	40357	34783
AChBP/ tubulin	blots								
	1	2.795485	1.864111	1.27984	1.500086	1.003117	2.0587662	0.955085	1.404311
	3	0.489542	0.815683	0.53158	1.08462	1.06294	0.7452625	0.767148	0.985222
	5	0.760515	0.584821	0.818863	0.711374	1.030288	1.3994752	1.224528	0.752787
	22	3.745081	5.856936	2.848332	3.981459	5.323447	4.2325581	3.51493	3.319164
	24	0.43034	0.410259	0.405533	0.671906	0.422224	0.3348004	0.338826	0.396343
	average	1.118971	0.918718	0.758954	0.991997	0.879642	1.1345761	0.821397	0.884666
	% control	100	82.1039	67.82612	88.65261	100	128.98153	93.37851	100.5711
	% scramb	121.7969	100	82.61011	107.9761	77.53048	100	72.39681	77.97325
	± SEM	0.563441	0.325884	0.193975	0.193206	0.152962	0.3780989	0.186236	0.211344
	± % SEM	50.35349	29.12352	17.33515	17.26637	17.38915	33.325122	22.67304	23.88966

References:

Akopian, G. and Walsh, J. P. (2006) Pre- and Postsynaptic Contributions to Age-Related Alterations in Corticostriatal Synaptic Plasticity. Synapse, 60, 223-238.

Alcorta, D. A., XIONG, Y., PHELPS, D., HANNON, G., BEACH, D. and BARRETT, J. C. (1996) Involvement of the cyclin-dependent kinase inhibitor p16 (INK4a) in replicative senescence of normal human fibroblasts. Proceedings of the National Academy of Science USA, 93, 13742–13747.

Aldrich, S. (2009) http://www.sigmaaldrich.com/life-science/functional-genomics-and-rnai/mirna/learning-center/mirna-introduction.html.

Alkondon, M., Pereira, E. F. R., Barbosa, C. T. F. and Albuquerque, E. X. (1997) Neuronal Nicotinic Acetylcholine Receptor Activation Modulates gamma -Aminobutyric Acid Release from CA1 Neurons of Rat Hippocampal Slices. Journal of Pharmacology and Experimental Therapeutics, 283, 1396-1411.

Araiz, C., Château, M. T. and Galas, S. (2008) 14-3-3 regulates life span by both DAF-16-dependent and -independent mechanisms in Caenorhabditis elegans. Experimental Gerontology, 43, 505-519.

Ardini, E., Pesole, G., Tagliabue, E., Magnifico, A., Castronovo, V., Sobel, M. E., Colnaghi, M. I. and Menard, S. (1998) The 67-kDa laminin receptor originated from a ribosomal protein that acquired a dual function during evolution. Molecular Biology and Evolution, 15, 1017-1025.

Arking, R. (2006) The Biology of Aging: Observations and Principles Oxford University Press.

Arundell M, Patel B.A, Straub V, Allen M.C, Janse C, O'Hare D, Parker K, Gard P.R and M.S, Y. (2006) Effects of age on feeding behavior and chemosensory processing in the pond snail, Lymnaea stagnalis. Neurobiology of Aging, 27, 1880 - 1891.

Arundell, M., Patel, B. A., Straub, V., Allen, M. C., Janse, C., O'Hare, D., Parker, K., Gard, P. R. and Yeoman, M. S. (2006) Effects of age on feeding behavior and chemosensory processing in the pond snail, Lymnaea stagnalis. Neurobiology of Aging, 27, 1880 - 1891.

Avruch, J. (1998) Insulin signal transduction through protein kinase cascades. Molecular and Cellular Biochemistry, 182(1-2), 31-48.

Balaban, R. S., Nemoto, S. and Finkel, T. (2005) Mitochondria, Oxidants, and Aging. Cell, 120, 483 - 495.

Banks, G., Kemenes, I., Schofield, M., O'Shea, M. and Korneev, S. A. (2009) Acetylcholine binding protein of mollusks is unlikely to act as a regulator of cholinergic neurotransmission at neurite-neurite synaptic sites in vivo. FASEB Journal., fj.08-117135.

Bartel, D. P. (2004) MicroRNAs: Genomics, Review Biogenesis, Mechanism, and Function. Cell, 116, 281-297.

Bass, B. L. (2000) Double-Stranded RNA as a Template for Gene Silencing. Cell, 101, 235-238

Bear, M. F., Connors, B. and Paradiso, M. (2006) Neuroscience Exploring the Brain

Bell, R., Hubbard, A., Chettier, R., Chen, D., Miller, J. P., Kapahi, P., Tarnopolsky, M., Sahasrabuhde, S., Melov, S. and Hughes, R. E. (2009) A Human Protein Interaction Network Shows Conservation of Aging Processes between Human and Invertebrate Species. PLoS Genet, 5, e1000414.

Bellanger, C., Dauphin, F., Belzunces, L. P., Cancian, C. and Chichery, R. (1997) Central acetylcholine synthesis and catabolism activities in the cuttlefish during aging. Brain Research, 762, 219-222.

Benjamin, P. R. and Rose, R. M. (1979) Central Generation of Bursting in the Feeding System of the Snail, Lymnaea Stagnalis. Journal of Experimental Biology, 80, 93-118.

Bennett, R. G., HAMEL, F. G. and DUCKWORTH, W. C. (2000) Insulin Inhibits the Ubiquitin-Dependent Degrading Activity of the 26S Proteasome. Endocrinology, 141.

Benuck, M., Schwartz, M. B., DeGuzman, T. and Lajtha, A. (1996) Changes in Brain Protease Activity in Aging. Journal of Neurochemistry, 67, 2019-2029.

Bernstein, E., Caudy, A. A., Hammond, S. M. and Hannon, G. J. (2001) Role for a bidentate ribonuclease in the initiation step of RNA interference. Nature, 409, 363 -668.

Bi, G. Q., Morris, R. L., Liao, G., Alderton, J. M., Scholey, J. M. and Steinhardt, R. A. (1997) Kinesin- and Myosin-driven Steps of Vesicle Recruitment for Ca2+-regulated Exocytosis. The Journal of Cell Biology, 138.

Bickford, P. (1993) Motor learning deficits in aged rats are correlated with loss of cerebellar noradrenergic function. Brain Research, 620, 133-138.

Bodles, A. M. and Barger, S. W. (2004) Cytokines and the aging brain - what we don't know might help us. Trends in Neurosciences, 27, 621-626.

Boenisch, T., Farmilo, A. J., Stead, R. H., Key, M., Welcher, R., Harvey, R. and Atwood, K. N. (2001) Immunochemical Staining Methods, DakoCytomation.

Bonner, T. I., Buckley, N. J., Young, A. C. and Brann, M. R. (1987) Identification of a family of muscarinic acetycholine receptor genes. Science, 237, 527 - 531.

Bourne, Y., Talley, T. T., Hansen, S. B., Taylor, P. and Marchot, P. (2005) Crystal structure of a Cbtx-AChBP complex reveals essential interactions between snake [alpha]-neurotoxins and nicotinic receptors. European Molecular Biology Organisation Journal, 24, 1512-1522.

Brull, R. K., Koudinov, A. R. and Degani, H. (2002) Choline in the aging brain. Brain Research, 951, 158-165.

Calvanese, V., Lara, E., Kahn, A. and Fraga, M. F. (2009) The role of epigenetics in aging and age-related diseases. Ageing Research Reviews, 8, 268-276.

Carmell, M. A. and Hannon, G. J. (2004) RNase III enzymes and the initiation of gene silencing. Nature Structural and Molecular Biology, 11, 214-218.

Carrette, O., Burkhard, P. R., Hochstrasser, D. F. and Sanchez, J. C. (2006) Age-related proteome analysis of the mouse brain:
a 2-DE study. PROTEOMICS, 6, 4940 - 4949.

Celie, P. H. N., Klaassen, R. V., van Rossum-Fikkert, S. E., van Elk, R., van Nierop, P., Smit, A. B. and Sixma, T. K. (2005) Crystal Structure of Acetylcholine-binding Protein from Bulinus truncatus Reveals the Conserved Structural Scaffold and Sites of Variation in Nicotinic Acetylcholine Receptors. THE JOURNAL OF BIOLOGICAL CHEMISTRY 280, 26457-26466.

Cerutti, K., Mian, N. and Bateman, A. (2000) Domains in gene silencing and cell differentiation proteins: the novel PAZ domain and redefinition of the Piwi domain. Trends in Biochemical Sciences, 25, 481-482.

Chalfie, M. (1995) GREEN FLUORESCENT PROTEIN. Photochemistry and Photobiology, 62, 651-656.

Chang, J., Van Remmen, H., Cornell, J., Richardson, A. and Ward, W. F. (2003) Comparative proteomics: characterization of a two-dimensional gel

electrophoresis system to study the effect of aging on mitochondrial proteins. Mechanisms of Ageing and Development, 124, 33-41.

Charpantier, E., Besnard, F., Graham, D. and F., S. (1999) Diminution of nicotinic receptor alpha 3 subunit mRNA expression in aged rat brain. Developmental Brain Research, 118, 153-158.

Chen, W., Ji, J., Xu, X., He, S. and Ru, B. (2003) Proteomic comparison between human young and old brains by two-dimensional gel electrophoresis and identification of proteins. International Journal of Developmental Neuroscience, 21, 209-216.

Cheng, T. F., Brzostek, S., Ando, O., Van, S. S., Kumar, K. P. and Reich, N. C. (2006) Differential Activation of IFN Regulatory Factor (IRF)-3 and IRF-5 Transcription Factors during Viral Infection. The Journal of Immunology, 176, 7462-7470.

Chung, H. Y., Cesari, M., Anton, S., Marzetti, E., Giovannini, S., Seo, A. Y., Carter, C., Yu, B. P. and Leeuwenburgh, C. (2009) Molecular inflammation: Underpinnings of aging and age-related diseases. Ageing Research Reviews 8, 18-30.

Chung, H. Y., Kim, H. J., Kim, J. W. and Yu, B. P. (2001) The inflammation hypothesis of aging: molecular modulation by calorie restriction. Annals of the New York Academy of Sciences, 928, 327-335.

Coppe, J. P., Kauser, K., Campisi, J. and Beausejour, C. M. (2006) Secretion of vascular endothelial growth factor by primary human fibroblasts at senescence. Journal of Biological Chemistry, 281, 29568-29574.

Court, J. A., Lloyd, S., Johnson, M., Griffiths, M., Birdsall, N. J. M., Piggott, M. A., Oakley, A. E., Ince, P. G., Perry, E. K. and Perry, R. H. (1997) Nicotinic and muscarinic cholinergic receptor binding in the human hippocampal formation during development and aging. Developmental Brain Research, 101, 93-105.

Cowen, T. (2002) Selective vulnerability in adult and ageing mammalian neurons. Autonomic neuroscience : basic & clinical, 96, 20-24.

Dekker, N. H., Abels, J. A., Veenhuizen, P. T. M., Bruinink, M. M. and Dekker, C. (2004) Joining of long double-stranded RNA molecules through controlled overhangs. Nucleic Acids Research, 32, 1-8.

dos Santosa, P. C., Gottfried, C., Gehlen, G. n., Goncalves¸Carlos-Alberto and Achaval, M. (2005) Distribution and ontogeny of glial fibrillary acidic protein

in the snail Megalobulimus abbreviatus. Comparative Biochemistry and Physiology, 141, 140-145.

Duchen, M. R. (2000) Mitochondria and calcium: from cell signalling to cell death. Journal of Physiology, 529, 57-68.

Eckenstein, F. and Thoenen, H. (1982) Production of specific antisera and monoclonal antibodies to choline acetyltransferase: characterization and use for identification of cholinergic neurons. The EMBO Joumal, 1, 363 - 368.

Eglen, R. M., Choppin, A. and Watson, N. (2001) Therapeutic opportunities from muscarinic receptor research. . Trends in Pharmacological Sciences, 22, , 409-414

Elbashir, S. M., Martinez, J., Patkaniowska, A., Lendeckel, W. and Tuschl, T. (2001) Functional anatomy of siRNAs for mediating efficient RNAi in Drosophila melanogaster embryo lysate. European Molecular Biology Organisation Journal, 20, 6877-6888.

Elliott, C. J. H. and Andrew, T. (1991) Temporal Analysis of snail feeding rhythms: A three-phase relaxation oscillator. Journal of Experimental Biology, 157.

Elliott, C. J. H., Stow, R. A. and Hastwell, C. (1992) Cholinergic interneurons in the feeding system of the pond snail Lymnaea stagnalis. I.Cholinergic receptors on feeding neurons. Philosophical Transactions of the Royal Society of London series B Biology, 336, 157 - 166.

Elliott, C. J. H. and Susswein, A. J. (2002) Comparative neuroethology of feeding control in molluscs. The Journal of Experimental Biology 205, 877 - 896.

Evans, R. J., Wyllie, F. S., Wynford-Thomas, D., Kipling, D. and Jones, C. J. (2003) A P53-dependent, Telomere-independent Proliferative Life Span Barrier in Human Astrocytes Consistent with the Molecular Genetics of Glioma Development. Cancer Research, 63, 4854-4861.

Farooqui, T. and Akhlaq, A. (2009) Aging: An important factor for the pathogenesis of neurodegenerative diseases. Mechanisms of Ageing and Development, 130, 203-215.

Fei, G., Guo, C., Sun, H. S. and Feng, Z. P. (2007) Chronic hypoxia stress-induced differential modulation of heat-shock protein 70 and presynaptic proteins. Journal of Neurochemistry, 100, 50-61.

Finch, C. E. (2003) Neurons, glia, and plasticity in normal brain aging. Neurobiology of Aging, 24, 123-127.

Finkel, T. and Holbrook, N. J. (2000) Oxidants, oxidative stress and the biology of ageing. Nature, 408, 239.

Fire, A., Xu, S., Montgomery, M. K., Kostas, S. A., Driver, S. E. and Mello, C. C. (1998) Potent and specific genetic interference by double-stranded RNA in Caenorhabditis elegans. Nature, 391, 806 - 811.

Fischer, W., Chen, K. S., Gage, F. H. and Björklund, A. (1992) Progressive decline in spatial learning and integrity of forebrain cholinergic neurons in rats during aging. Neurobiology of Aging

13, 9-23.

Flanary, B. E. and Streit, W. J. (2004) Progressive telomere shortening occurs in cultured rat microglia, but not astrocytes. Glia, 45, 75-88.

Fountoulakis, M., Hardmaier, R., Schuller, E. and Lubec, G. (2000) Differences in protein level between neonatal and adult brain. Electrophoresis, 21, 673-678.

Frade, J. M. and Barde, Y. A. (1998) Nerve growth factor: two receptors, multiple functions. BioEssays, 20, 137-145.

Freeman, W. M., Walker, S. J. and Vrana, K. E. (1999) Quantitative RT-PCR: pitfalls and potential. Biotechniques, 26, 112-122.

Friedman, W. J. and Greene, L. A. (1999) Neurotrophin Signaling via Trks and p75. Experimental Cell Research, 253, 131-142.

Frolkis, V. V., Martynenko, O. A. and Timchenko, A. N. (1991) Potential-dependent Ca Channels of neurons in the mollusc Lymnaea stagnalis in aging: Effect of norepinephrine. Mechanisms of Ageing and Development, 58, 75-83.

Frolkis, V. V., Stupina, A. S., Martinenko, O. A., Tòth, S. and Timchenko, A. I. (1984) Aging of neurons in the mollusc Lymnaea stagnalis. Structure, function and sensitivity to transmitters. Mechanisms of Ageing and Development, 25, 91-102.

Fukunaga, R. and Doudna, J. A. (2009) dsRNA with 5[prime] overhangs contributes to endogenous and antiviral RNA silencing pathways in plants. The EMBO Journal, 28, 545-555.

Gall, C. M., . and Isackson, P. J. (1989) Limbic seizures increase neuronal production of messenger RNA for nerve growth factor. Science, 245, 758-761.

Galvin, J. E. and Ginsberg, S. D. (2005) Expression profiling in the aging brain: A perspective. Ageing Research Reviews, 4, 529-547.

Gardiner, J., Barton, D., Overall, R. and Marc, J. (2009) Neurotrophic Support and Oxidative Stress: Converging Effects in the Normal and Diseased Nervous System. Neuroscientist, 15, 47-61.

Geiss, G., Jin, G., Guo, J., Bumgarner, R., Katze, M. G. and Sen, G. C. (2001) A Comprehensive View of Regulation of Gene Expression by Double-stranded RNA-mediated Cell Signaling. journal of Biological Chemistry, 276, 30178-30182.

Gems, D. and Partridge, L. (2001) Insulin/IGF signalling and ageing: seeing the bigger picture. Current Opinion in Genetics & Development, 11, 287-292.

Giacobini, E. (1990) Cholinergic Receptors in Human Brain: Effects of Aging and Alzheimer Disease. Journal of Neuroscience, 27, 548-560.

Giniatullin, R., Nistri, A. and Yake, J. L. (2005) Desensitization of nicotinic ACh receptors: shaping cholinergic signaling. Trends in Neurosciences, 28, 371-378.

Glanzer, J. G., Enose, Y., Wang, T., Kadiu, I., Gong, N., Rozek, W., Liu, J., Schlautman, J. D., Ciborowski, P. S., Thomas, M. P. and Gendelman, H. E. (2007) Genomic and proteomic microglial profiling: pathways for neuroprotective inflammatory responses following nerve fragment clearance and activation. Journal of Neurochemistry, 102, 627-645.

Gorgoulis, V. G., Pratsinis, H., Zacharatos, P., Demoliou, C., Sigala, F., Asimacopoulos, P. J., Papavassiliou, A. G. and Kletsas, D. (2005) p53-Dependent ICAM-1 overexpression in senescent human cells identified in atherosclerotic lesions. Laboratory Investigation, 85, 502-511.

Gotti, C. and Clementi, F. (2004) Neuronal nicotinic receptors: from structure to pathology. Progress in Neurobiology, 74, 363–396.

Gourlay, C. W. and Ayscough, K. R. (2005) The actin cytoskeleton: a key regulator of apoptosis and ageing? Nature Reviews. Molecular Cell Biology, 6, 583.

Green, W. N. (1999) Ion Channel Assembly: Creating Structures that Function. journal of General Physiology, 113 163-169.

Gustilo, M. C., Markowska, A. L., Breckler, S. J., Fleischman, C. A., Price, D. L. and Koliatsos, V. E. (1999) Evidence that nerve growth factor influences recent memory through structural changes in septohippocampal cholinergic neurons. The Journal of Comparative Neurology, 405, 491-507.

Hahn, W. C. (2001) Telomerase and Cancer: Where and When? Clinical Cancer Research, 7, 2953-2954.

Hansen, B. C., Bodkin, N. L. and Ortmeyer, H. K. (1999) Calorie-restriction in non-human primate: Mechanisms of reduced morbidity and mortality. Toxicological Science 56 (supplement), 56-60.

Hansen, S. B., Sulzenbacher, G., Huxford, T., Marchot, P., Taylor, P. and Bourne, Y. (2005) Structures of Aplysia AChBP complexes with nicotinic agonists and antagonists reveal distinctive binding interfaces and conformations. The EMBO Journal 24, 3635-3646.

Hansen, S. B., Talley, T. T., Radic, Z. and Taylor, P. (2004) Structural and Ligand Recognition Characteristics of an Acetylcholine-binding Protein from Aplysia californica. THE JOURNAL OF BIOLOGICAL CHEMISTRY, 279, 24197-24202.

Harley, C. B., Futcher, A. B. and Greider, C. W. (1990) Telomeres shorten during ageing of human fibroblasts. Nature, 345, 458-460.

Harman, D. (1965) The Free Radical Theory of Aging: Effect of Age on Serum Copper Levels. Journal of Gerontology 20, 151-153.

Hayflick, L. (1965) The limited in vitro lifetime of human diploid cell strains. Experimental Cell Research, 37, 614 - 636.

Heale, B. S. E., Soifer, H. S., Bowers, C. and Rossi, J. J. (2005) siRNA target site secondary structure predictions using local stable substructures. Nucleic Acids Research, 33, 1-10.

Heidel, J. D., Hu, S., Liu, X. F., Triche, T. J. and Davis, M. E. (2004) Lack of interferon response in animals to naked siRNAs. Nature Biotechnology, 22, 1579(1574).

Hekimi, S., Lakowski, B., Barnes, T. M. and Ewbank, J. J. (1998) Molecular genetics of life span in C. elegans: How much does it teach us? Trends in Genetics, 14, 14-20.

Hemann, M. T., Strong, M. A., Hao, L. Y. and Greider, C. W. (2001) The Shortest Telomere, Not Average Telomere Length, Is Critical for Cell Viability and Chromosome Stability. Cell, 107, 67-77.

Hu, D., Cao, P., Thiels, E., Chu, C. T., Wu, G. Y., Oury, T. D. and Klann, E. (2007) Hippocampal long-term potentiation, memory, and longevity in mice that overexpress mitochondrial superoxide dismutase. Neurobiology of Learning and Memory, 87, 372-384.

Hulme, E. C., Lu, Z. L., Saldanha, J. W. and Bee, M. S. (2003) Structure and activation of muscarinic acetylcholine receptors. Biochemical Society Transactions, 31, 29 - 35.

Huschtscha, L. I. and Reddel, R. R. (1999) p16INK4a and the control of cellular proliferative life span. Carcinogenesis, 20, 921-926.

Inoue, T., Hirata, K., Kuwana, Y., Fujita, M., Miwa, J., Roy, R. and Yamaguchi, Y. (2006) Cell cycle control by daf-21/Hsp90 at the first meiotic prophase/metaphase boundary during oogenesis in Caenorhabditis elegans. Development, Growth and Differentiation, 48, 25-32.

Inoue T, H. K., Kuwana Y, Fujita M, Miwa J, Roy R, Yamaguchi Y (2006) Cell cycle control by daf-21/Hsp90 at the first meiotic prophase/metaphase boundary during oogenesis in Caenorhabditis elegans. Development, Growth and Differentiation, 48, 25-32.

Jackson, A. L., Bartz, S. R., Schelter, J., Kobayashi, S. V., Burchard, J., Mao, M., Li, B., Cavet, G. and Linsley, P. S. (2003) Expression profiling reveals off-target gene regulation by RNAi. Nature Biotechnology, 21, 635(633).

Jacobs, B. L. and Langland, J. O. (1996) When Two Strands Are Better Than One: The Mediators and Modulators of the Cellular Responses to Double-Stranded RNA. Virology, 219, 339-349.

Jacobs, B. L., Langland, J. O. and Brandt, T. (1998) Characterization of Viral Double-Stranded RNA-Binding Proteins. Methods, 15, 225-232.

Joose, J. (1964) DORSAL BODIES AND DORSAL NEUROSECRETORY CELLS OF THE CEREBRAL GANGLIA OF LYMNAEA STAGNALIS. Archives Neerlandaise de Zoologie, 16, 1-103.

Joseph, J. A. (1992) The putative role of free radicals in the loss of neuronal functioning in senescence. Integrative physiological and behavioral science, 27, 216-227.

Kahle, P. J. and Haass, C. (2004) How does parkin ligate ubiquitin to Parkinson's disease? EMBO reports 5, 681 - 685.

Kaji, V. T., Boland, B., Odrljin, T., Mohan, P., Basavarajappa, B. S., Peterhoff, C., Cataldo, A., Rudnicki, A., Amin, N., Li, B. S., Pant, H. C., Hungund, B. L.,

Arancio, O. and Nixon, R. A. (2004) Calpain Mediates Calcium-Induced Activation of the Erk1,2 MAPK Pathway and Cytoskeletal Phosphorylation in Neurons: Relevance to Alzheimer's Disease. American journal of pathology, 165, 795-805.

Kamath, R. S., Fraser, A. G., Dong, Y., Poulin, G., Durbin, R., Gotta, M., Kanapin, A., Le Bot, N., Moreno, S., Sohrmann, M., Welchman, D. P., Zipperlen, P. and Ahringer, J. (2003) Systematic functional analysis of the Caenorhabditis elegans genome using RNAi. Nature, 421, 231-237.

Kapp, L. D. and Lorsch, J. R. (2004) THE MOLECULAR MECHANICS OF EUKARYOTIC TRANSLATION. Annual Review of Biochemistry, 73, 657.

Kar, A., Kuo, D., He, R., Zhou, J. and Wu, J. Y. (2005) Tau Alternative Splicing and Frontotemporal Dementia. Alzheimer's Disease association disorder, 19, 29-36.

Karlen, Y., McNair, A., Perseguers, S., Mazza, C. and Mermod, N. (2007) Statistical significance of quantitative PCR. Biomed Central Bioinformatics 8, 1-16.

Karlin, A. (2001) The Acetylcholine-binding protein: 'What's in a name?' The Pharmacogenomics Journal, 1, 221 - 228.

Karp, N. A. and Lilley, K. S. (2005) Maximising sensitivity for detecting changes in protein expression: Experimental design using minimal CyDyes. PROTEOMICS, 5, 3105-3115.

Kelly, K. M., Nadon, N. L., Morrison, J. H., Thibault, O., Barnes, C. A. and Blalock, E. M. (2006) The neurobiology of aging. Epilepsy Research, 68S, S5 - S20.

Kemenes, G. and Elliott, C. J. (1994) Analysis of the feeding motor pattern in the pond snail, Lymnaea stagnalis: photoinactivation of axonally stained pattern-generating interneurons. J. Neurosci., 14, 153-166.

Kemenes, G., Hiripi, L. and Benjamin, P. R. (1990) Behavioural and biochemical changes in the feeding system of Lymnaea induced by the dopamine and serotonin neurotoxins. Philosophical Transactions of the Royal Society of London Biological Sciences, 329, 243–255.

Kim, J. H., Park, S. M., Kang, M. R., Oh, S. Y., Lee, T. H., Muller, M. T. and Chung, I. K. (2005) Ubiquitin ligase MKRN1 modulates telomere length homeostasis through a proteolysis of hTERT. Genes & Development, 19, 776-781.

Kim, T.-S., Jang, C.-Y., Kim, H. D., Lee, J. Y., Ahn, B.-Y. and Kim, J. (2006) Interaction of Hsp90 with Ribosomal Proteins Protects from Ubiquitination and Proteasome-dependent Degradation. Molecular Biology of the Cell, 17, 824-833.

Kirkwood, T. B. L. (1977) Evolution of ageing. Nature 270, 301 - 304.

Kirschner, P. B., Jenkins, B. G., Schulz, J. B., Finkelstein, S. P., Matthews, R. T., Rosen, B. R. and Beal, M. F. (1996) NGF, BDNF and NT-5, but not NT-3 protect against MPP+ toxicity and oxidative stress in neonatal animals. Brain Research, 713, 178-185.

Klaassen, L. J., Janse, C. and van der Roest, M. (1998) Multiple synaptic connections of a single neuron change differentially with age. Neurobiology of Aging, 19, 341-349.

Klein, R. L., Hirko, A. C., Meyers, C. A., Grimes, J. R., Muzyczka, N. M. and Edwin, M. M. (2000) NGF gene transfer to intrinsic basal forebrain neurons increases cholinergic cell size and protects from age-related, spatial memory deficits in middle-aged rats. Brain Research, 875, 144-151.

Korneev, S. A., Kemenes, I., Straub, V., Staras, K., E.I., K., Kemenes, G., Benjamin, P. R. and M., O. S. (2002) Suppression of Nitric Oxide (NO)-Dependent

Behavior by Double-Stranded RNA-Mediated Silencing of a Neuronal NO Synthase Gene. The Journal of Neuroscience, 22, 1-5.

Korsloot, A., van Gestel, C. A. M. and van Straalen, N. M. (2004) Environmental Stress and Cellular Response in Arthropods CRC Press.

Kourie, J. I. (1998) Interaction of reactive oxygen species with ion transport mechanisms. American journal of physiology, 275, 1 - 24.

Kruatrachue, M., Thongkukiatkul, A., Sobhon, P., Upatham, E. S., Wanichanon, C., Sretarugsa, P., Chitramvong, Y. and Linthong, V. (1999) The Ultrastructure of Neurons and Neuroglia in the Cerebral and Pleuro-Pedal Ganglia of Haliotis asinina Linnaeus. Science Asia, 25, 137 - 142.

Krulko, I., Ustyanenko, D. and Polischuk, V. (2009) Role of siRNAs and miRNAs in the Processes of RNA-Mediated Gene Silencing during Viral Infections. Cytology and Genetics, 43, 63-72.

Kumar, M., Gupta, G. P. and Rajam, M. V. (2009) Silencing of acetylcholinesterase gene of Helicoverpa armigera by siRNA affects larval growth and its life cycle. Journal of Insect Physiology, 55, 273–278.

Kyriakedes, M. A. and McCrohan, C. R. (1989) Effect of Putative Neuromodulators on Rhythmic Buccal Motor Output in Lymnaea stagnalis. Journal of Neurobiology, 20, 635 - 650.

Landfield, P. W. and Pitler, T. A. (1984) Prolonged Ca2+-dependent afterhyperpolarizations in hippocampal neurons of aged rats Science, 226, 1089-1092.

Langmead, C. J., Watson, J. and Reavilla, C. (2007) Muscarinic acetylcholine receptors as CNS drug targets Pharmacology & Therapeutics in press.

Lee C.K, W. R., Prolla T.A (2000) Gene-expression profile of the ageing brain in mice. Nature Genetics, 25, 294 - 297.

Lee, C. K., Weindruch, R. and Prolla, T. A. (2000) Gene-expression profile of the ageing brain in mice. Nature Genetics, 25, 294 - 297.

Lewin, G. R. and Barde, Y. A. (1996) Physiology of the Neurotrophins. Annual Review of Neuroscience, 19, 289.

Li, L. C., Okino, S. T., Zhao, H., Pookot, D., Place, R. F., Urakami, S., Enokida, H. and Dahiya, R. (2006) Small dsRNAs induce transcriptional activation in human cells. Proceedings of the National Academy of Science USA, 103, 17337–17342.

Li, W., Gao, B., Lee, S. M., Bennett, K. and Fang, D. (2007) RLE-1, an E3 Ubiquitin Ligase, Regulates C. elegans Aging by Catalyzing DAF-16 Polyubiquitination. Developmental Cell, 12, 235-246.

Liles, W. C. and Nathanson, N. M. (1987) Regulation of Muscarinic Acetylcholine Receptor Number in Cultured Neuronal Cells by Chronic Membrane Depolarization. The Journal of Neuroscience, 7, 2556-2563.

Lin, B., Rommens, J. M., Graham, R. K., Kalchman, M., MacDonald, H., Nasir, J., Delaney, A., Goldberg, Y. P. and Hayden, M. R. (1993) Differential 3' polyadenylation of the Huntington disease gene results in two mRNA species with variable tissue expression. Human Molecular Genetics, 2, 1541-1545.

Lin, K., Hsin, H., Libina, N. and Kenyon, C. (2001) Regulation of the Caenorhabditis elegans longevity protein DAF-16 by insulin/IGF-1 and germline signaling. Nature Genetics, 29, 139-145.

Lin, X., Ruan, X., Anderson, M. G., McDowell, J. A., Kroeger, P. E., Fesik, S. W. and Shen, Y. (2005) siRNA-mediated off-target gene silencing triggered by a 7 nt complementation. Nucleic Acids Research, 33, 4527-4535.

Linnane, A. W., Zhang, C., Baumer, A. and Nagley, P. (1992) Mitochondrial DNA mutation and the ageing process: bioenergy and pharmacological intervention. Mutation Research, 275, 195-208.

Liu, H., Zheng, F., Cao, Q., Ren, B., Zhu, L., Striker, G. and Vlassara, H. (2006) Amelioration of oxidant stress by the defensin lysozyme. Am J Physiol Endocrinol Metab, 290, E824-832.

Liu, J., Carmell, M. A., Rivas, F. V. and Marsden, C. G. (2004) Argonaute2 Is the Catalytic Engine of Mammalian RNAi. Science, 305, 1437.

Livak, K. J. and Schmittgen, T. D. (2001) Analysis of Relative Gene Expression Data Using Real-Time Quantitative PCR and the 2DeltaDeltaCT Method. Methods, 25, 402-408.

Lopez, J. C. (2001) Crystal-clear glia neuron interactions. Nature Reviews Neuroscience, 2, 380.

Ma, B., Zhang, K., Hendrie, C., Liang, C., Li, M., Kirby, A. D. and Lajoie, G. (2003) PEAKS: Powerful Software for Peptide De Novo Sequencing by MS/MS. Rapid Communications in Mass Spectrometry, 17, 2337-2342.

Martin, B., Mattson, M. P. and Maudsley, S. (2006) Caloric restriction and intermittent fasting: Two potential diets for successful brain aging. Ageing Research Reviews 5, 332 - 353.

Martinez, J., Patkaniowska, A., Urlaub, H., Lührmann, R. and Tuschl, T. (2002) Single-Stranded Antisense siRNAs Guide Target RNA Cleavage in RNAi. Cell, 110, 563-574.

Martnez, L. E., Siles, E., Hernandez, R., Canuelo, A. R., Luisa del Moral, M., Jimenez, A., Blanco, S., Lopez-Ramos, J. C., Esteban, F. J., Pedrosa, J. A. and Peinado, M. A. (2003) Glutathione S-transferase isoenzymatic response to aging in rat cerebral cortex and cerebellum Neurobiology of Aging, 24, 501 - 509.

Mattson, M. P. (2007) Calcium and neurodegeneration. Aging Cell, 6, 337 - 350.

Mattson, M. P. and Magnus, T. (2006) Ageing and neuronal vulnerability. Nature Reviews. Neuroscience, 7, 278 - 294.

Medawar, P. B. (1952) An Unsolved Problem of Biology, London.

Meier, C. A. (1995) Advances in the understanding of the molecular basis of obesity. European Journal of Endocrinology, 133, 761-763.

Melov, S. (2002) Animal models of oxidative stress, aging, and therapeutic antioxidant interventions. The International Journal of Biochemistry & Cell Biology 34 1395–1400.

Merrick, W. C. (1992) Mechanism and regulation of eukaryotic protein synthesis. Microbiology and Molecular Biology Reviews, 56, 291-315.

Meshorer, E. and Soreq, H. (2002) Pre-mRNA splicing modulations in senescence. Aging Cell, 1, 10-16.

Michalek, H., Fortuna, S. and Pintor, A. (1989) Age-related differences in brain choline acetyltransferase, cholinesterases and muscarinic receptor sites in two strains of rats. Neurobiology of Aging, 10, 143-148.

Miller, K. E. and Joshi, H. C. (1996) Tubulin Transport in Neurons. The Journal of Cell Biology, 133, 1355 - 1366.

Minamino, T., Miyauchi, H., Yoshida, T., Ishida, Y., Yoshida, H. and Komuro, I. (2002) Endothelial Cell Senescence in Human Atherosclerosis: Role of Telomere in Endothelial Dysfunction. Circulation, 105, 1541-1544.

Minamino, T., Yoshida, T., Tateno, K., Miyauchi, H., Zou, Y., Toko, H. and Komuro, I. (2003) Ras Induces Vascular Smooth Muscle Cell Senescence and Inflammation in Human Atherosclerosis. Circulation, 108, 2264-2269.

Mitsui, A., Hamuro, J., Nakamura, H., Kondo, N., Hirabayashi, Y., Ishizaki-Koizumi, S., Hirakawa, T., Inoue, T. and Yodoi, J. (2002) Overexpression of Human Thioredoxin in Transgenic Mice Controls Oxidative Stress and Life Span. Antioxidants & Redox Signaling, 4, 693-696.

Montgomery, M. K., Xu, S. and Fire, A. (1998) RNA as a target of double-stranded RNA-mediated genetic interference in Caenorhabditis elegans. Proceedings of the National Academy of Science USA, 95, 15502–15507.

Murchison, D. and Griffith, W. H. (2007) Calcium buffering systems and calcium signaling in aged rat basal forebrain neurons. Aging Cell, 6, 297–305.

Nalepa, G., Rolfe, M. and Harper, W. J. (2006) Drug discovery in the ubiquitin-proteasome system. Nat Rev Drug Discov, 5, 596-613.

Nardai, G., Csermely, P. and Söti, C. (2002) Chaperone function and chaperone overload in the aged. A preliminary analysis. Experimental Gerontology, 37, 1257-1262.

Nichols, N. R., Day, J. R., Laping, N. J., Johnson, S. A. and Finch, C. E. (1993) GFAP mRNA increases with age in rat and human brain Neurobiology of Aging, 14, 421-429

Nierop, P. V., Bertrandm, S., Munno, D. W., Gouwenberg, Y., Minnen, J. V., Spafford, J. D., Syed, N. I., Bertrand, D. and Smit, A. B. (2006) Identification and Functional Expression of a Family of Nicotinic Acetylcholine Receptor Subunits in the Central Nervous System of the Mollusc Lymnaea stagnalis. Journal of Biological Chemistry, 281, 1680-1692.

Nierop, P. V., Keramidas, A., Bertrand, S., Minnen, J. V., Gouwenberg, Y., Bertrand, D. and Smit, A. B. (2005) Identification of Molluscan Nicotinic Acetylcholine Receptor (nAChr) subunits involved in Formation of Cation- and Anion selective nAChRs. The Journal of Neuroscience, 25, 10617 - 10626.

Nikitin, E. S., Kiss, T., Staras, K., O'Shea, M., Benjamin, P. R. and Kemenes, G. (2006) Persistent Sodium Current Is a Target for cAMP-Induced Neuronal Plasticity in a State-Setting Modulatory Interneuron. J Neurophysiol, 95, 453-463.

Nordberg, A., Alafuzoff, I. and Winblad, B. (1992) Nicotinic and Muscarinic Subtypes in the Human Brain: Changes With Aging and Dementia. Journal of Neuroscience Research 31, 103-111

Novere, L. N., Grutter, T. and Changeux, J. P. (2002) Models of the extracellular domain of the nicotinic receptors and of agonist- and Ca2┌ -binding sites. Proceedings of the National Academy of Science USA, 99, 3210–3215.

O'Neill, M. J., Murray, T. K., Lakics, V., Visanji, N. P. and Duty, S. (2002) The role of neuronal nicotinic acetylcholine receptors in acute and chronic neurodegeneration. Current Drug Targets - CNS and Neurological Disorders, 1, 399-411.

Office for National Statistics (2007) Focus on Older People.

Paradis, S. and Ruvkun, G. (1998) Caenorhabditis elegans Akt/PKB transduces insulin receptor-like signals from AGE-1 PI3 kinase to the DAF-16 transcription factor. Genes & Development, 12, 2488-2498.

Pasquali, C., Fialka, I. and Huber, L. A. (1997) Preparative two-dimensional gel electrophoresis of membrane proteins. Electrophoresis 8.

Patel, B. A., Arundell, M., Allen, M. C., Gard, P., O'Hare, D., Parker, K. and Yeoman, M. S. (2006) Changes in the properties of the modulatory cerebral giant cells contribute to aging in the feeding system of Lymnaea. Neurobiology of Aging, 27, 1892 - 1902.

Patel, B. A., Arundell, M., Parker, K. H., Yeoman, M. S. and O'Hare, D. (2005) Decreases in the serotonin content of a pair of identified neurones can explain the effect of p-chlorophenylanaline on the feeding behaviour of the pond snail, Lymnaea stagnalis. Current Separations, 21, 53-58.

Pepeu, G. (2001) Overview and perspective on the therapy of alzheimer's disease from a preclinical viewpoint Progress in Neuro-Pschopharacology and Biological Psychiatry, 25, 193-209.

Peretz, B., Romanenko, A. and Markesbery, W. (1984) Functional history of two motor neurons and the morphometry of their neuromuscular junctions in the gill of Aplysia: Evidence for differential aging. Proceedings of the National Academy of Science USA, 81, 4232-4236.

Perlson, E., Medzihradsky, K. F., Darulas, Z., Munno, D. W., Syed, N. I., Burlingame, A. L. and Fainzilber, M. (2004) Differential proteomics reveals multiple components in retrogradely transported axoplasm after nerve injury. Molecular and Cellular Proteomics, 3, 510 - 520.

Pertusa, M., Garcı´a-Matas, S., Rodrı´guez-Farre´, E., Sanfeliu, C. and Cristo`fol, R. (2007) Astrocytes aged in vitro show a decreased neuroprotective capacity. Journal of Neurochemistry, 101, 794–805.

Pfaffl, M. W. (2001) Gene Expression Omnibus database

A new mathematical model for relative quantification in real-time RT-PCR. Nucleic Acids Res, 29, e45.

Pickart, C. M. (2004) Back to the Future with Ubiquitin. 116, 181-190.

Pinkston-Gosse, J. and Kenyon, C. (2007) DAF-16/FOXO targets genes that regulate tumor growth in Caenorhabditis elegans. Nat Genet, 39, 1403-1409.

Poon, H. F., Vaishnav, R. A., Getchell, T. V., Getchell, M. L. and Butterfield, D. A. (2006) Quantitative proteomics analysis of differential protein expression and oxidative modification of specific proteins in the brains of old mice. Neurobiology of Aging, 27, 1010-1019.

Prolla, T. A. (2002) DNA Microarray Analysis of the Aging Brain. Chemical Senses, 27, 299-306.

Proud, C. G. (2004) mTOR-mediated regulation of translation factors by amino acids. Biochemical and Biophysical Research Communications, 313, 429-436.

Rattan, S. I. S. (1996) Synthesis, modifications, and turnover of proteins during aging. Experimental Gerontology, 31, 33-47.

Rebrin, I. and Sohal, R. S. (2008) Pro-oxidant shift in glutathione redox state during aging. Advanced Drug Delivery Reviews, 60, 1545-1552.

Reddy, S. R. R., Houmeida, A., Benyamin, Y. and Roustan, C. (1992) Interaction in vitro of scallop muscle arginine kinase with filamentous actin. European Journal of Biochemistry, 206, 251-257.

Reynolds, A., Leake, D., Boese, Q., Scaringe, S., Marshall, W. S. and Khvorova, A. (2004) siRNA design tool: Rational siRNA design for RNA interference. Nature Biotechnology, 22, 326 - 330.

Ririe, K. M., Rasmussen, R. P. and Wittwer, C. T. (1997) Product differentiation by analysis of DNA melting curves during the polymerase chain reaction. Analytical Biochemistry, 245, 154-160.

Robinson, L. J., Karlsson, N. G., Weiss, A. S. and Packer, N. H. (2003) Proteomic Analysis of the Genetic Premature Aging Disease Hutchinson Gilford Progeria Syndrome Reveals Differential Protein Expression and Glycosylation. Journal of Proteome Research, 2, 556-557.

Rose, R. M. and Benjamin, P. R. (1981) Interneuronal control of feeding in the pond snail Lymnaea stagnalis. Journal of Experimental Biology, 92, 187 - 201.

Sanchez, C., Lachaize, C., Janody, F., Bellon, B., Roder, L., Euzenat, J., Rechenmann, F. and Jacq, B. (1999) Grasping at molecular interactions and genetic networks in Drosophila melanogaster using FlyNets, an Internet database. Nucleic Acids Research, 27, 89-94.

Sato, Y., Yamanaka, H., Toda, T., Shinohara, Y. and Endo, T. (2005) Comparison of hippocampal synaptosome proteins in young-adult and aged rats. Neuroscience Letters, 382, 22-26.

Schapira, A. H., Mann, V. M., Cooper, J. M., Krige, D., Jenner, P. J. and Marsden, C. D. (1992) Mitochondrial function in Parkinson's disease. The Royal Kings and Queens Parkinson's Disease Research Group. Annals of Neurology, 32, 116-124.

Scherder, E., Dekker, W. and Eggermont, L. (2008) Higher-Level Hand Motor Function in Aging and (Preclinical) Dementia: Its Relationship with (Instrumental) Activities of Daily Life -- A Mini-Review. Gerontology, 54, 333-341.

Schipper, H. M. (2004) Brain iron deposition and the free radical-mitochondrial theory of ageing. Ageing Research Reviews, 3, 265-301.

Shaffer, W. (2006) Neurophysiological methods in C. elegans: an introduction. http://www.wormbook.org/chapters/www_intromethodsneurophys/intromethodsneurophys.html.

Shay, J. W., Pereira-Smith, O. M. and Wright, W. E. (1991) A role for both RB and p53 in the regulation of human cellular senescence. Experimental Cell Research, 196, 33-39

Shimohama, S. (2009) Nicotinic Receptor-Mediated Neuroprotection in Neurodegenerative Disease Models. Biological and Pharmaceutical Bulletin 32, 332 - 336

Shimokawa, I., Chiba, T., Yamaza, H. and Komatsu, T. (2008) Longevity Genes: Insights from Calorie Restriction and Genetic Longevity Models. Molecules and Cells, 26, 427-435.

Shimokawa, I. and Higami, Y. (2001) Leptin signaling and aging: insight from caloric restriction. Mechanisms of Ageing and Development, 122, 1511-1519.

Sijen, T., Fleenor, J., Simmer, F., Thijssen, K. L., Parrish, S., Timmons, L., Plasterk, R. H. A. and Fire, A. (2001) On the Role of RNA Amplification in dsRNA-Triggered Gene Silencing. Cell, 107, 465-476.

Sixma, T. K. and Smit, A. B. (2003) Acetylcholine binding protein (Achbp): A secreted glial protein that provides a high resolution model for the extracellular domain of pentameric ligand gated ion channel. Annual Review of Biophysics and Biomolecular Structure, 32, 311 - 334.

Smit, B. A., Brejc, K., Syed, N. and Sixma, T. K. (2003) Structure and function of AChBP, homologue of the ligand-binding domain of the nicotinic acetylcholine receptor. Annals of the New York Academy of Sciences, 998, 81-92.

Smit, B. A., Syed, N. I., Schaap, D., Minnen, J. N., Klumperman, J., Kits, K. S., Lodder, H., Van deSchors, R. C., Elk, R. V., Sorgedrager, B., Brejc, K., Sixma, T. K. and Geraets, W. P. M. (2001) A glia derived acetylcholine binding protein that modulates synaptic transmission. Nature 411, 261 - 268.

Snider, W. D., Zhou, F.-Q., Zhong, J. and Markus, A. (2002) Signaling the Pathway to Regeneration. Neuron, 35, 13-16.

Song, J.-J., Smith, S. K., Hannon, G. J. and Joshua-Tor, L. (2004) Crystal Structure of Argonaute and Its Implications for RISC Slicer Activity. Science, 305, 1434.

Sontheimer, E. J. (2005) Assembly and function of RNA silencing complexes. Nature Reviews. Molecular Cell Biology, 6, 127.

Soreq, H. and Seidman, S. (2001) Acetylcholinesterase — new roles for an old actor. Nature Reviews, 2, 8-17.

Söti, C. and Csermely, P. (2002) Chaperones and aging: role in neurodegeneration and in other civilizational diseases. Neurochemistry International, 41, 383-389.

Souazé, F., Ntodou-Thomé, A., Tran, C. Y., Rostène, W. and Forgez, P. (1996) Quantitative RT-PCR: limits and accuracy. 21, 2.

Spafford, D. J., Munno, D. W., van Nierop, P., Feng, Z. P., Jarvis, S. E., Gallin, W. J., Smit, A. B., Zamponi, G. W. and Syed, N. I. (2003) Calcium channel structural determinants of synaptic transmission between identified invertebrate neurons. Journal of Biological Chemistry, Vol. 278, 4258–4267.

Stanley, B. G., Kyrkouli, S. E., Lampert, S. and Leibowitz, S. F. (1986) Neuropeptide Y chronically injected into the hypothalamus: a powerful neurochemical inducer of hyperphagia and obesity. Peptides, 7, 1189-1192.

Stein, P., Svoboda, P., Anger, M. and Schultz, R. M. (2003) RNAi: Mammalian oocytes do it without RNA-dependent RNA polymerase. RNA, 9, 187-192.

Stenmark, P., Grunler, J., Mattsson, J., Sindelar, P. J., Nordlund, P. and Berthold, D. A. (2001) A New Member of the Family of Di-iron Carboxylate Proteins. Coq7 (clk-1), A MEMBRANE-BOUND HYDROXYLASE INVOLVED IN UBIQUINONE BIOSYNTHESIS. Journal of Biological Chemistry, 276, 33297-33300.

Stevens, B. and Fields, R. D. (2002) Regulation of the Cell Cycle in Normal and Pathological Glia. Neuroscientist, 8, 93-97.

Streit, W., Graeber, M. B. and Kreutzberg, G. W. (1989) Expression of Ia antigen on perivascular and microglial cells after sublethal and lethal motor neuron injury. Experimental Neurology, 105, 115-126.

Streit, W., Sammons, N., Kuhns, A. and Sparks, D. (2004) Dystrophic microglia in the aging human brain. Glia, 45, 208-212.

Streit, W. J. (2005) Microglia and neuroprotection: implications for Alzheimer's disease. Brain Research Reviews, 48, 234-239.

Sullivan, D., Chiara, D. C. and Cohen, J. B. (2002) Mapping the Agonist Binding Site of the Nicotinic Acetylcholine Receptor by Cysteine Scanning Mutagenesis: Antagonist Footprint and Secondary Structure Prediction. Molecular Pharmacology, 61, 463 - 472.

Sun, W., Pertzev, A. and Nicholson, A. W. (2005) Catalytic mechanism of Escherichia coli ribonuclease III: kinetic and inhibitor evidence for the involvement of two magnesium ions in RNA phosphodiester hydrolysis. Nucleic Acids Research, 33, 807-815.

Syntichaki, P., TROULINAKI, K. and TAVERNARAKIS, N. (2007) Protein Synthesis Is a Novel Determinant of Aging in Caenorhabditis elegans. Annals of the New York Academy of Sciences, 1119, 289-295.

Tavernarakis, N. (2008) Ageing and the regulation of protein synthesis: a balancing act? Trends in Cell Biology, 18, 228-235.

Terry, A. V. J. and Buccafusco, J. J. (2003) The Cholinergic Hypothesis of Age and Alzheimer’s Disease Related Cognitive Deficits: Recent Challenges and

Their Implications for Novel Drug Development. American Society for Pharmacology and Experimental Therapeutics, 306, 821-827.

Thibault, O., Gant, J. C. and Landfield, P. W. (2007) Expansion of the calcium hypothesis of brain aging and Alzheimer's disease: minding the store. Aging Cell, 6, 307–317.

Toescu, E. C. (2005) Normail brain ageing: models and mechanisms. Philosophical transactions of the royal society, 360, 2347-2354.

Tschuch, C., Schulz, A., Pscherer, A., Werft, W., Benner, A., Hotz-Wagenblatt, A., L., B., Lichter, P. and Mertens, D. (2008) Off-target effects of siRNA specific for GFP. BMC Molecular Biology, 9, 60.

Tsugita, A., Kawakami, T., Uchida, T., Sakai, T., Kamo, M., Matsui, T., Watanabe, Y., Morimasa, T., Hosokawa, K. and Toda, T. (2000) Proteome analysis of mouse brain: Two-dimensional electrophoresis profiles of tissue proteins during the course of aging. Electrophoresis, 21, 1853-1871.

Tuppo, H. E. and Arias, H. R. (2005) The role of inflammation in Alzheimer's disease. The International Journal of Biochemistry & Cell Biology, 37, 289-305.

Turrens, J. E. (1997) Superoxide production by the mitochondrial respiratory chain. Bioscience Reports, 13, 3-8.

Utsugisawa, K., Nagane, Y., Tohgi, H., Yoshimura, M., Ohba, H. and Genda, Y. (1999) Changes with aging and ischemia in nicotinic acetylcholine receptor subunit [alpha]7 mRNA expression in postmortem human frontal cortex and putamen. Neuroscience Letters, 270, 145-148.

van Diepen, M. T., Spencer, G. E., van Minnen, J., Gouwenberg, Y., Bouwman, J., Smit, A. B. and van Kesterena, R. E. (2005) The molluscan RING-finger protein L-TRIM is essential for neuronal outgrowth. Molecular and Cellular Neuroscience, 29, 74– 81.

van Kesteren, R. E., Carter, C., Dissel, H. M. G., van Minnen, J., Gouwenberg, Y., Syed, N. I., Spencer, G. E. and Smit, A. B. (2006) Local Synthesis of Actin-Binding Protein-Thymosin Regulates Neurite Outgrowth. The Journal of Neuroscience, 26, 152–157.

Vasto, S., Candore, G., Balistreri, C. R., Caruso, M., Colonna-Romano, G., Grimaldi, M. P., Listi, F., Nuzzo, D., Lio, D. and Caruso, C. (2007) Inflammatory networks in ageing, age-related diseases and longevity. Mechanisms of Ageing and Development, 128, 83-91.

Vierstraete, E., Verleyen, P., Baggerman, G., D'Hertog, W., Van den Bergh, G., Arckens, L., De Loof, A. and Schoofs, L. (2004) A proteomic approach for the analysis of instantly released wound and immune proteins in Drosophila melanogaster hemolymph. Proceedings of the National Academy of Sciences of the United States of America, 101, 470-475.

Warburg, O. and Christian, W. (1942) Isolation and crystalisation of enolase. Biochemische Zeitschrift, 310

384-421.

Wehrman, T., He, X., Raab, B., Dukipatti, A., Blau, H. and Garcia, K. C. (2007) Structural and Mechanistic Insights into Nerve Growth Factor Interactions with the TrkA and p75 Receptors. Neuron, 53, 25-38.

Weihe, E., Tao-Cheng, J. H., Schäfer, M. K., Erickson, J. D. and Eiden, L. E. (1996) Visualization of the vesicular acetylcholine transporter in cholinergic nerve terminals and its targeting to a specific population of small synaptic vesicles. Proceedings of the National Academy of Science USA, 93, 3547–3552.

White, J. G., Southgate, E., Thomson, J. N. and Brenner, S. (1986) The structure of the nervous system of the nematode Caenorhabditis elegans. Philosophical Transactions of the Royal Society of London series B Biology 314, 1-340.

Williams, G. C. (1957) Pleiotropy, natural selection, and the evolution of senescence. Evolution, 11, 398-411.

Wu, Y., Zhang, A. Q. and Yew, D. T. (2005) Age related changes of various markers of astrocytes in senescence-accelerated mice hippocampus. Neurochemistry International, 46, 565-574.

Wullschleger S, L. R., Hall M.N (2006) TOR Signaling in Growth and Metabolism. 124, 471-484.

Wyss, M. and Kaddurah-Daouk, R. (2000) Creatine and Creatinine Metabolism. Physiological Reviews, 80, 1107-1213.

Yamamura, H. I. and Snyder, S. H. (1972) Choline: High-Affinity Uptake by Rat Brain Synaptosomes. Science, 178, 626-628.

Yan, K. S., Yan, S., Farooq, A., Han, A., Zeng, L. and Zhou, M. M. (2003) Structure and conserved RNA binding of the PAZ domain. Nature, 426, 469-474.

Yang, S., Liu, T., Li, S., Zhang, X., Ding, Q., Que, H., Yan, X., Wei, K. and Liu, S. (2008) Comparative proteomic analysis of brains of naturally aging mice. Neuroscience, 154, 1107-1120.

Yeoman, M. S. and Faragher, R. G. A. (2001) Ageing and the nervous system:insights from studies on invertebrates. Biogerontology, 2, 85 - 97.

Yeoman, M. S., Parish, D. C. and Benjamin, P. R. (1993) A cholinergic modulatory interneuron in the feeding system of the snail, Lymnaea. Journal of Neurophysiology, 70, 37 - 50.

Yeoman, M. S., Patel, B. A., Arundell, M. and O'Hare, K. P. D. (2008) Synapse-specific changes in serotonin signalling contribute to age-related changes in the feeding behaviour of the pond snail, Lymnaea. Journal of Neurochemistry, 106, 1699-1709.

Young, K. W., Billups, D., Nelson, C. P., Johnston, N., Willets, J. M., Schell, M. J., Challiss, R. A. J. and Nahorski, S. R. (2005) Muscarinic acetylcholine receptor activation enhances hippocampal neuron excitability and potentiates synaptically evoked Ca2+ signals via phosphatidylinositol 4,5-bisphosphate depletion Molecular and Cellular Neuroscience 30, 48-57.

Yu, B. P. and Chung, Y. H. (2006) The inflammatory process in aging. Reviews in Clinical Gerontology, 16, 179-187.

Zimmermann, R. A. (2003) The Double Life of Ribosomal Proteins. Cell, 115, 130-132.

Zou, S., Meadows, S., Sharp, L., Jan, L. Y. and Jan, Y. N. (2000) Genome-wide study of aging and oxidative stress response in *Drosophila melanogaster*. Proceedings of the National Academy of Science USA, 97, 13726 - 13731.